Republic of Iraq
Ministry of Higher Education and Scientific Research
University of Babylon
College of Materials Engineering
Department of Engineering of Polymers
and Petrochemical Industries

Influence of Curing Conditions on the Kinetics Parameters of an Epoxy System and Its blends

A Thesis Submitted to the Council College of Materials Engineering / University of Babylon in Partial Fulfillment of the Requirements for the Degree of Doctor of Philosophy in Materials Engineering / Polymer

By:

Zahraa Imran Mousa Hussien

(B.Sc. in Non-Metallic Materials Engineering , 2011)
(M. Sc. In Polymers Engineering , 2014)

Supervised by:

Prof.Dr. Najim Abd Al-Ameer Saad (Ph.D.)

2024 A.D **1445 A.H**

بِسْمِ ٱللَّهِ ٱلرَّحْمَٰنِ ٱلرَّحِيمِ

(قَالُواْ سُبْحَانَكَ لاَ عِلْمَ لَنَا إِلاَّ مَا عَلَّمْتَنَا إِنَّكَ أَنتَ الْعَلِيمُ الْحَكِيمُ).

صدق الله العلي العظيم

سورة البقرة

الآية(32)

Supervisors Certification

We certify that this thesis entitled "**Influence of Curing Conditions on the Kinetics Parameters of an Epoxy System and Its Blends**" had been carried out under our supervision for the student (**Zahraa Imran Mousa Hussien**) at the university of babylon/collage of material's engineering/ department of engineering of polymers and petrochemical industries in partial fulfillment of the requirements for the degree of doctor of philosophy in materials engineering/polymer.

Signature:

Prof. Dr. Najim Abd Al-Ameer Saad

Supervisor

Date: / /2024

Examination Committee Certification

We certify that we have read this thesis entitled "**Influence of Curing Conditions on the Kinetics Parameters of an Epoxy System and Its Blends**" and as an Examination Committee examined the student (**Zahraa Imran Mousa Hussien**) on its contents and that, in our opinion, it meets the standard of a thesis and is adequate for the award of the Doctor Degree of Philosophy in Materials Engineering/ Polymer Engineering.

Signature:

Prof. Dr.Zuhair Jabbar Abdul Ameer

Date: / /2024

(Chairman)

Signature:

Prof. Dr. Zoalfokkar Kareem Mezaal

University of Babylon / College of Materials Engineering Department

Date: / /2024

(Member)

Signature:

Prof. Dr. Auda Jabbar Braihi

University of Babylon/ College of Materials Engineering polymer and petrochemical industries Department

Date: / /2024

(Member)

Signature:

Prof. Dr. Ahmed Fadhil Hamzah

University of Babylon/ College of Materials Engineering

Polymer and Petrochemical Industries Department

Date: / /2024

(Member)

Signature:

Assist. Prof. Dr.Ammar Emad Al-Kawaz

University of Babylon/ College of Materials Engineering

Polymer and Petrochemical Industries Department

Date: / /2024

(Member)

Signature:

Prof. Dr. Najim Abd Al-Ameer Saad

University of Babylon / College of Materials Engineering

Polymer and Petrochemical Industries Department

Date: / /2024

(Member)

Approval of Department of Engineering of Polymers and Petrochemical Industries

(Head of the Department)

Signature:

Assist. Prof. Dr.Ammar Emad Al-Kawaz

Date: / /2024

Approval of Materials Engineering College

(Dean of the College)

Signature:

Prof. Dr. Abdul Raheem K. Abid

Date: / /2024

Dedications

To My Husband

My Father and Mother

My Children

My Sisters

My Brothers

To My Friend Dalal and

My Friends

Acknowledgments

F**irst and foremost, I am indebted to the all-powerful almighty "god", for giving me the strength and ability to understand, learn and complete this research it gives me great pleasure and profound privilege to place on record my deep sense of gratitude and indebtedness to my supervisors,* ***Prof. Dr. Najim Abd Al-Ameer Saad *whose constructive comments, unflagging optimism, and scholarly guidance throughout the present work have driven me towards the success of this endeavor without their supervision and guidance, this work would not have been completed I wish to thank all the staff of the laboratories of the collage of materials engineering, especially in the polymers laboratories (ali yhea , fadaa ather, yaser ammar, nabeel and battol) for their support during this work I do not know how can I reach my big respect and thank to my family for their care, patience and encouragement throughout the study period," Iam really indebted to them finally, I would like to thank my family; my friends and everyone help me to accomplish the present work.*

Zahraa Imran witwit

2024

Abstract

Epoxy resin market is faced with an ever increasing demand for a designer range of properties for the epoxy end-use products. Therefore, it is necessary to obtain a complete mechanism and accurate kinetic model that has predictive capabilities. In this study four different mixing ratios of epoxy/hardener pure samples with second set of samples with PS were used to study the cure kinetic of pure epoxy resin and blends with different conditions of curing parameters. The different conditions of curing are including different formulation of epoxy to hardener ratio different cure time and different temperature of curing. Series of epoxy samples were obtained with variations of these conditions and studied the the cure kinetic, TGA, FTIR, tensile properties, fracture toughness strength, impact strength, hardness and SEM.

Based on the results acquired the cure kinetics of epoxy resin utilising under various curing conditions, such as temperature, time ratios of toughened material, and resin to hardener indirect parameters, such the degree of cure and the pace of reaction, were calculated. The findings of DSC epoxy and its blends demonstrated that, depending on the circumstances, a number of parameters altered the kinetics mechanism additionally, the addition of PS has a lowering effect on Tg indicating that toughening agents operate on flexibility chains and have a plasticizer effect.

The findings of the FT-IR analysis of the toughening agent/epoxy blends demonstrate that there is only physical interaction between the polar epoxy polymer and the various toughening agents, not any chemical

reaction with PS. In the SEM images of the epoxy blends, PS altered the epoxy matrix, demonstrating that PS domine purphas phase separated from the epoxy matrix and that pinning morphology appeared in the fracture surface region after curing at RT may be according to solvent evaporation.

Tensile strength, elastic modulus and elongation at break were studied. The best values of tensile strength that best value for pure samples with different conditions are at 1:0.5 pure cured at 80 ℃ followed by 1:0.5 pure at 120 ℃ and 1:0.5 pure at RT while at percent 1:1 pure the best value at RT followed by 1:1 pure at 120 ℃ and the samples at this ratio showing steady value for all the nature of this percent was soft at all conditions while at percent 1.5:1 the best value is at 1.5:1 pure at RT followed by 1.5:1 pure at 120 ℃ followed by 2.5:1.5 + 5 wt.% PS mixture cured at 50 ℃ and at percent of 2.5:1.5 the best value is pure cured at RT similar to that cured at 120 ℃ followed by 2.5:1.5 pure cured at 50 ℃ while for mixture 5:3+5%PS cured at 120 ℃ is the best followed by 2.5:1.53+2.5 wt.% PS cured at 80 ℃ as it is seen this variation in value of tensile strength related to different conditions of curing which enable us to benefits from this in appling of epoxy resin and its blends under different temperatures according to the application requirement in different fields .

Under certain conditions, the elastic modulus reaches its maximum for a 1:0.5 ratio with 5 wt.% PS cured at 80°C and shows optimal values for a 1:10.5 ratio of pure material cured at 50°C. On the other hand, when the ratio is 1:1, the material's rubber-like quality during testing results in an elastic modulus that is the same for every sample. The optimal result is achieved in the case of a 1.5:1 ratio for both pure material cured at 50 °C and a 1.5:1 ratio with 5 weight percent PS cured at 80 °C. On the other

hand, under all circumstances, the elastic modulus values of all percentages in the 2.5:1.5 ratio decrease the results show that the sample treated with a 1:0.5 ratio of curing agent to polymer, plus an extra 7.5 wt.% PS at RT, had the maximum elongation at break.

The fracture toughness of epoxy compositions containing the formulation with a ratio of 1:0.5, when cured at temperatures of 120 ℃, 80 ℃, and room temperature, respectively, exhibited a steady value at 50 ℃, 80 ℃, and 120 ℃, which is superior to the formulation with a ratio of 1:0.5 and 7.5 wt.% PS. At formulation 1:1, the value is observed to be zero due to the rubber-like appearance of the sample.

List of Contents

Sequence	Subject	Page No.
	Abstract	I
	List of Contents	IV
	Abbreviation	VIII
	List of Symbols	XII
	List of Figures	XIII
	List of Tables	XVIII
Chapter One: Introduction		
1.1	General Introduction	1
1.2	Aim of this study	3
1.3	Objectives	3
Chapter Two: Theoretical Part and Literature Review		
2.1	Introduction	5
2.2	Curing Mechanism	8
2.3	Curing Techniques	10
2.3.1	Thermal Curing	10
2.3.2	Microwave Curing	11
2.3.3	Radiation Curing	11
2.3.3.1	Electron Beam Curing	11
2.3.3.2	Gamma Ray Irradiation	12
2.4	Cure Monitoring Techniques	12
2.5	Epoxy Resins	13
2.6	Physcochemical properties	14
2.7	Curing of Epoxy Resin	16
2.8	Epoxy Curing Agents	21
2.8.1	Amine – Curing Agents	21
2.9	Type of Reaction and Curing Agents	23
2.10	Coupling Agent	25
2.11	Kinetic Modeling	26
2.11.1	Kamal Model (Isothermal Kinetic Model)	26
2.11.2	Kissinger Method (Dynamic Kinetic Model)	29
2.11.3	Flynn Wall – Ozawa Method (Dynamic Kinetic Model)	29
2.12	Kinetic Analysis Using DSC	30

2.12.1	DSC Analysis of Curing Kinetic	32
2.12.2	Isothermal Analysis	34
2.13	Polystyrene	35
2.14	Grades of Polystyrene	36
2.14.1	General Purpose Polystyrene	36
2.14.2	High Impact Polystyrene	36
2.14.3	Expanded Polystyrene	37
2.15	Application of Epoxy Blends	38
2.16	Literature Review	39
2.17	Summary of literature review	50
Chapter Three: Experimental Part		
3.1	Introduction	51
3.2	Materials Used	53
3.2.1	Epoxy Resin	53
3.2.1.1	Characteristics / Advantages of Epoxy Resin	53
3.2.2	The hardener	54
3.2.3	Polystyrene	55
3.2.4	Silane Coupling Agent	56
3.3.5	Toluene	56
3.3	Preparation of unmodified Epoxy Samples	57
3.4	Solvent Seleaction	58
3.5	Preparation of Polystyrene Solution	60
3.6	Preparation of an Epoxy Polystyrene Blends	61
3.7	Thermal Tests	63
3.7.1	Differential Scanning Calorimatry (DSC)	63
3.7.2	Thermo Gravimetric Analysis (TGA)	63
3.8	Characteristic Test	64
3.8.1	Infrared Fourier Transform Spectrometer (FTIR)Test	64
3.9	Mechanical Tests	64
3.9.1	Tensile Test	64
3.9.2	Hardness Test	65
3.9.3	Impact Test	66
3.9.4	Fracture Toughness test	68
3.9.5	Crack Path Deflection	68
3.9.6	Crack Pinning	69
3.9.7	Plastic Deformation	69

3.9.8	Plastic Void Growth	70
3.10	Morphology Test	70
3.10.1	Scanning Electron Microscopy (SEM)	70
Chapter Four: Results and Discussion		
4.1	Introduction	71
4.2	Solvent selection results	71
4.3	Analysis of Curing Kinetics Parameters of DSC Results	72
4.4	TGA Results	99
4.5	FTIR Results	112
4.6	Mechanical Characterization	124
4.6.1	Tensile Test	124
4.6.1.1	Tensile Strength Results	124
4.6.1.2	Elastic Modulus Results	133
4.6.1.3	Elongation at Break Results	137
4.6.2	Hardness Results	140
4.6.3	Impact Results	143
4.6.4	Fracture Toughness Results	148
4.7	SEM Test Results	152
Chapter Five : Conclusions and Recommendations		
5.1	The Conclusions	161
5.2	Recommendations	163
	References	164

List of Abbreviations

Abbreviation	Definition
$d\alpha/dt$	Rate of reaction
H(t)	Enthalpy of the reaction
H_T	Total enthalpy of the reaction
α	Degree of cure
ΔHt	The reaction heat at particular time
ΔHT	The total reaction heat
EB	Electron beam
UV	Ultraviolet
Tg	Glass transition temperature
R	Universal gas constant
$K_0, A_1, A_2, \Delta E_C, \Delta E_1$ and ΔE_2	Experimental constants
T	Temperature
ASTM	American Society for Testing and Materials
CTBN	Carboxyl-terminated acrylonitrile-butadiene
CTPB	Carboxyl-terminated polybutadiene
DSC	Differential scanning calorimetry
DGEBA	Diglycidyl ether of bisphenol A
DMA	Dynamic mechanical analysis
DDM	4,4'-diaminodiphenylmethane
EP	Epoxy
TETA	Triethylene triamine
DICY	Dicyandiamine

NMR	Nuclear magnetic resonance spectroscopy
GPC	Gel permeation chromatography
OH	Hydroxyl group
NH	Amino group
fe,fa	Functionalites of epoxy resin and amine
r	Ratio of the amine hydrogen to epoxy group
Qt	Certain time
Q	Entire reaction
m-PDA	m-phenylenediamine
TGPAP	Triglycidylp-Aminophenol
LCERs	Liquid crystalline epoxy resins
Kd	Rate constant
Tcure	Curing temperature
RTM	Resin transfer molding
RIM	Resin injection molding
H	Heat of polymerization
OG	An organic – inorganic hybrid epoxy resin
P	Polymer
S	Solvent
Ro	Interaction radius
H	Hydrogen bond interaction
P	Polar interaction
D	Dispersive force
δ	Solubility parameter
CED	Cohesive energy density

AP	Aniline point
DR	Dilution ratio
KB	Kauri-butanol value
δ	Solubility parameter
CED	Cohesive energy density
$\delta_D, \delta_p, \delta_H$	Solubility sphere
COD	crack-opening displacement
δ_{tc}	Crack opening displacement
PS	Polystyrene
GPPS	General purpose polystyrene
HIPS	High impact polystyrene
EPS	Expandable polystyrene
FESEM	Field Emission Scanning Electron Microscopy
FTIR	Fourier transform infrared spectroscopy
TGA	Thermo gravimetric analysis
AFM	Atomic force microscopic
IPN	Inter-penetrating network
LEFM	linear elastic fracture mechanics
MWCNTs	Multi-walled carbon Nano- tubes
PU	Polyurethane
SEM	Scanning electron microscopy
SENB	Single edge notch bending fracture toughness
ISO	The International Organization for Standardization
RT	Room temperature
Ea	Activation energy

K(T)	Temperature dependent of constant
F(α)	Corresponds to the reaction model
Ea	Activation energy
A	Pre-exponential factor or Arrhenius frequency factor
β	Heating rate
ΔH_R	Residual heat of reaction for isothermally cured sample for a certain period of time
Tg	Glass transition temperature
Tc gel	Crystalline temperature
X	Electron donating species
Y	Electron – accepting species
LC	Liquid crystalline
NH	Amino group
Pc	Critical degree of epoxy conversion
TTT	Time – Temperature –Transformation diagram
CHT	The continuous heating transformation cure diagram
Tgo	Glass transition temperature of unreacted resin
Tg∞	Glass transition temperature of fully cure value
Tp	Peak temperature
To	Onset temperature
T_E	Endset temperature
Kc	Rate constant for chemical kinetics
C	Diffusion coefficient
RIPS	Reaction induced phase-separation
h	Hardener

PCL	Poly-caprolactone
Mc	Average molecular weight

List of Symbols

Symbol	Meaning	Unit
A	The Cross-Sectional Area	mm
A_{cu}	Impact Strength	KJ/m^2
B	Width	mm
E	Modulus of Elasticity	Gpa
H	Thickness	mm
K_{IC}	Critical Stress Intensity Factor	Mpa
P	Force	N
t	Time	min
T_g	Glass Transition Temperature	°C
E	Strain	mm
σ	Stress	Mpa
Φ	Heat flow	-
n	Order of reaction	-
K	Constant rate of reaction	-
m	Order of reaction	-
c	Temperature dependent particle constant	-
α	Degree of cure	-
$α_c$	Temperature dependent particle constant	-
$α_c$	Cure critical degree	-
$α_{max}$	Upper extremely cure degree at a particular temperature	-
G_c	The impact strength	KJ/m^2
U_c	The needed energy for fracture the sample	J
E_B	Flexural Modulus	MPa
V_{fp}	volume fraction of particles	-
$γ_m$	the specific fracture energy of matrix	
δtc	crack-opening displacement	μm
ν	Poisson ratio	-

List of Figures

Figure No.	Subject	Page No.
1.1	Schematic representation of the physical changes occurring during the curing of epoxy resin	2
2.1	Reaction between Amine-Curing Agent and Epoxy Resin	6
2.2	The cure of epoxy resin. Stage A: Uncured resin, Stage B: Partially cured resin (small branched molecules are present), Stage C: Gelation (critical point where branched structures extend throughout the whole sample)	18
2.3	A-Generalized Time - Temperature - Transformation isothermal diagram (TTT) with isoconversion confours. B-Schematic Tg -Temperature - Property diagram (Tg TP) for thermosetting systems	19
2.4	Reaction schemes of chain-growth ring-opening polymerization with (a) cationic and (b) anionic modes	24
2.5	Reaction scheme of step growth ring opening polymerization of epoxy and amine (a) without and (b) with autocatalytic reaction. Panel b only shows the first step reaction	25
3.1	Procedure of Preparing Unmodified Epoxy Samples	58
3.2	Procedure Used to Prepare Modified Epoxy Blends	62
3.3	Represent The Standard Dimensions of Tensile Test Specimen and Experimental Tensile Test Specimen	65
3.4	Represent the standard of Impact Test Specimen	67
3.5	Represent of Fracture Toughness Specimen	68
4.1	The DSC chart test of samples (a: 1:0.5pure, b: polystyrene, c: 1:0.5+2.5 wt.% PS, d: 1:0.5+5 wt.% PS and e:1:0.5+7.5 wt.% PS cured at RT)	75
4.2	Relation between degree of cure and unmodified mixing ratio EP/h cured at RT	78
4.3	Represent the relation between Tg and mixing ratios of	81

	epoxy and its blends at different curing temperature a: 50℃, b:80℃ and 120℃	
4.4	Represent relation between degree of cure and mixing at different curing temperates of a:50℃, b:80℃ and c:120℃	83
4.5	The rate of reaction of epoxy and its blends at different curing temperature	88
4.6	Relation between activation energy and mixing ratios of epoxy and its blends	91
4.7	Relation between curing time and degree of cure for epoxy and its blends at different curing temperature	92
4.8	Relation between curing time and degree of cure for epoxy and its blends at different curing temperature	93
4.9	Relation between curing time and degree of cure for epoxy and its blends at different curing temperature	93
4.10	Relation between 1/Tp and different heating rate	98
4.11	TGA Chart of Samples of a:1:0.5, b:1:0.5+2.5 wt.%, c:1:0.5+5 wt.% 1:0.5+7.5 wt.% PS Cured at RT.	102
4.12	Represent TGA chart of samples of a: 1.5:1 + 7.5 wt.% PS, b:2.5:1.5+7.5 wt.% PS, c: 1:1 + 7.5 wt.% PS and 1:0.5+7.5 wt.% PS Cured at RT	105
4.13	Represent TGA chart od samples of a: 1:0.5+2.5 wt.% PS and b: 1:0.5 + 7.5 wt.% PS curing at 120 ℃	107
4.14	Represent TGA chart of sample 1:0.5+2.5 wt.% PS cured at 80 ℃	108

4.15	Reperesent TGA chart of samples a: 1:0.5 + 2.5 % wt. PS and b:1:0.5 + 5 wt.% PS cured at 50 ℃.	110
4.16	FTIR Spectrum of Uncured Resin - hardener and cured epoxy	117
4.17	FTIR spectrum of sample (1:0.5+2.5 wt.% PS) cured at RT and 120℃	117
4.18	FTIR spectrum of polystyrene	120
4.19	FTIR spectrum of Samples a1:0.5 wt.% PS, b:1:0.5+5 wt.% PS, c:1:0.5+7.5 wt.% PS and d:1:1+7.5 wt.% PS cured at RT	123
4.20	The Tensile strength of pure samples vs. curing temperature	125
4.21	The Tensile strength of samples with 2.5 % wt. PS vs. curing temperature	121
4.22	The Tensile strength of different formulations of EP/h with content of 5wt.% PS	128
4.23	The Tensile strength of different formulations of EP/h with content of 7.5wt.% PS	129
4.24	Represent the tensile strength of epoxy and its blends at different curing temperature for a:1:0.5 ratio, b:2.5:1.5 ratio, c: 1.5:1 ratio and d:1:1 ratio	132
4.25	Represent elastic modulus of a:1:0.5, b:2.5:1.5, c:1.5:1 and d:1:1	134
4.26	Represent a: pure samples, b: 2.5 wt.% PS , c: 5 wt.% PS , and d: 7.5 wt.% PS of elastic modulus with cure temperature for pure samples, and blends under different	137

	curing temperatures	
4.27	Represent the elongation at break of a: 1:0.5, b:1:1, c:1.5:1 and d:2.5:1.5 unmodified epoxy and blends at different temperature and content of PS	140
4.28	Relation between hardness and mixing ratios a: unmodified, b: 2.5 wt.% PS, c: 5 wt.% PS and d: 7.5 wt.% PS of epoxy and its blends at different curing temperature	143
4.29	Represent samples of a: 1:0.5, b:1:1, c:1.5:1 and d:2.5:1.5 impact strength of epoxy and its blends at different temperature	147
4.30	Represent the fracture toughness of epoxy with blends at different temperature	151
4.31	The SEM images at 20μm for samples a: 2:1+7.5 wt. % , b: 2:1+5 wt.%, c: 2:1+2.5 wt. % and d: 2:1pure cured at RT with curing time 24h for different percent of concentration of PS	153
4.32	The SEM image at 20μm for samples a: 2:1+7.5 wt. % and b: 2:1+2.5 wt. % cured at 120 ℃ for 4h with different concentration of PS	154
4.33	The SEM image at 50μm for different samples a: 2:1+7.5 wt.%, b: 2:1+5 wt.%, c: 2:1+2.5 wt. %and d: 2:1pure cured at RT for 24h with different concentration	157

	of PS	
4.34	The SEM images at 50μm for different samples a: 2:1+7.5 wt.% and 2:1+2.5 wt.% cured at 120 ℃ for 4h with different concentration of PS	157
4.35	The SEM images of different samples a: 2:1+7.5 % wt. PS, b: 2:1+5 % wt. PS c: 2:1+2.5% wt. PS and d: 2:1pure cured at RT of EP/h/PS blends	159
4.36	The SEM images of different samples a: 2:1+7.5% wt. PS and b: 2:1+2.5 % wt. PS cured at 120℃ of EP/h/PS blends	159
4.37	The SEM Images of Different Samples a: 2:1 pure, b: 2:1+2.5 % wt. PS, 2:1+5 % wt. PS and 2:1+7.5 % wt. PS cured at RT of EP/h/PS Blends	160
4.38	The SEM images of different samples a: 2:1+2.5%PS and b: 2:1+7.5%PS cured at 120 ℃ of EP/h/PS blends	160

List of Tables

Table No.	Subject	Page No.
(3-1)	Properties of Epoxy Resin	53
(3-2)	Properties of the Hardener	55
(3-3)	properties of polystyrene	55
(3-4)	Properties of Toluene	57
(3-5)	Technical information of tescan mira is a high-resolution (hr) analytical SEM	70
(4-1)	The Hanson solubility parameters of target polymers	71
(4-2)	The Hanson solubility parameters values of the currently used solvents, and their miscibility with polystyrene (PS)	72
(4-3)	The value of Tg for epoxy and its blends cured at RT	76
(4-4)	The relation between hardener ratios and degree of cure of epoxy and its blends at RT	78
(4-5)	Value of kinetics parameters at Different Heating Rates for Different Samples	95
(4-6)	Ratios of total mass loss of different samples curing at different temperatures	99

(4-7)	Represent the FTIR peaks	113

Chapter One
Introduction

1.1 General Introduction

Uncured epoxy resins are not very beneficial, to give them superior mechanical qualities and thermal stability, they must react with an appropriate curing agent, such as amines and anhydrides, to create three-dimensional cross-linked structures. Their applications in the domains of adhesive, coating, electronic encapsulation material, and the matrix for advanced fiber-reinforced plastics are also expanded by their inherent high adhesion strength and good process ability [1].

The cured epoxy resins offer strong mechanical and adhesive qualities, good water resistance, heat resistance, chemical resistance, and superior insulating and electrical properties once they have fully set, as a result, they are frequently employed in reinforced composite matrices, coatings, encapsulants, and adhesives. Most commercial epoxy resins currently on the market are based on the interaction between bisphenol A and epichlorohydrin [2].

The curing mechanism of the epoxy/amine system follows the autocatalytic model due to the increasing concentration of the hydroxyl group during the curing reaction that accelerates the curing reaction [3]. cure by the reaction of epoxy groups with the amine groups following the step-growth polymerization process, the physical changes occurring during the curing of epoxy resin as shown in Figure (1.1) this curing process is complicated and involves the ring-opening reaction of the epoxy ring, which produces secondary amines that further react with the epoxy groups to produce tertiary amines, causing branching or crosslinking. The hydroxyl group produced during the polymerization can form hydrogen

bonds with the unreacted epoxy groups, thereby promoting the nucleophilic attack of the amino groups on the epoxy groups [4].

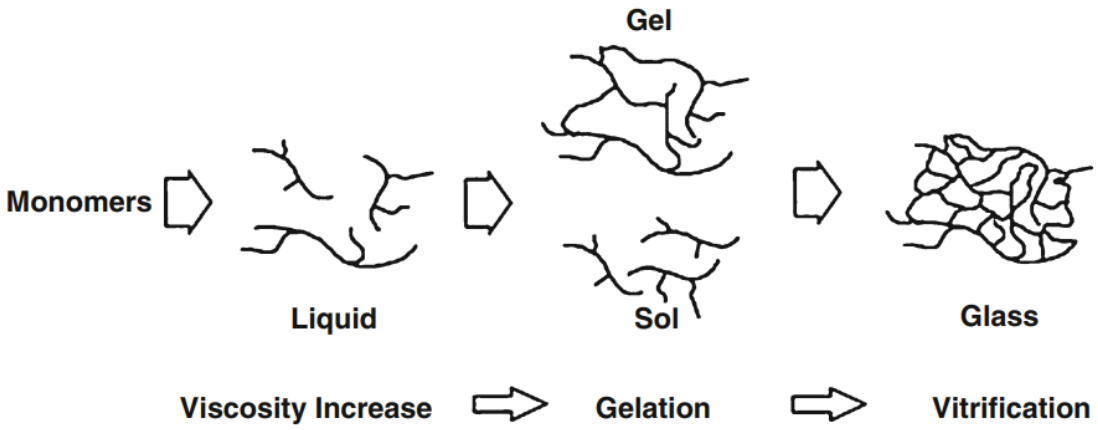

Figure (1.1) : Schematic representation of the physical changes occurring during the curing of epoxy resin [1].

The study of the curing kinetics plays a crucial role in developing and optimizing the industrial manufacturing process. Curing kinetics can be used to minimize the cycle time heat transfer and micromechanics to calculate and minimize the generated internal stresses. In this way, it is possible to improve the process development and ultimately the quality and performance of the final product [5]. The kinetic parameters of the cure reaction can be obtained by fitting the data obtained from the DSC measurements to the phenomenological reaction models the rate of reaction is assumed to be proportional to the rate of heat generation and can be expressed as [6]:

$$\frac{d\alpha}{dt} = \frac{1}{HT}\frac{dH(t)}{dt} \quad \ldots\ldots (1.1)$$

where $d\alpha/dt$ is the rate of reaction, $H_{(t)}$ is the enthalpy of the reaction up to time t and H_T refers to the total enthalpy of the reaction.

One of the application of effects on kinetic is that during the application of such coatings to steel structures, on different parts of a ship in a yard, cure kinetics play a significant role in determining the cost of application.

For example, at low application temperatures during winter, a fast-curing epoxy-amine coating can reduce the over coating interval, thereby increasing the application speed and reducing the overall cost of the application process after application, curing kinetics govern how quickly the coating (or the coating system) can develop its required chemical, mechanical, and barrier properties since all these properties are strongly dependent on the final epoxy-amine polymer (along with other non-reactive additives such as extenders, hydrocarbon resins, etc.) present in the commercial coatings nevertheless, an optimum curing speed is always required, since too fast curing can generate significant internal stresses that cause cracking. Delamination of epoxy-amine coatings from the metallic substrate or from other coating layers is also sometimes attributed to high curing speeds, which do not allow entanglements of polymer chains [4].

1.2 Aim of this study

Study the influence of curing conditions on curing kinetics of epoxy and its blends.

1.3 Objectives:

In order to achieve the previous aim, the following activities will be carried out:

1- In order to study the influence of cure kinetics on cure parameter of epoxy resin it will use different procedure for curing epoxy resin under different parameters with using tough material thermoplastic polystyrene with using saline coupling agent to modification polystyrene thermoplastic polymer and improve their surface to avoid separation and increase the ability to bond with the base material.

2- The samples will undergo different tests such as DSC (in order to configuration of Tg, T_p, T_{onset}, ΔH_{total}, ΔHt, Ea, rate of reaction and degree of cure, TGA test (to configuration of thermal stability of material under different temperature), mechanical tests (tensile strength, hardness test, fracture toughness and impact strength) morphological tests SEM, FTIR as characterization test.

Chapter Two
Theortical Part and Literature Review

2.1 Introduction

Curing is the principal process in the production of thermosetting polymers which gelation plays an important role for product quality control. In the curing process, the epoxy resin reacts with the curing agent to form a highly cross-linked molecular network through a step-growth polymerization. The viscosity, density and other physical properties of the resin change continuously with the progress of the curing reaction. When the reaction proceeds to a certain time, the resin viscosity rises exponentially and the gelation initiates [7].

The cure kinetics associated with the epoxy resin is very important aspect. With the help of the modeling of cure kinetics, scientists, engineers or process control managers can get valuable information useful for optimizing processing conditions or predicting the thermosetting resins or composites shelf life time. Differential scanning colorimetery (DSC) can be used so that the kinetic parameters are determined by using isothermal and dynamic methods [8].

Epoxy resins are characterized by a three-membered ring known as epoxy, epoxide, oxirane, or ethoxylene group, consisting of an oxygen atom attached to two interconnected carbon atoms, the strained three-membered ring structure makes epoxy resin reactive. Hence it is attacked by nucleophilic and electrophilic reagents. The ultimate properties of epoxy resin are achieved by converting them to insoluble and infusible network. This is achieved by reaction with various chemical compounds known as curing agents or hardeners [1].

The reaction of epoxide with amine as shown in Figure (2-1) involves several reactions like addition of amine to epoxide, homopolymerization of epoxy by etherification or ionic polymerization, cyclisation, and various side transformations and degradation reactions. In most cases, the addition of amine is the predominating reaction. The reaction between epoxy resin and an amine-curing agent [1].

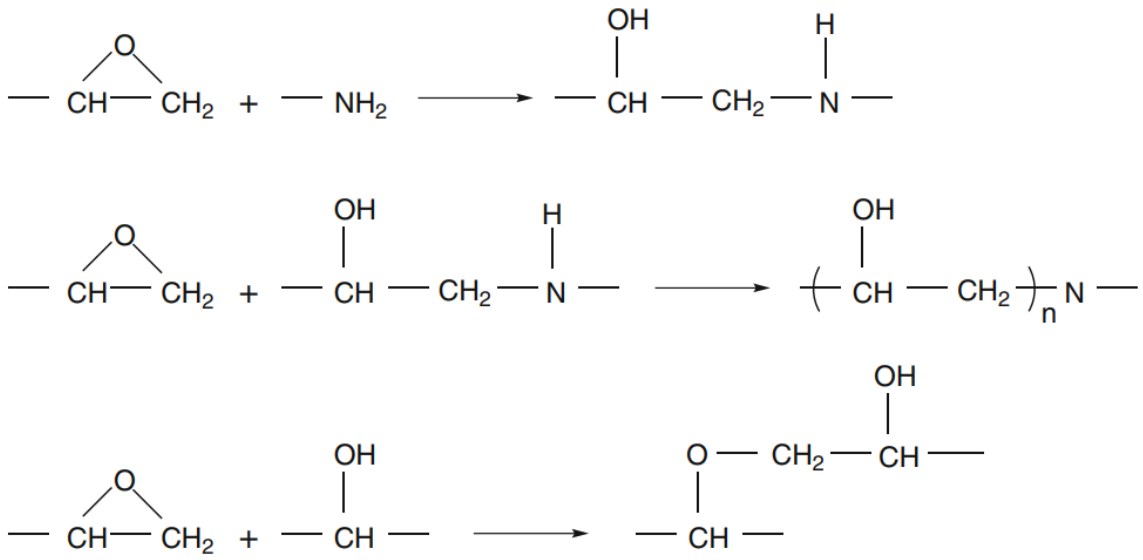

Figure (2.1) : Reaction between amine-curing agent and epoxy resin [1]**.**

Epoxy resins are the most frequently used precursors for syntheses of thermoset materials. Many applications of epoxy systems include adhesives, coatings, electronic applications, high-performance materials, etc., according to the application, a great variety of hardeners are used to form epoxy networks under both low- and high-temperature curing regime [9].

The most widely used low-temperature hardeners include polyamide and amidoamine curing agents as well as aliphatic amines (such as diethylenetriamine, triethylenetetramine and their derivatives, catalytic amines, sulfur-containing curing agents and amine adducts. The main disadvantage of curing at low temperatures is low glass transition temperature of the cured resin. Although room temperature curing epoxy resins are very convenient in many applications, polymer bulletin their short working life and long curing time often become serious disadvantages of their use [4]. The hardening effect is achieved through the formation of cross-links between the resin polymer chain and the hardener, or by direct linkage among the epoxy groups [11].

To toughen epoxy resin, a common method is introducing particles in the resin, including liquid rubbers, thermoplastics, copolymers, silica nanoparticles, silicate layers, core shell particles, and combinations of these. The major toughening mechanisms involve rubber particle debonding/cavitation, localized shear banding of matrix as well as rubber particle bridging. Fracture toughness of rubber toughened epoxy resin will be improved obviously, while many other desirable properties, such as elastic modulus and failure strength, will decrease significantly [12].

The cross linked network structure of epoxy resins can be tuned via different approaches, controlling the curing process, changing the chemical structures epoxy resins and curing agents, and so on, for an epoxy-amine system with the specific curing process, design of the crosslinking network structure of the thermosets can be obtained by changing the stoichiometric ratio of active-hydrogen to epoxy-group, on the other hand, epoxy resin system with high temperature curing process

usually exhibits superiority in mechanical and thermal properties at elevated temperature. However, materials served at cryogenic engineering always suffer from low temperature or alternating hot and cold temperature. Compared with the high-temperature curing process, low-temperature curing process will significantly decrease the large temperature gradient from the curing temperature to the operating temperature. Therefore, the internal stress caused by the contraction during the decrease of temperature is likely to be reduced. This unique advantage endows low temperature curing system with possible applications in cryogenic engineering. Additionally, as the properties of the thermosets are deeply affected by curing temperature, it is desirable to investigate the effects of the stoichiometric ratio on curing characteristic and morphology of low-temperature cured epoxy resins [13].

2.2 Curing Mechanism

The term curing is used to describe the process by which one or more kinds of reactants, an epoxide and a curing agent, are transformed from low-molecular-weight materials to a highly cross-linked network. The network is composed of segments involving only the epoxide or both the epoxide and the crosslinking agent. Under basic or neutral conditions, all ring-opening reactions are essentially similar and involve the attack of a nucleophile on one of the epoxide carbon atoms, as in the case of an amine curing agent [14].

A real difference exists when the reactions are carried out under acidic conditions. The addition of most nucleophiles is accelerated considerably by acids or electrophilic species because of the reversible formation of the

more reactive conjugated acid of the epoxide, as in the case of a Lewis acid. There is very little doubt that the ring-opening reactions of epoxides take place by ionic mechanisms. The bond that is broken is the highly polar carbon-oxygen bond, which would be expected to break ionically; the reactions are generally carried out in polar solvents, such as the resin itself, and can be accelerated by adding polar reagents [15].

The cure degree α, is utilized to reveal the degree of conversion of small molecular weight pre-polymers into high molecular weight cross-linked, having three dimensions construction, α increases with increase in heat given off due to bonds creation, on the other hand, for resin which is completely cured α equal or less than one. It is presumed that the curing rate is proportionate to rate of heat generation and the following expression, to characterize the process of curing, many phenomenological models have been developed to study the system of different resins, α increases with increase in heat given off due to bonds creation and it can be described as follows [16]:

$$\alpha = \frac{\Delta H_t}{\Delta H_{totat}} \ldots\ldots (2.1)$$

Where α represent the cure degree, ΔH_t represents the reaction heat being accumulated up at a particular time t of curing process, and ΔH_{total} represents the total heat which is liberated when the reaction is completed.

2.3 Curing Techniques

Epoxy resin systems are cured by various methods. These include chemical curing (under ambient or increased temperature as with conventional thermal curing), microwave curing, and radiation curing (electron-beam (EB) and ultraviolet (UV) curing). The mechanism of curing methods differs in these methods. Thermal curing takes place through a step polymerization mechanism, which follows throughout the curing process, whereas radiation curing leads to chain polymerization involving initiation, propagation, and termination steps. The mechanical characteristics of the cured matrix differ in both cases [17].

Many different analytical methods have been studied to characterize the cure reaction and monitor the cure process of thermosets, such as differential scanning calorimetry (DSC) and dynamic mechanical analysis (DMA) these methods, however, typically are not practiced for in-situ cure monitoring because they are only performed in laboratories under ideal conditions. Nevertheless, these methods can provide excellent information about glass transition temperature (T_g), onset of cure, heat of cure, maximum rate of cure, completion of cure and degree of cure [18].

2.3.1 Thermal Curing

The thermal curing process of resin matrix is a thermo-chemo-coupled process. The resin is taken as not flowing in the stage of curing, and the convection and thermal conduction are neglected, thus the thermal conduction equation with the chemical reaction as written in Eq.2 can be used to describe a full three-dimensional cure process [19]:

$$\frac{d\alpha}{dt} = K_0 exp - \frac{\Delta E_c}{RT\alpha^m\ 1\ - \alpha^n} \ldots\ldots (2.2)$$

$$\frac{d\alpha}{dt} = K_1 + K_2\ \alpha^m 1 - \alpha^n \ldots\ldots (2.3)$$

Where

$$\mathrm{K_1} = \mathrm{A_1 exp} - \frac{\Delta \mathrm{E_1}}{\mathrm{RTK_2}} = \mathrm{A_2 exp} - \frac{\Delta \mathrm{E_2}}{\mathrm{RT}} \ldots\ldots (2.4)$$

Where R is the universal gas constant; T is the temperature; and k_0, A_1, A_2, ΔE_c, ΔE_1, and ΔE_2 are the experimental constants.

2.3.2 Microwave Curing

Microwave curing can reduce the time of the epoxy resin substantially. The cure times can be reduced to the range of minutes from hours through the use of microwave curing. As the microwave energy is largely concentrated on the sample with greater efficiency, curing is highly economic for commercial manufacturing with shorter cure cycles [17].

2.3.3 Radiation Curing

2.3.3.1 Electron Beam(EB)Curing

Electron beam curing of composites is an innovative processing method, begun in the late 1970s, that uses high-energy electrons from an accelerator to initiate polymerization and cross-linking of a matrix resin. Reduced cure time, low-temperature cure, greater design flexibility, and unlimited material shelf life are some of the advantages of this method compared to the conventional thermal curing. As a low-cost and nuisance-

free technology [17].

2.3.3.2 Gamma Ray Irradiation

Surface properties of polymeric materials, such as films, fibers, powders, and molded objects, can be altered by a new technique using irradiation-induced grafting. This can induce chemical reactions at any temperature without any catalyst in the solid, liquid, and gas phase, and is a safe method against environmental pollution [17].

2.4 Cure Monitoring Approaches

Cure monitoring is a means of tracking the real-time changes in physical state or chemical reaction that occur during the curing process, indicates measurements being carried out on a timescale which allows process conditions to be modified before completion. Cure monitoring enables several important transition stages or critical points during cure to be detected and identified, including:

• resin flow/position of flow front

• minimum viscosity

• gelation

• vitrification

• post-cure

• degradation

• degree of cure.

These characteristic cure stages help streamline processes in several ways, once gelation is achieved no more flow is possible and continued application of pressure achieves no further consolidation and so can be removed. At vitrification, no more cure is attained at the defined processing temperature and so the part can be removed from the process and allowed to cool down. Alternatively, monitoring for the initial signs of degradation can be used as a trigger for part removal. Solid cured parts can then be collected and given a post-cure heat treatment together. The final measured degree of cure can then be used to ensure the part meets the specifications and requirements of the application [20].

For in-situ monitoring processes such as curing, phase separation or even ageing, the interpretation of the spectra and the assignment of the bands are critical. Mid infrared spectroscopy has been widely used for characterization of organic compounds and plenty of reliable information and spectra libraries can easily be found. Both qualitative and quantitative information can be obtained by this technique, although its use in epoxy systems is quite restricted because of the location and intensity of the oxirane ring absorptions. For monitoring the curing reaction, the intensity of the bands in this region is much lower than in the mid-range, allowing the use of thicker and undiluted samples to get good quality data [21].

2.5 Epoxy Resins

Epoxy resins are a class of versatile polymers containing two or more oxirane rings or epoxy groups in their molecular structure, which can be hardened into thermosetting plastics with the use of a suitable curing agent. Epoxy resins have found a wide range of applications as coatings,

adhesives, electrical insulators, electronic encapsulation materials, and matrices for fibrous components due to their excellent adhesiveness, chemical resistance and physical properties [22]. The cross-links form during the polymerization of the liquid resin and hardener, so the structure is almost always amorphous, on reheating, the additional secondary bonds melt, and the modulus of the polymer drops; but the cross-links prevent true melting or viscous flow so the polymer cannot be hot-worked (it turns into a rubber). Further heating just causes it to decompose [23].

2.6 Physicochemical Properties

The properties of the epoxy resin depend on the extent of reaction. The knowledge of the mechanism and cure kinetics is necessary for assigning structure, property relationships. The viscosity of the epoxy resin depends on the molecular weight distribution of the polymer. It increases with the increase in equivalent weight that results in solid resin at room temperature. Cross-linking densities can be lowered by increase in fracture toughness to a small extent. These resins are generally used in solution form for coating application and as granular molding compounds. The functional group of the epoxy resin decides the thermomechanical behavior of the resin. Increase in epoxy functionality increases the cross-linking density and thus forms a rigid molecule. Hence, multifunctional epoxies have a glass transition temperature higher than difunctional epoxy even after cured with the same hardener. It can be further classified into different categories on the basis of the structure of the phenol-containing molecule and the number of phenol groups per molecule [24].

In order to understand the following reaction's relationship between the hardener/resin ratio and the mechanical properties and epoxide group[25]:

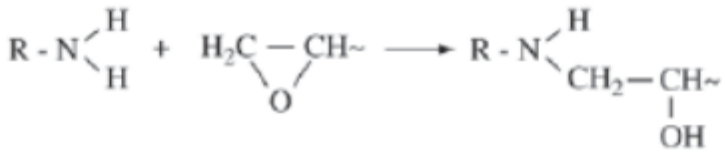

Which leads to the formation of strongly hydrophilic hydroxyl groups (-OH) for non-stoichiometric formulations with excess of epoxy monomer the epoxy ring can react with hydroxyls groups, leading to the formation of ether groups according to the reaction [25]:

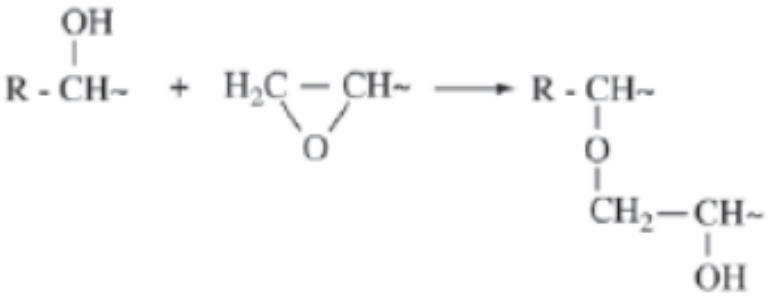

Finally, homopolimerization reactions can be catalysed by steric hindered tertiary amines [25], leading to the formation of the p-dioxane ring structure:

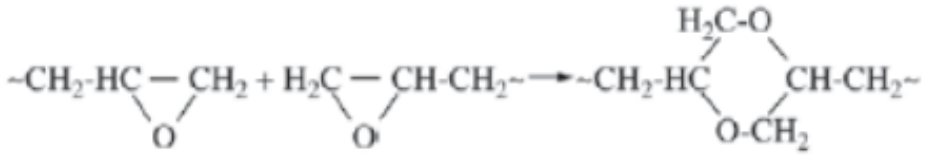

Or to the step like structure [25]:

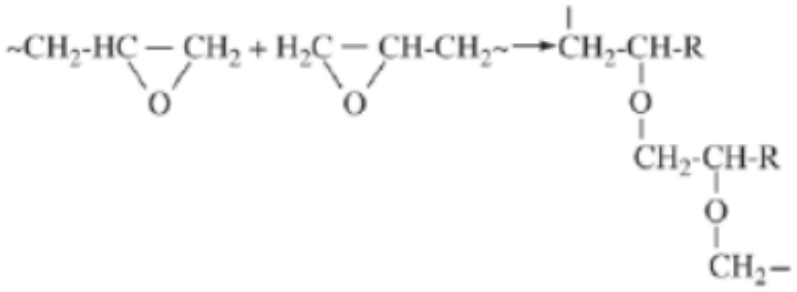

2.7 Curing of Epoxy Resin

The basic reaction of epoxides based on diglycidyl ether of bisphenol A (DGEBA) with primary and secondary amines, in the absence of catalyst, involves the addition of the primary and secondary amino groups of the polyamine to the epoxy group, with the simultaneous evolution of one hydroxyl group due to opening of the epoxy ring. This reaction scheme can be represented by the following reactions [26]:

- **Primary Amine Addition**

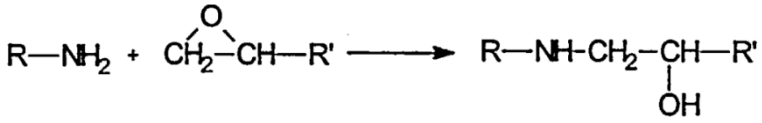

- **Secondary Amine, Addition**

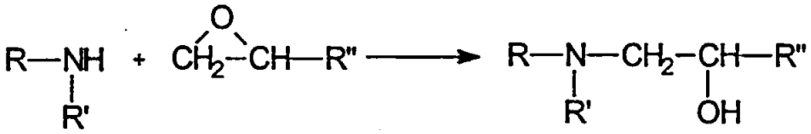

Experimental evidence shows that the two epoxy groups of this type of resins have the same reactivity, hence these reactions proceed with the -

NH amino group attacking the epoxy ring randomly. These reactions are catalysed by acids such as (Lewis acids), phenols and alcohols. The hydroxyl groups formed by the amine/epoxide addition reaction can act as catalysts, accelerating the reaction at the early stages and showing the typical performance of an auto-catalysed reaction. In cases where the amine is present in less than stoichiometric concentrations, further reaction of the epoxy groups with the hydroxyl groups may occur, producing an ether group according to the general reaction [26]:

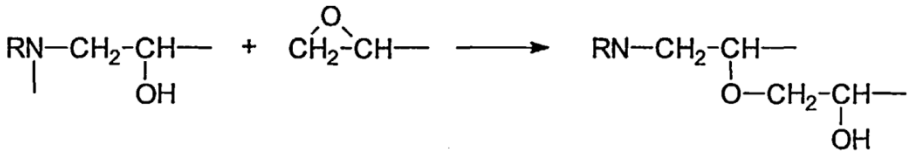

According to the type of the epoxy/amine system, some other reactions can also become operative to various extents, anionic or cationic polyinerisation reaction of the epoxy groups, initiated by an interaction of the epoxy group with tertiary amine or a Lewis acid, occasionally also in the presence of a proton donor. For a biftmetional epoxy-amine system, with the only reaction occurring being the epoxy/amine addition, the mathematical formula that gives the critical point of epoxy conversion for gelation is given by [26]:

$$Pc = \left(\frac{1}{(fe-1).(fa-1).r}\right)^{1/2} \quad \ldots\ldots (2.5)$$

Where p_c , is the critical degree of epoxy curing, f_e , and f_a are the functionalities of epoxy resin and amine respectively, and r is the ratio of amine hydrogen's to epoxy groups initially present in the resin system. At

epoxy conversions below p_c , all the molecules have finite size, whereas at higher conversions, some are infinite. Eventually, a network will be formed, with one single molecule in the total mass as shown in Fig.2.2 [26].

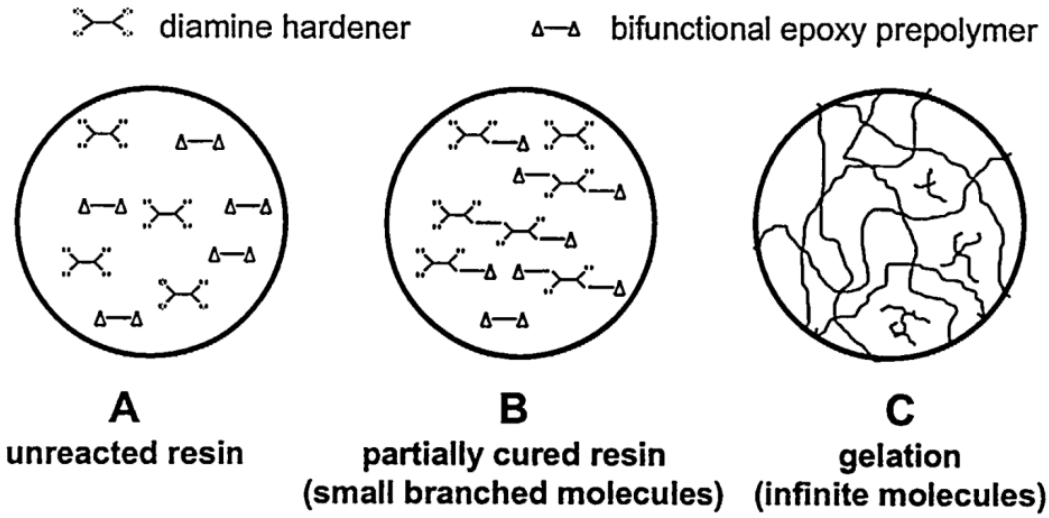

Figure (2.2) : The cure of epoxy resin. Stage A: Uncured resin, Stage B: Partially cured resin (small branched molecules are present), Stage C: Gelation (critical point where branched structures extend throughout the whole sample)[26]**.**

Many other changes in the physical state of the epoxy - amine system take place during the cure reaction as a consequence of the changes in the free volume and in the glass transition temperature of the reactive system. During cure to full conversion at isothermal conditions, the glass transition temperature (T_g) increases from the value representative of the uncured monomer mixture (T_{go}) to the fully cured value ($T_{g\infty}$) [26].

In Figure (2.3) on the well-known Time - Temperature -Transformation (TTT) diagram, which was first adopted for the epoxy resin cure by Gillham, provides an intellectual framework for the understanding of the

curing process and the optimisation of the processing and the final material properties [26].

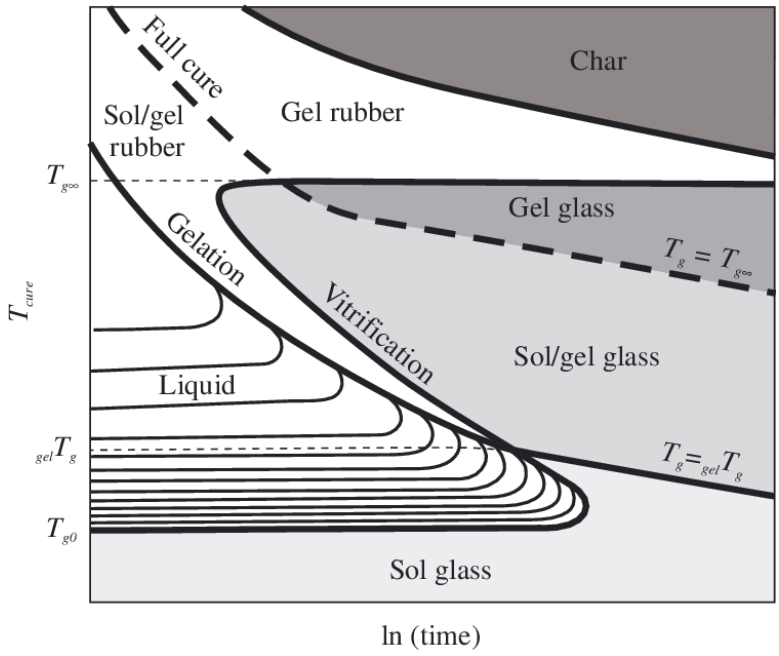

Figure (2.3) : Generalized isothermal time-temperature-transforma tion (TTT) cure diagram for a thermosetting system, showing three critical temperatures (Tg_0, Tg_{gel} and Tg_∞), various stages of the material, and contours characterizing the curing and degradation processes [27]**.**

During curing, epoxy resin is converted into a hard infusible material as a result of cross-linking reactions, which ultimately lead to a network structure. Initially, linear growth of the chain occurs followed by branching and finally leads to cross-linking. This irreversible reaction leads to an increase in molecular weight, which results in the physical transformation of the system from a viscous state to an elastic gel. As curing proceeds further, the viscosity of the system increases because of the increase in molecular weight, and the reaction becomes diffusion controlled and eventually quenched as the material vitrifies. This is again

another physical transformation and occurs during the curing reaction called vitrification of the growing chain or network. During this conversion, a substantial increase in cross-link density, Tg and ultimate properties takes place. The change in the state of the system from viscous liquid to elastic gel and finally to glassy solid begins to occur as the Tg of the developing network becomes equal to the curing temperature.

At the vitrification point, the reaction shifts from chemically controlled to a diffusion-controlled state. The net changes during the curing of the thermoset can be expressed in terms of a TTT diagram, the S-shaped gelation curve and the vitrification curve divide the time-temperature plot into four distinct states of the thermosetting cure process: liquid, gelled rubber, ungelled glass, and gelled glass, Tg is the glass transition temperature of the resin at its gel point, the temperature region below the glass transition of the unreacted resin Tg_0 represents the solid state and hence the reaction is believed to occur very slowly, this temperature region defines the storage temperature for unreacted resins, the reaction initiates above Tg_0 and continues till the rise in Tg becomes equal to the cure temperature at which vitrification will commence, thereafter, the reaction becomes diffusion controlled and is eventually quenched when vitrification is complete [28].

In a stage between gel Tg and Tg, gelation precedes vitrification, and a cross-linked rubbery network forms and grows until its Tg coincides with the cure temperature. The reaction will be quenched at this stage. Tg is the minimum cure temperature required for the completion of cure. Above Tg, the thermoset will remain in the rubbery state, unless other oxidative cross-linking or chain scission occurs. Gelation and vitrification determine

the handling, processing, and development of the ultimate properties of the cured resin [17].

2.8 Epoxy Curing Agents

Epoxy curing agents promote or control the epoxy resin curing reaction. Epoxy resin curing is accomplished by adding a curing agent. Irreversible changes in the epoxy resin occur during the curing process. The cure kinetics and Tg of epoxy resins are dependent on the molecular structure of the curing agents. Curing agents can be divided into amine-type curing agents, alkali curing agents, anhydrides, and catalytic curing agents according to their chemical compositions [29].

2.8.1 Amine-Curing Agents

The most common curing agents for the epoxy resin cure are:

A. Curing agents containing nitrogen.

1. aliphatic amines and derivatives (EDA, DETA, TETA), cycloaliphatic amines and derivatives (PACM, DACH, IPDA),
2. aromatic amines and derivatives (DDM, DDS, DETDA). They act as curing agents for the polyaddition reaction.
3. Catalysts and co-curing agents (tertiary amines, imidazoles, ureas). They act either as catalysts for the crosslinking by homopolymerisation or as accelerators and co-curing agents for polyamines, polyamides and anhydrides, or as activators.

B. Curing agents containing oxygen.

1. Carboxylic acids and anhydrides (TGIC, HBPA, TMA), phenol formaldehyde resins (P-F resins).

2. Amino formaldehyde resins (M-F resins).

C. Curing agents containing sulphur (polysulphides, polymercaptons).

In general, epoxy resin curing reactions involve opening of the epoxide ring followed either by a homopolymerisation reaction with further epoxide, or reaction with other curing agents to form additional products. Amongst the curing agents of greatest technological importance are the polyamines and anionic or cationic catalysts [26].

Amine compounds are classified into primary, secondary, and tertiary amines, in which one, two, and three hydrogen molecules of ammonia (NH_3) have been substituted for hydrocarbon, respectively. Amines are called monoamine, diamine, tri-amine, or polyamine according to the number of amines in one molecule. According to the types of hydrocarbons involved, amines are classified into aliphatic, alicyclic and aromatic amines and they all are important curing agents for epoxy resin [30].

These curing agents are cross-linking agents which are labile hydrogen compounds, such as acids, anhydrides, amines, etc. Aliphatic amine is a curing agent which is capable of curing epoxy resin at room temperature. The cured resin has outstanding properties. It is only the active hydrogen present in primary amine helps to cure reacts with an epoxy group to form secondary amine, and the latter reacts with epoxy group. The role of the tertiary amine generated is to polymerize the epoxy groups. Tertiary amines are very important as accelerator especially for acid anhydrides but less used as curing agent. The amines cured end product has been found highly dependent on the curing speed, amount of hardener loaded, and the

type of epoxy resin. Aliphatic amines cured epoxy have good bonding properties and excellent resistance toward water and some solvents. The major disadvantage is skin irritation and its toxicity [24].

2.9 Type of Reactions and Curing Agents

An oxirane in an epoxy monomer is a class of three-membered ring. Such a small ring exhibits high reactivity dominated by the effect of ring strain, whose strain energy is estimated to be about 115 $kJ \cdot mol^{-1}$. Thus, epoxy monomers can generate a cross-linked network structure by either chain-growth ring opening polymerization or step-growth polymerization, depending on the type of curing agent. Chain-growth ring-opening polymerization can be further classified into cationic and anionic polymerizations. The propagation reaction proceeds via an active oxonium at the end of the growing chain as shown in Figure (2.4).

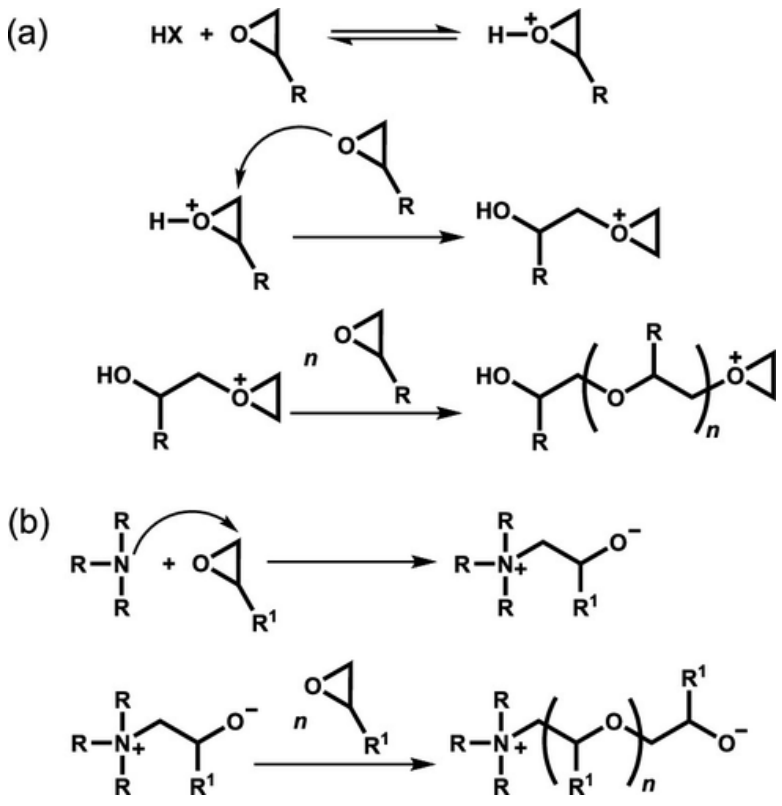

Figure(2.4):Reaction schemes of chain-growth ring-opening polymerization with (a) cationic and (b) anionic modes [31]**.**

Common initiators are boron trifluoride (BF_3) complexesand onium salts including diaryliodonium, triarylsulfonium, or phosphonium salts. Section b of Figure (2.5) shows the scheme for anionic polymerization which is generally initiated by imidazoles or highly reactive tertiary amines. It is based on the formation of alkoxide, which then reacted with an epoxy monomer, leading to the generation of another alkoxide. The step-growth ring-opening polymerization of epoxy monomers can be performed using amines, acids, isocyanates, and mercaptans, of these amines have been widely used.

In this case, the reactivity and thereby the kinetics of the curing reaction are determined by the electrophilicity of the epoxy group and the nucleophilicity of the amino group. Section a of Figure (2.5) shows the reaction scheme of epoxy monomers with an amine. A primary amino group first reacts with an epoxy group. This produces a secondary amino group that further reacts with another epoxy group and then a tertiary amino group is generated. Since the resultant tertiary amino group gives a branching or cross-linking structure, the amines used are often referred to as curing agents or hardeners [25].

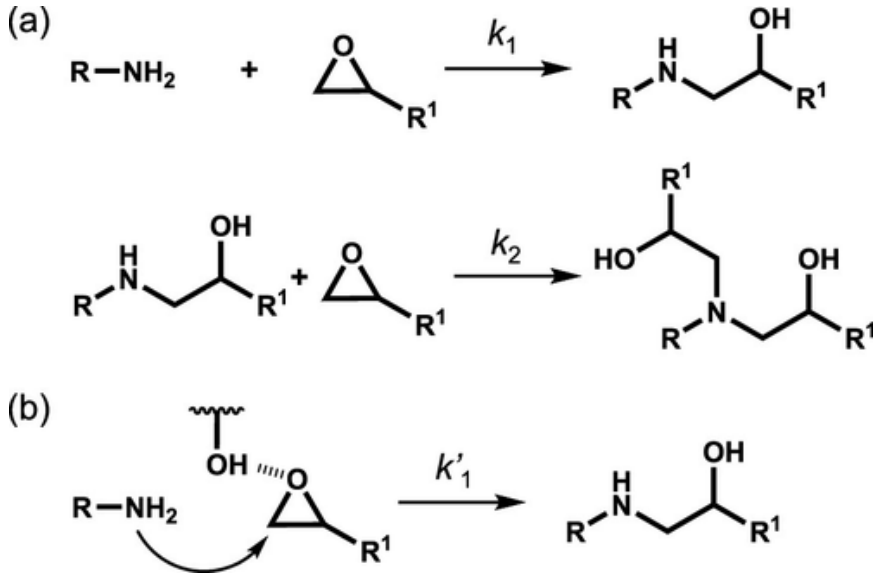

Figure(2.5): Reaction scheme of step growth ring opening polymerization of epoxy and amine (a) without and (b) with autocatalytic reaction. Panel b only shows the first step reaction[31]**.**

2.10 Coupling Agents

The property of a polymer blend or a filled polymer system largely depends on the compatibility between the constituent polymers in the blends or between the polymer and filler in filled-polymer systems. Other terminologies such as wetting and interfacial adhesion are sometimes used to reflect compatibility. For filled polymer systems, the incompatibility generates weak interfaces, leading to a drastic reduction in mechanical properties. Coupling agents are used to improve the compatibility, wetting or interaction between the constituent polymers in the blends, or between the polymer and filler in filled polymer systems. Coupling agents have been found to be very successful for improving the properties of thermoplastic blends. However, in thermosetting resin systems, coupling agents are mostly used to improve the wetting of filler by the resin matrices. Silane compounds, such as trichlorovinyl silane, triethoxyvinyl

silane, and G-glycidoxypropyl-trimethoxy silane are examples of coupling agents for thermosetting resins [32].

2.11 Kinetic Modeling

Two types of equations are used for kinetic modeling; one is based on the reaction pathway and the other is the phenomenological kinetic equations. The model proposed by Horie et al. (1970) and simplified by Kamal and Sourour is the most widely used phenomenological kinetic equation and the Kissinger and Flynn–Wall–Ozawa models are also used in the kinetic analysis of epoxy curing [1].

2.11.1 Kamal Model (Isothermal Kinetic Model)

This model is simple to use and does not need prior knowledge of the reaction mechanism. It has been used widely in various thermosetting systems for resin transfer molding (RTM), filament winding, resin injection molding (RIM), microwave curing, etc. The model assumes that the epoxy–amine reaction is catalyzed by the hydroxyl groups formed during curing and those existing in the resin or by acidic impurities present in the system. Also the degree of reactivity of primary and secondary amine hydrogen's toward epoxy group is the same. The kinetic equation is [1]:

$$\frac{d\alpha}{dt} = (K_1 + K_2\,\alpha^{\,m})(1-\alpha)^n \ldots\ldots (2.6)$$

where k_1 is the rate constant for the reaction catalyzed by groups initially present in the resin, k_2 is the rate constant for the reaction catalyzed by hydroxyl groups formed during the reaction, and m + n gives

the overall order of the reaction. In a modified version of the Kamal equation, it was assumed that the curing reaction followed second-order process, but as cure reaction proceeds the glass transition temperature Tg of the system approaches the curing temperature T_{cure}. In addition, the viscosity of the system will also increase. When Tg approaches T_{cure}, the reaction becomes diffusion controlled, and the reaction rate becomes zero before complete reaction. So the final conversion is dependent on the cure temperature. The effect of cure temperature is incorporated in the models replacing the term1 α with $\alpha_{max} - \alpha$, where α_{max} represents the final degree of cure reached at the investigated temperature. The equation becomes [1]:

$$\frac{d\alpha}{dt} = (K_1 + K_2\,\alpha^m)(\alpha_{max} - \alpha)^n \ldots\ldots (2.7)$$

Plot of $d\alpha/dt = (\alpha_{max} - \alpha)$ versus α gives a straight line with intercept k_1 and slope k_2. These constants follow the Arrhenius relationship with cure temperature[1].

$$k_i = A_i e - \frac{E_i}{RT} \ldots\ldots (2.8)$$

i=1,2

In these models, the kinetic parameters were determined using least squares method without any constraints. Toward the end of the curing reaction, the reaction becomes diffusion controlled. In order to incorporate diffusion control, a semi empirical equation was used. When degree of cure reaches critical value α_c, diffusion becomes the dominant phenomenon, and rate constant k_d is given by:

$$k_d = K_c\, e - C(\alpha - \alpha_c) \ldots\ldots (2.9)$$

Where k_c is the rate constant for chemical kinetics and C is the diffusion coefficient. According to this equation, diffusion control begins when α becomes equal to α_c. But in actual conditions, the onset of diffusion control is a gradual process, and there is a certain curing stage where both chemical and diffusion factors are controlling the reaction. The overall effective rate constant k_e is given by:

$$\frac{1}{K_e} = \frac{1}{K_d} + \frac{1}{K_C} \ldots\ldots (2.10)$$

The diffusion factor f(α) is given by:

$$f(\alpha) = \frac{K_e}{K_c} = \frac{1}{1+\exp[C(\alpha-\alpha_c)]} \ldots\ldots (2.11)$$

The diffusion factor is the ratio of the experimental reaction rate to the reaction rate predicted by Kamal model. When α is much smaller than critical value ($\alpha << \alpha_c$), $f(\alpha)$ approximates unity, and the reaction is kinetically controlled, and diffusion effect is negligible. As α approaches α_c, $f(\alpha)$ begins to decrease and approaches zero as the reaction effectively stops. The effective reaction rate at any conversion is equal to the chemical reaction rate multiplied by $f(\alpha)$. The values of α_c and C are determined by the nonlinear regression analysis to $f(\alpha)$ versus α plot [1].

2.11.2 Kissinger Method (Dynamic Kinetic Model)

In the Kissinger method, the activation energy is obtained from the maximum reaction rate where d/dt (dα/dt) is zero under a constant heating rate condition.

$$\frac{d\left[\ln\left(\frac{q}{T^2p}\right)\right]}{d\left(\frac{1}{Tp}\right)} = -\frac{E}{R} \dots\dots (2.12)$$

where T_p is the maximum rate temperature, q is the constant heating rate, E is the activation energy, and R is the gas constant. A plot of $\ln(q/T_{p2})$ versus $1/T_p$ gives the activation energy without a specific assumption on the conversion-dependent function [1].

2.11.3 Flynn–Wall–Ozawa Method (Dynamic Kinetic Model)

In this method, it is assumed that the extent reaction is proportional to the heat generated during the reaction. The reaction rate is expressed as:

$$\frac{d\alpha}{dt} = K(T)f(\alpha) \dots\dots (2.13)$$

Where t is the time, k(T) is the Arrhenius rate constant, and $f(\alpha)$ is a function that depends on the reaction mechanism. The integrated form of the above equation is:

$$g(\alpha) = \int_0^{\infty} \frac{dx}{f(\alpha)} = k(T)t \dots\dots (2.14)$$

Where g(α) is the integrated form of the conversion dependent function. Flynn–Wall–Ozawa modified the equation for g(α) as:

$$\log(q) = \log\left[\frac{AE}{g(\alpha)R}\right] - 2.315 - \frac{0.457E}{RT} \ldots\ldots (2.15)$$

Where A is a pre-exponential factor, q is the heating rate, R is the universal gas constant, and T is the temperature. The activation energy (E) at different conversion can be calculated using this equation. The activation energy can be calculated from the: (slope = 0.457E / RT), obtained from a plot of log(q) versus 1/T. It is also assumed that the degree of cure is independent of heating rate once exothermic peak is reached [1].

2.12 Kinetic Analysis Using DSC

DSC is a convenient and simple-to-use tool for monitoring cure reaction since precise results were obtained with a small amount of sample in a relatively short time span. The basic assumption is that the heat evolution recorded by DSC is proportional to the extent of consumption of the functional groups, such as the epoxide groups in the epoxy resin or amine groups in the curing agent. DSC has two advantages: (i) it is the reaction rate method that permits to measure with great accuracy both the rate of reaction and degree of conversion, and (ii) the DSC cell may be considered as a mini-reactor without temperature gradient. Both isothermal and dynamic measurements can be used to follow the cure reaction. The dynamic measurements are fast compared to isothermal measurements. DSC kinetics provides heat flow and heat generation data required for the solution of the heat/mass transfer equation. The basic assumption for the

application of DSC technique to the cure of the epoxy resin is that the rate of reaction is proportional to the measured heat flow (ϕ) [1].

$$Rate\ of\ reaction, \frac{d\alpha}{dt} = \frac{\Phi}{\Delta H} \ldots\ldots (2.16)$$

Where ΔH is the enthalpy of curing reaction. The curing involves several reactions including primary and secondary amine attack on epoxy group, homopolymerization, etherification, and degradation. This makes the analysis of polymerization kinetics from dynamic DSC measurements difficult. But in isothermal mode, the overall process can be analyzed, and more information regarding the kinetics can be obtained. The isothermal measurements provide more reliable heat of reaction and kinetic parameters. The important parameters required for kinetic analysis are the total heat of the reaction ΔH_{tot} and the fractional cure degree α at time t. The ΔH_{tot} can be obtained from dynamic and isothermal methods in the following ways. (i) ΔH_{tot} was taken as the average of the enthalpy values obtained from the calorimetric measurements at different heating rates in dynamic mode. (ii) The sample is analyzed isothermally at a particular temperature, and after the measurement, the same sample was analyzed in dynamic mode for examining the completeness of the curing reaction. The sum of the heat of reaction obtained from isothermal measurement and the subsequent dynamic mode is taken as ΔH_{tot}. In order to calculate the cure degree (α) at time t, the heat of reaction at time t (ΔH_t) is required. The isothermal scan of the sample was done and the curve was integrated at different times from the area of the curve at a particular time, the heat of reaction at that time interval can be calculated. In another approach, the sample was cured isothermally and the curing reaction was quenched at

different time intervals. The dynamic DSC scan of the quenched samples gave the residual heat of reaction. The difference between the total heat of reaction and the residual heat will give the value of ΔH_{tot}, from these values the cure degree α at time t is calculated using the equation below [1]:

$$\alpha = \frac{\Delta HT - \Delta HR}{\Delta HT} \dots\dots (2.17)$$

Where ΔH_T equals the total enthalpy of reaction measured at a certain heating rate for an unreacted sample, and ΔH_R is the residual heat of the reaction.

2.12.1 DSC Analysis of curing Kinetic

The module applied here is Ozawa method according to the program of the device that were the test is applied , the general equation expressing reaction rate is as follow :

$$\frac{dx}{dt} = A.exp\left(-\frac{\Delta E}{RT}\right)(1-x)^n \dots\dots (2.18)$$

Where as :

dx/dt: Reaction rate.

A: Frequency factor.

ΔE: Kinetic energy.

1-x: Incomplete reaction percent.

R: Gas constant.

n: reaction order.

Now the temperature rises at the heating rate $\Phi = dT/dt$ the approximation calculations etc., based on the P function can be used to express equation as follow:

$$\log_{10} \emptyset = -0.4567 \frac{\Delta E}{R} \cdot \frac{1}{T} + const. \dots \dots (2.19)$$

Where T is peak temperature , in other words when peak temperature are performed with different heating rates and a plot is made of the invers of the peak temperature as horizontal axis and the common logarithm of the heating rate as the vertical axis Arrhenius plot and the equation 16 above will yield a straight line and the slope of line is expressed as follow :

$$slope = 0.4567 \frac{\Delta E}{R} \dots \dots (2.20)$$

Where R and T are known so that kinetic energy ΔE can be calculated from equation above. Using the determined kinetic energy reaction factor can be calculated from the following equation:

$$\frac{\emptyset \Delta E}{R\, T^2} - A\boldsymbol{exp}\left(-\frac{\boldsymbol{\Delta E}}{\boldsymbol{RT}}\right) \cong \mathbf{0} \dots \dots (2.21)$$

Further the reaction percent (1-C_m) at the beak apex becomes :

$$1 - C_m = \begin{cases} \frac{1}{e} & (n = 1) \\ n^{\frac{1}{1-n}} & (n \neq 1) \end{cases} \dots \dots (2.22)$$

Therefore if the area from the peak start point to the peak apex is taken as a ratio (C_m) with respect to the entire peak area reaction order n can be deduced. These calculation is preformed to the DSC kinetic analysis program is based on Ozawa method and as such the reaction parameters (kinetic energy, reaction rate, frequency factor) are calculated and followed by isothermal analysis (rate constant , reaction time) .

2.12.2 Isothermal analysis

This referees to the determination of reaction percent and time in the case of heating is performed at constant temperature. However since it is necessary to use parameters determined by kinetic analysis as mentioned above so that kinetic analysis must be conducted prior to the isothermal analysis, Rate constant K at fixed temperature T is expressed as :

$$K = A\ exp\left(-\frac{\Delta E}{R}\right) \ldots\ldots (2.23)$$

Where :

A:Frequency factor.

ΔE: kinetic energy.

R: Gas constsnt.

T: absolute temperature.

The equation can be solved using the parameters determined from the DSC kinetic analysis(kinetic energy ΔE , reaction order n , frequency factor A) further , K can be used to calculate the relationship between reaction percent (C) at fixed temperature and time t,

$$\frac{dC}{dt} = K(1-C)^n \dots\dots (2.24)$$

If this is integrated with respect to time , reaction time t becomes :

$$t = \frac{1}{k(n-1)}\{(1-C)^{1-n} - 1\} \qquad (n = 1) \dots\dots (2.25)$$

$$t = \frac{1}{k}\ln(1-C) \qquad (n \neq 1) \dots\dots (2.26)$$

2.13 Polystyrene (PS)

PS is the most employed aromatic thermoplastic polymer. PS finds a wide range of application from food contact packaging to thermal insulator in buildings. PS within polyolefins is a very interesting material to be pyrolyzed due to the absence of a well-established protocol for disposal of waste and/or contaminated PS and the presence of an aromatic ring which is very attractive as feedstock for several industrial processes. Polystyrene is employed for outside housing of computers, other electronic devices and it also is used in the form of foam for packaging and insulation [33].

It is a polymer made from the monomer styrene, a liquid hydrocarbon that is commercially manufactured from petroleum. At room temperature, PS is normally a solid thermoplastic but can be melted at higher temperature for molding or extrusion, then solidified. PS is clear, rigid, brittle and moderately strong. Its electrical properties as a dielectric material are good, though it has relatively low heat resistance. PS is soluble in most chlorinated and aromatic solvents, though not in alcohols. PS is considered to be the most durable thermoplastic polymer. It is used in a wide range of products due to its versatile properties. Polystyrene is characterized by the resistance to biodegradation, stiffness or flexibility

(with plasticizers), light weight, good optical ,chemical and insulation properties and facile synthesis. It is an inexpensive resin per unit weight. It is a poor barrier to oxygen and water vapor and has a relatively low melting point [34].

In chemical terms, PS is a long chain hydrocarbon wherein alternating carbon centers are attached to phenyl groups.

2.14 Grades of polystyrene

Different types of polystyrene are available in the market and all the various categories depend on end use requirement performances. The varieties include general purpose polystyrene (GPPS), high impact polystyrene (HIPS) and expandable polystyrene (EPS) [35].

2.14.1 General purpose Polystyrene (GPPS)

A tactic polystyrene is another alternative name for general-purpose polystyrene (GPPS). It is produced by simple thermal initiated radical bulk polymerization. It is further subdivided into two grades i.e. high performance grade and conventional grade. The excellent physical and processing properties make GPPS suitable for many applications as compared to any other plastics. It has glass transition temperature (Tg) of 100 ℃ which leads to limit its use in certain applications. GPPS is clear, hard and can be used in packaging, household items, and electronics [35].

2.14.2 High Impact polystyrene(HIPS)

HIPS a process of adding rubbers to rigid plastics in order to increase their fracture resistance was first used commercially in 1948, with polystyrene being the matrix. The early success of high impact polystyrene

led to the development of similar blends based on other rigid polymers, giving rise to the rubber toughened grades, which are now available for most commercial plastics and thermosets of any significance. HIPS is one of the well-known toughened polymers. The high toughness is given by the rubbery phase. (HIPS) is generally produced by the radical polymerization of styrene monomer with polybutadiene rubber. It is a thermoplastic polymer, which micro-structure is composed of an amorphous polystyrene matrix containing spheroid domains which are responsible for HIPS elastacity, elongation, craze plasticity and energy absorption. The thermal and oxidative degradation of this polymer is caused by double carbon-carbon bonds (C=C). HIPS has very good properties in comparison to common thermoplastics, such as the impact resistance, flexibility, low cost, shatterproof and easy process-ability. This material is commonly used for the production of toys, housewares, packaging, bottles light-duty industrial components and electronic appliances [35].

2.14.3 Expanded Polystyrene (EPS)

In the early 1940s, it took an accidental discovery to create a variant of polystyrene known as foamed polystyrene. Blowing gases into heated polystyrene produces foamed polystyrene. The result is a product that is over 95- percent air, making it a poor conductor of heat. The suspension process is a batch polymerization process that may be used to produce crystal, impact, or expandable polystyrene beads. EPS bead typically consists of high molecular weight crystal grade polystyrene (to produce the proper structure when the beads are expanded) with 5 to 8 percent being a low-boiling-point aliphatic hydrocarbon blowing agent dissolved

in the polymer bead. EPS is manufactured through 3 main stages namely Pre-expansion, Intermediate maturing and final moulding. At Pre-expansion stage, the raw material is heated in special machines called pre-expanders with steam at temperatures of between (80-100) °C. During pre-expansion, the raw materials compact beads turn into cellular plastic beads with small closed cells that hold air in their interior [35].

2.15 Applications of Epoxy Blends

The wide range of applications of epoxy resins has considerably increased during the last decades, since cured resins display outstanding properties as low shrinkage, adhesion to many substrates, good chemical and abrasion resistances, high mechanical strength, and high electrical resistance. Epoxy resins possess good properties and show excellent performance, but provide poor resistance to initiation and propagation of cracks, nevertheless, the toughness of these thermosets may be improved by incorporating thermoplastic components, by forming blends of the ductile thermoplastics with the thermosetting resins, which are widely used as matrices for high performance composites. Known examples are blends of epoxy resins with polysulfones, with polystyrene, and with poly(ether imides). The main requirements for the thermoplastic incorporation to the resin are: (i) the thermoplastic should initially dissolve in the liquid resin or, in its case, in the resin hardened mixture and (ii) it should form a separate phase during subsequent curing or it should be segregated in the course of polymerization leading to a randomly dispersed phase in the epoxy matrix. This mechanism is known as polymerization induced phase separation [36].

2.16 Literature Review

Shanyi Du, etal., 2004, studied the cure reaction of HD_{03} epoxy resin that followed an autocatalytic kinetic mechanism in the chemical controlled stage and can be described by the modified Kamal model. The parameters, which include cure rate constant k and reaction orders m and n, are determined by a nonlinear multiple regression method. In order to consider the diffusion control in the latter cure stage, a diffusion factor is introduced into the modified Kamal model. The combined equation of the modified Kamal model with a diffusion term is useful for describing the whole cure reaction of this resin. The critical degree of cure increases with increasing cure temperature [37].

N. L. D. Filho, etal., 2006, studied the cure kinetic of a hybrid epoxy resin, denominated octa[dimethylsiloxypropylglycidylether] octasiloxane (OG), in presence of 3,3-methylenedianiline (MDA) as hardener, was examined by DSC technique at various experimental conditions. The results of heat of polymerization and activation energy obtained by DSC technique show the same profile with respect to OG content, in the sense that they exhibit maxima around 70 wt% OG ($\varphi \approx 0.50$). Dynamic mechanical analysis suggests that the maximum cross-link density is obtained at 83 wt% OG ($\varphi = 1$, components are mixed at stoichiometric amount), whereas fracture toughness and tensile modulus mechanical properties are maximized at 70 wt% OG ($\varphi \approx 0.50$). Thus, this formulation of $\varphi \approx 0.50$ containing excess of amine, is not the composition where the highest crosslinked density is reached for the OG/MDA composites [38].

K. P. Unnikrishnan, etal., 2006, used 10–15 phr of rubber that was necessary to generate toughness properties in epoxy systems. In an initially miscible blend, curing may cause phase separation curing reaction and phase separation are competitive chemical toughening leads to an increase in mechanical and thermal properties due to the formation of strong covalent bonds whereas physical blending produces only marginal toughening effect. Toughening of epoxies by particulates improves the modulus of the cured system which is uncommon in elastomer toughening. With the advent of new telechelic liquid rubbers with reactive terminal functional groups, the technology of toughened epoxies assumes new dimensions and it will be interesting to look ahead for developments in this field in the years to come [39].

X. Luo , etal. , 2009, studied the phase-separated blend of epoxy and poly(-caprolactone) (PCL) which was initially miscible and contained 15.5 wt.% PCL, experiences phase separation due to polymerization when the epoxy is cross-linked. This results in a morphology akin to bricks and mortar, where the PCL matrix percolates through the epoxy phase, forming interconnected spheres known as bricks. After fully cured, the material is robust, hard, and long-lasting. The spontaneous wetting of all free surfaces by the molten PCL phase was seen as a heating-induced bleeding behaviour. This bleeding is capable of mending damage through crackwicking and subsequent recrystallization with very slight concurrent softening during that process which is caused by the volumetric thermal expansion of PCL over its melting temperature above the expansion of epoxy bricks. In carefully regulated thermal-mending tests, heating a fractured sample caused PCL to extrude from the bulk, producing a liquid

layer that filled the crack. A "scar" made of PCL crystals developed at the crack site as it cooled, restoring a sizable amount of the mechanical strength. Thermal-mending efficiency topped 100% when a moderate force was used to aid in crack closing [40].

Hussein Ali Shnawa, etal., 2009, studied the use of tannins and natural polyphenols as sustainable and biodegradable fillers in epoxy composites. Utilizing the differential scanning calorimetry (DSC) technology, it was determined how adding tannins affected the thermal and curing characteristics of epoxy-tannin composites. A single exothermic peak caused by crosslinking processes was seen in the temperature range of 85℃ - 155℃ and distinguished composites comprising 5, 20, and 40% of tannins. The curing of the composites was discovered to behave in the same way as unmodified epoxy, proving that the tannins do not impede the curing reactions. The kinetics demonstrate that the activation energy of the curing operations of epoxy-tannin composites was determined to be in the range of 48–56 $kJ.mol^{-1}$. The same temperature range as the neat epoxy resin might be used to cure the epoxy-tannin composites. $T_{onset's}$ curing properties did not significantly increase or decrease, however T_p and T_{endset} can be seen. The epoxy-tannin composites' glass transition temperature and cure enthalpy were lower than for neat epoxy according to the kinetic parameters, tannins have little effect on epoxy resin's reactivity [41].

Gulnare Ahmetli, etal., 2011, investigated how the structure and quantity of polymer affected the physico-mechanical and thermal properties of epoxy, Fatty acid waste was recycled as a raw material and used to create polymers with epoxy or unsaturated ester groups. Styrene and cationic acid were also used in the radicalic polymerization process by

esterifying reaction with epichlorohydrin, styrene-itaconic acid copolymer glycidyl ester was produced. Diglycidyl ether of bisphenol A type commercial epoxy resin was mixed with the polymers to create composites. Over the pure epoxy matrix, the elastic modulus of the composites reinforced with bio-based polymers increased by around 74.55-243%. Composites made of styrene-based polymers have higher obtained Young's modulus values. Comparing all composites to a pure epoxy matrix, they all exhibit superior elongation at break and tensile strength. Hardness also significantly improved as a result of the integration of the various polymers. The elongation at break values for composites with OEE in the tensile test were the best composites containing HP are characterized by greater hardness and heat resistance [42].

N. Abdulrazack, etal., 2014, studied the mechanical characterization, thermogravimetric analysis (TGA), and differential scanning calorimetry (DSC) tests used to compare the two methods of curing diglycidyl ether of bisphenol A (DGEBA), a low molecular weight epoxy resin, utilising both aliphatic and aromatic hardeners. Two aliphatic and two aromatic hardeners were used in stoichiometric amounts in this experiment. These consist of diaminodiphenyl sulfone (DDS), dicyandiamide (DICY), m-phenylenediamine (mPDA), and triethylene tetramine (TETA). The shear and peel strength tests conducted as part of the mechanical characterisation indicate that aromatic compounds outperform aliphatic compounds. Comparing the behaviours of aromatic and aliphatic amines was another goal of the experiment. The DSC studies and mechanical characterization results show that the system's

effectiveness varies in the following order: mPDA > DDS > DICY > TETA [30].

M. Pramanik, etal., 2014, studied the degree and strength of the epoxy-cross-linker curing reactions had a major impact on any epoxy system's performance adverse effects such as etherification may occur during the curing process of an epoxy pre-polymer containing an amine functional group. Commercial amines were used to cure commercial epoxy pre-polymers at low and high temperatures even after post-curing at 200°C, observed only epoxy-amine interactions using epoxides based on diglycidyl ether of bisphenol-A (DGEBA) it was discovered that epoxides with a tertiary amine moiety undergo the side reaction of etherification at a cure temperature of 200°C [43].

S. K. Sardiwal, etal., 2014, used the unaltered epoxy-polymer's fracture energy that was 495 J/m^2, but the maximum strain-energy release rate during a fatigue cycle that had a threshold value of 155 J/m^2, below which significant crack propagation did not occur. The values of Gth and GIc increased to around 445 J/m^2 and 2475 J/m^2 for these PU-based epoxy polymers, respectively according to the methods of toughening brought about by the inclusion of the polymer-blend modifier, a multiphase was necessary to generate suitably high values of GIc and Gth in the epoxy-blend polymer. This resulted from the second-phase particles' major mechanism of energy loss and toughening—the plastic deformation of the epoxy-matrix phase this degree of ductility exhibited by this phase of the epoxy-blend polymer is clearly related to the amount of energy dissipated during the plastic deformation of the epoxy-matrix phase [44].

H. Ma, etal., 2016, looked at the chemical makeup and molecular weight of an epoxy resin toughening agent after presenting a production method for the substance. The results of the tests show that this toughening agent can create a tiny two-phase structure in the epoxy-amine system, which results in stable chemical properties and outstanding physical properties. EP E54 and the synthetic toughening agent work well together. Under the right circumstances, the epoxy resin E54 system can be fully cured. Since the curing heat peaks at a heating rate of 11 ℃/min, it is important to choose the right heating rate. The amount of the toughening agent has a significant impact on the bonding strength of the epoxy resin system when the curing agent and epoxy resin ratio are fixed [45].

D. A. Lakho, etal., 2016, used differential scanning calorimetry (DSC) to in-situ cure multiple formulations of commercially available diglycidylether epoxy resin using both isothermal and non-isothermal modes. The system's long aliphatic chain diluent often lowers the formulation's glass transition temperature, which in turn reduced the cure rate by reducing the sample's viscosity. Imidazole could be added to the mixture to account for the cure rate as well as the glass transition, during the curing process, the Lewis base activity of imidazole and an anionic chain-growth reaction mechanism cause the crosslinking density and in turn the glass transition temperature to rise. The curing agent, imidazole, diluent, and epoxy are combined to allow for design freedom in changing the behaviour of the resin during the curing process. It takes less than five minutes for the sample to reach at least a 97% degree of cure when the resin is put into a heated mould maintained at 100℃ [46].

B. B. Johnsen, etal., 2017, displayed the toughness of cured epoxy was greatly increased by the addition of modest amounts of the semi-crystalline thermoplastic sPS. There was spherical particle presence of the sPS phase and plastic void formation in the epoxy matrix. Blends undergoing phase-separation caused by crystallisation have the sPS phase as spherulites with a thin fibrillar substructure. The primary micromechanisms for toughening in this instance are fracture deflection and bifurcation when used in very tiny quantities, the semi-crystalline thermoplastic sPS can greatly increase the toughness of cured epoxy. The sPS/epoxy mixtures' toughness is greatly increased by the RIPS microstructure. The plastic gaps formed in the epoxy matrix by the simple debonding of sPS particles are responsible for the notable increase in toughness. The sPS phase is present in the mixes as spherulites with a thin fibrillar substructure [47].

H. Li, etal., 2018, used dynamic mechanical analysis and FTIR to investigate the average molecular weight and integrity of the cross-linked network structure in PUE thermosets, as well as how the stoichiometric ratio of active hydrogen to the epoxy group affects the cross-linked network structure and cryogenic properties of a polyurethane modified epoxy resin. The results show that increasing the [H]/[E] stoichiometric ratio from 0.7 to 1.3 can reduce the Mc of PUE thermosets cured at low temperature at 77 K, the thermosets' tensile strength increases to about 105 MPa as the [H]/[E] stoichiometric ratio becomes closer to 1.3 to get the greatest mechanical properties for these PUE thermosets that have been cured at low temperatures, an adequately high amount of curing agent is needed [13].

E. O. Ozgul, etal., 2018, used three distinct epoxy resins were mixed with three distinct reactive diluents based on glycidylether. The combinations of six different amine-based hardeners consisted of two cycloaliphatic and four aliphatic hardeners. The creation of dangling ends was probably the reason why the monofunctional diluent drastically decreased the strengths of the combinations with both TETA and MXDA. The strength of the tertiary amine (TDMAP) hardener was enhanced as a result of the favourable contribution of DGEBF's mobility to the polymerization reaction. All hardeners used in epoxy mortars had higher flexural strengths when diluents were added; this could be because the wetting properties improved. The strongest adhesion strength was achieved with an MXDA hardener for a DGEBA resin, most likely as a result of the methyl joints in this hardener's molecular structure, which allowed for greater mobility than in the other hardeners examined [48].

B. Massoumi, etal., 2019, used a small addition of O-MMT and curing the mixture with PSt that had its amines altered had a synergistic effect on the thermal stability of the ENR resin. The generated nanocomposite in this study has an exfoliated structure, and the silicate layers are distributed randomly inside the matrix according to a TGA investigation. Because of its exceptional thermal stability and cheap manufacturing cost, the new resin nanocomposite is expected to find application in a variety of industrial areas, such as building and commodities, coatings, composite matrices, and electronics [49].

M. Michel and E. Ferrier, etal., 2019, explained the relationship between four common epoxy polymers (Liquid bisphenol-A based epoxy

resin hardener based on aliphatic polyamines[1], two-component epoxy resin without solvent nor MDA[2], epoxy-based solution without solvent amine hardener[3] and Liquid bisphenol-A based epoxy resin Polyetheramine based hardener[4]) and time, curing, and temperature, in the summer the Tg values of every polymer under investigation rose with higher temperatures; however, the Tg values remained unchanged when the polymer was exposed to a lower temperature by raising the temperature following a low curing temperature: this initiates the epoxy's crosslinking process and raises the Tg value until the thermal energy reaches a level that facilitates ideal curing and keeps the Tg value constant. At temperatures of 5 ℃and 10 ℃, the minimum curing time needed is more than two weeks, whereas at temperatures of 20 ℃ and 40 ℃, it is less than one week [50].

L. Liu, etal., 2019, used liquid bisphenol A epoxy resin that may be used at room temperature and had a variety of toughness and curing agents. When comparing the energy per unit area combined with the tensile test, bending strength, compressive strength, and steel-steel tensile shear strength, the 10% amount of A2364 toughened and polyamide A350A curing agent demonstrated the highest performance in the various tests. Shear strength is 23.2 MPa, bending strength is 96.9 MPa, and Tg is 74.6 °C. The characteristic temperature of the epoxy strengthening system is determined using DSC. The kinetic equation of the toughened epoxy curing system is found, providing theoretical support for practical implementation. The appropriate addition volume for a number of curing agents is first determined by Tg. The addition of 10% A2364 toughened to these greatly improves the mechanical characteristics [51].

Xingming Bian, etal., 2019, studied the boron nitride-epoxy hybrid system was strengthened by using carboxyl-terminated butadiene nitrile liquid rubber (CTBN). Different CTBN contents were examined for their effects on the composites' mechanical properties, dielectric properties, thermal conductivity, glass transition temperature, and thermal stability. Comparing the composite to pure epoxy resin, the toughness improved by about 32%, the breakdown strength by about 15%, and the heat conductivity increased by about 15%. The dielectric constant and dielectric loss rose while the thermal stability and glass transition temperature of the composite dropped as the CTBN content increased. An better all-around toughened epoxy composite material is produced with a 10-15 weight percent CTBN component. The tensile strength of the 15 wt.% CTBN composite was barely affected, although the impact strength and elongation at break both rose by about 32 %. The addition of CTBN to the epoxy resin decreased the composite's crosslink density, glass transition temperature, and thermal stability. In the composite with the maximum thermal conductivity roughly 173% higher than that of pure epoxy resin five wt.% of CTBN was included when CTBN was added, the composite's dielectric constant increased due to the effects of dielectric relaxation, and a peak appeared in the dielectric loss curve [52].

Subhi A. Al –Bayaty, etal., 2020, investigated the kinetics of epoxy deterioration when combined with 10, 15, or 20 weight ratios of polystyrene powder to create epoxy composites. The experiment involved heating at a rate of 10 ℃/min all experiments were carried out in an oxidising air environment, with the exception of one test that looked into the impacts of a non-oxidative process using nitrogen. The kinetics result

was obtained for the statistical investigations using MINITAB 16. The TGA profiles showed signs of three different stages of degradation but there are two peaks seen in the DSC profile. The resilience of composites was enhanced by every study conclusion about the impact of polystyrene powder content on epoxy breakdown [56].

U. Farooq, etal., 2020, studied the state-of-the-art for creating IPN structures that toughen epoxy matrix systems utilising thermosets or thermoplastics. Better mechanical qualities (such as fracture toughness) are often obtained by this way of modifying the epoxy system. In theory, IPNs provide a synergistic blend of the advantageous qualities of two distinct polymers: thermosets offer high service temperatures, while toughened polymers offer greater toughness. Creating an interpenetrating polymer network (IPN) by mixing brittle epoxy with thermoplastic or thermoset materials is the most alluring method to increase the fracture toughness of the modified system. The formation of the IPN structure suggests that the fracture toughness of epoxy resin consistently increases with a rise in toughened content. Impact and tensile strength frequently show a diminishing tendency beyond a particular hardened concentration. The branching and structure of the thermosetting toughened epoxy can be experimented with to counteract this drop in the impact strength of the epoxy system [54].

V. E., etal., 2021, studied the toughening effects of in situ polytriazoleketone and polytriazolesulfone toughening agents were evaluated when employed with a range of epoxy resins, including diglycidyl ethers of bisphenol A (DGEBA), bisphenol F (DGEBF), and triglycidyl p-aminophenol (TGAP). PTK increased the fracture toughness

by 27% and the tensile strength by 8.6% in comparison to DGEBF that had not been hardened. The fracture toughness rose by 51% when PTS was applied to TGAP as opposed to TGAP that had not been toughened. DGEBF's tensile properties improved with the addition of polytriazoleketone, boosting its fracture toughness by 27%. When polytriazolesulfone was added to TGAP, its fracture toughness increased by 51% while its tensile strength and tensile modulus remained unaltered [55].

2.17 Summary of Literature Review

The review of the literature looks at several researchers that have investigated the kinetic curing of epoxy under various settings from different curing agents to different fillers and different technique of curing process using various experiments to characterize the kinetic parameter of epoxy and their effects on epoxy's qualities. Investigated how different conditions of curing process and filler content as toughening materials affected the characteristics and parameters of cure kinetics of epoxy and its blends.

.

Chapter Three
Experimental Part

3.1 Introduction

Epoxy resins can be designed with a cross-linked network structure by varying the hardener's content in addition to the epoxy and hardener's chemical compositions. The experimental work is explained in this chapter, with special attention to the material selection, qualities, sample preparation methods, and testing procedures. Along with directions for preparing materials and samples and an explanation of the test equipment used, it provides a comprehensive examination of the experimental methods. This chapter describes the qualities of the materials utilised, as well as the experimental methods used to manufacture and assess epoxy resin samples with different hardener formulations and curing temperatures.

Thermoplastic polystyrene was used as toughened material with varying contents (2.5 wt.%, 5 wt.%, and 7.5 wt.%) with epoxy resin at various formulations of EP/h (1:0.5, 2.5:1.5, 1:1 and 1.5:1). DSC analysis, TGA analysis, FTIR, and mechanical properties (tensile strength, elastic modulus, elongation at break, hardness, impact strength, and fracture toughness) structural properties were used to explore the kinetics of epoxy resin and its blends while SEM morphology tests were carried out. Utilising a mechanical stirrer, mixes were created and then poured into moulds to form plates that were prepared for testing and CNC cutting into different forms. The following chart represents the work:

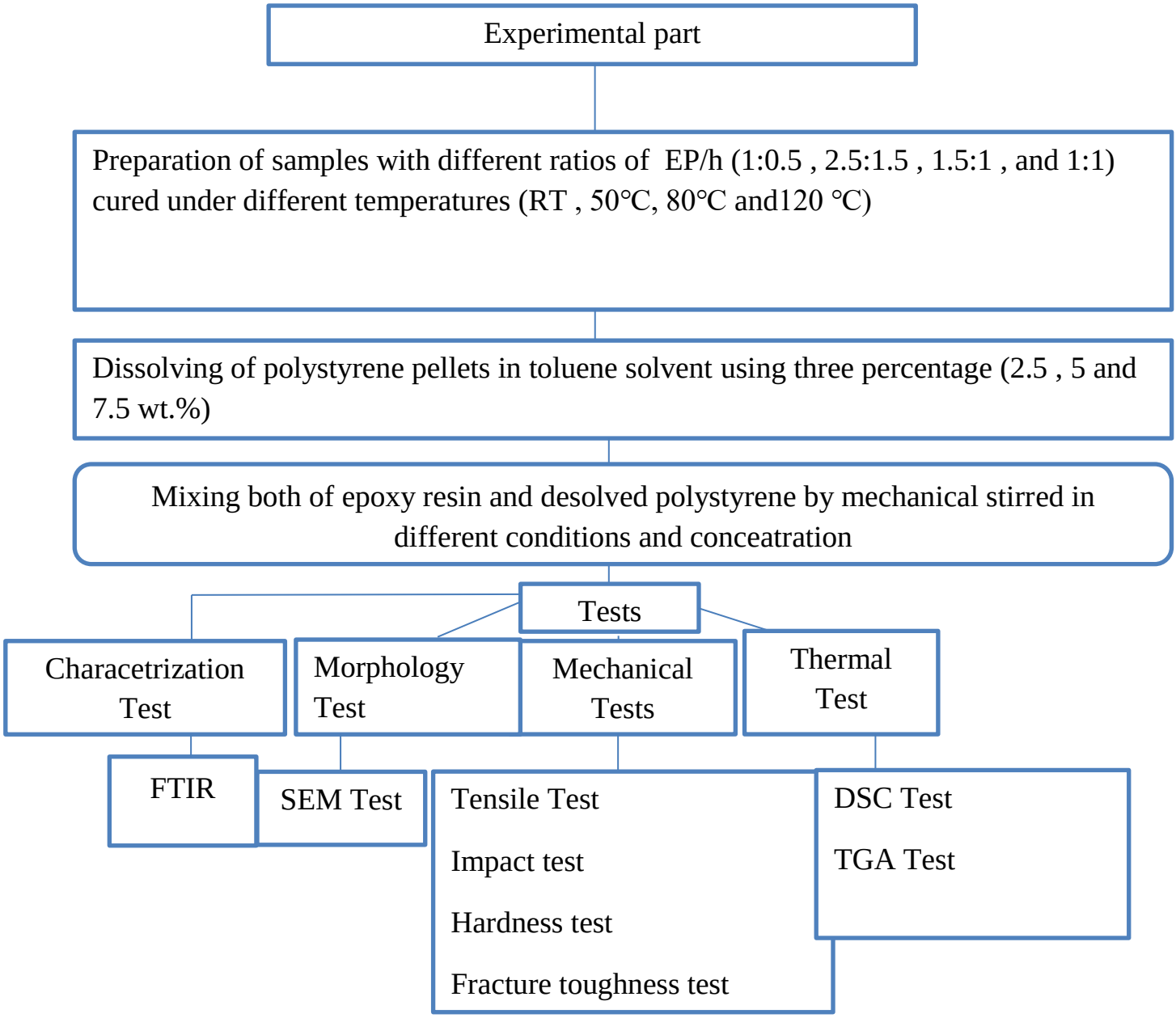
Experimental part
Preparation of samples with different ratios of EP/h (1:0.5 , 2.5:1.5 , 1.5:1 , and 1:1) cured under different temperatures (RT , 50℃, 80℃ and120 ℃)
Dissolving of polystyrene pellets in toluene solvent using three percentage (2.5 , 5 and 7.5 wt.%)
Mixing both of epoxy resin and desolved polystyrene by mechanical stirred in different conditions and conceatration
Tests
Characetrization Test
Morphology Test
Mechanical Tests
Thermal Test
FTIR
SEM Test
Tensile Test
Impact test
Hardness test
Fracture toughness test
DSC Test
TGA Test

3.2Materials Used

3.2.1 Epoxy Resin

Resin type of Sikadur®-52 LP Bisphenol A (epichlorohydrin) oxiran, mono(C-12-14 alkyloxy) methyl derives, is a two part, solvent free, low viscosity injection liquids, based on high strength epoxy resins was used.

3.2.1.1 Characteristics / Advantages of Epoxy Resin

- Solvent free
- Suitable for both dry and damp conditions
- Shrinkage free hardening
- High mechanical and adhesive strengths
- Hard but not brittle
- Low viscosity
- Injectable with single component pumps.

Table (3-1) :Properties of Epoxy Resin [56].

Property	Data
Mixing Ratio	A : B = 2 : 1 parts by weight and by volume
Color	Part A Transparent Part B Brownish Part A+B Yellowish-brownish
Density	+20 °C Part A+B mixed (2:1) ~1.06 kg/l
Viscosity	Temperature Part A+B mixed (2:1) +10 °C +20 °C ~330 MPa +30 °C ~150 MPa

	+40 °C ~95 MPa
Compressive Strength	≥70 N/mm^2 (7 d / 30 °C) (ASTM D695)
Tensile Strength	~27 N/mm^2 (7 d / 30 °C) (ISO 527)
Tensile Adhesion Strength	Curing time Curing temperature 25 °C 2 days ≥7 N/mm^2 14 days ≥10 N/mm^2 (ASTM C882)
Pot Life	Temperature 1 kg mixture +5 °C - +10 °C - +23 °C ~70 min +30 °C ~30 min +40 °C ~10 min The pot life begins when the resin and hardener are mixed. It is shorter at high temperatures and longer at low temperatures. The greater the quantity mixed, the shorter the pot life. To obtain longer workability at high temperatures, the mixed injection resin may be divided into portions. Another method is to chill components A+B before mixing them (not below +5 °C).

3.2.2 The hardener

3-aminomethyl-3,5,5-trimethylcyclohexylamine3,6-dizaoctanethylene diamine was used as a hardener.

Table (3-2): Properties of the Hardener [57].

Property	Data
Melting point	45.5°C
Boiling point	301.29 °C (rough estimate)
Density	0.9690 g/cm^3
vapor pressure	8.9 Pa at 20 ℃
refractive index	1.4904
Water Solubility	528.1g/L at 20 ℃
Molecular Weight	171.28 g/mol

3.2.3 Polystyrene(PS)

Type of API 390 polystyrene was used as toughened material is a general purpose polystyrene produced in pellet form for injection molding. API 390 has excellent clarity and easy flow. It used in the manufacture of cosmetic containers, housewares, toys, and medical applications. Information provided by American Polymers, Inc company.

Table (3-3) : Properties of polystyrene [58].

Physical Properties	**Metric**	**English**	**Comments**
Density	1.05 g/cc	0.0379 Ib/in^3	ASTMD792
Melt flow	8.0 g/10min	8.0 g/10min	ConditionG; ASTMD1238
Mechanical properties	Metric	English	Comments
Hardness , Rockwell L	**74**	**74**	**ASTM D785**
Tensile strength, ultimate	**43.4 MPa**	**6300psi**	**ASTM D638**

Elongation at break	**1.0%**	**1.0%**	**ASTM D638**
Tensile modulus	**2.88 GPa**	**417 ksi**	**ASTM D638**
Izod impact, notched	**0.16 J/cm**	**0.33 ft-Ib/in**	**Injection molded sample, ASTM D256**
Thermal Properties	Metric	English	Comments
Deflection temperature at 1.8 MPa	**87.8 °C**	**190 °F**	**Annealed, ASTM D648**
Vicat softening point	**98.3 °C**	**209 °F**	**ASTM D1525**

3.2.4 Silane Coupling Agent

3-(Trimethoxysilyl)propyl methacrylate 98% Silane A174, [3-(Methacryloyloxy)propyl] Trimethoxysilane was used as coupling agent to create connection between resin and polystyrene, Linear Formula: $H_2C=C(CH_3)CO_2(CH_2)_3Si(OCH_3)_3$ with Molecular Weight: 248.35g/mol, Used in dental materials and adhesives and adhesives with primer systems; Used to make organosiloxane copolymers, prosthetics, and contact lenses; Also used as coupling agent (Room Temperature-Cured Polymers, Resin-glass, Resin-Metal, and Resin-Resin Bonds) and silylating agent for plastic surfaces.

3.2.5 Toluene

Toluene was used as solvent for polystyrene pellets with formula ($C_6H_5CH_3$, toluene sulphure free) was obtained from Thomas Baker Chemicals, India. The chemical composition with some properties as obtained.

Table (3-4) : Properties of Toluene [59].

Property	Data
Chemical composition	$C_6H_5CH_3$
Molecular weight	92.14 g/mol
Minimum assay	99.0 %
Maximum limits of impurities : Water	0.04 %
Maximum limits of impurities : Sulphur compound (C S_2)	0.0005 %
Maximum limits of impurities : Non-volatile matter	0.02

3.3 Preparation of Unmodified Epoxy Samples

The resin was mixed with hardener (in formulations of 1:0.5 EP/h, 2.5:1.5 EP/h, 1.5:1 EP/h and 1:1 EP/h) by using mechanical stirrer at 500 rpm for 15-30 minutes. The mixture was put under vacuum at room temperature for 10-15 minutes to eliminate bubbles using of vacuum oven. Then the mixture was put it into the mold which was previously prepared, then left it for 24 hours at room temperature for curing process to happened.

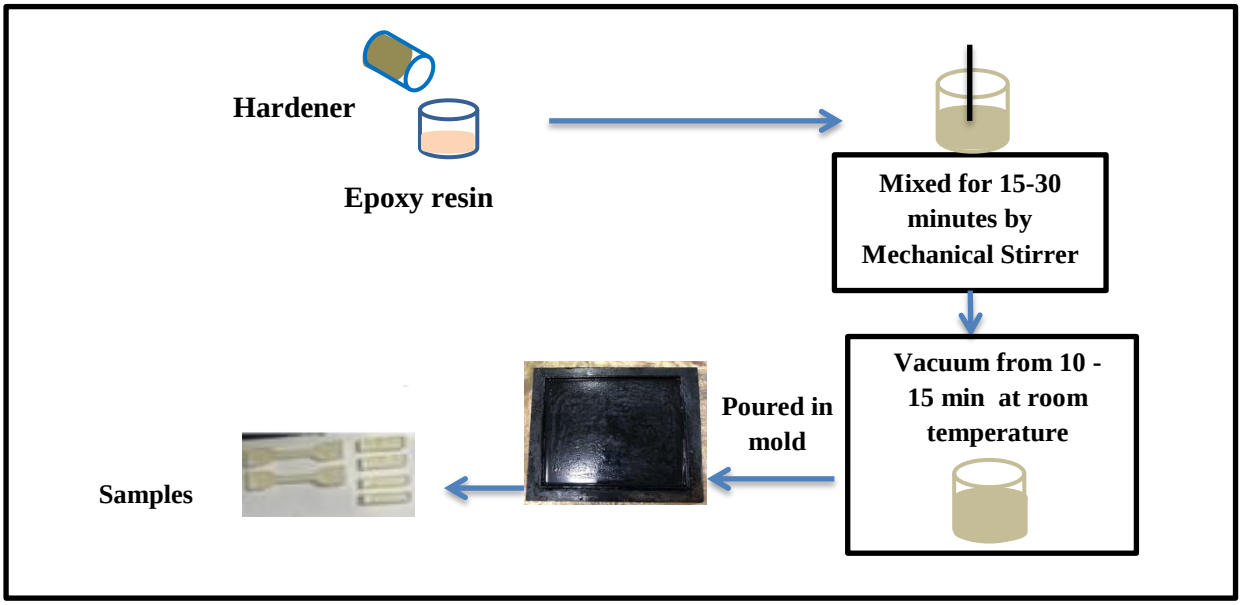

Figure (3.1) : Procedure of preparing unmodified epoxy samples

3.4 Solvent Selection:

The usual problem of polymer engineering is a selection of proper solvent for a given polymer[46].

This selection implies that the solvent must form with polymer a thermodynamically stable mixture in the whole range of concentrations and temperatures. Such choice is facilitated by use of numerical criterion of a solvent power. Solvent power might be taken from the thermodynamic treatment (for example, a change of Gibbs free energy or chemical potentials of mixing of polymer with solvent), but these criteria depend not only on the solvent properties but also on polymer structure and its concentration. Therefore, various approaches were proposed to estimate the solvent power, such as Kauri-butanol value (KB), dilution ratio (DR), aniline point (AP) and solubility parameter (δ).

The dissolution of polymer is determined by chain flexibility. The mechanism of dissolution consists of separating chains from each other and their transfer into solution. If a chain is flexible, its segments can be

separated without a large expenditure of energy. Thus functional groups in polymer chain may interact with solvent molecules. Thermal movement facilitates swelling of polymers with flexible chains. The flexible chain separated from an adjacent chain penetrates easily into solvent and the diffusion occurs at the expense of sequential transition of links. The rigid chains cannot move gradually because separation of two rigid chains requires large energy. Crystalline polymers dissolve usually less readily than amorphous polymers. Dissolution of crystalline polymers requires large expenditures of energy for chain separation.

The presence of even a small amount of crosslinks hinders chain separation and polymer diffusion into solution. Solvent can penetrate into polymer and cause swelling. The swelling degree depends on crosslink density and compatibility of polymer and solvent. The higher the melting temperature of the polymer, the worse its solubility. Substances having higher melting heat are less soluble, with other characteristics being equal. The solubility parameter (δ) is a function of the cohesive energy density (CED)[47].

A low molar mass compound can be described by the three parameter values, δ_D, δ_P, and δ_H, while the polymer is described not only by these three values but also by a parameter called interaction radius, R_0, which is the radius of the "solubility sphere" in the " $2\delta_D$ - δ_P - δ_H " space. In this space, the three parameters determine a center of a sphere, which has the R_0 as its radius.

Also in this space, a low molar mass compound can be positioned as a dot based on its parameters, and if the compound is within the space limited by the "solubility sphere", it is a solvent for the polymer, and vice versa.

The distance between the center of the "solubility sphere" and the position the compound belongs to is expressed as below:

$$D_{S-P} = \sqrt{(2\delta_{D,P} - 2\delta_{D,S})^2 + (\delta_{P,P} - \delta_{P,S})^2 + (\delta_{H,P} - \delta_{H,S})^2} \quad \ldots\ldots(3.1)$$

Where: S = solvent, P refers to polymer.

Usually, the ratio DS-P/R0 is used as the criterion:

$D_{S\text{-}P}/R_0 > 1 \rightarrow$ the compound is a non-solvent;

$D_{S\text{-}P}/R_0 < 1 \rightarrow$ the compound is a solvent;

$D_{S\text{-}P}/R_0 = 0 \rightarrow$ the compound may cause swelling[].

3.5 Preparation of Polystyrene Solution

- Weighing (6.25 g, 12.5 g and 18.75 g)of polystyrene pellets.
- Dried pellets in an oven at 100 ℃ for one hour to get rid of any existing moisture.
- Put the pellets in beaker with 50 ml of toluene.
- Put the beaker on magnetic stirr with heat up to 70℃ to ensure complete solubility of pellets degree with speed at 5 degree until the pellets soluble.
- Keep the beaker to cooled at room temperature.

3.6 Preparation of An Epoxy Polystyrene Blends

- Weighing of epoxy resin in desired formaulations(1:0.5, 1:1, 1.5:1 and 2.5:1.5).
- Mixing soluble polystyrene to epoxy resin with addition of silane coupling agent in rang og 1ml to ensure good consistency between resin and polystyrene solution for one hour by mechanical stirrer to get good mixing between compounds.
- After that added the hardener to the mixture with mixing by mechanical stir for 30 min.
- The mixture was put under vacuum at room temperature for 10 minutes to eliminate bubbles.
- The mixture after that poured in mold that was prepared then left it for 24 hours for curing process to take place at room temperature.
- These procedures was repeated for all samples with different formulations resin to hardener of blends as shown:
    a) (1:0.5) EP/h + 2.5 wt.% PS, (1:0.5) EP/h + 5 wt.% PS, (1:0.5) EP/h + 7.5 wt.% PS).
    b) (1:1) EPh +2.5 wt.% PS, (1:1) EP/h +5 wt.% PS, (1:1) EP/h + 7.5 wt.% PS).
    c) (1.5:1) EP/h +2.5 wt.% PS, (1.5:1) EP/h + 5 wt.% PS, (1.5:1) EP/h + 7.5 wt.% PS).

d) (2.5:1.5) EP/h + 2.5 wt.% PS, (2.5:1.5)EP/h + 5 wt.% PS, (2.5:1.5) EP/h + 7.5 wt.% PS).

- First all formulations of EP/h and EP/h/PS was prepared with curing at room temperature(RT) for 24 hours' time of curing.
- Second the formulations of EP/h and EP/h/PS was prepared by the same procedure above at different curing temperatures (50 ℃ , 80 ℃ , 120 ℃) for curing time at 4 hour for curing process in an oven after the time set up finished leave until cooled then removed from the oven and mold prepared for cutting by using CNC machine .

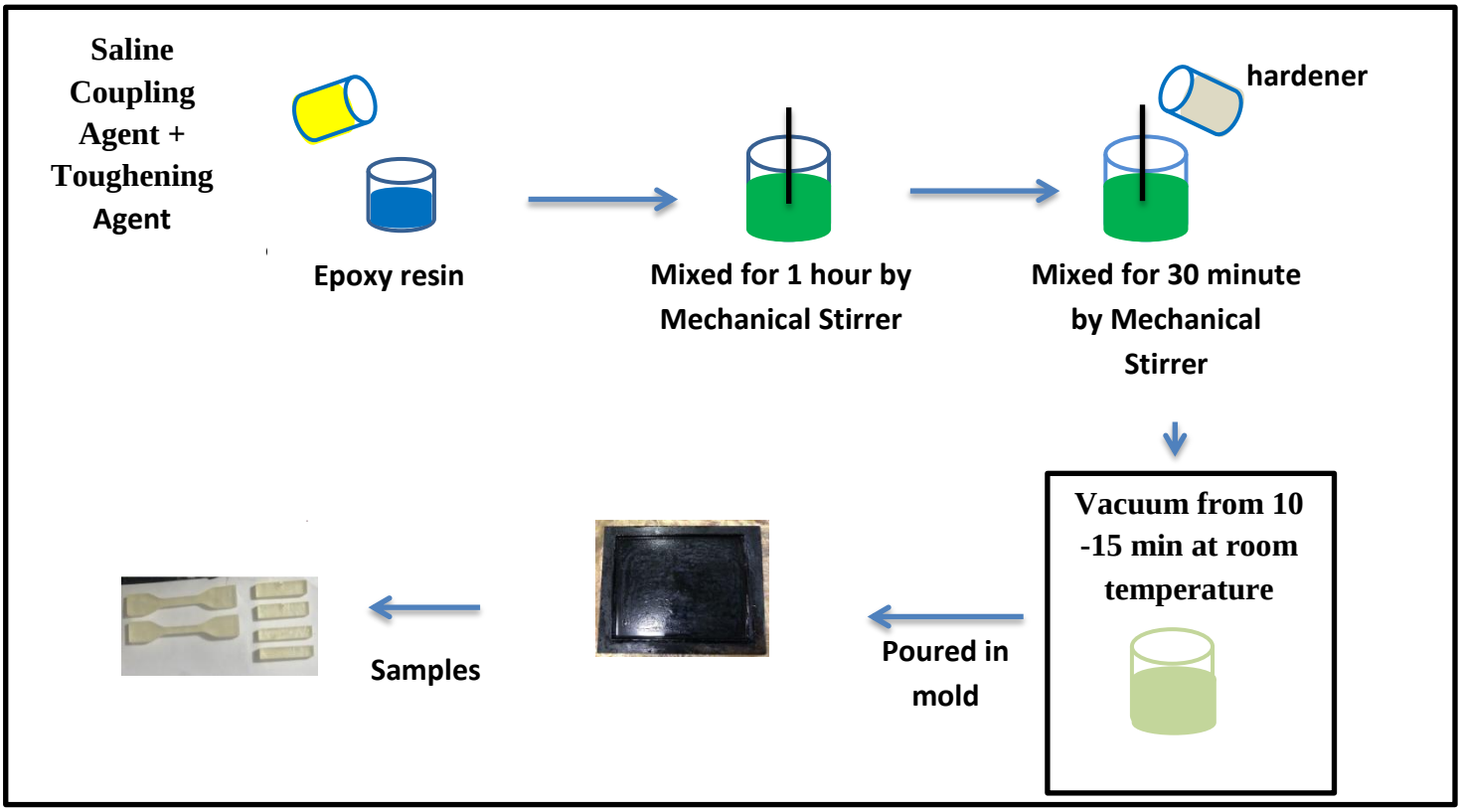

Figure (3.2): Procedure of preparing modified epoxy blends.

3.7 Thermal Tests

3.7.1 Differential Scanning Calorimetry Test (DSC)

Differential scanning calorimetry measurements (DSC) were carried out according to ASTM D3418-03 under nitrogen gas atmosphere. DSC techniques are used to study the thermal transition behavior of a polymer. A sum of basic physical changes in a polymer are carried out when a polymer is heated, which can be measured via DSC, these involve: (T_m), (T_g), (T_c), and (T_d). Also, chemical changes due to polymerization and degradation reactions, and other reactions affecting the specimen can be estimated. The prepared samples with weight in (mg) were mounted in aluminum pans and heated were evaluated in powder form and a heating rate of 10°C/min using the SH1MADZ-4 DSC-60 apparatus, Pure epoxy and epoxy/polystyrene blends. The test was being done in laboratory of Babylon University/ Collage of Materials Engineering /Department of polymer and petrochemicals industries [62].

3.7.2 Thermal Gravimetric Analysis (TGA)

(TGA) measure weight change (loss or gain) and the rate of weight change as a function of temperature, time, and atmosphere. Thermogravimetric data is critical to setting proper temperature limits for Differential Scanning Calorimetry method development. Other common usages include thermal and oxidative stability of materials, moisture and volatile contents, composition of multi-component materials, decomposition kinetics and estimated lifetime of a product by instrument type SDT Q600 V20.9 Build 20 with Method: Dual Ramp.

TGA measures the amount and rate (velocity) of change in the mass of a sample as a function of temperature or time in a controlled atmosphere. The measurements are used primarily to determine the thermal and/or oxidative stabilities of materials as well as their compositional properties. The technique can analyze materials that exhibit either mass loss or gain due to decomposition, oxidation or loss of volatiles (such as moisture).

3.8 Characteristic Test

3.8.1 Infrared Fourier Transform Spectrometer Test (FTIR)

The test of FTIR was used to obtain specific information about the chemical bonds and molecular structure of epoxy system samples. The (FTIR) test is performed according to (ASTM E1252) by using FTIR instrument type IR Affinity-1 (made in Japan) [63]. It is available in the laboratory of the Materials Engineering Faculty/Polymer Engineering and Petrochemicals Industries Department/ University of Babylon. It is supplied with a DTGS detector that operates at ambient temperature and a KBr beam splitter. The infrared spectrum was used within a range of (400–4000)cm^{-1}. FTIR was performed on a spectrum of neat epoxy polymers, epoxy blends. Annual Book of ASTM Standard, [63].

3.9 Mechanical Tests

3.9.1 Tensile Test

The specimens for tensile strength evaluation were made according to ASTM 638 standards. Tensile strength, elongation at break and modulus of elasticity were concluded from tensile test by using the universal tensile instrument at a cross head speed of (5 mm/min) and the load was

applied which equals to (5 KN) until break of the specimen occurs. Three specimens were used for this test and final results represent the average data for three specimens which were tested. Figure (3.3) represent the standard dimensions of tensile test specimen and experimental tensile test specimen respectively. The test was being done in laboratory of Babylon University/ Collage of Materials Engineering /Department of polymer and petrochemicals industries [64].

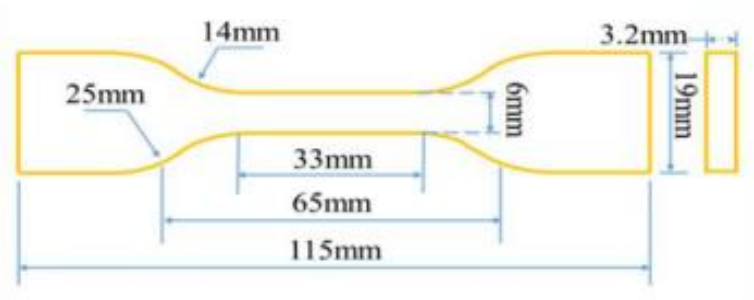

Figure (3.3) : Represent the standard dimensions of tensile test specimen and experimental tensile test specimen [64]**.**

3.9.2 Hardness Test

A hardness test is required to measure the resistance of a material to indentation. A Shore D durometer instrument was used to test hardness samples. The test was done according to ASTM (D2240) [65]. The Shore device has a needle applied in a perpendicular direction to the sample to obtain correct readings, the surface of the sample must be smooth and clean with a thickness of not less than 3 mm. Each specimen was tested six times at different positions on each specimen at the same time, and the final hardness is an average of them. The test was being done in Laboratory of light of rizy company in Bagdad.

3.9.3 Impact Test

It is considered one of the most important mechanical tests that accord the absorption of energy that is required for fracture of the sample which is taken directly from the device. Impact test was performed according to Standard ISO 179-1 with dimensions (55×10×4mm) without notched point as shown in Figure (3.4) using Charpy method where the sample was placed horizontally, the testing procedure was included lifting of pendulum to its maximums height and fixing it firmly where its potential energy would have been changed to kinetic energy. The instrument measured the absorbed energy of fracture but the impact strength and fracture toughness are calculated. The used instrument of Charpy test is done in Dept. of Eng. of Polymers and Petrochemical Industries/Materials Engineering faculty /Babylon University. Model WP 400 charpy type made in German, pendulum impact tester was employed, impact strength can be intended from the following equation:-

$$Gc = \frac{Uc}{A} \dots \dots (3.2)$$

Where Gc :

The impact strength (KJ/m^2).

Uc: The needed energy for fracture the sample (J).

A: - the cross section area of the specimen (m^2).

Impact strength depends on material type, kind of the stress that is applied, process conditions, shape and the dimensions of specimen. Fracture toughness can be intended as the following equation:-

$$Kc = \sqrt{GcEB} \ldots\ldots (3.3)$$

K_C: Fracture toughness (MPa$\sqrt{m}$)

G_C: Impact strength (J/m^2).

E_B: Flexural Modulus (MPa) [66].

Figure (3.4): Represent the standard dimensions of impact test specimen[67]**.**

3.9.4 Fracture Toughness Test

SENB(Single Edge Notched Beam) test was carried out to investigate the toughness of epoxy neat and blends specimens, They were tested using a universal testing machine type (WDW/5E). Standard Sample Geometries such as shown in Figure (3.5) The cross-head speed was held constant and was chosen (10mm/min), span length was (40 mm), At room temperature, according to ASTM D5045[68]. The stress intensity factor (K_{IC}) was obtained using the relationships shown below.

$$K_{IC} = \left(\frac{P}{BW^{\frac{1}{2}}}\right) f\left(\frac{a}{w}\right) \ldots\ldots (3.4)$$

where (0 < x < 1), P is the critical load for split propagation, B is the specimen thickness, W is the specimen width, a is the crack length, and f (x) is a non-dimensional shape factor with x = a/W.

$$\boldsymbol{f}(\mathrm{x}) = 6\mathrm{x}^{\frac{1}{2}} \frac{[1{,}99 - \mathrm{x}(1-\mathrm{x})(2{,}15 - 3{,}93\mathrm{x} + 2{,}7\,\mathrm{x}^2)]}{(1+2\mathrm{x})(1-\mathrm{x})^{\frac{3}{2}}} \ldots\ldots\ldots (3.5)$$

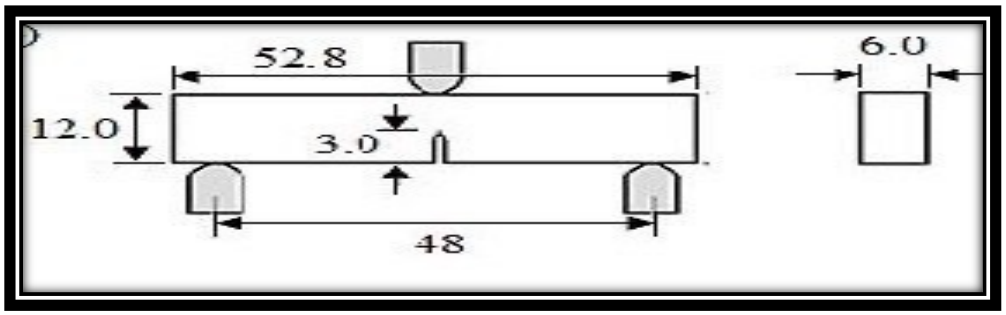

Figure (3.5): Represent the standard dimensions of fracture toguhness test specimen[68]**.**

3.9.5 Crack Path Deflection

Crack path deflection mechanism at particle obstacles in a matrix have been recommended to play an important role in the toughening. According to this assumption, when a crack front encounters the particles, it is forced to tilted and even twisted out of its original plane and hence passes around them. This causes an increase in the total fracture surface area. An indication for the change in fracture surface can be acquired by measuring the average surface roughness, Sa, of a fracture surface, which should increase if deflection processes are occurred. Other works showed that there was a linear relationship between the surface roughness and the overall toughening contribution [69]. An analytical model that describes the increment of fracture energy, ΔG, due to the crack deflection effect was used:

$$\Delta G = \frac{3\gamma m V f p}{2} \ldots\ldots (3.6)$$

Where V_{fp} is the volume fraction of particles and γ_m is the specific fracture energy of matrix [69].

3.9.6 Crack Pinning

This theory stated that as the crack begins to propagate through the resin, the crack front bows out between the filler particles but remains pinned at the particles. In these cases, crack pinning occurred when the particles were larger than the crack-opening displacement (COD).

The plastic zone ahead of the crack tip can be modeled as a line-zone using the Irwin analysis. Under plane-strain conditions, the crack-opening displacement, δtc, can be calculated using the relationship [69]:

$$\delta_{tc} = \frac{K_{IC}^2}{E\sigma_y}(1-\upsilon^2) = \frac{G_{IC}}{\sigma_y} \qquad \ldots\ldots(3.7)$$

Where δtc: crack-opening displacement (μm), E: tensile modulus (GPa), σy: yield stress of the matrix (MPa), ν: Poisson ratio (-),G_{IC} : fracture energy and K_{IC} : is stress intensity factor.

3.9.7 Plastic Deformation

The molecular cross-linked network topology of thermosetting polymers confers greater resistance to plastic deformation. However, under load, it can distort and even flow plastically by blunting the crack tip, plastic deformation lowers the concentration of localized stress in the material and enables it to withstand larger loads before failing. Under plane-strain conditions and presuming that the zone is circular, the nominal of the plastic zone forward of the crack tip can be computed [69]:

$$r_y = \frac{1}{6\pi}\left(\frac{K_{IC}}{\sigma_y}\right)^2 \quad \text{……(3.8)}$$

Where r_y :radius of plastic zone (μm), σ_y : yield stress of the matrix (MPa) and K_{IC} : is stress intensity factor.

3.9.8 Plastic Void Growth

Plastic void growth is initiated by cavitation or debonding of the particles. Matrix–particle debonding is essential in the matrix plastic void growth mechanism, which is a significant part of the matrix plastic deformation in epoxy modified [70].

3.10 Morphology Test

3.10.1 Scanning Electron Microscopes (FESEM-EDS)

Scientific instruments that take pictures of details as small as 10 nm and study items on a very fine scale using an extremely intense electron beam. High-resolution imaging combined with scanning electron microscopy is a valuable combo. Therefore, composite materials were spluttered with 130 gold to obtain superior electrical conductivity. This test can provide information on the morphology (size and shape of the particles inside the item) and topography (characterizing surface aspects of an item and establishing the nature of the fracture process). The test is conducted using the High-Resolution (HR) Analytical SEM TESCAN MIRA, which has a high brightness field emission electron source (FEG).

Table (3-5) : Technical information of tescan mira is a high-resolution (hr) analytical SEM [71]**.**

Technical Specifications / Electron Optics:

Electron Gun:	High Brightness Schottky Emitter	
Electron Optics:	Wide Field Optics™ Technology with Intermediate Lens™ and In-Flight Beam Tracing™	
Resolution:	**High Vacuum Mode:**	**Low Vacuum Mode:**
	1.2 nm at 30 keV	2.0 nm at 30 keV with BSE detector*
	3.5 nm at 1 keV	1.5 nm at 30 keV with LVSTD detector*
	1.8 nm at 1 keV with BDT	* optional detectors
Maximum Field of View:	>50 mm at max WD	

Chapter Four
Results and Discussion

4.1 Introduction

This chapter covers a detailed discussion of all the results which were obtained from the experimental work. It includes the results of thermal test DSC results and TGA results are presented in this chapter. It also includes the results of mechanical tests: tensile, fracture toughness, impact, and hardness tests. Moreover, the present chapter contains the results of structural and morphological tests: FTIR, SEM that presented in this chapter.

4.2 Solvent Selection Results

According to the Hanson solubility parameter (δ) concept, Toluene was selected as a co-solvent for PS DS-P = $\sqrt{(2*\ 21.28-2*18)^2}$ + $(5.75-1.40)^2$ +$(4.30-2)^2$ =8.198. Then D_{S-P}/R_0 = 8.198/12.70 = 0.64551.

Our ideal solvents should show DS-P/R0 ratios less than 1 with in value of D_{S-P} = 0.64551 after calculation. Usually, the ratio DS-P/R0 is used as the criterion:

$D_{S-P}/R_0 > 1 \rightarrow$ the compound is a non-solvent;

$D_{S-P}/R_0 < 1 \rightarrow$ the compound is a solvent;

$D_{S-P}/R_0 = 0 \rightarrow$ the compound may cause swelling based on the information from [72].

Table (4-1) : The Hanson solubility parameters of target polymers [61].

POLYMER	δd	δp	δh	Interaction Radius
Polyisoprene	16.57	1.41	-0.82	9.60
Polystyrene	21.28	5.75	4.30	12.70
Polyethylene glycol	17.00	11.00	8.90	22.00

Table (4-2): The Hanson solubility parameters values of the currently used solvents, and their miscibility with polystyrene [61]**.**

SOLVENT	HSP			D_{S-P}/R_0		
	δd	δp	δh	with PI	with PS	with PEG
Acetone	15.50	10.40	7.00	1.26	1.00	0.16
Methanol	15.10	12.30	22.30	2.68	1.79	0.64
Ethanol	15.80	8.80	19.40	2.25	1.49	0.50
Toluene	18.00	1.40	2.00	0.42	0.65	0.55
Tetrahydrofuran	16.80	5.70	8.00	1.02	0.76	0.25
Water	15.50	16.00	42.40	4.76	3.24	1.55

4.3 Analysis of Curing Kinetics Parameters of DSC Results

- **Glass Transition Temperature (Tg)**

Figure (4-1) displays various resin/hardener combinations DSC curves, both pure and with blends samples, which have been permitted to cure for a further 24 hours at RT similar to [73].

Tg is found to be 66.30 °C in an epoxy system that has not been altered. In comparison to the unaltered epoxy system, Tg has started to decrease with the addition of thermoplastic polymer and rising PS% load content; this represents a reduction of about 19% when modified with 2.5 wt.% of PS curing at RT. Because PS may serve as plasticizers, it can be argued that the decreased crosslinking degree of the PS areas leads to the conclusion that the addition of PS influences the Tg of epoxy resin. Furthermore, the value of Tg decreased by around 12.669% as content of PS increased. For all samples that were cured at RT for 24 hours, the drop rose to 25% when 7.5 wt.% PS was added agreement with [74] this phenomena may have a possible explanation in the shape of a second phase that prevents the density of thermoset cross-links from increasing aggrement with [75] the fact that some PS chains will may be impede

progress of curing process of the epoxy while others were miscible with it suggests that the matrix plasticization process was what led to the decreased Tg similar to [79,80].

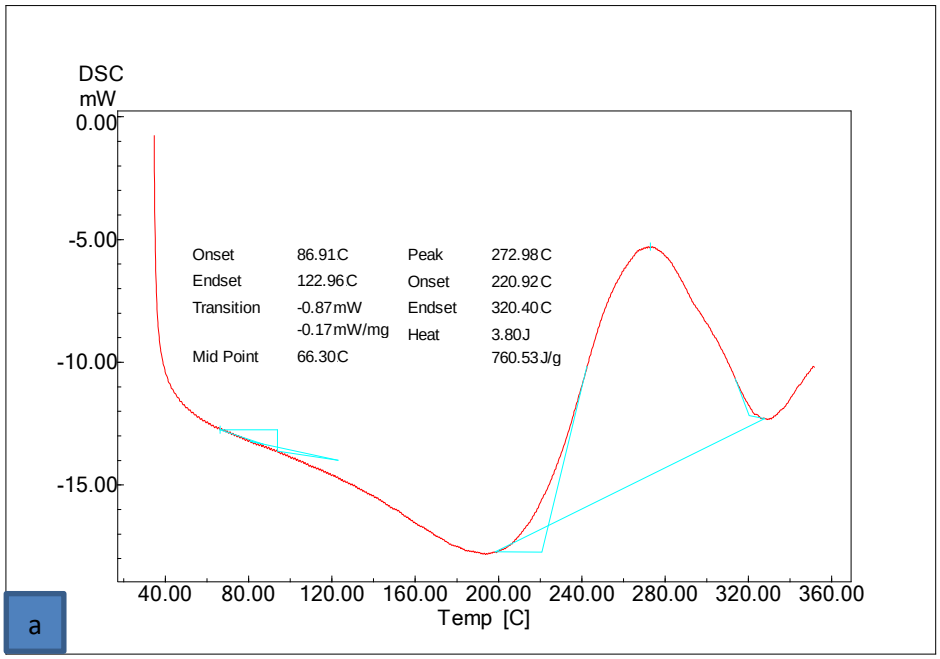

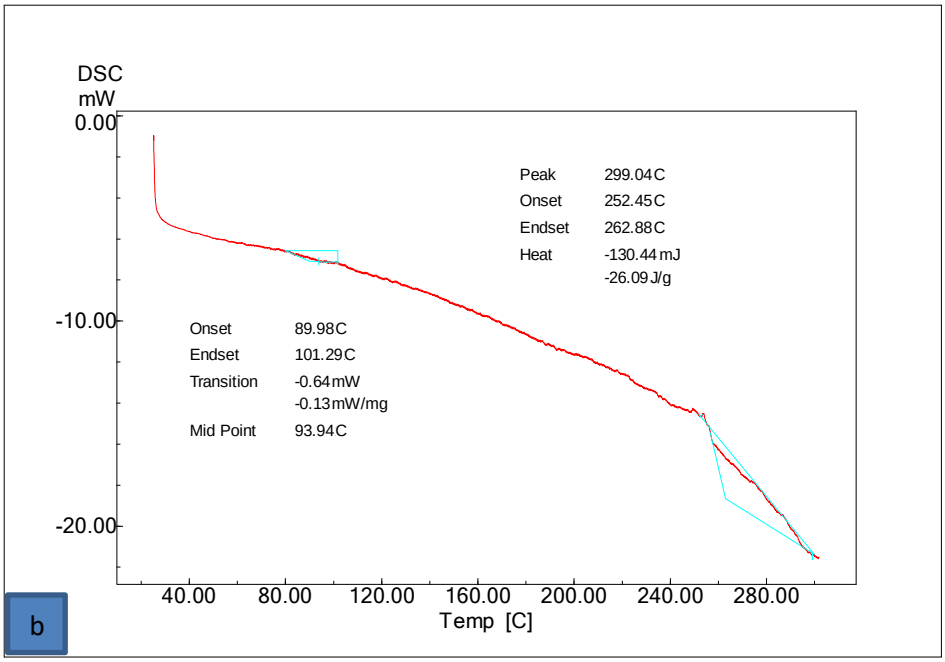

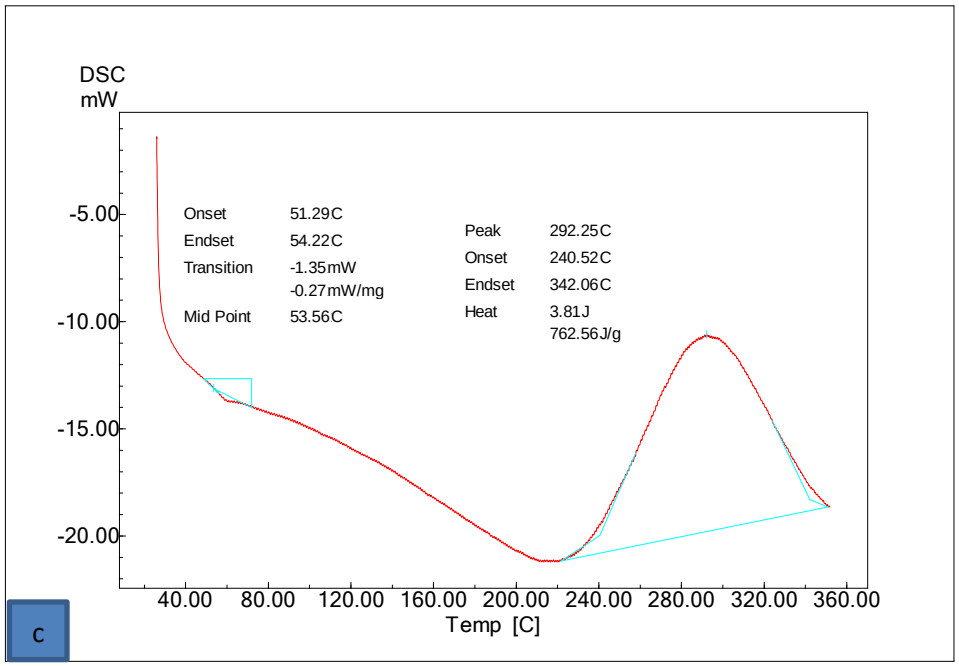
DSC
mW
-5.00
-10.00
-15.00
-20.00
Onset 51.29C
Endset 54.22C
Transition -1.35mW
-0.27mW/mg
Mid Point 53.56C
Peak 292.25C
Onset 240.52C
Endset 342.06C
Heat 3.81J
762.56J/g
40.00 80.00 120.00 160.00 200.00 240.00 280.00 320.00 360.00
Temp [C]
c

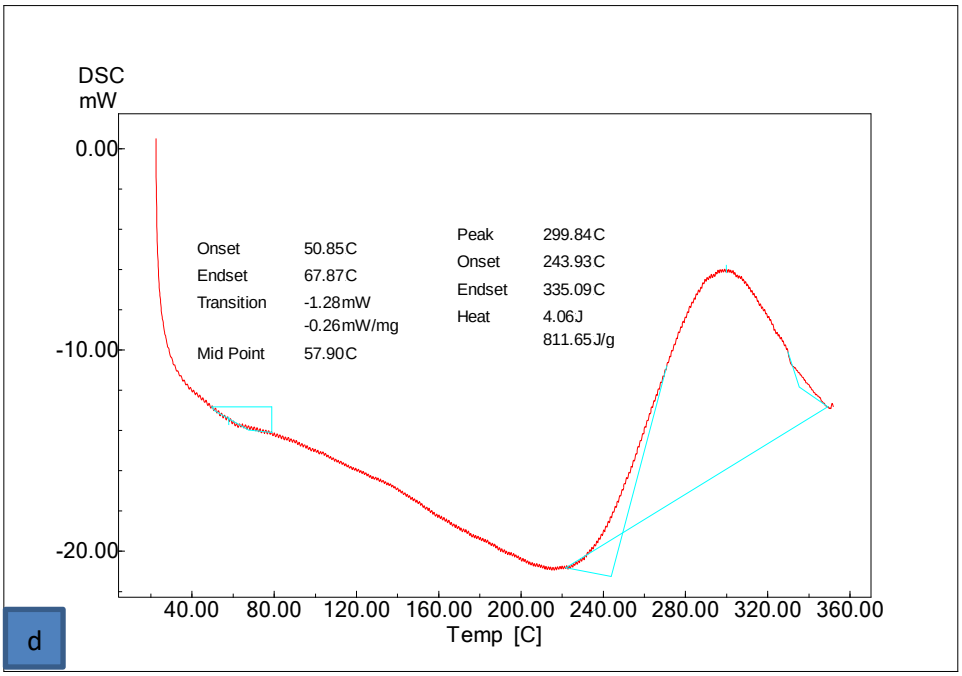
DSC
mW
0.00
-10.00
-20.00
Onset 50.85C
Endset 67.87C
Transition -1.28mW
-0.26mW/mg
Mid Point 57.90C
Peak 299.84C
Onset 243.93C
Endset 335.09C
Heat 4.06J
811.65J/g
40.00 80.00 120.00 160.00 200.00 240.00 280.00 320.00 360.00
Temp [C]
d

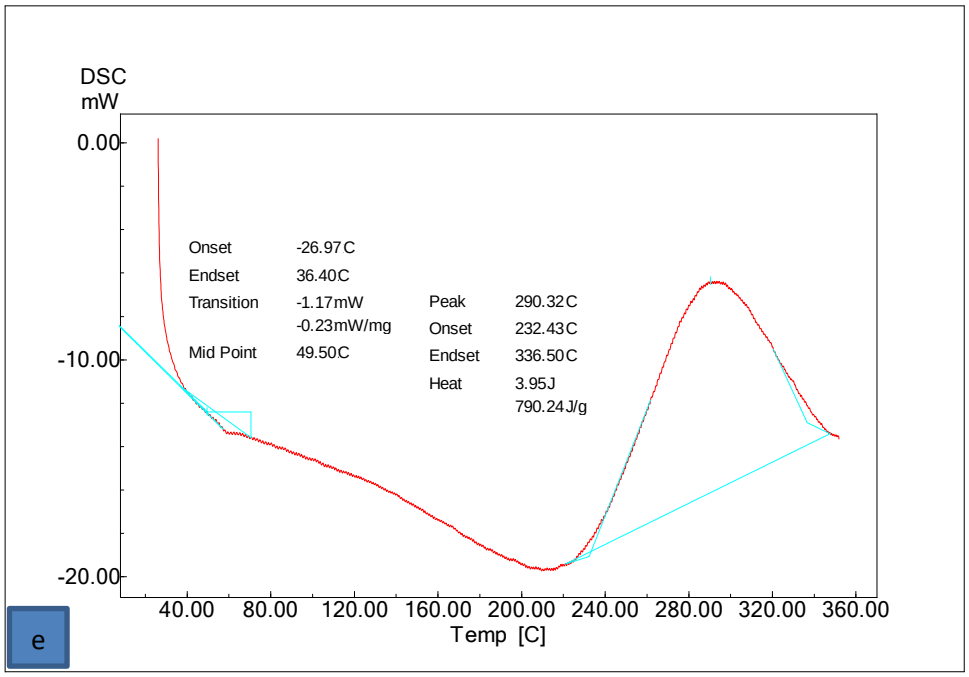

Figure (4.1): The DSC chart test of samples a: 1:0.5pure, b: polystyrene, c: 1:0.5+2.5 wt.% PS, d: 1:0.5+5 wt.% PS and e:1:0.5+7.5 wt.% PS cured at RT.

Depending on the variations in treatment circumstances, the degree of cross-linking, the elasticity of the material's chain, and the strength of the intermolecular hydrogen bonding interaction (amino group) all have a significant kinetic influence on the Tg of cured epoxy similar to [78].

In Table (4-3) illustrate samples were cured at RT, in some samples exhibit two values of the Tg, in samples of 1.5:1 + 2.5wt.% PS and 2.5:1.5 + 2.5 wt.% when the variation in curing temperature causes a sharp sifting or lowering of the Tg value were cured at 50 °C its may be attributed to phase separation ocuured between epoxy and polystyrene resulting in immiscible compounds, or because the heat wasn't enough to accelerate the reaction, that may be causing the polystyrene to agglomerate and agglomartion in one place inside the epoxy matrix.

Table (4-3): The value of Tg for epoxy and its blends cured at RT.

Hardener	**33%** **1:0.5**	**37%** **2.5:1.5**	**40%** **1.5:1**	**50%** **1:1**
PSwt.%	**Tg ℃**	**Tg ℃**	**Tg ℃**	**Tg ℃**
0	**66.30**	**48.42**	**42.49**	**50.68**
2.5	**53.56**	**50.88**	**54.11**	**84.88**
5	**57.9**	**60.88**	**60.18**	**64.88**
7.5	**49.50**	**59.38**	**54.63**	**64.10**

Table 4-3 illustrates the Tg value varation with increasing hardener ratios in contrast to growing PS content Tg increasing with increasing hardener ratios in horizontally direaction in the Table(4-3). In the first the Tg of pure samples, which was dropped to around 25%, were one of these these observation may be explained by the presence of a polystyrene phase, which caused the cross-link density to decrease this, in turn, led to an internal plasticizing effect in the modified epoxy resin and an inadequate conversion of epoxy groups in other samples. Initial Tg decreases with increasing PS content may have occurred because PS reduced Tg by impeding the mobility of the polymer chain similar to [79]. The value of Tg > 120 °C cannot be achieved in a network system made of epoxy cured with aliphatic amines, as shown in results which is its primary drawback use of aromatic amines and high temperature curing are required to create an epoxy network with a high Tg similar to [32].

Figure (4.1) the samples illustrated appearance of single glass transition, may be suggests the existence of a closed network or cross-linked structure in addition it was discovered that overloading PS had appreciable impact on the Tg in order that with rasing and decreasing of

Tg value may be due to the interlacing polymeric chains between the two phases or increasing or decreasing hardener value additionally, it was noted that the transition temperature value decreased as the PS loading increased and the cure temperature altered, most likely as a result of PS acting as a plasticizer phase in the matrix similar to [80].

In DSC measurements α or degree of cure, is an additional parameter that ranges from 0 totally uncured to 1 fully according to the equation(2.17).

Figure (4.2) illstruated that with incrasing of hardener ratios in which increasing from hardness whith appearance of craks in the structure. The enthalpy can be calculated from the area of the exothermic peak, which is the integration of the heat flow a DSC is commonly used to measure the heat flow when epoxy resins are cured by DSC, a sizable exothermic peak appears and as the heating rate increases, so does the exotherm's intensity.

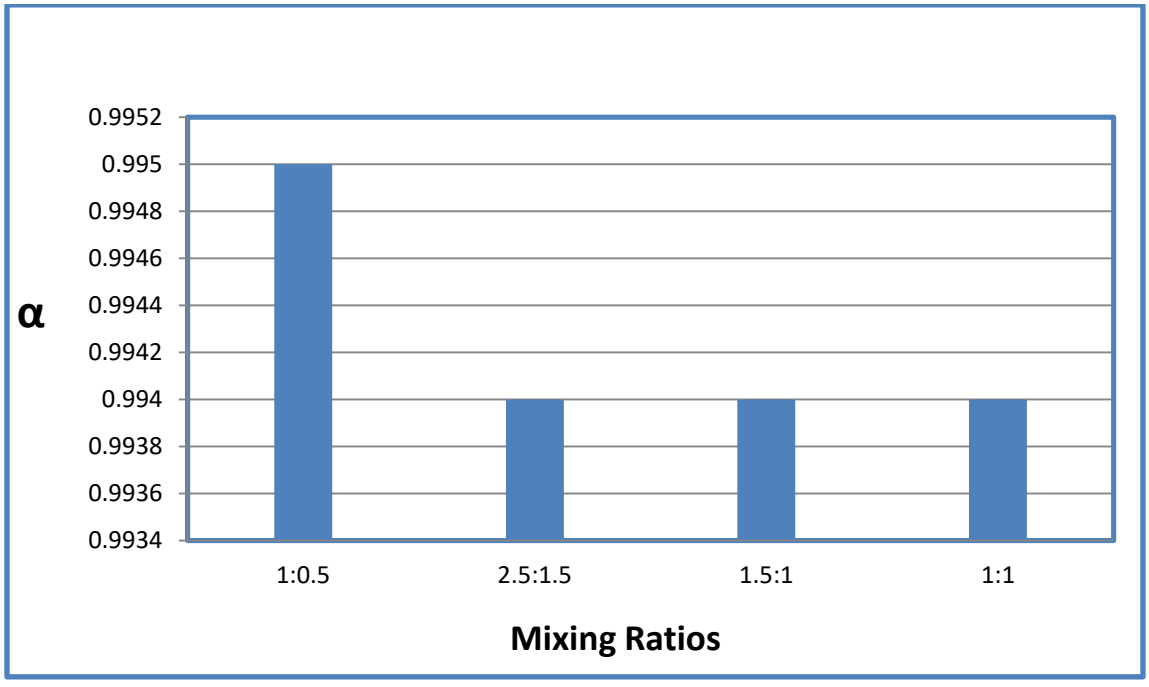

Figure (4.2): Relation between degree of cure and unmodified mixing ratio EP/h cured at RT.

Table(4-4): The relation between hardener ratios and degree of cure of epoxy and its blends at RT.

Hardener	33% 1:0.5	**37% 2.5:1.5**	**40% 1.5:1**	**50% 1:1**
PS wt.%	**α**	**α**	**α**	**α**
0	**0.995**	**0.994**	**0.994**	**0.994**
2.5	**0.995**	**0.994**	**0.995**	**0.995**
5	**0.995**	**0.994**	**0.994**	**0.995**
7.5	**0.995**	**0.995**	**0.994**	**0.994**

- **Effect of Curing Temperature**

Illustrated a range of Tg and degree of cure in contrast with changing the curing temperature (RT, 50℃, 80℃, and 120℃) and other condition , as shown in the figures below when the ratio of hardener to epoxy was changed.

At Figure (4.3), it was noticed that two values of Tg were found for formulations of 1.5:1 and 2.5:1.5 at 50 ℃ this could be attributed to the discovery of excessive hardener material in the mixture or phase separation between two polymers prior to the use of coupling agents [81]**,** in this temperature range, the mixes' composition changes from miscible to immiscible and back to miscible.

This shows that blends are miscible below a certain temperature for any composition, even though the miscibility behaviour is similar to an

immiscibility window at a particular temperature the trend of this miscibility behaviour matches the experimental one additionally, cloud point a different phenomenon, is connected to this behavior as in Figure (4.3) demonstrate different Tg and degrees of cure when changed in formulation of the hardener to epoxy ratio and contrasted it with modifying the curing temperature and time. The blend samples' behaviour at two Tg values during the phase transition from homogeneity to phase separation are shown in the DSC chart similar to [82].

A mixture containing an excessive amount of hardener material or separate polystyrene phases may also hinder the formation of the epoxy resin's cross-linking structure, which initially joins the styrene and epoxy groups.

The glass transition temperature is lowered when there is less crosslinking because it increases the material's free volume and improves the chain segments' mobility as the temperature goes over 120°C, separation occurs, resulting in displacement between the chains and a reduction in crosslinking strength similar to [83].

Furthermore, it is noted that a decrease in the transition temperature value with increased PS loading may be the result of the blend being less stiff, which acts as a plasticizer phase in the matrix similar to [87,83], But in other cases, like the 1:1 ratio, where adding 2.5 wt.% PS increased the percentage to about 64%, and adding 7.5 wt.% increased the percentage to about 26%, which was still higher than pure this could be because the PS phases to go deep rather than increasing from the density of cross-link chains, which could act as a bridge connection which increasing the density of chains since the formultion of epoxy group and amine is equal, as shown in Figure (4.3).

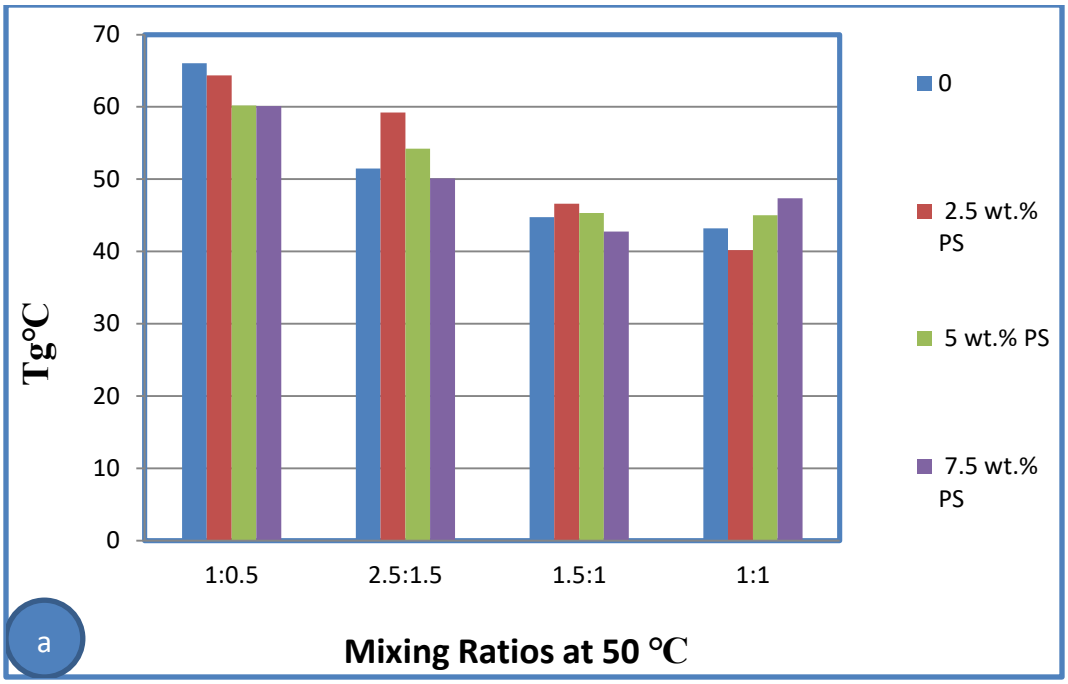
70
60
50
40
30
20
10
0
Tg°C
1:0.5
2.5:1.5
1.5:1
1:1
0
2.5 wt.% PS
5 wt.% PS
7.5 wt.% PS
a
Mixing Ratios at 50 °C

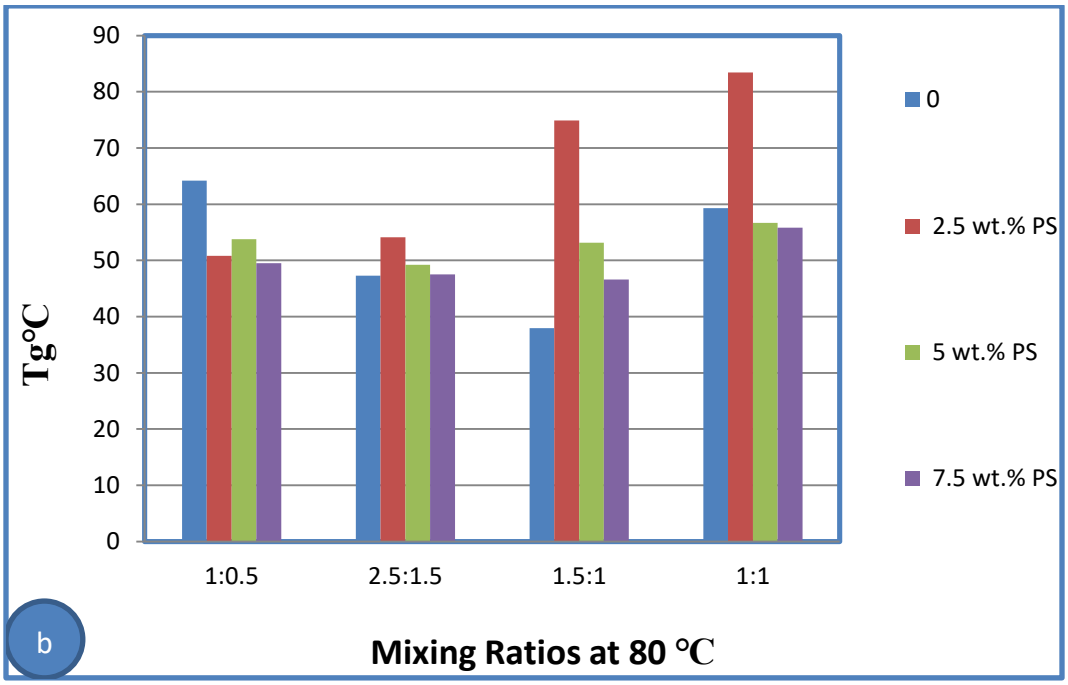
90
80
70
60
50
40
30
20
10
0
Tg°C
1:0.5
2.5:1.5
1.5:1
1:1
0
2.5 wt.% PS
5 wt.% PS
7.5 wt.% PS
b
Mixing Ratios at 80 °C

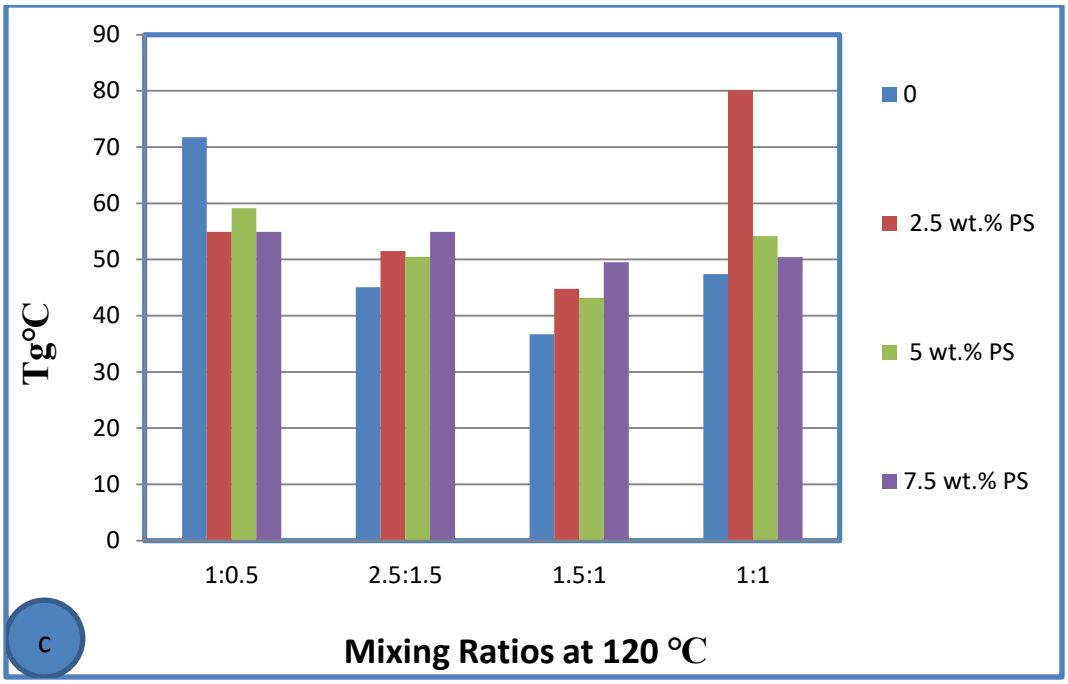

Figure (4.3): Represent the relation between Tg and mixing ratios of epoxy and its blends at different curing tempearture a:50°C, b:80°C and c:120°C.

When compared to the other samples toughened by polystyrene, Tg increased in the neat epoxy sample when PS was added this is because the presence of flexible PS chains, a decrease in the stiffness of the polymer chains, and a decrease in the density of crosslinks are all contributing factors the samples compounded with different concentrations of resin and hardener cured at room temperature are decreased by adding PS.

depends on how cross-linked a thermoset is and to what extent with increasing polystyrene content found that the Tg changed to a lower value and dropped; nevertheless, only a few very slight changes occur to the glass transition features because of the wide range of polymer combinations chains have a lower Tg because they are more mobile and versatile than other materials cross-links function as long-lasting entanglements that limit the motion of the chain.

Stated differently, at low cross-link densities, the temperature at which glass transitions occur increases almost linearly with the number of cross-links materials with a high cross-link density usually exhibit an inaccurate and hazy glass transition.

The presence of secondary components causes the free volume to drop quickly and the Tg to be impacted by the polymer chain mobility similar to [85] assumes that the degree of cure is proportionate to the reaction heat since the curing process is an exothermic reaction, and the cumulative heat produced during the reaction phase is often connected to the degree of cure.

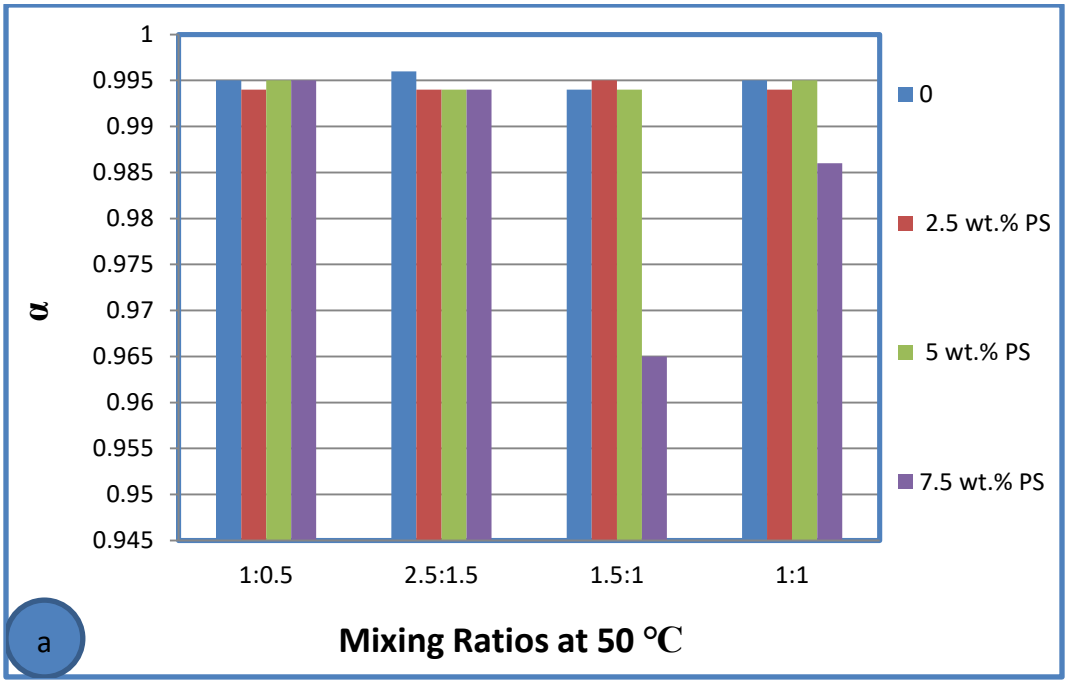

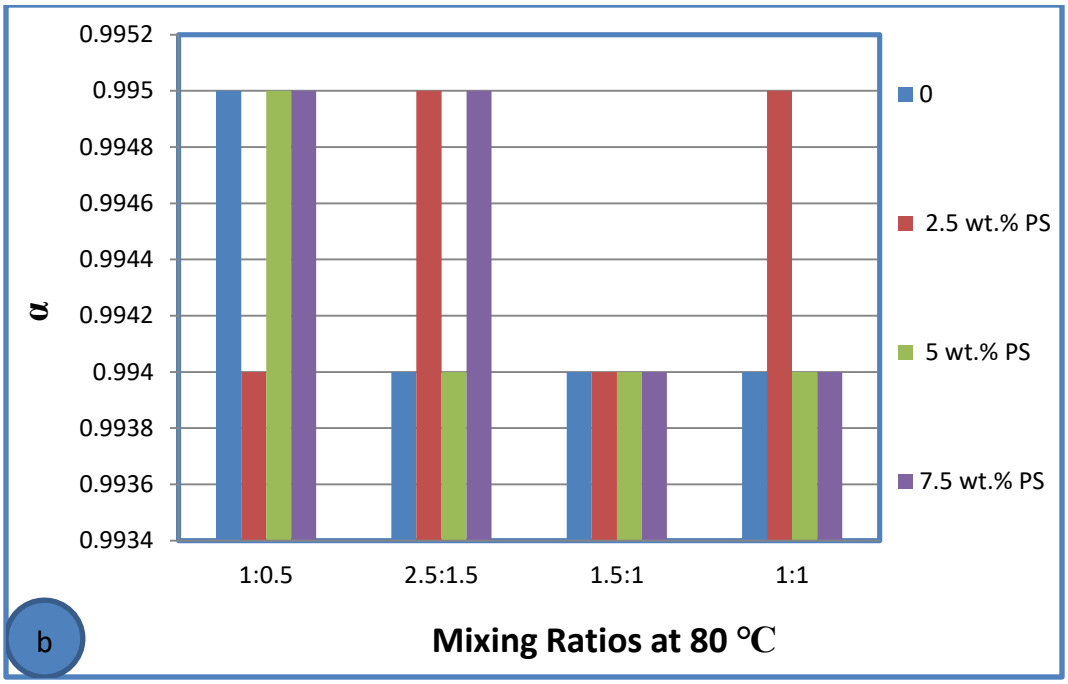

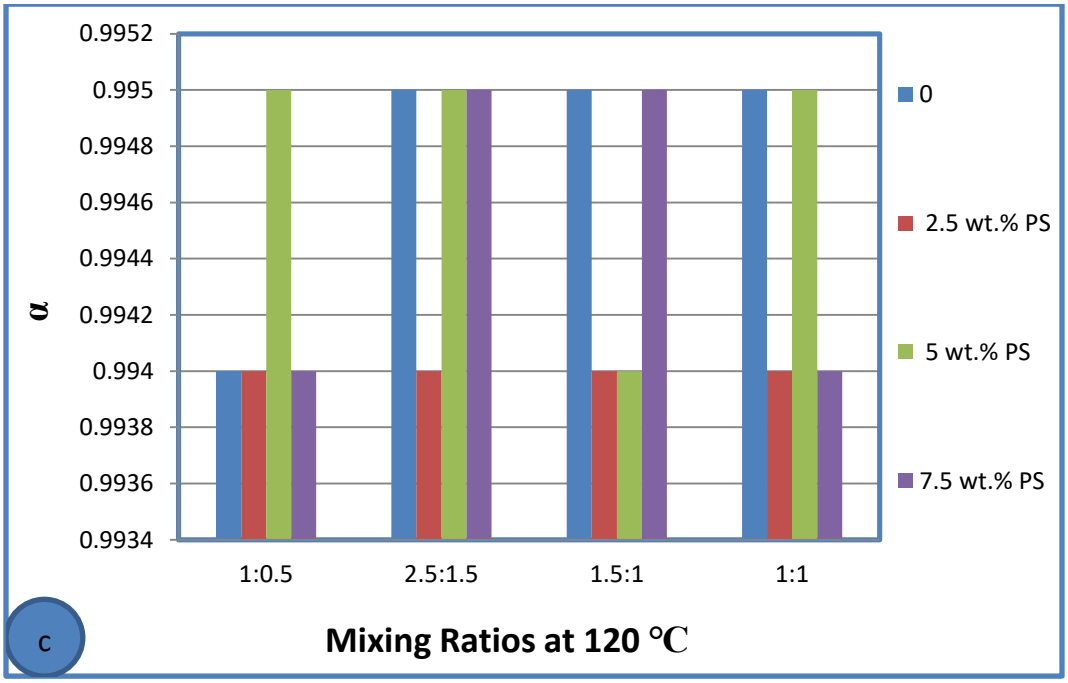

Figure (4.4): Represent relation between degree of cure and mixing ratios at different curing temperature a: 50℃, b:80℃ and c:120℃.

In Figure (4.4) the variation in the degree of cure with different formulation of EP/h ratios under different curing conditions, noticed that at 50 ℃ curing temperature the best value was at 2.5:2.5 EP/h pure sample inorder that because of may be increasing of unmber of cross linking network while the addition of of PS leads to decrased of degree of cure up to increasing content of PS to 7.5 wt.% noticed sharp decreased in value of degree of cure at formulation of 1.5:1 proply that was because of restricted of PS the curing process.

For curing temperature at 80 ℃ noticed the best value of degree of cure was at 1:0.5 pure sample comperaing to the other formulations and with the addition of PS noticed decreased in value of degree of cure then with increasing of PS content the value of degree of cure increased, at formulation 1.5:1 the value of degree of cure had steady value at a;ll addition of PS as shown in Figure (4.4 b).

In Figure (4.4 c) presented samples that cured at 120 ℃ at this temperature the degree of cure at samples 1:0.5 and 2.5:1.5 with PS content of 5 wt. % showed high value of degree of cure comparing to other samples, with increasing of PS content the degree of cure increased properly because of increasing of amino group and decreasing at 2.5wt. % PS may because that PS act as pasteurized the restricted the curing process.

Related to the value of Tag that is higher for 1:0.5 when cured at RT, concluded that the best ratio was at 1:1 + 2.5 wt.% PS when cured at RT, which had higher Tg compared to other formulations like 1:0.5 and 1.5:1 and 2.5:1.5 when PS content adding there was a reduction in value of Tg

according to this may be attributed to the fact that when the amine group is increased, it becomes equal to the epoxy group, and the addition of PS increases the connection and density of cross link, this is for formulation of 1:1, while for other formulations, the Tg of the epoxy resin was not raised but rather lowered.

This may occur when the epoxy resin is unable to cure adequately due to the PS macromolecular chain coming into contact with the curing agent additionally; the PS addition increases the viscosity of the system, leading to a slower curing process similar to [92]. The Tg of the epoxy resin was decreased rather than increased by adding PS the chain flexibility, cross-linked structure, and hydrogen bonding contact between molecules all affect the Tag of cured epoxy.

The Tg of modified epoxy resins would decrease and the cross-linked structure would be strengthened with the addition of PS because of the PS addition, the system becomes more viscous, which causes incomplete curing responses for this reason, compared to pure epoxy, the Tg of epoxy/PS blends is lower similar to [78]. In Figure (4.4) Both the cure kinetics and the finished material's physical properties are affected by the cure situation in the transition state, the primary function of the hydroxyl groups was to facilitate the opening of additional epoxide rings by hydrogen bonding generated by the ring opening reaction of epoxide groups, thus accelerating the epoxy cure reaction, curing raises the molecular weight of a thermoset resin.

A macroscopic network structure that limits chain mobility forms when a threshold for gel formation is crossed, assuming a continuous decrease in

fluidity until viscosity reaches an infinite level as the scanning rate increased, expected the peak temperature, which represents the maximum reaction rate, to rise when a reacting medium's glass transition temperature is higher than the reaction temperature, vitrification occurs.

- **Rate of Reaction (dα/dt)**

During the DSC curing process, epoxy resin and its blends experience a large exothermic peak because the intensity of the exotherm increases with the rate of reaction according to the equastion (1.1), the value of Tg after PS is introduced may have fluctuated. In addition, as the curing reaction advanced, the exothermic peaks became sharper and moved towards higher temperatures, as demonstrated by the DSC chart.

However, as the rate of reaction increased during the curing of the EP/PS system, as shown in Figure (4.5) presented the investigation found, the thermal inertia and heat flux also increased as a result, the thermal effect's temperature difference widened, and the curing exothermic peak shifted to a higher temperature. Furthermore, a modest rate of heating gives the system adequate time to respond, allowing the curing response to happen at low temperatures.

Furthermore, the system's values steadily decreased as the heating rate increased, showing that the system's curing reaction was more fully developed at lower heating rate values the investigation and computation of the kinetic parameters of the curing reaction of the EP/PS polymer system have substantial theoretical and practical relevance for its use in industry. In Figure (4.5) illustrated that with increasing of curing temperature the rat of reaction incresced in the beginging stages of the cure reaction, the cure rate at a higher cure temperature is faster than it is

at a lower temperature; however, in the later stages, it is begin to slower similar to [86].

The exothermic peak temperature (Tp) shifted to higher values in the blends. The increased shift in Tp is due to the decrease in the polymerization rate due to a dilutional effect where the presence of thermoplastic reduces the concentration of reactive groups, thus decreasing the cure rate. The decrease in reaction rate can also be due to the decrease in the amount of catalytic group.

As the curing process comes to a finish, the sample is almost solidified since there are significant restrictions on the movement of the reacting groups and products, diffusion rather than chemical kinetics governs the rate of reaction because there is no clear pattern in the behaviour of reaction heats, which shows that a non-uniform process is occurring, it is believed that the information from the results complements each other and can help in the understanding of processes to be represented with the cure equations similar to [87]**.**

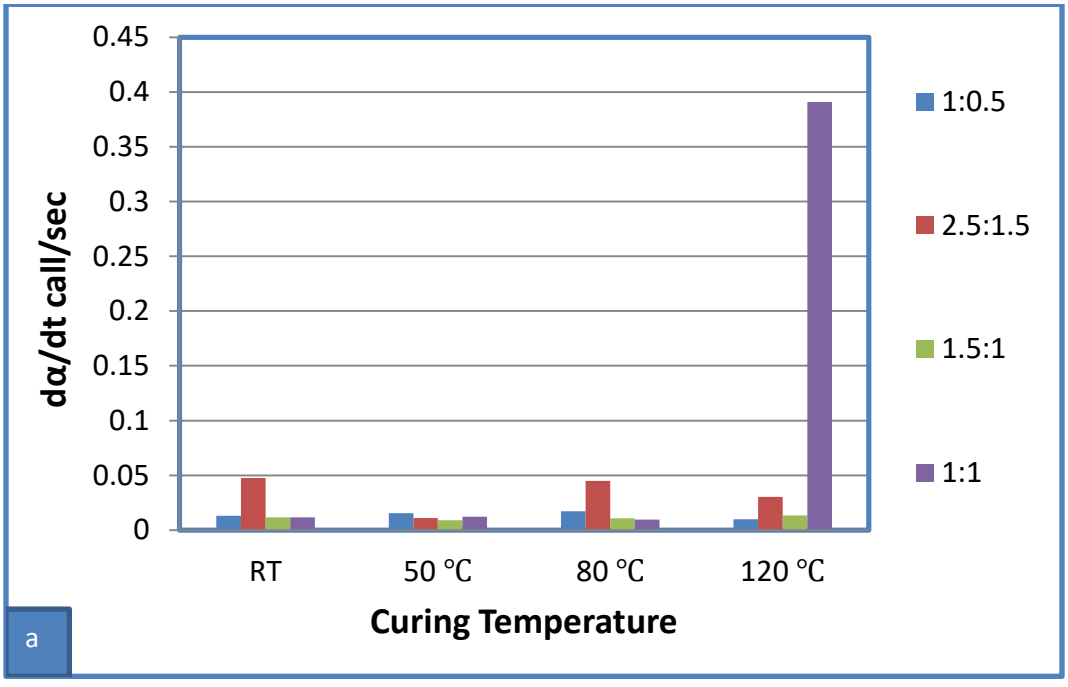

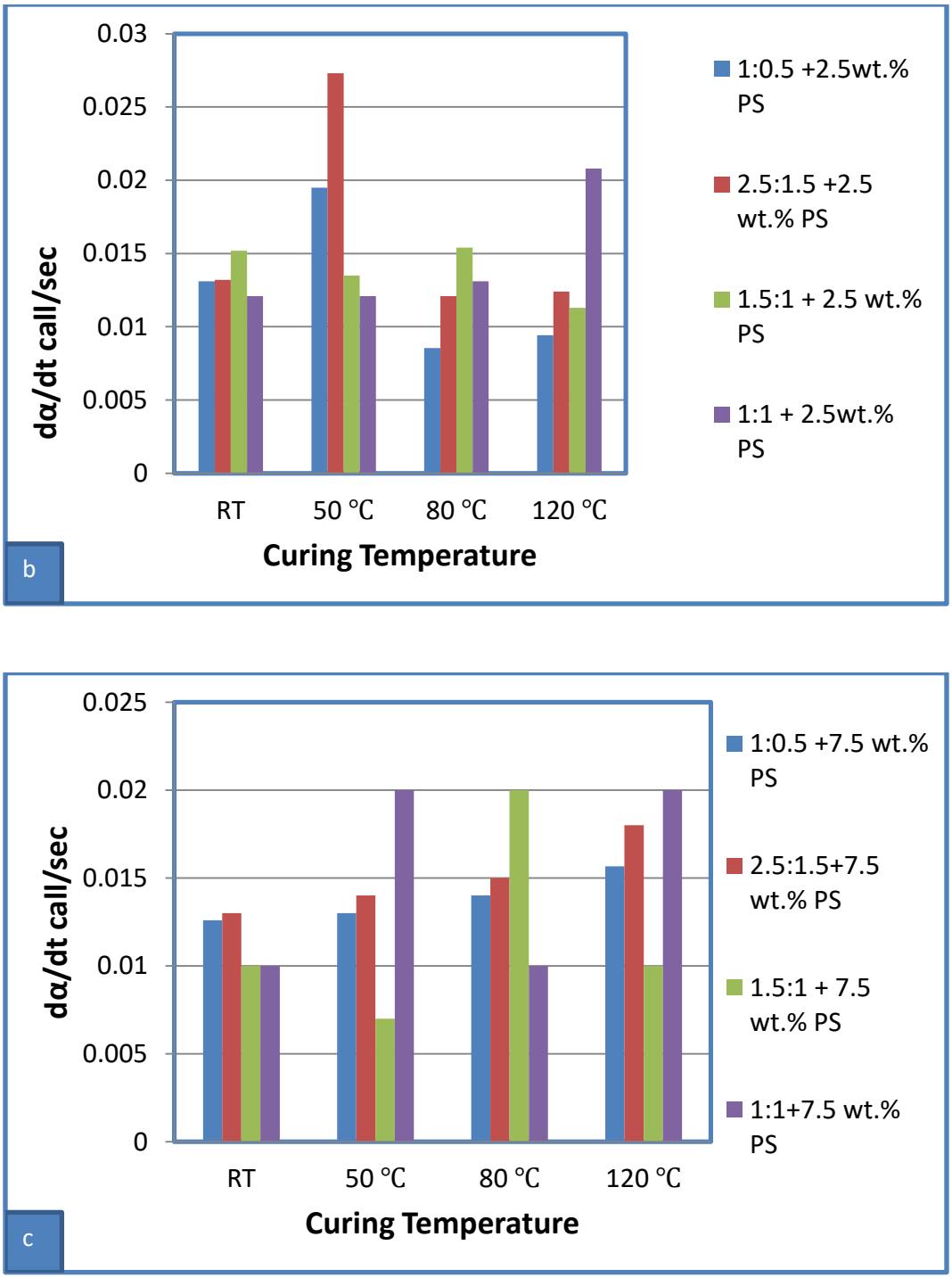

Figure (4.5): The rate of reaction of epoxy and its blends at different curing temperatures.

- **Activation energy (Ea)**

The apparent activation energy (Ea) according to the eqution value correlates with the system's curing difficulty to initiate the reaction and initiate the curing process.

According to the equation $\frac{\ln \beta}{\frac{1}{Tp}} = \frac{-1.052}{R} Ea$ [88].

The presence of thermoplastic causes very little effect on the activation energy suggesting that no relevant changes in the energy barrier required for initiation of the reaction occur compared to the corresponding non-toughened of epoxy resin.

In Figure (4.6) a slightly different activation energy evolution the activation energy initially decreased due to the formation of hydroxyl groups which catalyzed the curing reaction, and at a later stage, it increased due to increased system viscosity similar to [89].

The reduction in activation energy is more for amine-terminated the PS may be acted as catalyst at lower concentration, and at higher compositions they obstructed the curing reaction.

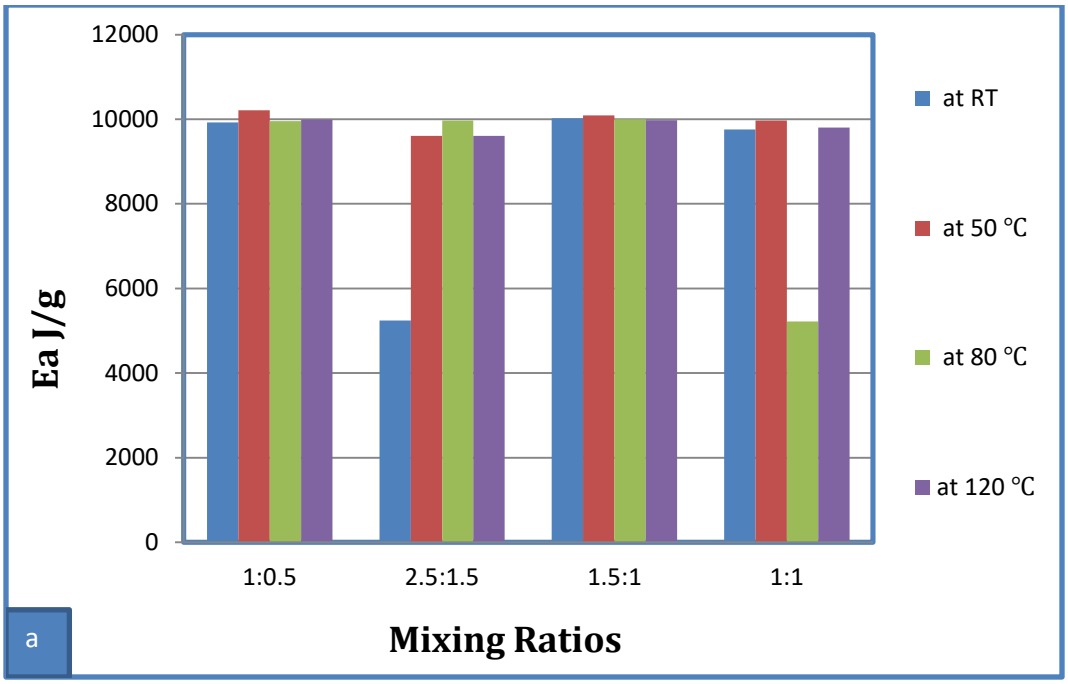
12000
10000
8000
6000
4000
2000
0
Ea J/g
1:0.5
2.5:1.5
1.5:1
1:1
at RT
at 50 °C
at 80 °C
at 120 °C
a
Mixing Ratios

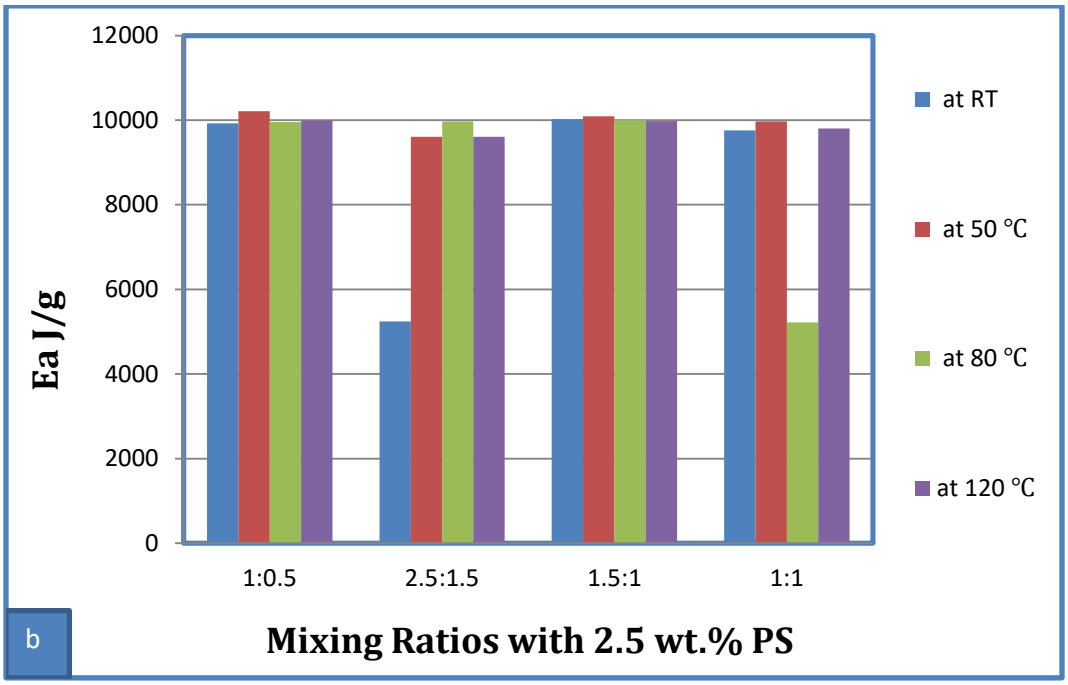
12000
10000
8000
6000
4000
2000
0
Ea J/g
1:0.5
2.5:1.5
1.5:1
1:1
at RT
at 50 °C
at 80 °C
at 120 °C
b
Mixing Ratios with 2.5 wt.% PS

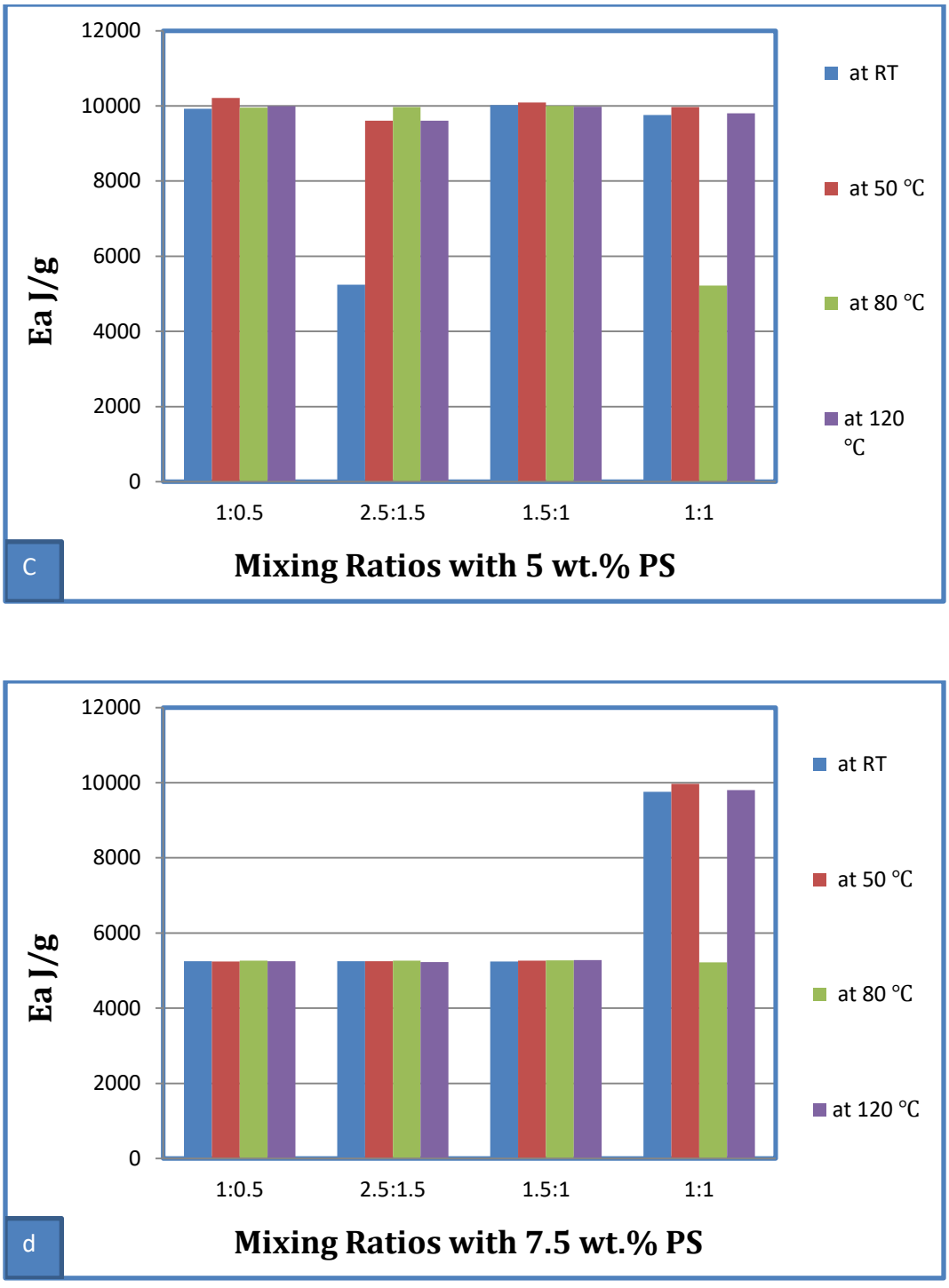

Figure (4.6): Relation between activation energy and mixing ratios of epoxy and its blends.

- **Effects of Curing Time**

The effects of curing time on degree of cure are shown in Figure (4.7), Figure (4.8), and Figure (4.9) it is evident that as curing temperature rises and curing time decreases, industry benefits because it allows for faster attainment of the same degree of curing through increased production for specific applications.

As shown in Figure (4.7) the best value of curing faste was at 2.5:1.5 EP/h formulation pure sample probly because of increasing of epoxy group with increasing amino group leaded to faster connection in the presence of temperature.

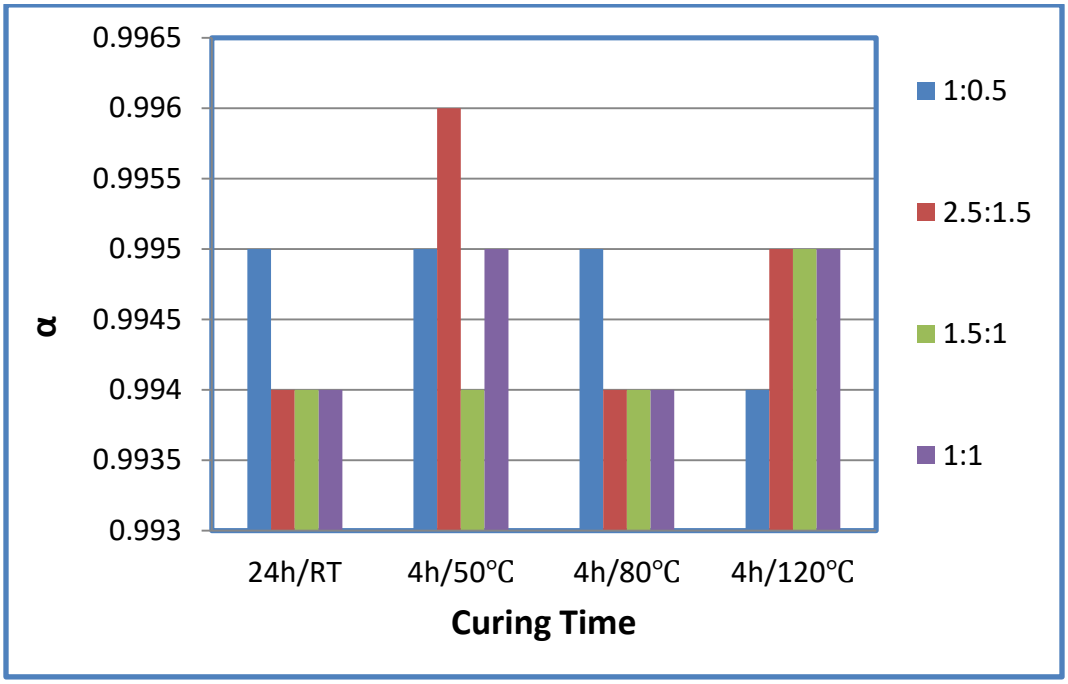

Figure (4.7): Relation between curing time and degree of cure for epoxy pure samples at different curing temperature.

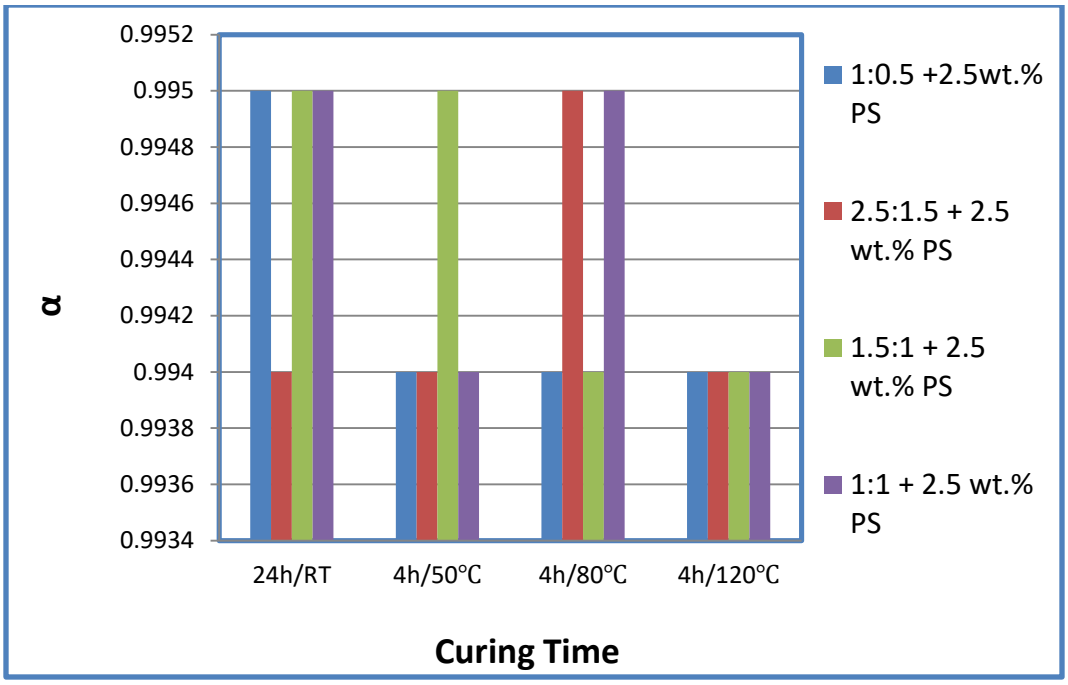

Figure (4.8): Relation between curing time vs degree of cure for epoxy and its blends at different curing temperature.

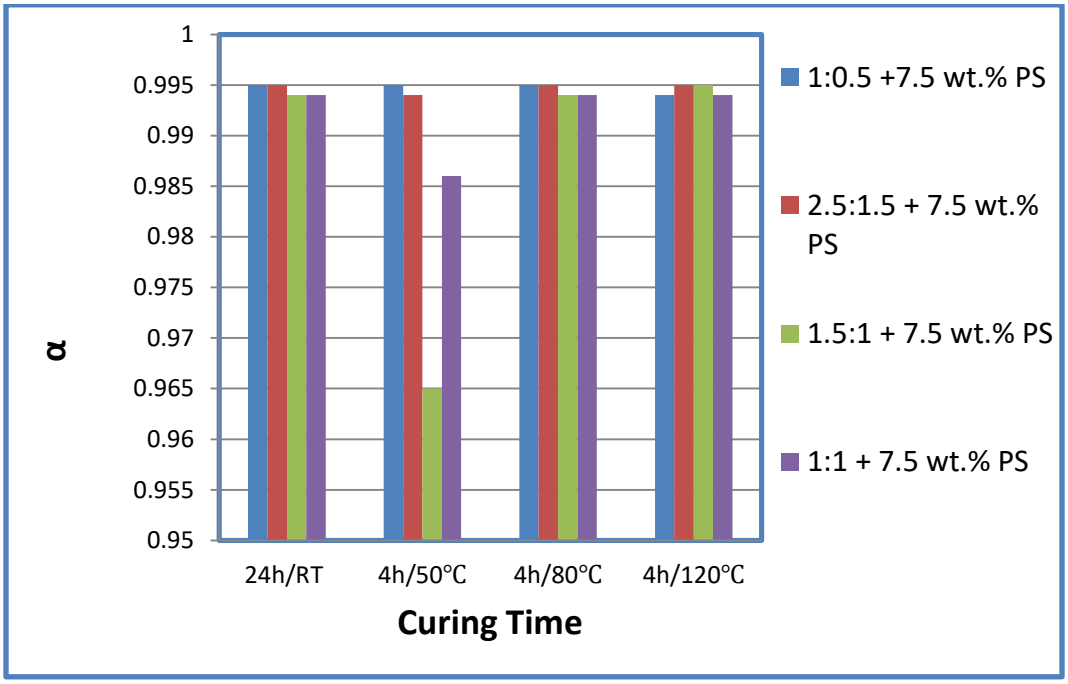

Figure (4.9): Relation between curing time vs degree of cure of epoxy and its blends at different curing temperature.

As shown in Figure (4.8) a result, with an increase in the heating rate, the peak temperature, changes to a wider temperature range as expected.

as represented by the value of formulations of 1:0.5 + 2.5 wt.%PS (T_p= 292.25 °C) compared to formulations of 1:1+ 2.5% PS, 1.5:1+2.5% wt. PS, and 2.5:1.5 + 2.5 wt.% PS of value (T_p=272.59 °C), (T_p=276.73 °C) and (T_p=283.10 °C).

While in Figure (4.9) there is varation in time for curing as shown above these thermal properties can be tuned by varying the concentration of polymeric blends the minimum in the peak temperature, corresponds to the maximum heat flow due to the epoxy-amine reaction it can be seen that, the T_{peak} maximum in the exotherm increases as the weight percentage of PS in the matrix increases this may be due to the plasticization effect that with increasing content of PS causes retardation in cure reaction or there occurs delay in cure kinetics.

The same behavior could be noticed in the other heating rates too as shown in Table (4-5) similar to [34 , 75]. The $1/T_p$ against heating rate should be created for each degree of cure in order to determine the appropriate activation energy and pre-exponential component similar to [18]**.**

In Table (4.5) with rising heating rate, the amplitude of the exotherm also increases with an increase in heating rate, the peak temperature moves to a greater temperature range but at heating rate 20℃/min noticed that found reduction in peak temperature. The degree of glass transition Tg is identified by the abrupt reduction in heat flow, and the vast exothermic peak area that follows corresponds to the reaction's residual heat, or ΔH_R. As one may anticipate, as the isothermal cure time increases, the reaction's residual heat of reaction diminishes.

The progression of the cure reaction over time is indicated by a decrease in the reaction's residual heat and an increase in Tg the level of cure at four distinct temperatures over a different of time. Another facter was exchanged of heating rate in DSC test, the cure of epoxy resin is characterized by a broad exothermic peak using varied heating rates for 12 samples employing different heating rate of (10, 20, 25 °C/min). The reaction is crosslinking process is carried out by the amine, because of the presence of more amine groups, resulting in a lower peak temperature (Tp) as shown in Table (4-5).

Table (4-5): Value of kinetic parameters at different heating rates for different samples.

EP:h+wt.% PS	Tg at 10 ℃/min	Tg at 20 ℃/min	Tg at 25 ℃/min	Curing temperature	Tp at 10 ℃/min	Tp at 20 ℃/min	Tp at 25 ℃/min	To at 10 ℃/min	To at 20 ℃/min	To at 25 ℃/min	ΔH total J/g at 10	ΔH total J/g at 20	ΔH total J/g at 25
1:0.5:	66.30	56.32	65.93	RT	272.98	125.73	317.76	220.92	161.78	248.38	760.30	355.4	510.43
1:0.5+2.5	53.56	53.71	64.26	RT	292.25	123.99	319.98	240.52	159.20	256.12	762.56	338.4	505.20
1:0.5+5	57.90	56.45	63.88	RT	299.84	124.11	323.32	243.93	161.35	259.16	811.65	369.7	562.06
1:0.5+7.5	49.57	54.29		RT	290.32	118.79		232.43	158.94		790.24	298	
1:1+7.5	64.10		53.42	RT	272.48		330.45	264.81	128.51	400.60	707.53	941.6	31.25

1.5:1+7.5	**54.63**	**53.23**	**59.20**	**RT**	**282.36**	**117.89**	**319.99**	**214.83**	**158.76**	**253.90**	**983.24**	**752.1**	**733.58**
2.5:1.5+7.5	**59.38**	**68.56**	**59.29**	**RT**	**285.07**	**137.22**	**301.24**	**241.42**	**170.56**	**252.10**	**748.56**	**554.4**	**1.69KJ/g**
1:0.5+2.5	**50.83**	**51.33**	**64.39**	**80 ℃**	**295.60**	**114.47**	**319.79**	**240.62**	**155.72**	**257.52**	**1.17 kj/g**	**402.8**	**590.54**
1:0.5+2.5	**84.19**	**45.82**	**63.26**	**120 ℃**	**275.39**	**108.12**	**320.77**	**210.64**	**151.53**	**256.02**	**898.68**	**562.9**	**792.20**
1:0.5+7.5	**60.03**	**49.60**	**61.84**	**120℃**	**286**	**112.99**	**317.92**	**245.50**	**152.93**	**249.90**	**638.32**	**456.8**	**753.72**
1:0.5+2.5	**64.35**			**50 ℃**	**280.02**	**89.97**		**243.71**	**122.99**		**511.69**	**653.5**	
1:0.5+5		**53.47**	**66.53**	**50 ℃**		**120.41**	**320.31**		**158.58**	**260.08**		**466.3**	**641.64**

In Figure (4.10) represented the relation between different heating rates and peack temperature. The appearance of the exothermic peak of the resin system increases with the rate of temperature rise and moves to the right, that is, at heating rate 20 ℃/min in the direction of high temperature; with the increase in the heating rate, the curing temperature rises, the curing rate increases, and the curing time is shortened while at 25 ℃/min the peak temperature decreased.

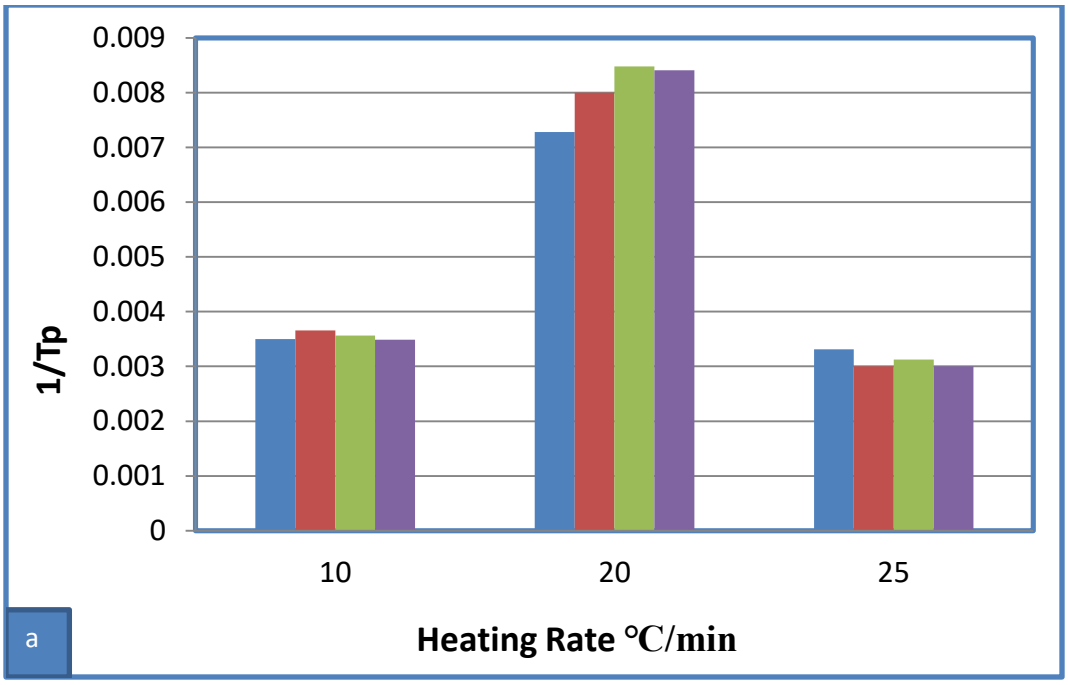
0.009
0.008
0.007
0.006
0.005
0.004
0.003
0.002
0.001
0
1/Tp
10
20
25
Heating Rate °C/min
a

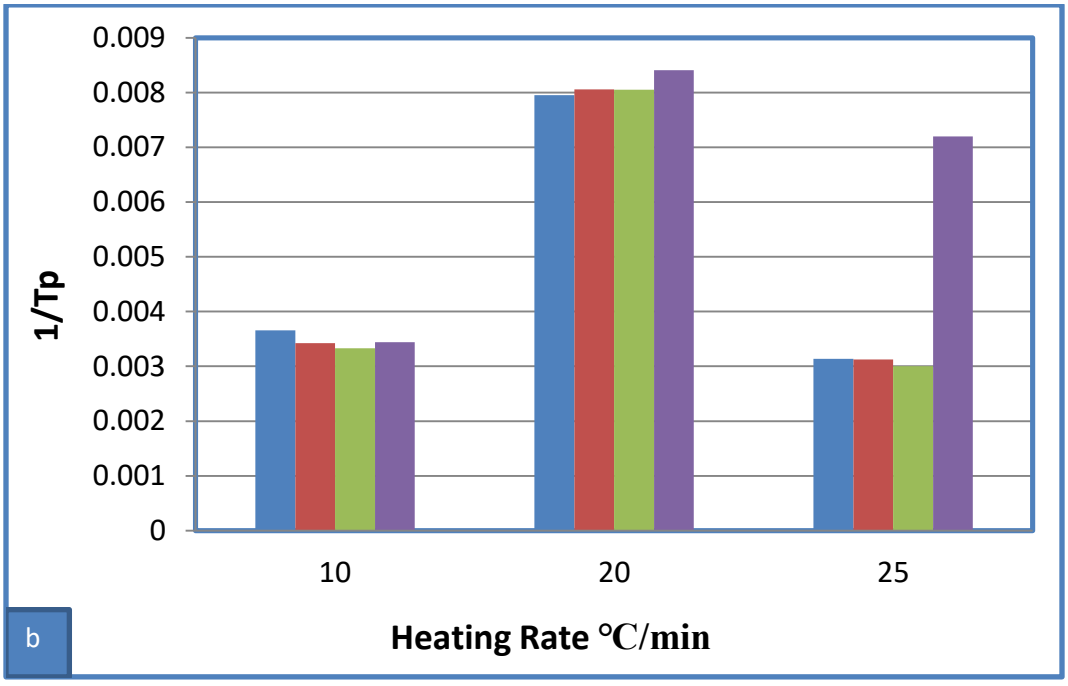
0.009
0.008
0.007
0.006
0.005
0.004
0.003
0.002
0.001
0
1/Tp
10
20
25
Heating Rate °C/min
b

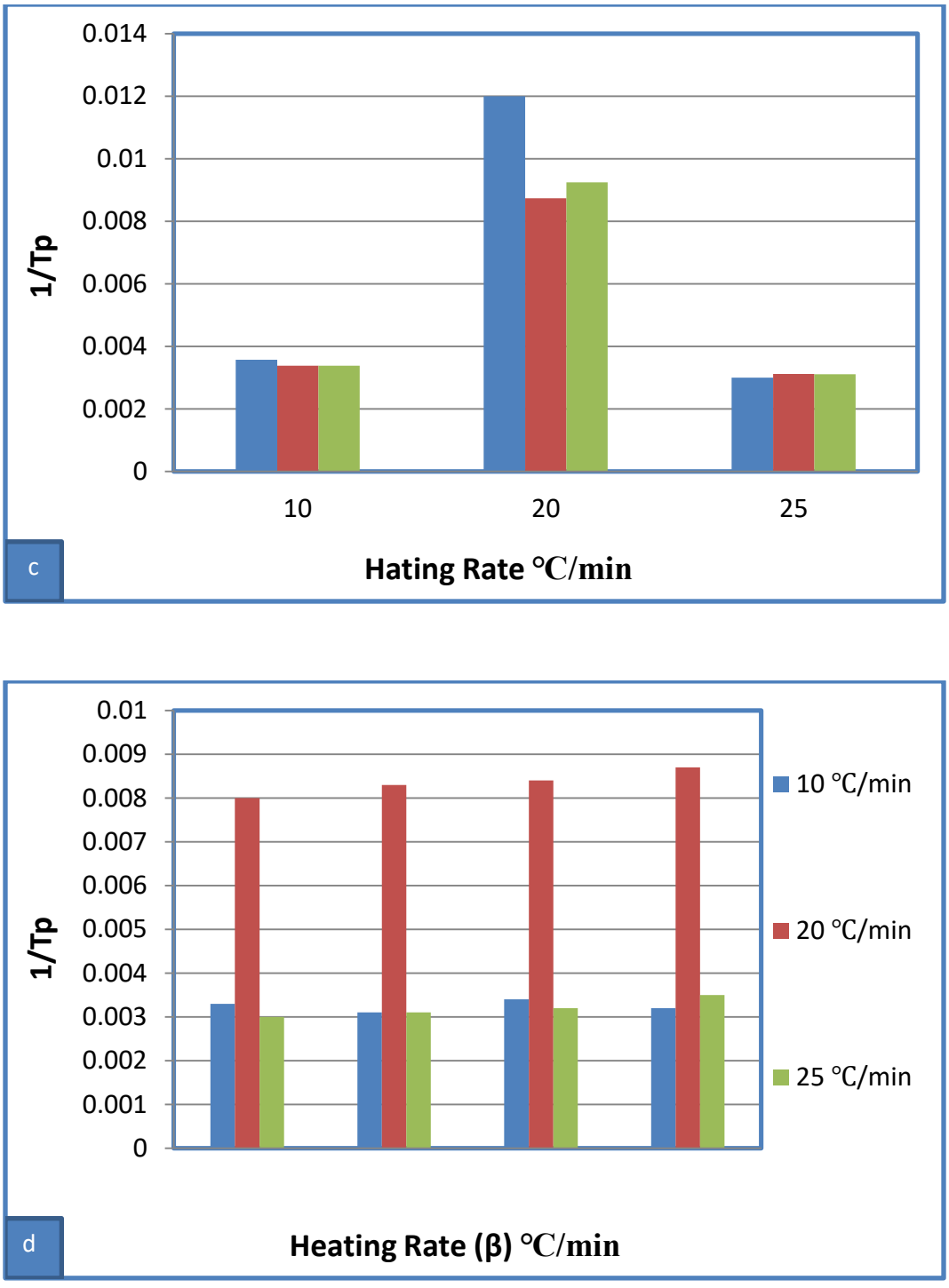

Figure (4.10) : Relation between (1/Tp) with different heating rate for different samples.

4.4 TGA Results

In Figure (4.11) illstrutes the TGA decomposition information can be used to predict the useful product lifetimes of some polymeric materials, such as the coatings for electrical or telecommunication cables, one of the most important applications of TGA is the assessment of the compositional analysis of polymeric blends.

Table(4-6): Ratios of total mass loss of different samples curing at different temperatures.

wt. %	Curing Temperature°C	Total weight loss %
1:0.5	**RT**	**41.68**
1:0.5+2.5 PS	**RT**	**41.68**
1:0.5+5 PS	**RT**	**44.29**
1:0.5+7.5 PS	**RT**	**35.91**
1:0.5+ 2.5 PS	**50**	**40.97**
1:0.5+5 PS	**50**	**44.15**
1:0.5+2.5 PS	**80**	**38.51**
1:0.5+2.5 PS	**120**	**35.91**
1:0.5+7.5 PS	**120**	**68.92**
1:1+7.5 PS	**RT**	**59.82**
1.5:1+7.5 PS	**RT**	**57**
2.5:1.5+7.5 PS	**RT**	**66.87**

Based on the Table (4-6), it was determined that 1:0.5+2.5 weight percent PS cured at 120°C had the best thermal stability value and the least amount of mass loss compared to the total weight when the curing

temperature was varied this could be explained by the amount of thermoplastic that was added, may be slows down the rate of decomposition, and reduction the epoxy resin's stiffness and brittleness these properties will affect the epoxy resin's mechanical characteristics, as will be demonstrated later.

While the elongation rises, these numbers compress to the Tg value as it lowers, since a reduction in Tg results in a loss of toughness and strength, in contrast to the standard value of epoxy, which has decreased due to a number of variables.

The phase separation of combined compounds resulted in two values of Tg in certain samples. First, pure epoxy resin usually undergoes two stages of heat degradation, the first one happened between 150℃ and 280 °C and was possibly brought on by the breakdown of the end hydroxyl group of epoxy resin that had been polyamine-cured and the generation of olefins the second stage of degradation became apparent at 335 °C, indicating the disintegration of the bisphenol-A group as the values grow, there is a weight loss in multiple regions as shown in Figure (4.11) below.

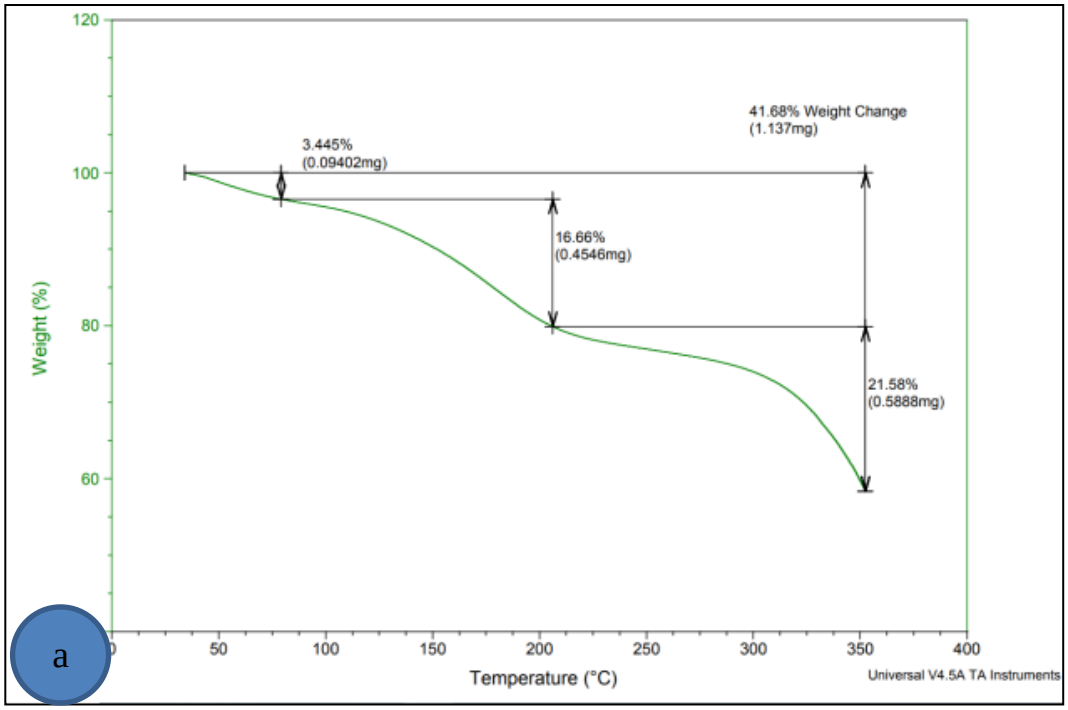
120
100
80
60
Weight (%)
41.68% Weight Change
(1.137mg)
3.445%
(0.09402mg)
16.66%
(0.4546mg)
21.58%
(0.5888mg)
50
100
150
200
250
300
350
400
Temperature (°C)
Universal V4.5A TA Instruments
a

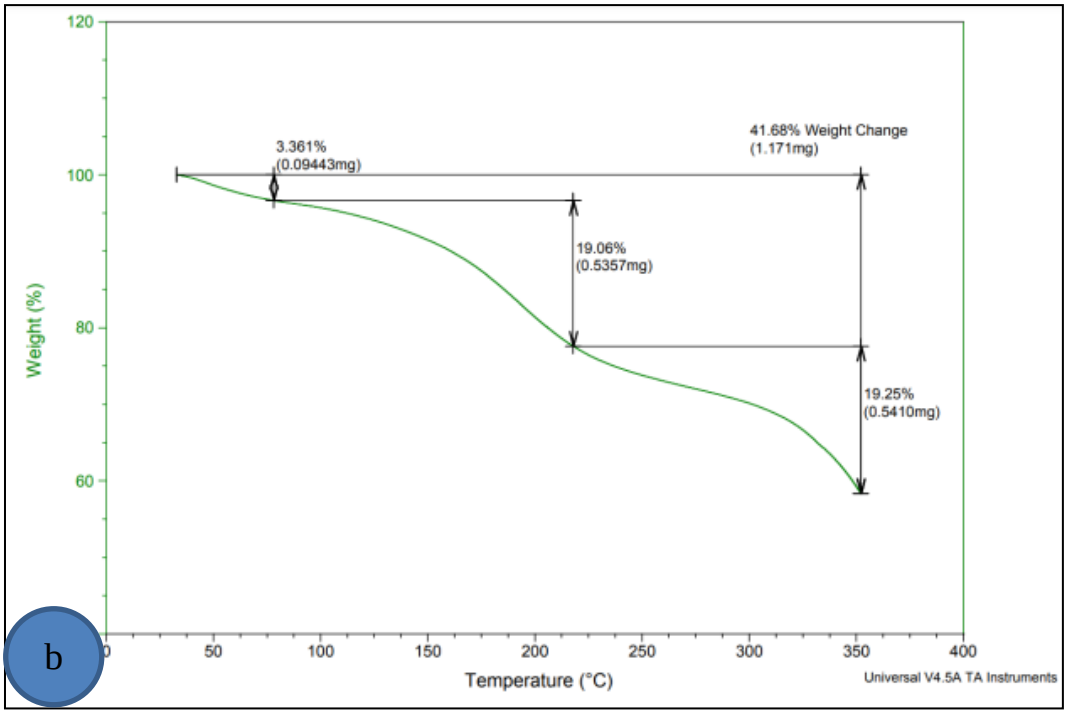
120
100
80
60
Weight (%)
41.68% Weight Change
(1.171mg)
3.361%
(0.09443mg)
19.06%
(0.5357mg)
19.25%
(0.5410mg)
50
100
150
200
250
300
350
400
Temperature (°C)
Universal V4.5A TA Instruments
b

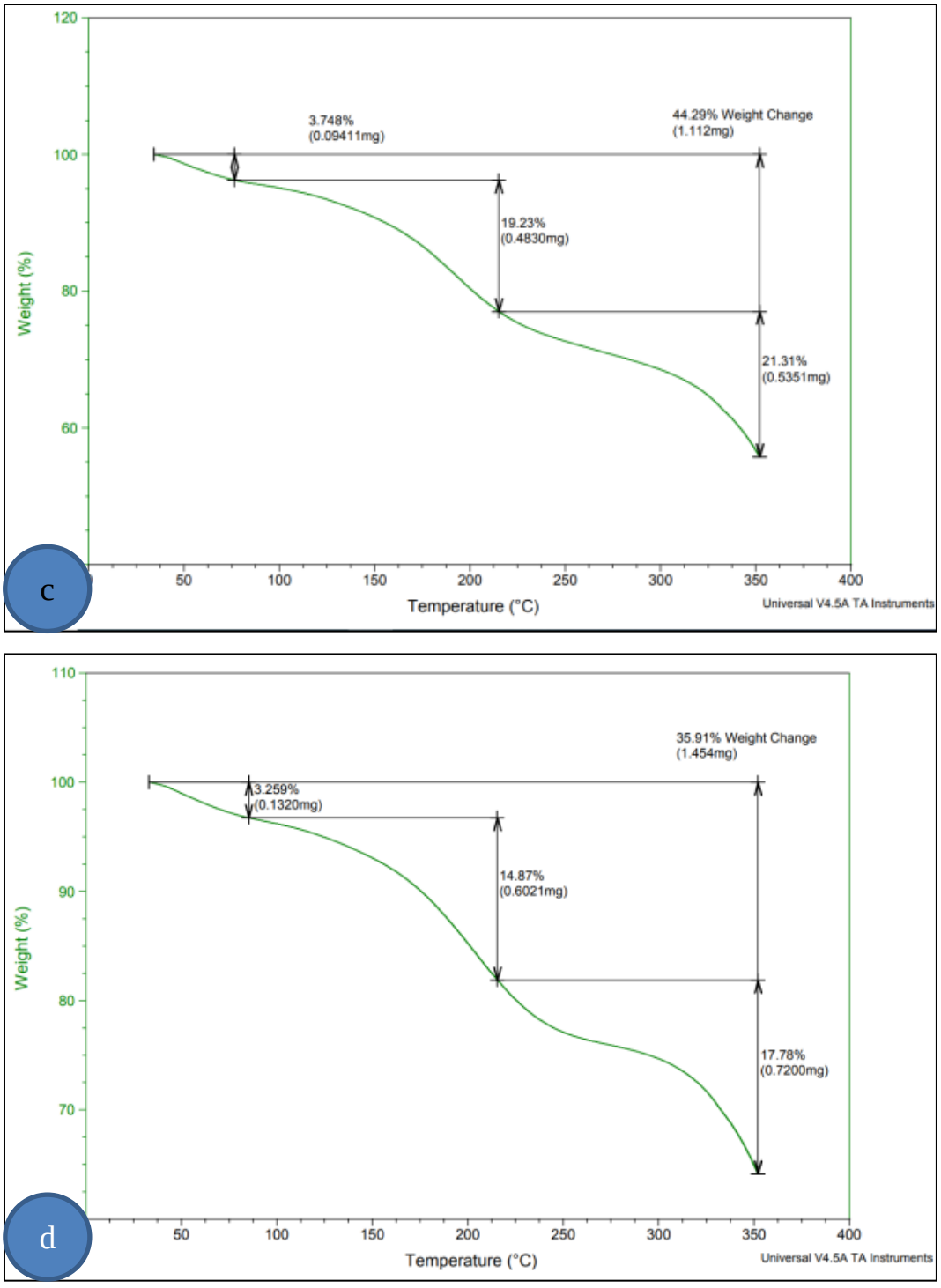

Figure (4.11): Represent TGA charts of samples of a:1:0.5 , b: 1:0.5+2.5 wt.% PS, c: 1:0.5 + 5 wt.% PS and d:1:0.5+7.5 wt.% PS cured at RT.

In order to that there is relation between thermal stability and pot life of the mixed resin also related to the worakability regine of the material

begins when the resin and hardener are mixed it is shorter at high temperatures and longer at low temperatures the greater the quantity mixed, the shorter the pot life, to obtain longer workability at high temperatures, the mixed resin may be divided into portions another method is to chill components A+B before mixing them (not below +5 °C).

In order to determine the workability, the thermal decomposition rates of epoxy and epoxy/Polystyrene systems were calculated using TGA. The higher the provided decomposition temperature, the faster the applied heating rate. With this method, the polymer decomposition process is linked to temperature and time, and the decomposition kinetics may be modelled using this data.

Thermal stability of a material is the primary criterion for establishing the limit of working temperature of a material and the ambient conditions for safer usage, the test was conducted in a nitrogen flow at a temperature ramp rate of 20 °C/min. It has to do with the material's thermal decomposition temperature and rate of breakdown.

The sample's extraction of moisture and volatiles, which causes the sample to begin losing weight, is seen in the first region below 120 ℃ If continue the test until 300 °C, the primary degradation process should conclude around 200-300 °C as predicted, it begins in the 210–230 °C temperature range this stage which concludes with a tiny hump in the curve could be categorised as the first rapid decline stage.

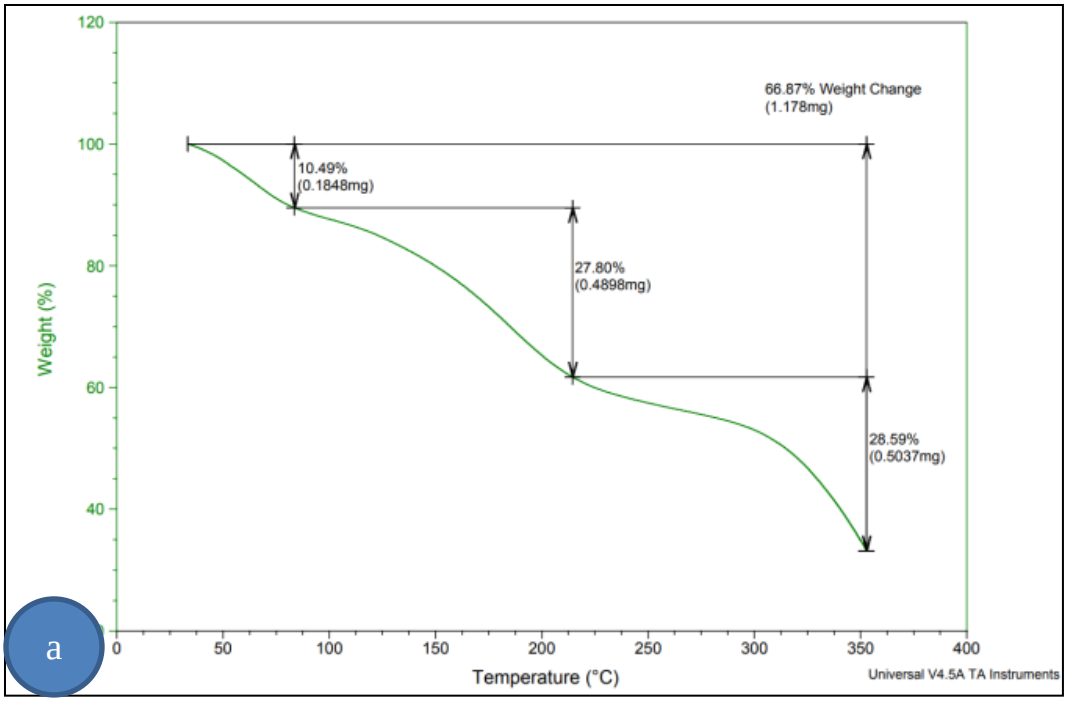
66.87% Weight Change
(1.178mg)
10.49%
(0.1848mg)
27.80%
(0.4898mg)
28.59%
(0.5037mg)
Weight (%)
Temperature (°C)
Universal V4.5A TA Instruments
a

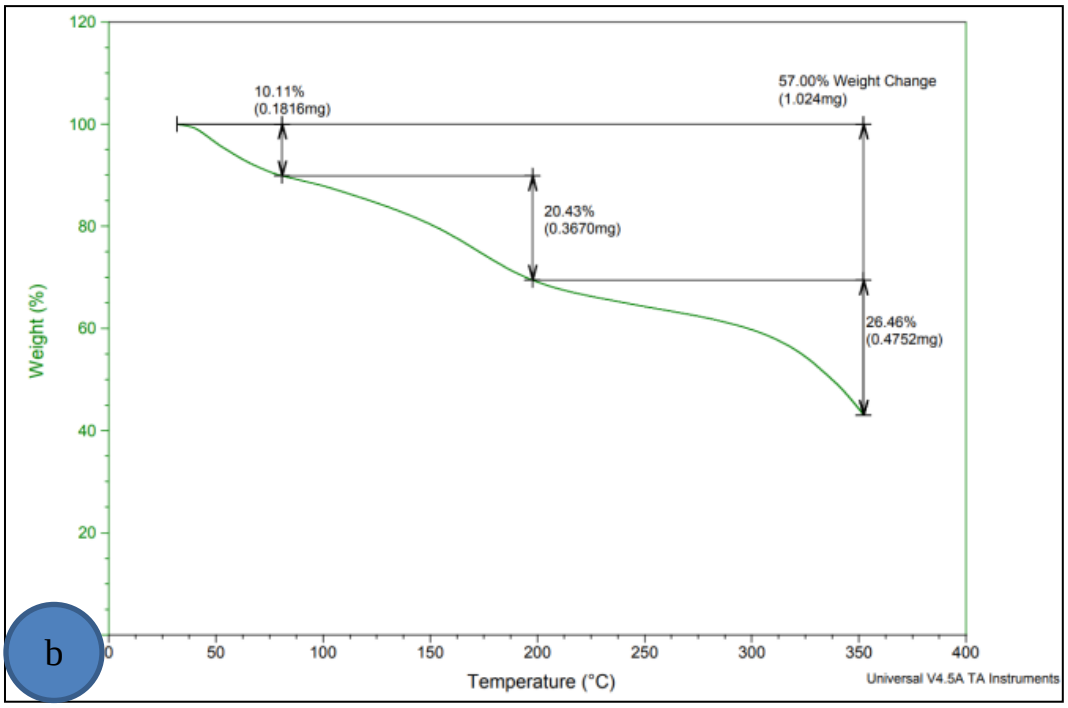
57.00% Weight Change
(1.024mg)
10.11%
(0.1816mg)
20.43%
(0.3670mg)
26.46%
(0.4752mg)
Weight (%)
Temperature (°C)
Universal V4.5A TA Instruments
b

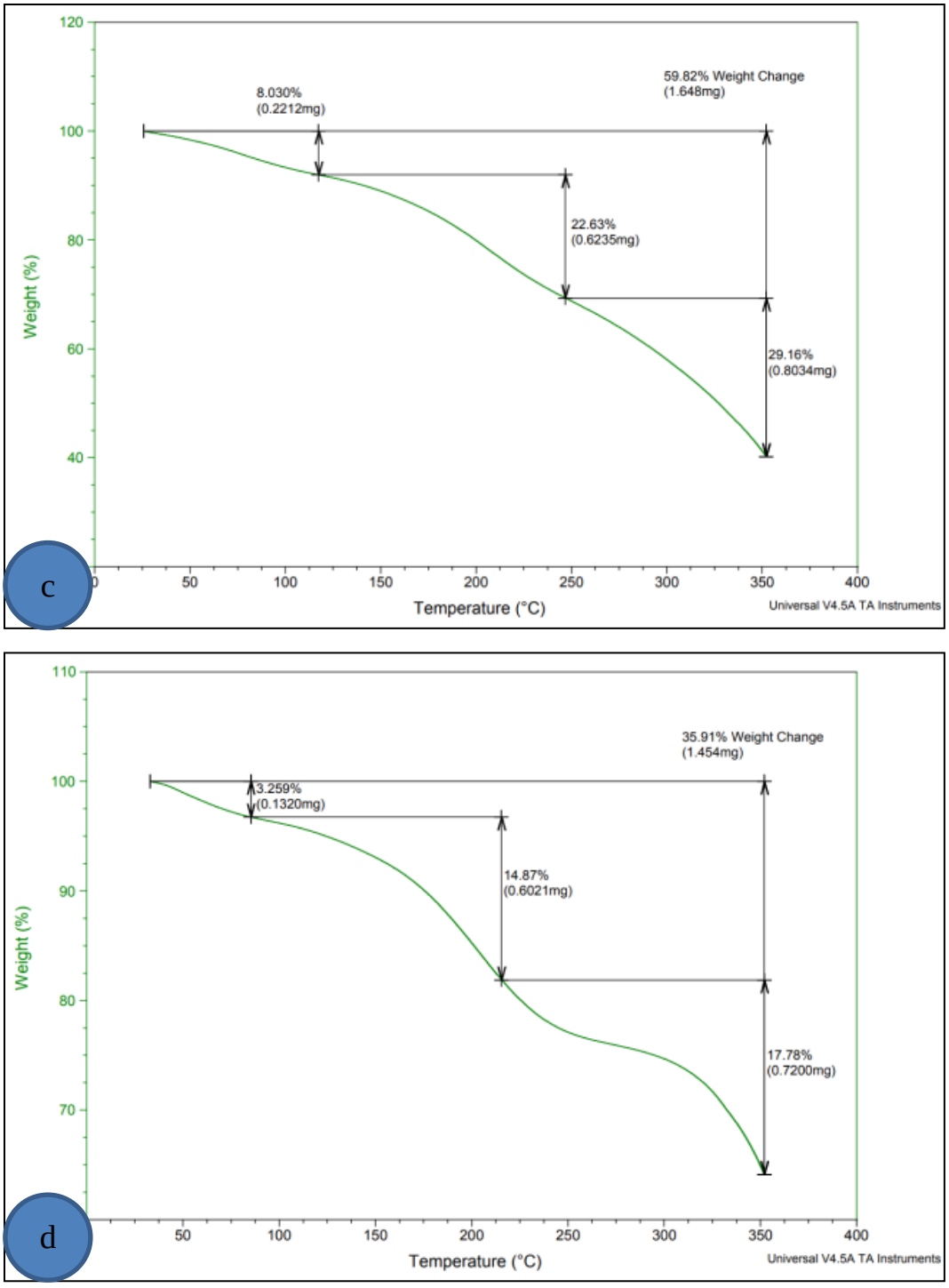

Figure (4.12) : Represent TGA chart of samples of a: 1.5:1 + 7.5 wt.% PS, b:2.5:1.5+7.5 wt.% PS, c: 1:1 + 7.5 wt.% PS and 1:0.5+7.5 wt.% PS Cured at RT.

The mass loss during the first stage of thermal decomposition was 10.49% at temperatures close to 100 °C in Figure (4.12) above for sample

2.5:1.5+7.5 wt.% PS that was cured at room temperature for 24 hours as the temperature rose past 200 °C, the decomposition accelerated and produced mass losses of 27.8% and 28.59% before the material charred as sample 1.5:1+7.5 wt.% PS curing at room temperature for 24 hours is shown in Figure (4.12), the decomposition starts before it reaches 100℃ with a mass loss of 10.11% and continues until it reaches 200℃, at which point it loses 20.43% of its mass when it reaches 350, the mass loss has increased to 26.46%.

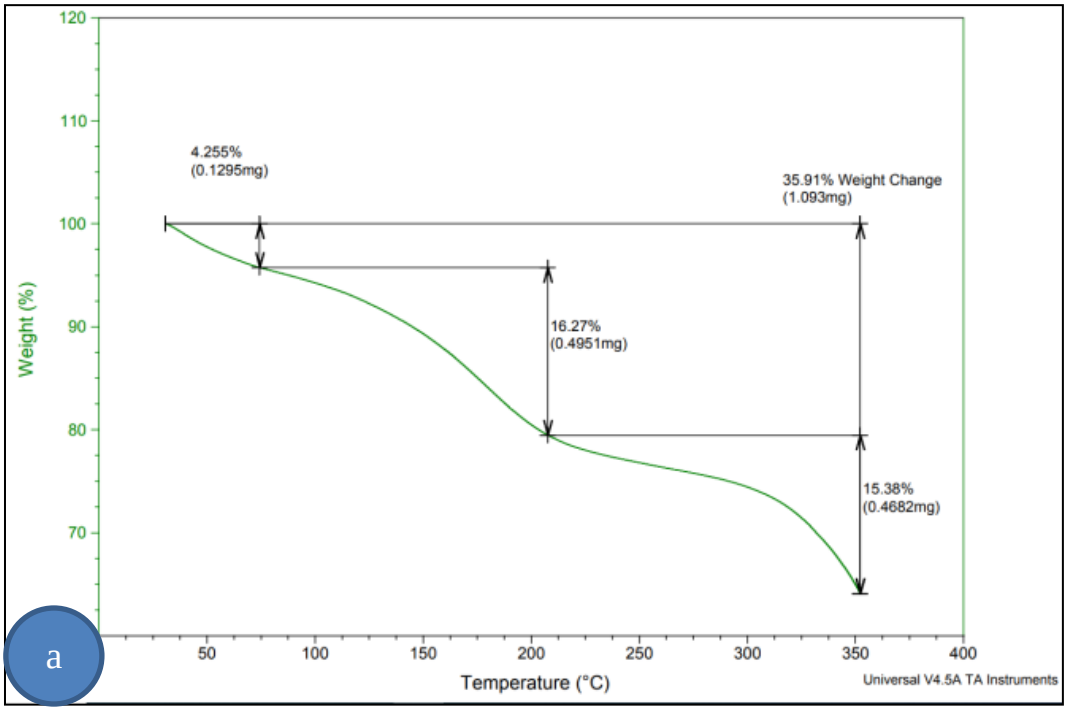

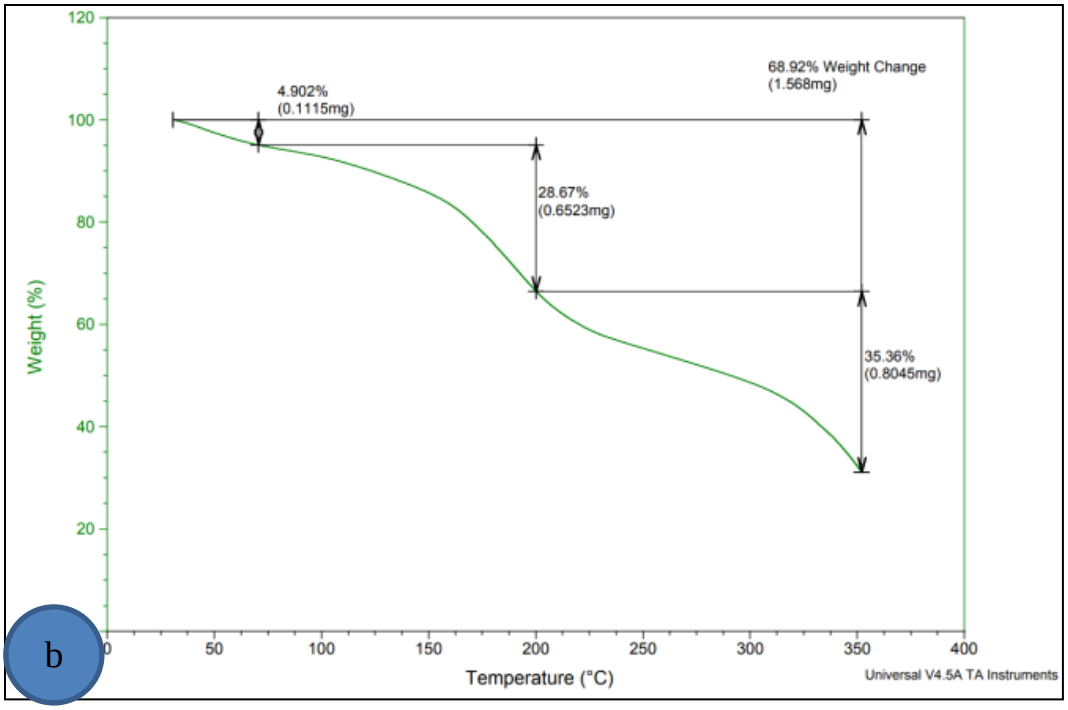

Figure (4.13): Represent TGA chart od samples of a: 1:0.5+2.5 wt.% PS and b: 1:0.5 + 7.5 wt.% PS curing at 120 ℃.

In Figure (4.13) In contrast, sample 1:0.5+7.5 wt.% PS curing at 120°C for 4 hours in the first in the middle between 50°C and 100°C the mass loss was 4.902%, which is lower and steady until it approaches 200℃ the mass loss rising to 28.67% and then 35.36% above the low point of 350°C this abrupt drop in mass loss could be explained by the possibility that the cross linking between the polymer chain and toughening may not have had enough time to occur during the 120°C curing process.

The mass loss for the sample 1:0.5+2.5 wt.% PS curing at temperature 120 °C for 4h is (4.255% first stage- 16.27% second stage- 15.38% third stage), as can be seen in comparison to the sample 1:0.5+2.5 wt.% PS curing at temperature 80 °C for 4h in Figure (4.14) the mass loss for the sample is displayed in three steps (3.203%-19.23%-16.08); and in between 50 and 100 °C is the temperature range where the mass loss is first observed the first stage (4.217%) between 200 ℃ and 250 °C was the

temperature at which the mass loss occurred in the second stage. 19% of all the sample 1:0.5+5 wt.%PS cured at room temperature is represented by (3.748% - 19.23% and 21.31%) in the three degradation phases for the sample treated 1:0.5+2.5 wt.% PS cured at RT the three stages of degradation are represented by (3.361% - 19.06% and 19.25%). The thermal deterioration of a cured at 350 °C in a pure epoxy sample is given by (20.68%). The mass loss was (8.030%–22.63% and 29.16%) for sample 2:2+7.5% PS cured at RT, as indicated in in Fig.(4.12), at three phases (3.445%–16.66% and 21.58%).

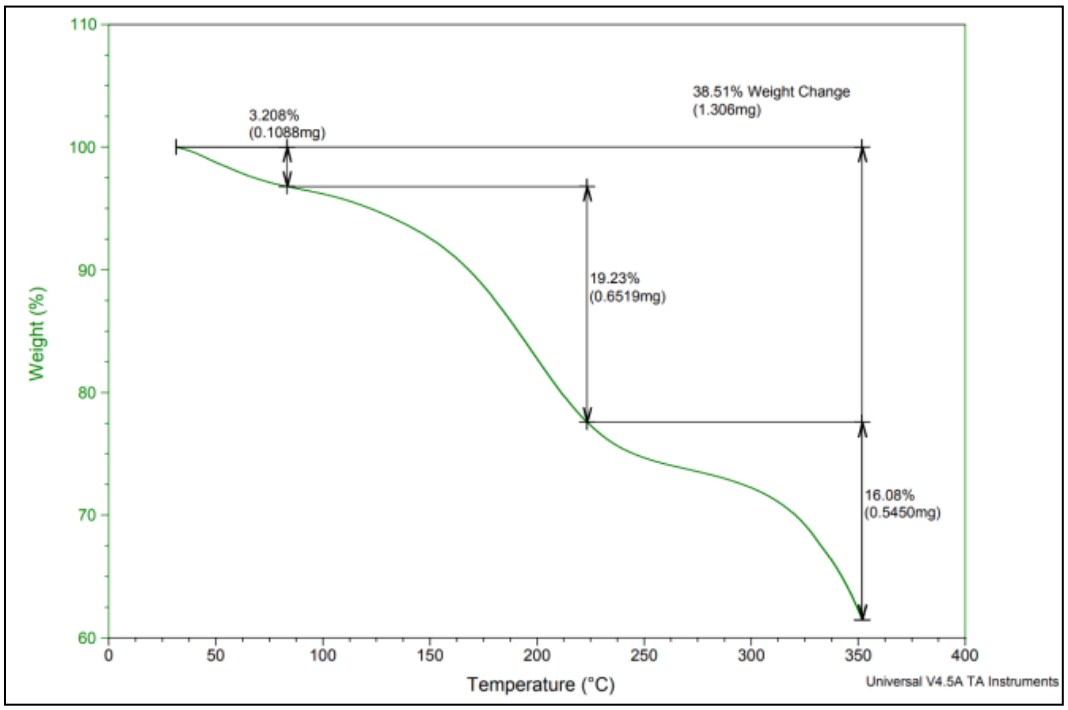

Figure (4.14): Represent TGA chart of sample 1:0.5+2.5 wt.% PS cured at 80 ℃.

In Fig.(4.15) the three stages of degradation of PS (1.605%-17.74% and 21.62%) were cured at 50℃ for 4 hours the samples that were cured had may be enough time to fully complete the cross-linking or curing process showed little mass loss in the beginning for pure and low PS content after reaching above 200℃, but started losing mass quickly until it charred,

while the PS content was 7.5 wt.% by weight in the first step much and increasing unlit reach 350 ℃ after that charred this differences in degradation was according to that in the first step the loss of mass consider as solvent when the temperature between 50 ℃-100 ℃ as think when the temperature skip the 100 ℃ mild or aromatic ingredients decomposing until the temperature reach from 200 ℃ – 350 ℃ the real decomposition of material start which considers the temperature of starting is the onset of actual decomposition of material until reach the completely loss of mass at 350 ℃ or over this temperature with this differences of mass losing is related also with Tg and mechanical properties, Polymer degradation behavior was investigated by TGA; it was observed that the mass loss started at 260 ℃, reaching a maximum degradation temperature at 350 ℃, which is attributed to main-chain pyrolysis similar to [90].

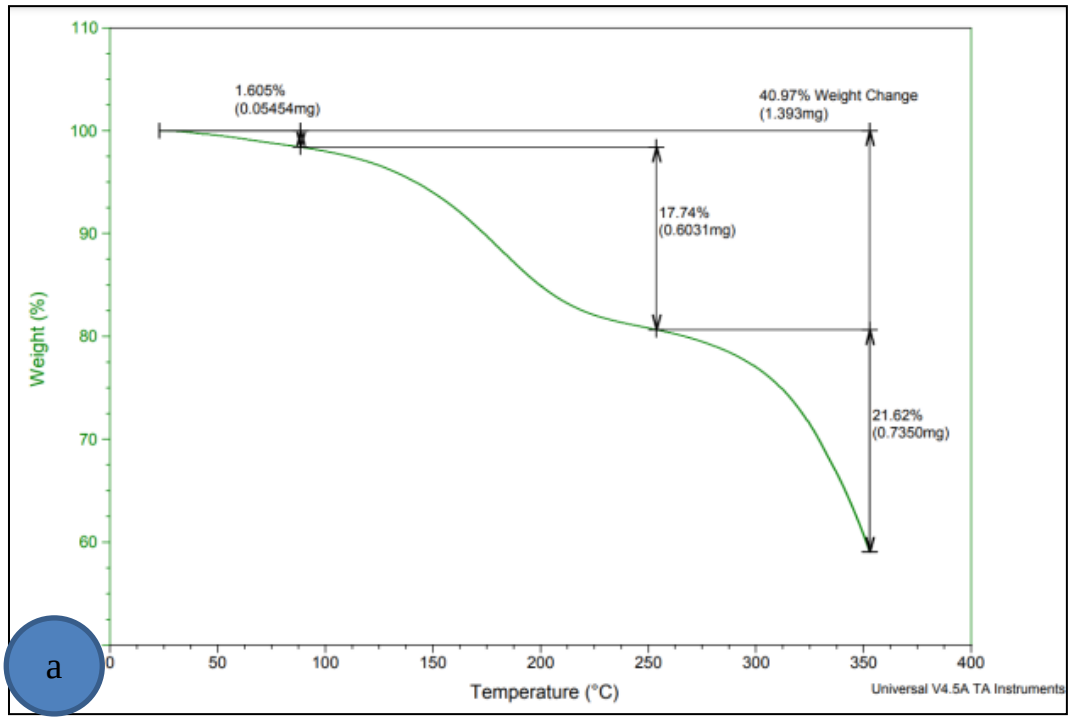

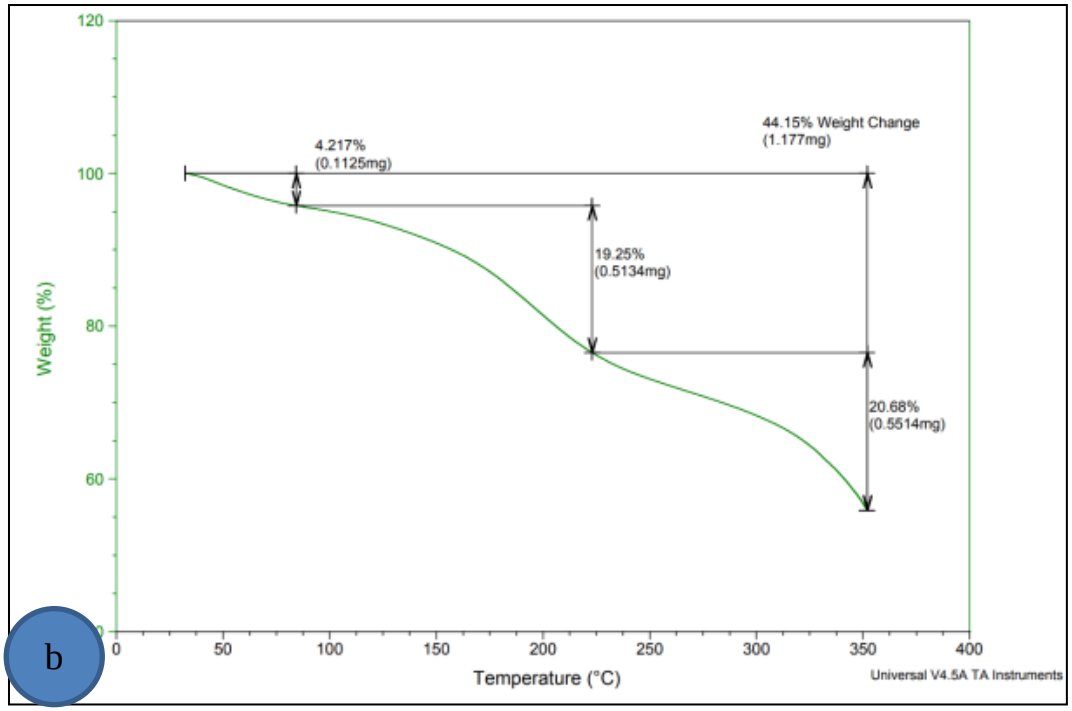

Figure (4.15): Reperesent TGA chart of samples a: 1:0.5 + 2.5 % wt. PS and b:1:0.5 + 5 wt.% PS cured at 50 ℃.

The early degradation up to 300°C showed a distinct pattern for every one of blends. The relative mass losses were as follows in order to assess the thermal stability: Between 0 and 100 °C, 27.80% between 200℃ and 250 °C, and between 350 and 400 °C, 28.59% This indicates that between 330 and 400 °C is when polymer breakdown happens most frequently it is clear from the data that the epoxy's heat breakdown profile is represented by owing to the altered linkage between epoxy and polystyrene, epoxy is more stable during the test's first stage, losing mass at (3.445%, 3.361%, 3.74%, 3.2%, and 3.2%) for all samples below with varying ratios and curing temperatures however, as temperatures increased during the middle stage, the mass loss increased (16.66%, 19.08%, 19.23%, 14.87%, and 19.23%) for all samples, and in the test's final stage (0-350°C).

In the second major stage, the polymer deteriorated very efficiently due to the destruction of the three-dimensional cross-linking skeleton and

the breakdown of the polymer's backbone carbon chains at various points along the chain.

This breakdown of weaker linkages, such as epoxy's dehydration, hydrogen bonds within and between backbones, and the interaction between epoxy and polystyrene, may be the cause of the increased rate of weight loss that is correlated with an increase in the percentage loading of PS similar to [53].

The final product's end use qualities (such as thermal expansion, stiffness, and damping) can be greatly influenced by the PS level. The final product's end use qualities (such as thermal expansion, stiffness, and damping) can be greatly influenced by the PS level.

The thermal stability of epoxy pure and its mixes is demonstrated in the preceding figures in the temperature range of 0 to 120 °C however, the rate of deterioration increases with increasing temperature up to 350 °C, at which point the sample would burn.

These results suggest that the thermal stability of the composite improved in the first step and to some extent in the second stage the following conclusions were drawn from these observed phenomena: in the first stage, the rate of degradation of the resin chain's epoxy cross-linking network is significantly higher than the rate of carbon-carbon bond breaking; in the second stage, the rate of degradation will be much higher, leading to an increase in activation energies and decomposition entropies; and in the final stage, a trend similar to the first stage is evident, with the exception that gasification aggrement with [53].

4.5 FTIR Results

FTIR was utilised to assess the degree of reaction of the epoxy groups in the thermosets that were allowed to cure for 24 hours and for 4 hours at RT in order to look into the integrity of the cross-linked network structure further. The FTIR spectra of neat polystyrene, hardener, and uncured resin are displayed in Figures (4.16), accordingly, for the purposes of simplification and comparison.

The oxirane ring's characteristic vibration in the resin sikadur-LP can be detected at 910 cm^{-1}, the O-H bending vibration at approximately 3400 cm^{-1}, and the stretching vibration of the C=C aromatic ring at 1506 cm^{-1}. The kinetics of epoxy-amine reactions have also been extensively studied using FTIR spectroscopy. Generally, the near-infrared wavenumber range absorption band intensity changes are used to track the reaction similar with [31]. The system was examined for potential reactive sites or functional groups in order to comprehend the chemistry of potential reactions taking place in the formulations.

First, the uncured resin epoxy group was at 910.40 cm^{-1}, and at 833.25 cm^{-1}, also that the peak intensity of the absorptions for the epoxide ring stretching had decreased, at these two peak numbers (833.25 cm^{-1} and 910.40 cm^{-1}), a decrease in the normalised peak intensity denotes a decrease in the epoxide group concentration similar with [91]. In order to demonstrate a decrease in peak intensity or an increase in accordance with the ratio as will be explained later, the epoxy/hardener ratio must be adjusted. Further investigation is needed to see whether any new bond results or bond shifting is evident from the wavenumbers associated with the vibrational spectra of the various groups found in the sample: a large

peak resulting from O-H group stretching is seen between 3400 and 3600 cm^{-1}.

Furthermore, epoxy and amine conversions cannot be individually determined by DSC, which only offers an overall conversion degree. Conversely by band integrating the matching infrared signals (epoxy and amino), infrared spectroscopy makes it possible to determine both conversions extremely accurately, this is because the integration error is low and the values obtained at high conversions are more precise, based on the reaction mechanism the amount of reaction can be expressed in terms of epoxy groups (α) and N-H bonds (β) derived from the oxirane ring and N-H absorption regions, respectively. where (t) denotes a specific reaction time stands for epoxy, N-H amine, and (0) initial while working in the near range yields more accurate findings, epoxy and amino groups have absorptions in the mid-range.

- For the formulation 1:0.5 pure sample cured at RT,

$$\alpha_e = 1-(A_{e(0)} - A_{e(t)} / A_{e(0)}) = 1- ((910.40)-(933.55)/(910.40)) = 0.9745 \text{ [92]}.$$

$$\beta_{N-H} = 1-(A_{N-H(0)} - A_{N-H(t)} / A_{N-H(0)}) = (3363.86)-(3425.58)/(3363.86) = 0.99 \text{ [92]}.$$

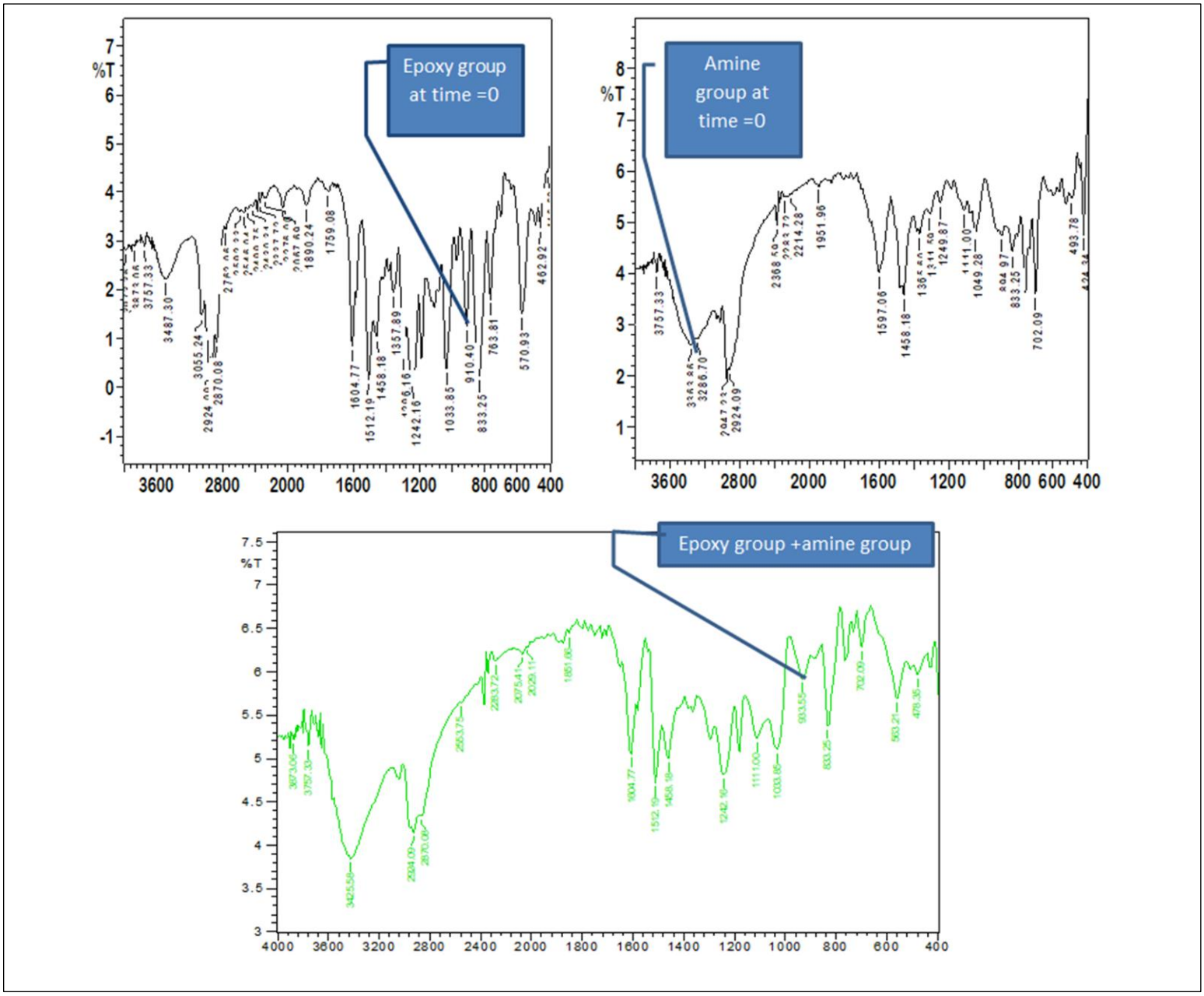

Figure(4.16): FTIR Spectrum of Uncured Resin - hardener and cured epoxy.

Another parameter was also can calculated in order to quantitatively analyze the curing extent of epoxy resin by IR, the internal standard method was taken in this research. Internal standard was the characteristic absorption peak of benzene ring in at 1604.77 cm $^{-1}$. Thus, the ratio of absorbance values at 910 cm $^{-1}$ and at 1604.77 cm $^{-1}$ could be used to

represent the conversion extent of epoxy groups. The curing degree of epoxy resin (α) could be calculated as equation bleow similar with [93]:

$$\alpha = [1- \{(A910)(A1604.77)_t/(A910)(A1604.77)_0\}]*100 \text{ [93].}$$

So that can ably this eq. on FTIR spectrum that give a %T as shown:

$$\alpha= 1-((933.55)(1604.77)_t/(910.40)(1604.77)_0) = -0.02542*100=-2.542$$

Another concept that related to FTIR was one of the most common analytical techniques to monitor oxidation reactions is FTIR spectroscopy to observe changes in the carbonyl band (C = O) which has given rise to a method called the carbonyl index (CI) in other word FTIR analysis is capable of monitoring other chemical changes that take place throughout the lifetime of a material, by detecting the functional groups present at distinct bands.

The CI is used to specifically monitor the absorption band of the carbonyl species formed during photo or thermo-oxidation processes in the range of 1850–1650 cm^{-1}, by measuring a ratio of the carbonyl peak relative to a reference peak. This parameter capable for used to measure oxidation occurring throughout the lifetime of epoxy resin , but it is also employed to predict their service life and to develop stabilization additives for materials.

Carbonyl index [CI= Area of absorption peak of carbonyl bond / Area of absorption peak for reference bond] since absorption, A = 1/transition T so able to connect and benefit from these spectrum of FTIR. Also a carbonyl index can be calculated from a FTIR spectrum by analyzing the peak that indicate the presence of carbonyl groups and comparing it with a

reference peak that does not change as the polymer degrades as shown in Figure (4.17) from observation to detect CI we noticed that carbon storage at RT is more than in sample cured at 120 ℃ while C=O(carbonyl) is more at 120 ℃. This factor also definition as ratio between absorption intensities of C=O and CH_2. It's a kind of expression to talk about hydrophillicity of polymers.

The FTIR spectra indicate the possible intramolecular hydrogen bonding interactions that may arise from combining the epoxy matrix with the identifiable hardener peaks at around 3487.30 and 3425.58 cm^{-1} for hydroxayl and amine groups, and around 910.40 cm^{-1} for epoxy groups, are attributed to the various functional groups of epoxy (EP) in which when hardener added to epoxy for curing process these peaks shifted to 925.83 cm^{-1} and 933.55 for epoxy group and only one of amine group (N-H) still at here position according to this one of them is connected to epoxy group and the characteristic absorption peak of benzene ring located at 1607 cm^{-1} and kept stable in curing process if the curing agent had no aromatic ring peaks at Table (4.7) similar with [94]:

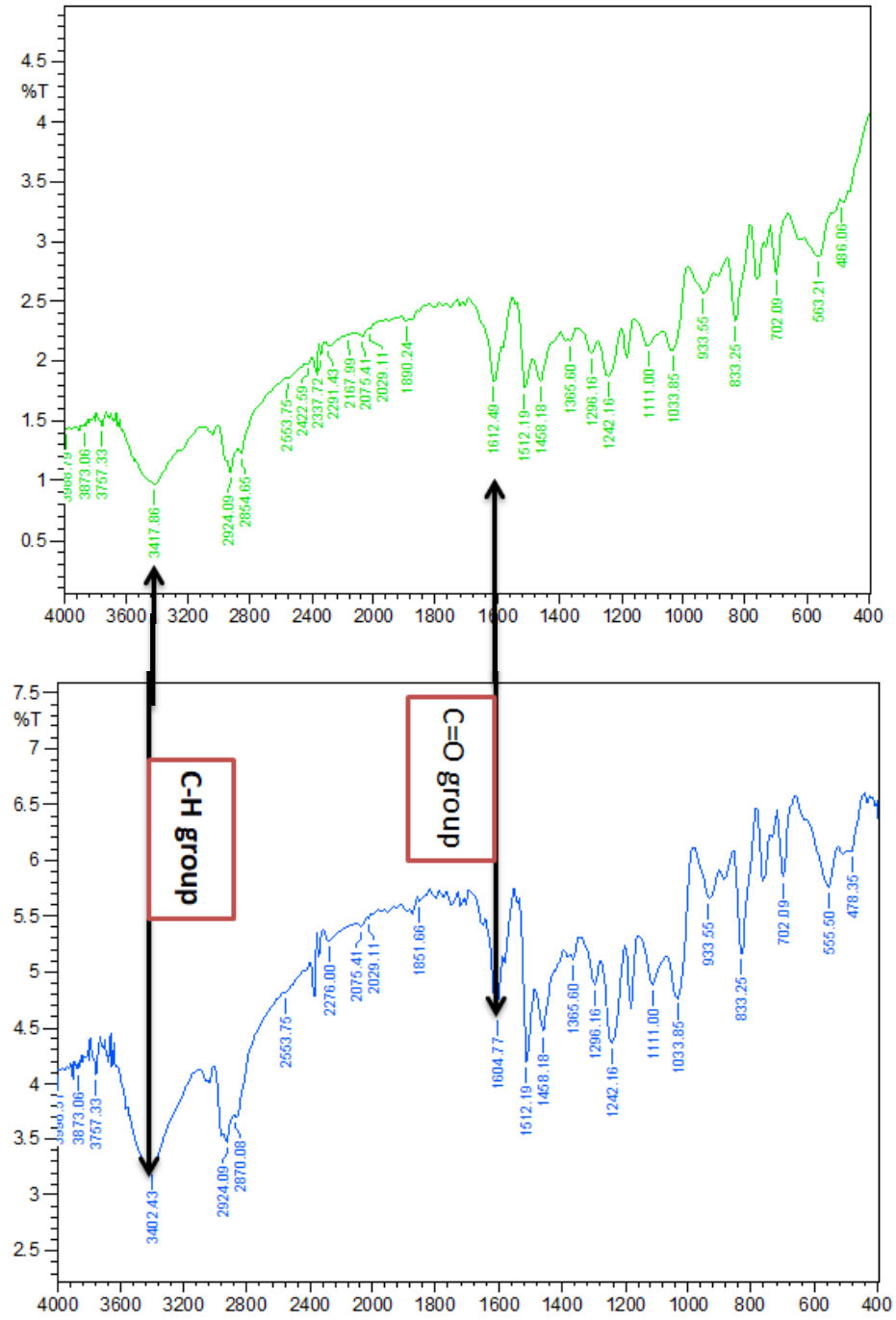

Figure (4.17):FTIR spectrum of sample (1:0.5+2.5 wt.% PS) cured at RT and 120°C.

FTIR spectra of a sample displayed bands in the region from 2600 to 3000 cm^{-1}, which are characteristic of the C–H group stretching and bending vibrations.

Table (4-7): Represent the FTIR peaks.

3500-3400 cm^{-1}	medium N-H stretching primary amine.
3400-3300 cm^{-1}	medium N-H stretching primary amine.
3330-3250 cm^{-1}	medium N-H stretching aliphatic primary amine.
3350-3310 cm^{-1}	medium N-H stretching secondary amine.
3054.89 cm^{-1}	symmetrical & asymmetrical C-H stretch in aromatics.
2966.18 cm^{-1}	asymmetrical C-H stretch of $–CH_3$ group.
2927.61 cm^{-1}	asymmetrical C-H stretch of $–CH_2$ group.
2871.68 cm^{-1}	symmetrical C-H stretch of $–CH_3$ group.
1606.52 cm^{-1}, 1581.44 cm^{-1}, 1508.16 cm^{-1} and 1456.09 cm^{-1}	C-C stretching vibration in aromatic.
1296.01 cm^{-1}	asymmetrical $–CH_2$ deformation.
1245.87 cm^{-1}	asymmetrical aromatic C-O stretch.
1184.16 cm^{-1}	asymmetrical aliphatic C-O stretch.
1033.72 cm^{-1}	symmetrical aromatic C-O stretch.
970.08 cm^{-1} - 914.15 cm^{-1} and 862.03 cm^{-1}	epoxide ring vibrations.(characteristic peak)
829.29 cm^{-1}	CH out of plane deformation in aromatic.

460-580 cm^{-1}	characteristics frequency of C6H4X2-para. (X represents any functional group).

FT-IR spectroscopy was carried out in wavelengths of 4000–400 cm^{-1} . The most important functional group of this compound, is the epoxy group which has an absorption peak in 910 cm^{-1}.

The absorption bond of 1188.15 cm^{-1} represents the presence of C–O stretching of aromatic rings and the peak around 3487.30 cm^{-1} indicates the hydroxyl groups of epoxy resin.

Two absorption peaks at 2924.09 cm^{-1} and 2870.08 cm^{-1} are assigned to the stretching CH_2 and CH of aromatic and aliphatic, Absorption peaks appeared at 1512.9–1573.91 cm^{-1} and 1242.16 cm^{-1} are characteristic peaks of aromatic C═C bonds and phenols group. The peaks at 1033.85 and 833.25 cm^{-1} are also related to stretching C–O–C of ether and stretching C–O–C of oxirane groups, Moreover, vibration bond at 1458.18 cm^{-1} corresponds to methylene groups similar with [95].

PS spectrum is characterized by the disappearance of the signal at 1683 cm^{-1} corresponding to C=C double bond stretching vibration of styrene vinyl group. Also, signals between 3000–2780 cm^{-1} associated to C–H bonds stretching modes became more intense due to the polymer backbone formation.

Finally a slight shift of C–C aromatic stretching modes towards higher wavenumbers can be observed and can be explained by a lower mobility of these aromatic carbons as the polymer is formed similar with [90].

In the FTIR spectra, the absence of a peak at 910 cm^{-1} (indicating complete cure) and a shoulder at 3620 cm^{-1} (ruling out the presence of free hydroxyl groups) in the hydroxyl groups formed by the epoxy-amine curing reaction are of particular interest this indicates that the majority of secondary hydroxyl groups produced by the curing reaction participate in intramolecular hydrogen bonding interactions.

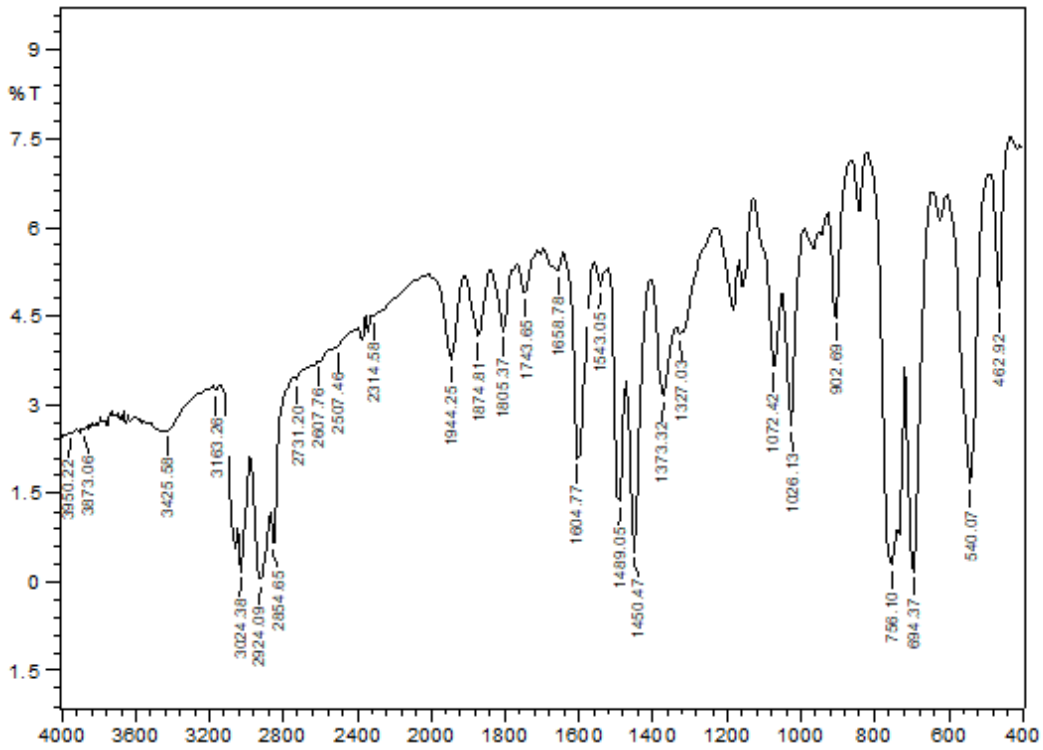

Figure (4.18): FTIR spectrum of polystyrene.

In Fig.(4.18) obviously, in polystyrene FTIR chart there are several absorption peaks within the involved wavenumber range. There are absorption peaks at the wave numbers of 3024.38 due to aromatic C-H stretching vibration absorption and there are three absorption peaks at the wave numbers of 1604.77 cm^{-1}, 1489.05 cm^{-1}, and 1450.47 cm^{-1} due to

aromatic C=C stretching vibration absorption. These absorption peaks indicate the existence of benzene rings.

The absorption peaks at the wave numbers of 756.10 cm^{-1} and 694.37 cm^{-1} correspond to C-H out-of-plane bending vibration absorption and indicate that there is only one substituent in the benzene ring. absorption peaks at the wave numbers of 2924.09 cm^{-1} and 2854.56 cm^{-1}, corresponding to the existence of methylenes.

These FTIR results have confirmed that the styrene reacts to produce polystyrene through polymerization reaction. In addition, the absorption peaks at the wave number of 3425.58 cm^{-1} is for the stretching vibration absorption of O-H, which indicates the existence of hydroxyl similar with [96].

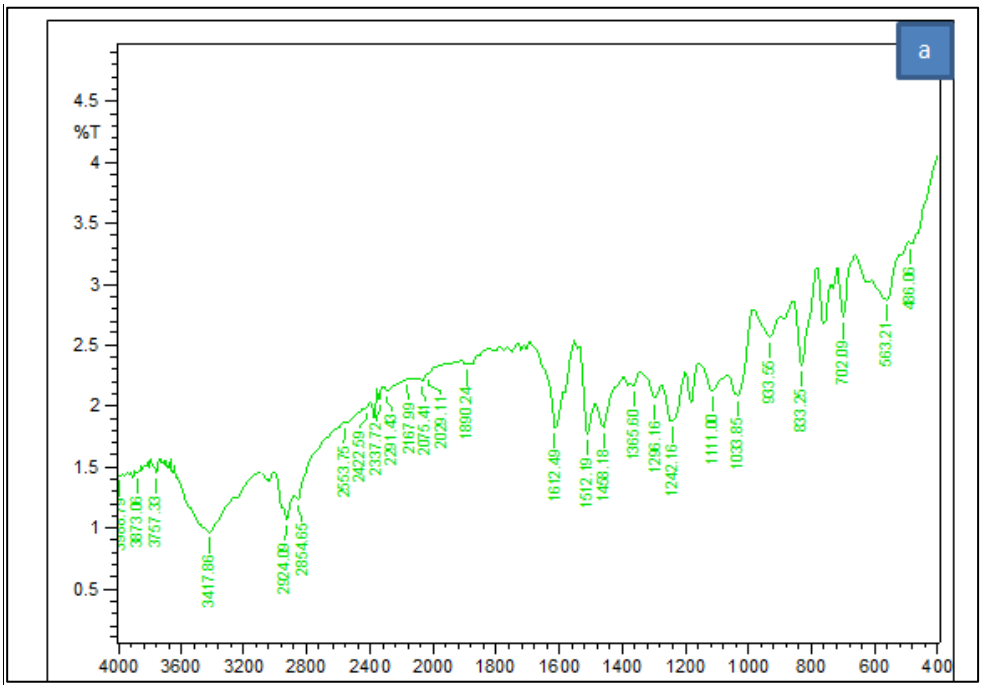

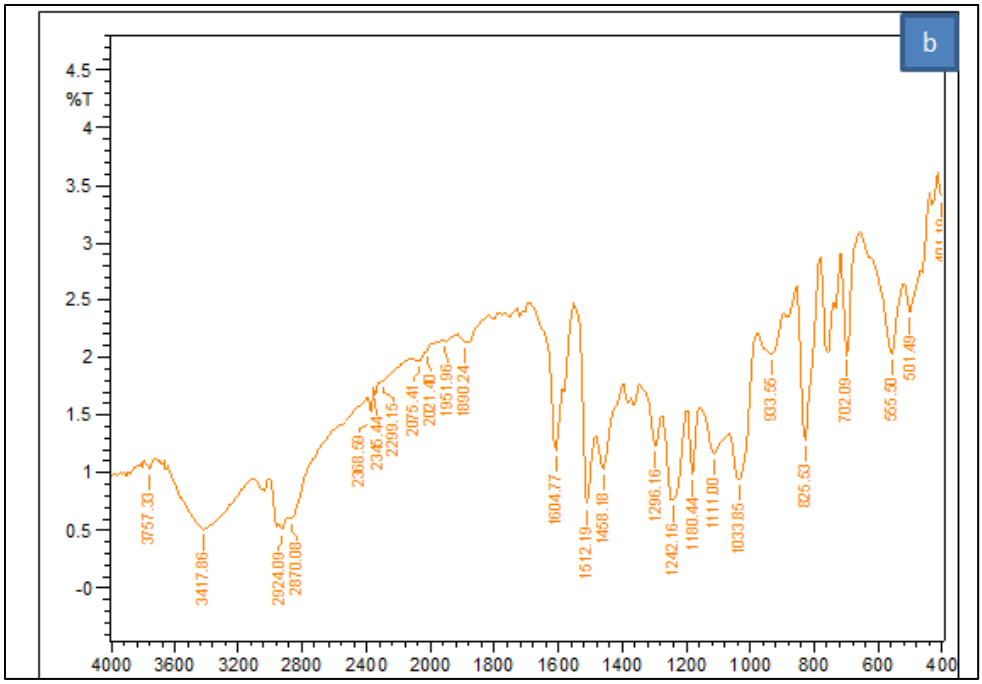
b
%T
4.5
4
3.5
3
2.5
2
1.5
1
0.5
-0
3757.33
3417.86
2924.09
2870.08
2368.59
2345.44
2299.15
2075.41
2021.40
1951.96
1890.24
1604.77
1512.19
1458.18
1296.16
1242.16
1180.44
1111.00
1033.85
933.56
825.53
702.09
565.50
501.48
4000 3600 3200 2800 2400 2000 1800 1600 1400 1200 1000 800 600 400

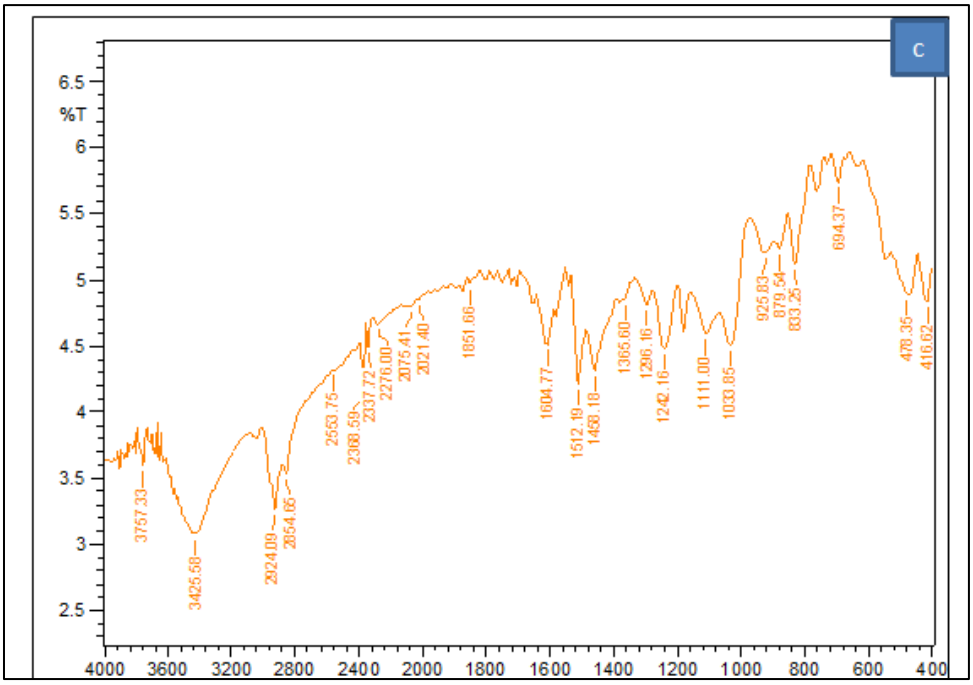
c
%T
6.5
6
5.5
5
4.5
4
3.5
3
2.5
3757.33
3425.58
2924.09
2854.05
2553.75
2368.59
2337.72
2276.00
2075.41
2021.40
1851.66
1604.77
1512.19
1458.18
1365.60
1296.16
1242.16
1111.00
1033.85
925.83
879.54
833.25
694.37
478.35
416.62
4000 3600 3200 2800 2400 2000 1800 1600 1400 1200 1000 800 600 400

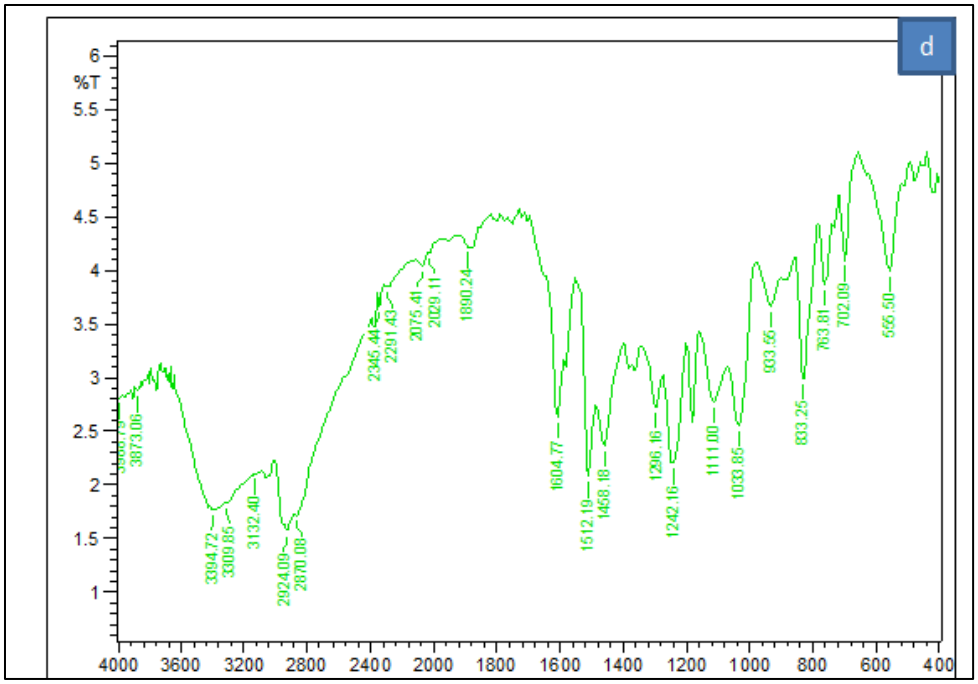

Figure (4.19) : FTIR spectrum of Samples a1:0.5 wt.% PS, b:1:0.5+5 wt.% PS, c:1:0.5+7.5 wt.% PS and d:1:1+7.5 wt.% PS cured at RT.

In Figure (4.19) the vibration absorption peak of epoxy band in PS is located at 933.55 cm^{-1} which is in accord with the fact that the typical epoxy absorption is 910~916 cm^{-1} for uncured epoxy resin as shown in Figure (4.16) the declined vibration absorption of the epoxy-groups with the increased formulation ratio confirms the reaction between epoxy-groups and active-hydrogen's.

In all figures the downward trend of epoxy vibration absorption in FTIR is in good agreement with the degree of cure data, implying the continuous improvement of cross-linked network structure when the EP/h stoichiometric ratio is beyond 1 this could be attributed to the entrapment of the reactive-hydrogen in the rigid 3-dimensional network because the vitrification of the thermosets hindered the further reaction of epoxy and hardener molecules agreement with [13]. The result also suggests that the

excessive content of curing agent is necessary to make full reaction of the epoxy-group for room temperature curing systems.

4.6 Mechanical Characterization

4.6.1 Tensile Test

4.6.1.1 Tensile Strength Results

The phase morphology that forms during the mixing of the epoxy resin and polystyrene, as well as the interfacial adhesion between the phases, have a significant impact on the mechanical performances of the blend materials. Enhancing the mechanical characteristics of the blends requires strong interactions and good dispersion of the polystyrene. It was anticipated that the application of surface functionalization would improve both the dispersion and interfacial bonding of the epoxy blends, thereby improving their performance.

The 1:0.5 pure amine formulation in Figure (4.20) displayed the maximum stress at break at 80 °C. The tensile strength of the EP/h/PS system increased with higher temperature curing and declined with increasing PS content and hardener ratios. In contrast to the epoxy formulations 1:0.5, 1.5:1, and 2.5:1.5, which break brittlely because of the presence of ether groups and homo-polymerization, the amine formulations 1:0.5, 1.5:1, and 2.5:1.5 pure samples require less strength to shatter.

This is a result of the material's higher degree of cross-linking, which gives it strength and rigidity while also causing ductile behaviour. When cured at room temperature, the amine formulation 1:0.5 has the best resistance to pulling loads because it contains a substantial number of ether

groups and homo-polymerization byproducts, but the carbon-amine nitrogen linkage makes up the majority of the structure similar to [25].

Although the 1:1 formulation exhibits less resistance to pulling loads, the material is less stable due to a significant quantity of unreacted hardener molecules. For the EP/h/PS system, the material exhibits excellent resistance to the stretching force up until the specimen fails as the hardener/resin ratio rises. This may be because the sample's nature makes it appear like rubber when it is being pulled by a load. Pure epoxy is represented by a polystyrene concentration of zero. shows unmistakably that the tensile strength has improved significantly even with relatively low polystyrene loadings.

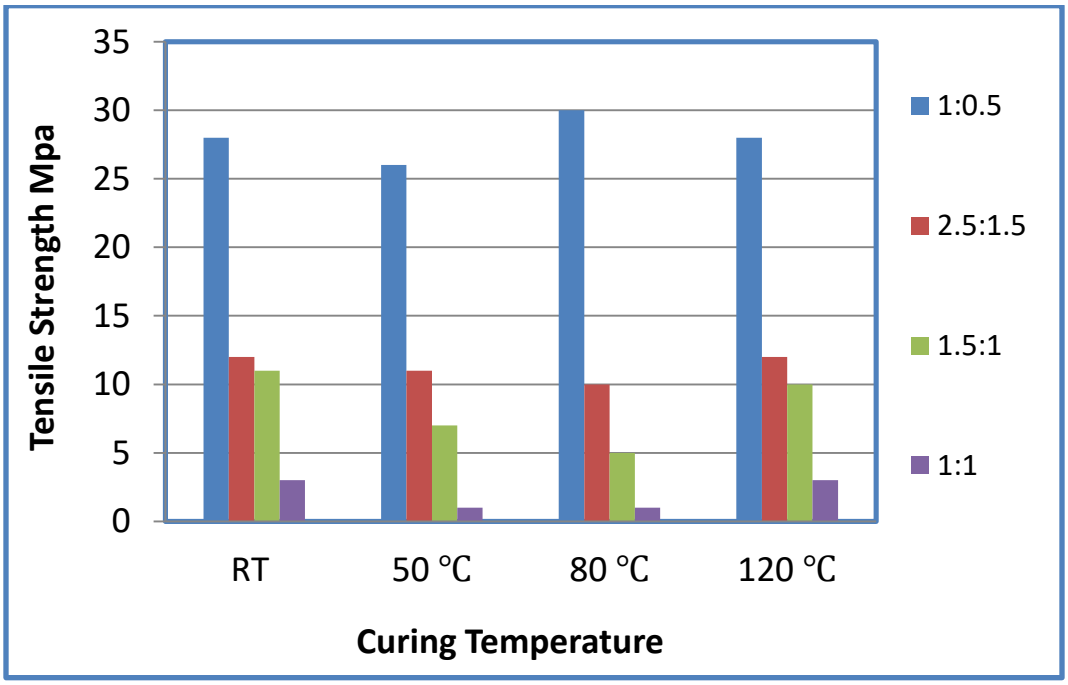

Figure(4.20): The tensile strength of pure samples vs. curing temperature.

As shown in Figure (4.20), blends exhibited better tensile properties at low polystyrene loadings than the pure 1:0.5 formulation, whose tensile

strength peaked at 80 °C. The rate of enhancement was found to be higher at low PS loading than it was at higher PS loading. The epoxy-PS mixes' tensile strength showed a distinct trend from the other composites. It began to diminish after initially growing. The enhanced dispersion of EP-PS led to a greater tensile strength at lower concentrations when compared to raw EP resin. Consequently, the increase in tensile strength was attributed to specific interactions between the filler and the polymer matrix. Because PS is poorly dispersible, it may hinder the polymer chains from packing densely and lower the overall tensile strength of the blends.

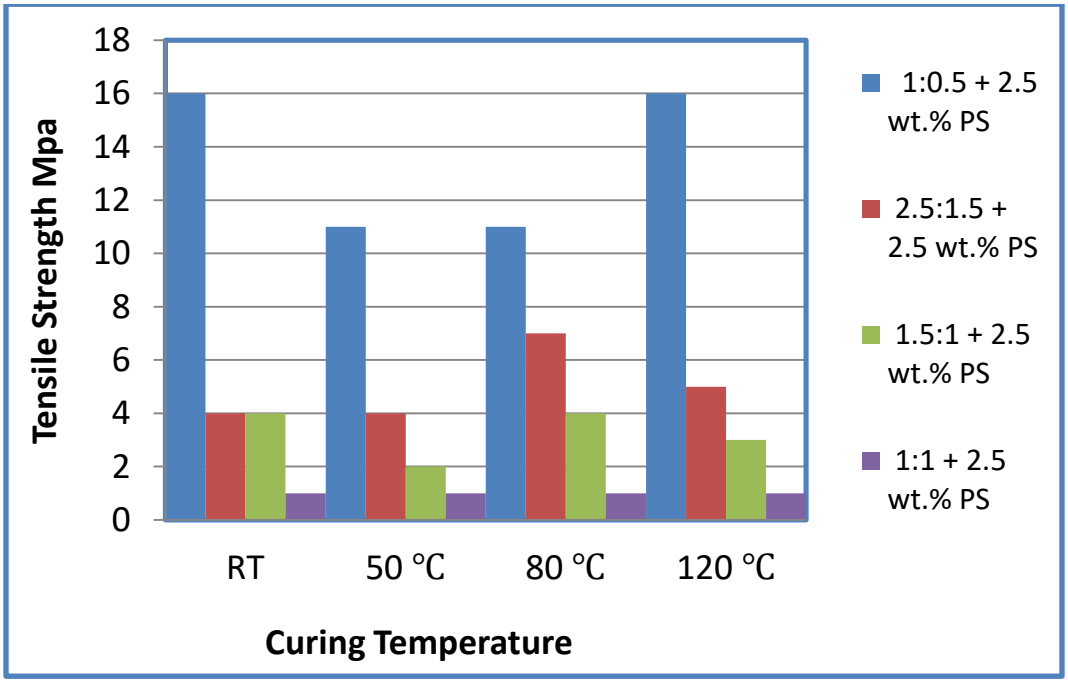

Figure(4.21): The tensile strength of samples with 2.5 % wt. ps vs. curing temperature.

As shown in Figure (4.21) that the tensile strength decreases as the temperature of curing rises when the amount of polystyrene increases. The potential for phase separation between epoxy resin and polystyrene, which occurs when coupling agents are introduced, is the reason for this decrease in load transfer capability.

Furthermore, when the temperature rises, the polystyrene inside the epoxy matrix stabilises and the epoxy resin solidifies more quickly, giving the impression of frozen waves inside the matrix. The polystyrene also does not fully cure, resulting in the formation of crooked lines the shrinkage that occurs during the cooling process from the curing temperature to room temperature causes large internal stresses in cured EP resin, which toughen the material's lower modulus and tensile strength. Microcracks and voids caused by internal strains impair performance similar to [97].

The decrease in tensile strength and modulus with the addition of PS concentration may be due to the fact that the interaction between the epoxy networks, crosslinking densities, and resin defects predominantly affect the tensile property. Adding PS actually reduces crosslinking densities and attracts some defects to the epoxy resin, which affects the tensile properties regardless of the kind of phase structure similar to [98].

In Figure (4.22) and Figure (4.23) the results of the epoxy resin/polystyrene companion show that the tensile strength in the blends decreases with increasing polystyrene content and then slightly increases at 7.5 wt.% content of polystyrene addition to prevent polystyrene migration due to the significant difference in surface tension between thermoset and thermoplastic therefore we use an silane coupling agent.

The reason for this is that the epoxy resin was improperly cured, which caused the elastic modulus to increase, start to stabilize with an increase in PS, and then decrease after being heated, the elastic modulus of the modified epoxy system seems to have decreased similar to [99] the

properties of blend strongly depend on the morphology, that is, on miscibility, size and form of dispersed phase, character and size of the interphase domain.

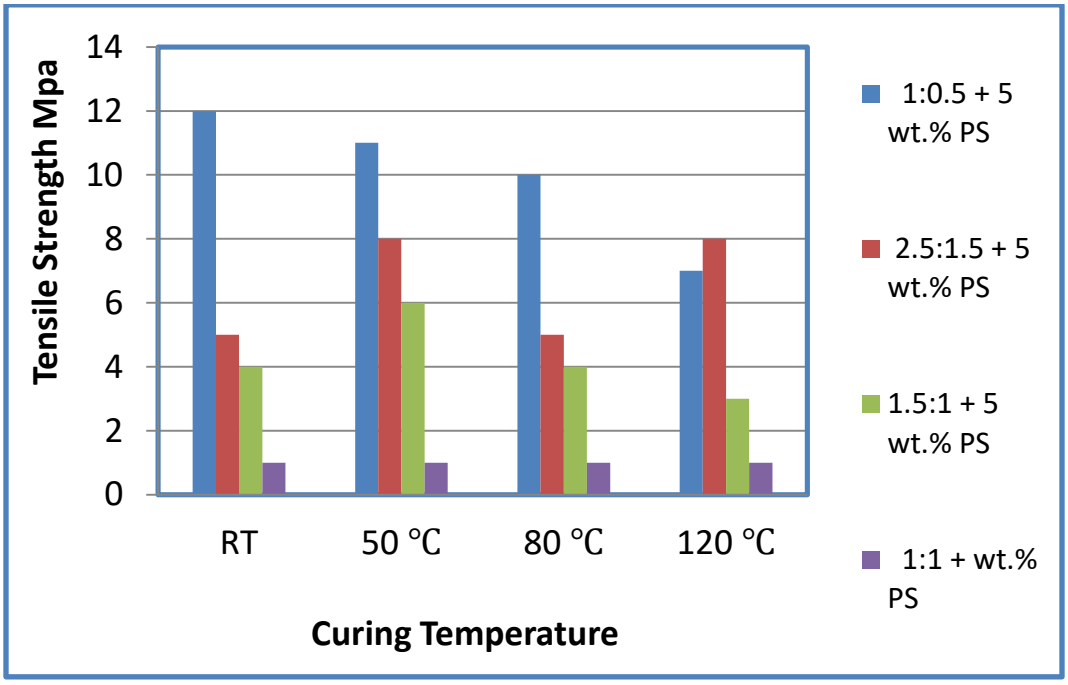

Figure (4.22): The tensile strength of different formulations of EP/h with content 5 wt.% PS.

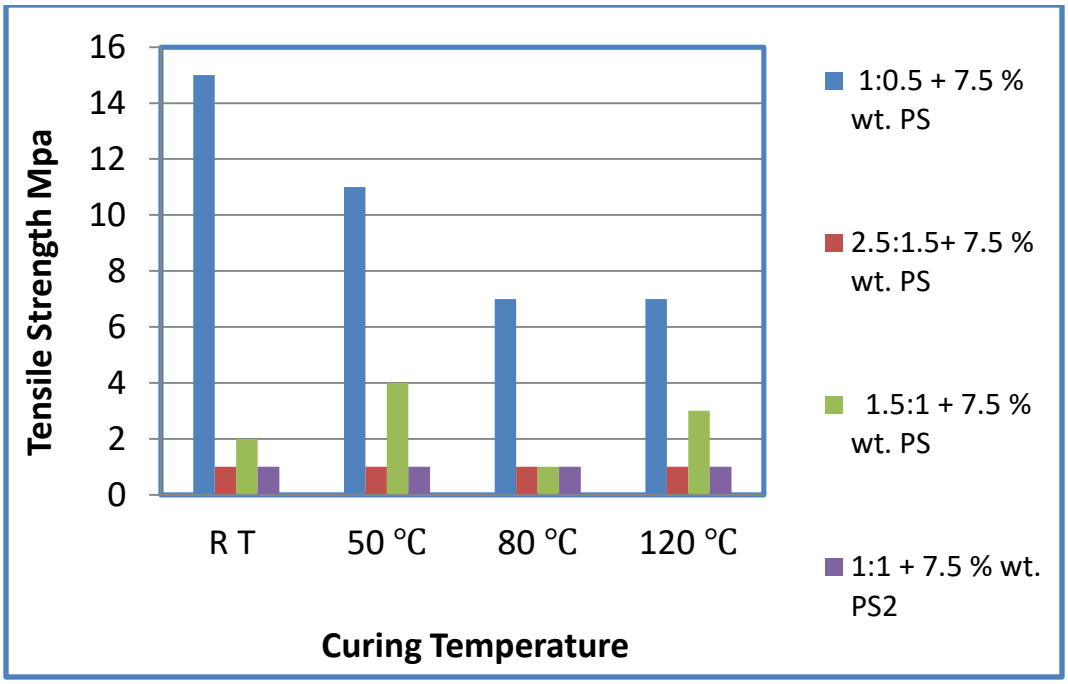

Figure (4.23): The tensile strength of different formulations of EP/h with content 7.5 wt.% PS.

In Figures (4.21), (4.22) and (4.23) the tensile strength at the various curing temperatures indicated, with varying hardener to epoxy resin ratios and polystyrene concentrations there is a sharp decline in tensile strength when compared to the standard ratio of mixing, but all blends then stay stable at the same value of tensile strength at different temperatures. The tensile strength were presented better at room temperature than after that, when the values varied in their value between rising and sharp decreasing.

The tensile strength of the epoxy matrix decreases to a value less than that of neat EP as the polystyrene component rises, causing the matrix to become plasticized while the hardener to resin ratio varies amongst epoxy brands, it is usually remain steady at the formulation ratio established by assuming that both epoxy groups and amine groups will fully react similar to [100].

In Figure (4.24) presented that depicts the effects of varying ratios of epoxy resin to hardener with varying the concentration of PS content with effect of curing temperature can see that in the first, the value of tensile strength increased for unmodified epoxy resin/hardener, at room temperature and then there were sharp decrees at 2.5% content of PS.

As increased the concentration of PS with inecrasing of hardener ratios , the value of tensile strength increased slightly, which may indicate that PS phase provided some ductility for epoxy at varied concentrations of polystyrene in the polymer matrix, the tensile strength and elongation at break of several epoxy-polystyrene blend systems are compared.

The differences in macromolecular structures that are formed and/or the potential reactions that could take place given a boundary condition (i.e., when a variable like temperature or the amount of monomers is changed) may be considered the direct causes of the changes in mechanical properties that are observed when the epoxy resin to hardener ratio is varied. The primary amino addition reaction, which takes place between the primary amines (NH_2), dominates the cure reaction scenarios for the epoxy resin system under study agreement with [25].

Despite a higher crosslinking rate , a loss in tensile strength indicates that one (or both) of the blend's components were altered during the high-temperature curing process. The modulus and failure tensile strength of epoxy resin at ambient temperature decrease when the curing temperature is above or close to the resin Tg due to heat deterioration or oxidative crosslinking (crosslinking within the epoxy polymer). Additionally, there is a very little color shift (from translucent to light yellow) that is linked to

an early oxidation of the epoxy resin As shown in figures below similar to [101].

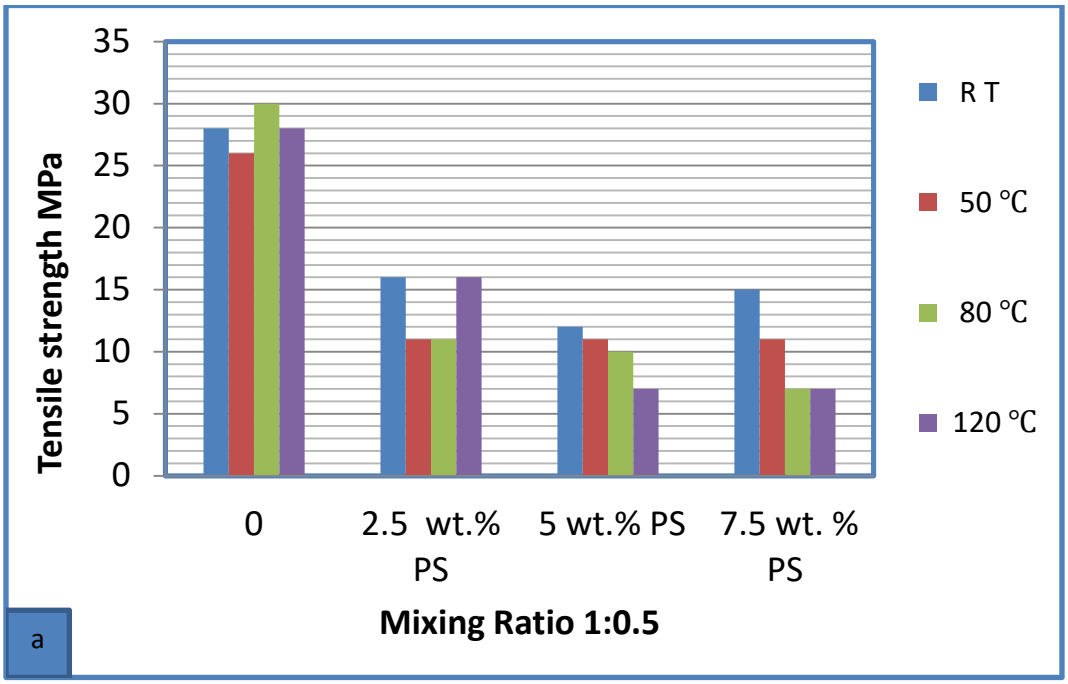

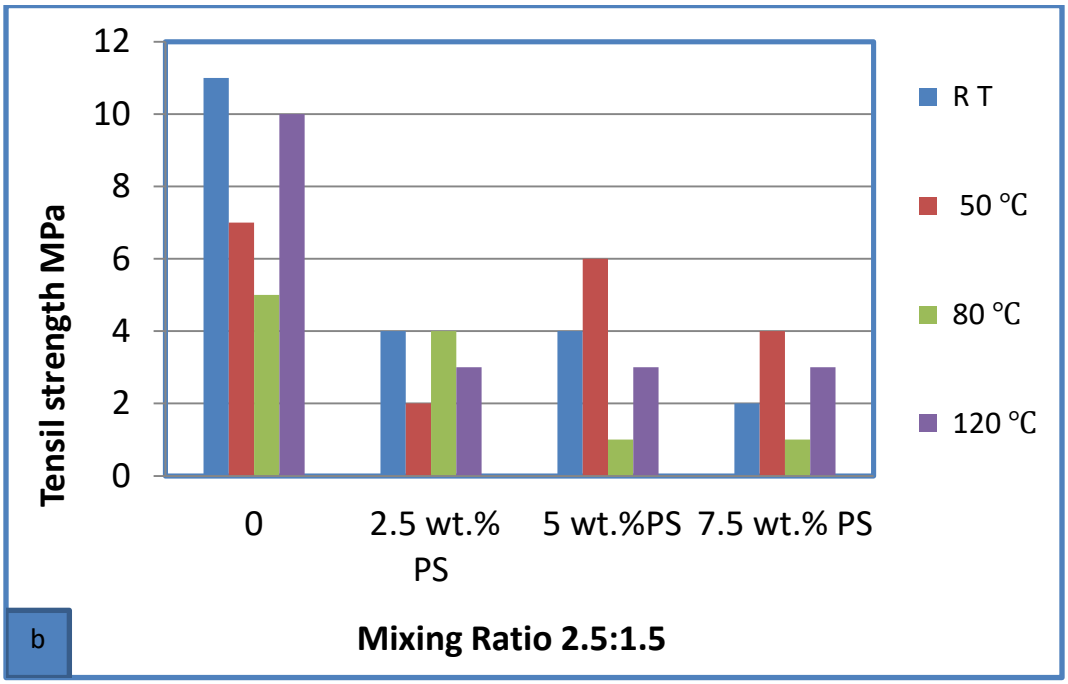

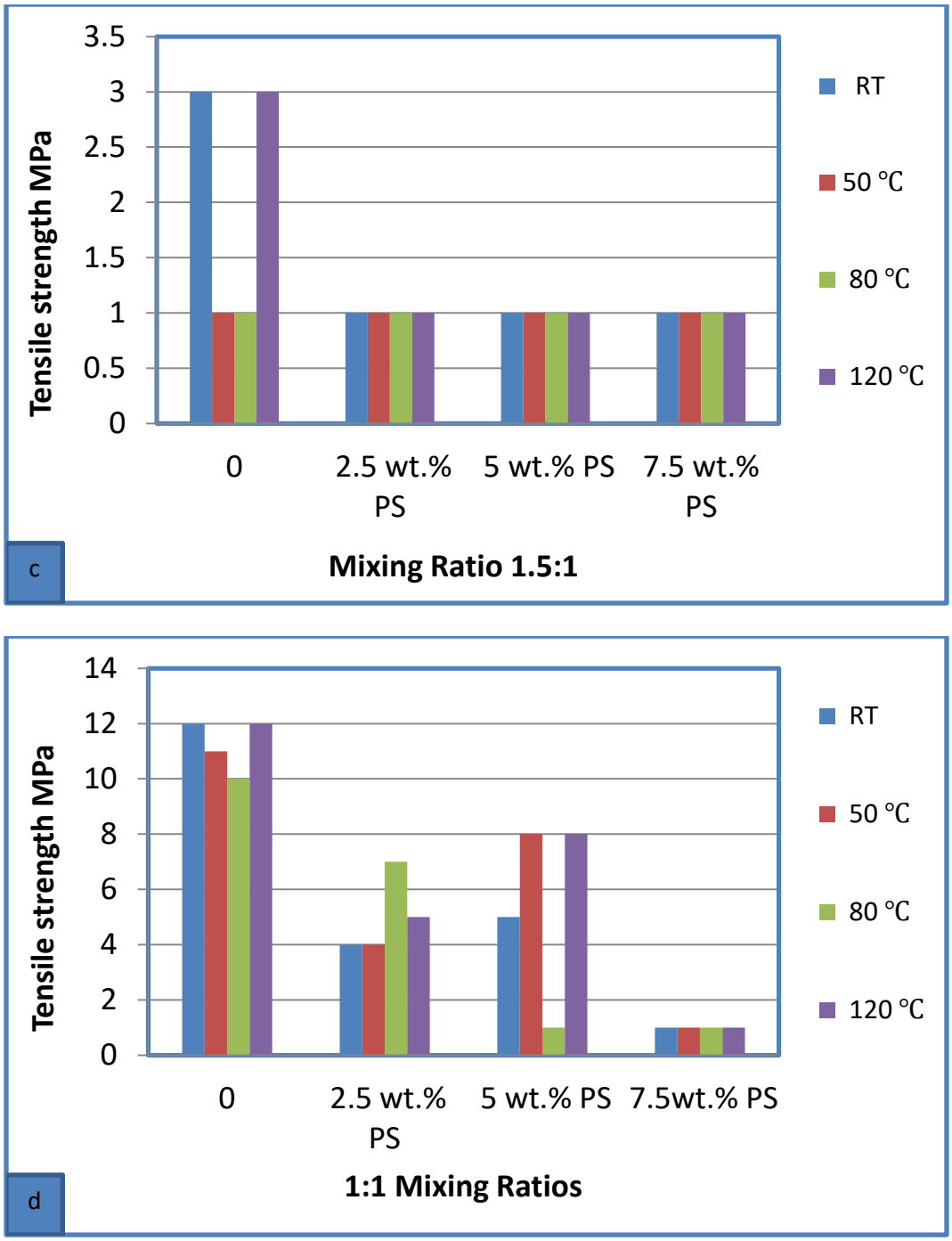

Figure(4.24): Represent the tensile strength of epoxy and its blends at different curing temperature of a:1:0.5 ratio, b:2.5:1.5 ratio, c: 1.5:1 ratio and d:1:11 ratio.

4.6.1.2 Elastic Modulus Results

Fig.(4.25) reviews the elastic modulus of the EP/h and its blends under different condition of kinetic curing in first we observed that with ratio of 1:0.5 having best value at curing temperature 50 ℃ for pure sample cured with different curing temperatures while with the addition of PS thermoplastic as tough material the best value was at curing temperature 80 ℃ with the addition of PS 5 wt.% the elastic deformation which is due to intermolecular force of attraction can be estimated in terms of Young's modulus which describes tensile elasticity or the tendency of an object to deform along an axis when opposing forces are Effect of the hardener/resin Ratio on the elastic modulus applied along that axis. The elastic modulus of a sample is a measure of its stiffness. The higher the modulus the stiffer the material. The value of elastic modulus is normally derived from the initial slope of the stress-strain curve similar to [25].

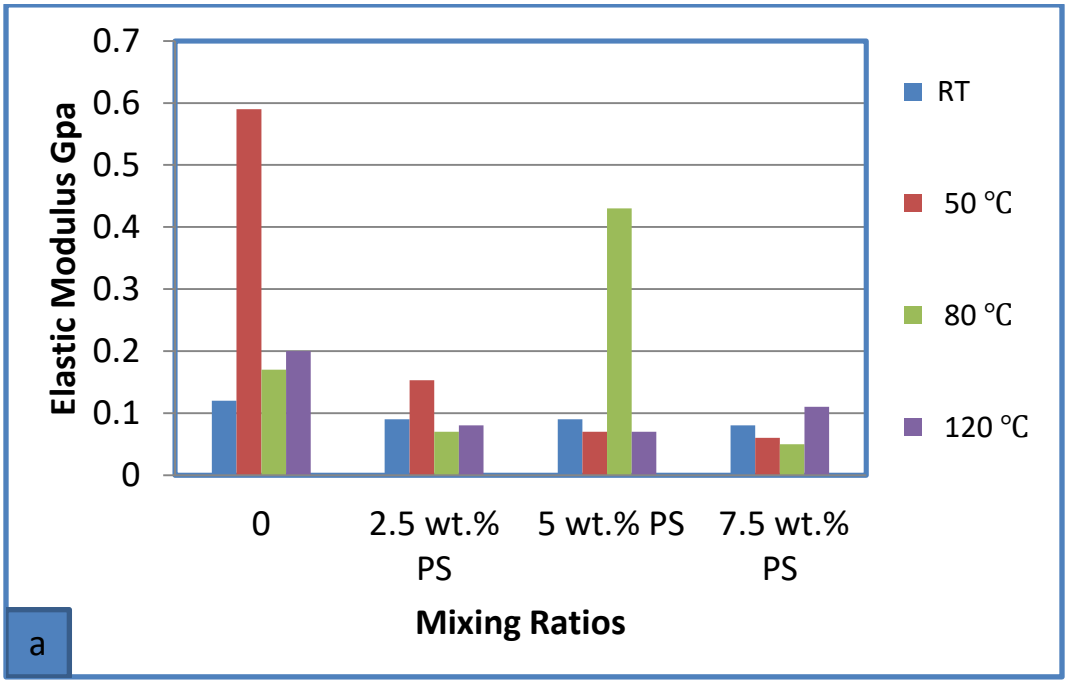

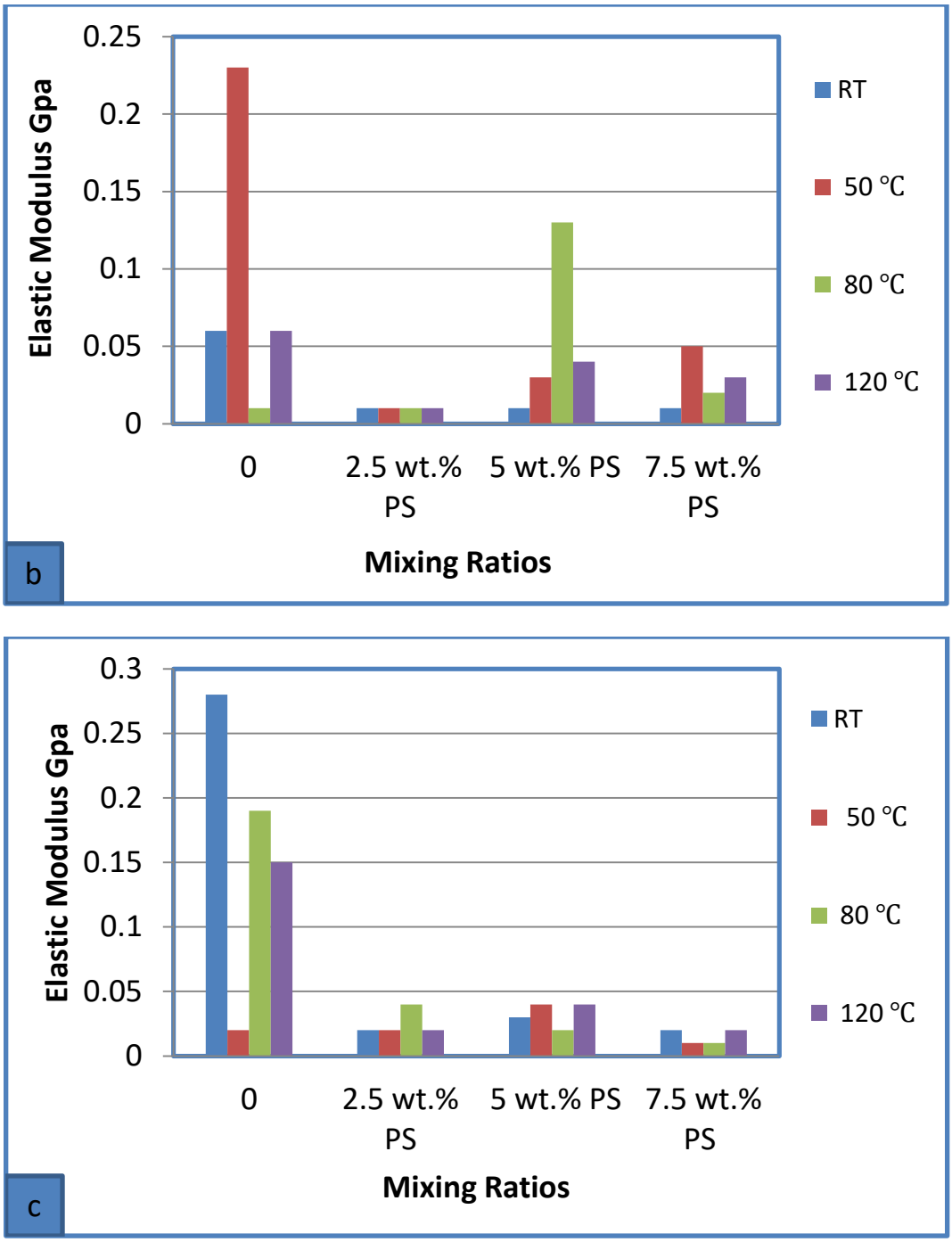

Figure (4.25): Represent elastic modulus of a:1:0.5 EP/h, b:2.5:1.5 EP/h and c:1.5:1 EP/h of epoxy and its blends.

The relationship between the elastic modulus and the curing temperature is reviewed in Figure (4.26) contrary to an increase in plastic deformation, the elastic modulus decreases as cure temperatures rise with the right application, this allows one to determine the working temperature.

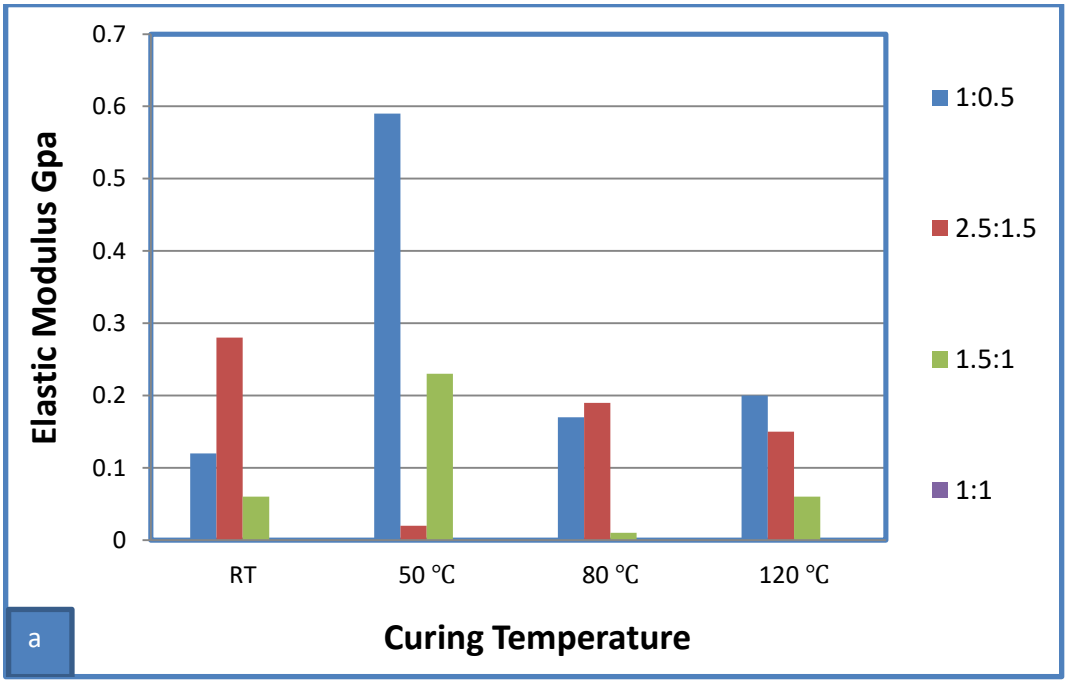

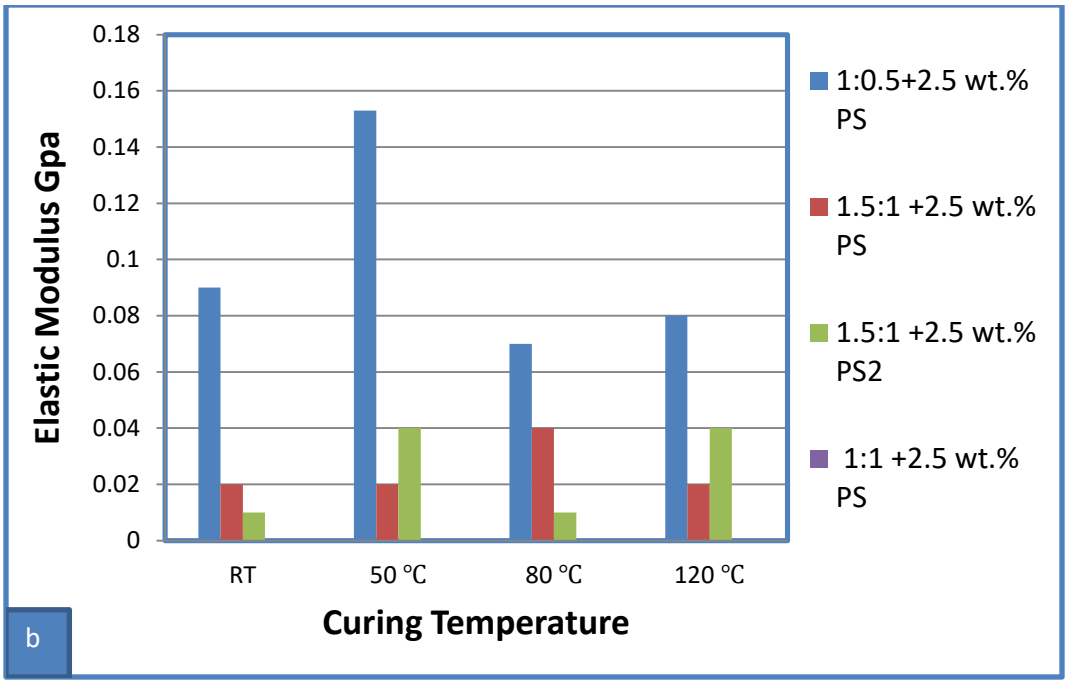
0.18
0.16
0.14
0.12
0.1
0.08
0.06
0.04
0.02
0
Elastic Modulus Gpa
RT
50 ℃
80 ℃
120 ℃
Curing Temperature
1:0.5+2.5 wt.% PS
1.5:1 +2.5 wt.% PS
1.5:1 +2.5 wt.% PS2
1:1 +2.5 wt.% PS
b

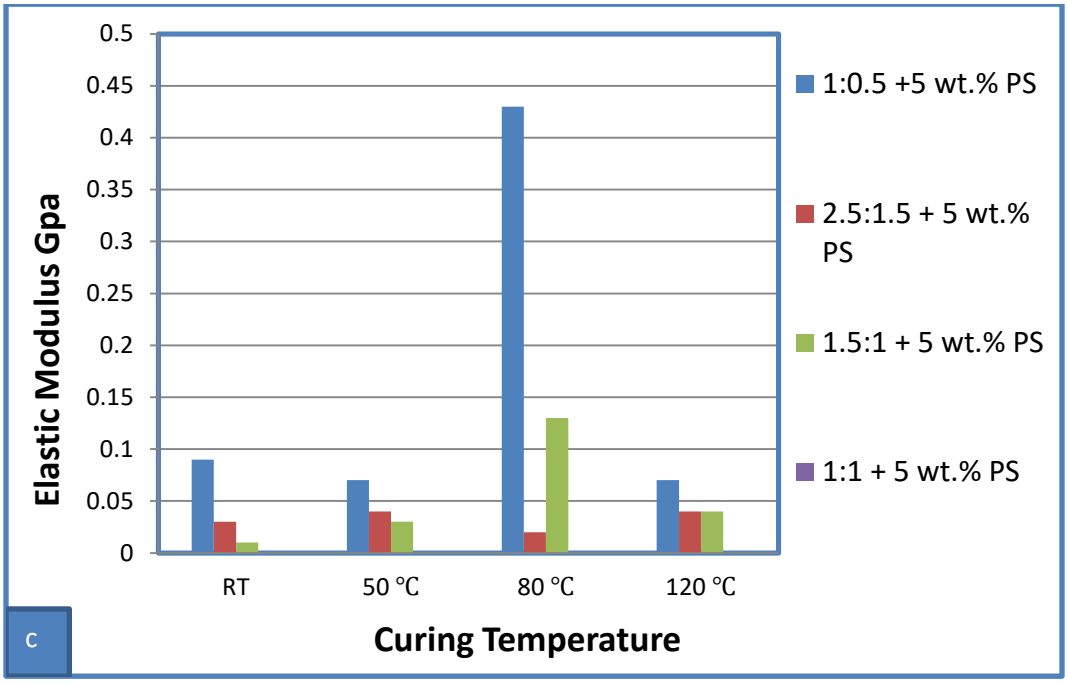
0.5
0.45
0.4
0.35
0.3
0.25
0.2
0.15
0.1
0.05
0
Elastic Modulus Gpa
RT
50 ℃
80 ℃
120 ℃
Curing Temperature
1:0.5 +5 wt.% PS
2.5:1.5 + 5 wt.% PS
1.5:1 + 5 wt.% PS
1:1 + 5 wt.% PS
c

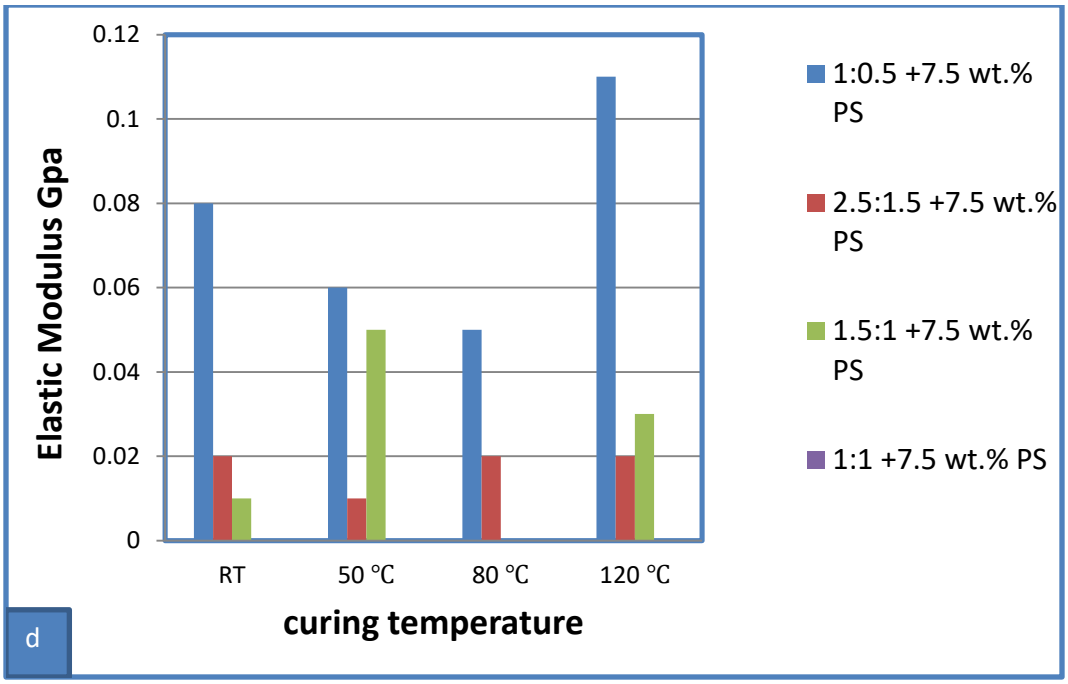

Figure (4.26): Represent a: pure samples, b: 2.5 wt.% PS , c: 5 wt.% PS , and d: 7.5 wt.% PS of elastic modulus with cure temperature for pure samples, and blends under different curing temperatures.

4.6.1.3 Elongation at Break Results

The effect of varying PS content on elongation at break is shown in Fig. (4.27) and it is clear that all blends had a decrease in elongation of break as the PS level increased. For pure samples, the 1:1 formulations for the EP/h/PS/ system show the maximum elongation when cured at room temperature, this is because the material is more flexible due to the carbon-amine nitrogen coupling which allows the chains to stretch significantly before breaking. Less elongation is seen in the formulation 2.5:1.5, since the ether groups and homopolymerization process affect the amine addition reaction between the hardener and epoxy resin, causing the material to become brittle and less flexible than in the other formulations.

The formulation 1.5:1 shows superior elongation than the epoxy 2.5:1.5 and 1:0.5 because of the amine addition reaction, which

predominates despite the presence of a considerable quantity of ether groups and the outcomes of homopolymerization. In order for the material to bear the imposed load, this makes it more ductile and flexible the amine rich formulation 2.5:1.5 is showing less elongation than the amine rich formulation 1.5:1 because the non-reacted hardener molecules make the material brittle similar to [102]. The mechanical properties of the mix can be maximised by adding the ideal amount of PS, according to tensile strength and EAB values the findings of this investigation are consistent with those from Tricca where discovered that when the increased the hardener/resin ratio, the epoxy resin system's elongation increased similar to [103]

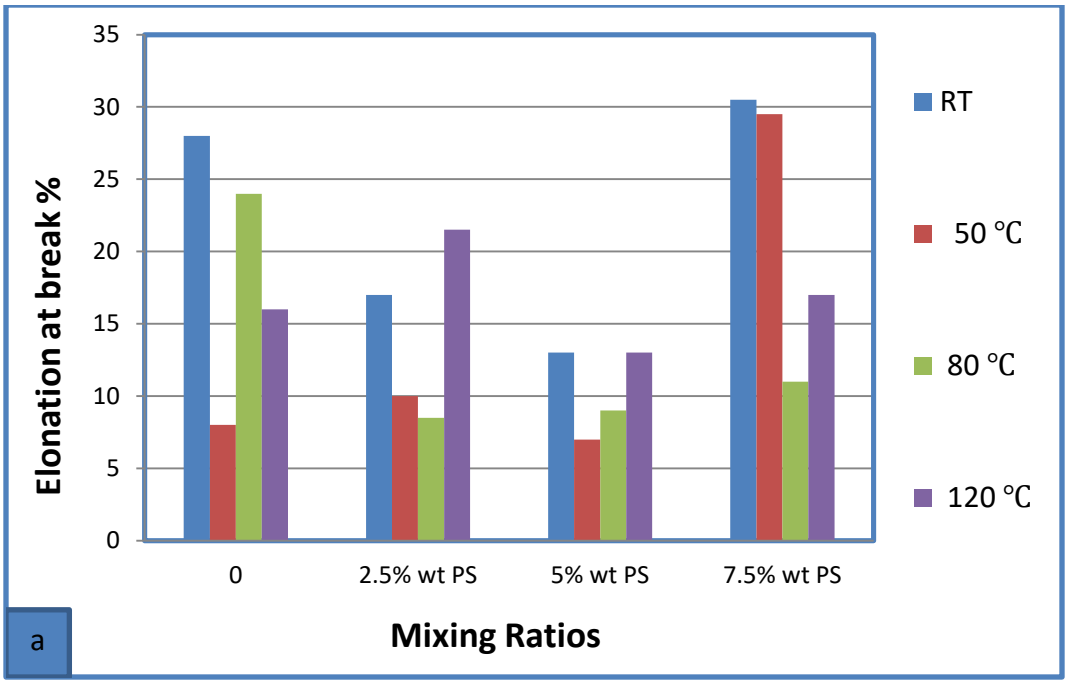

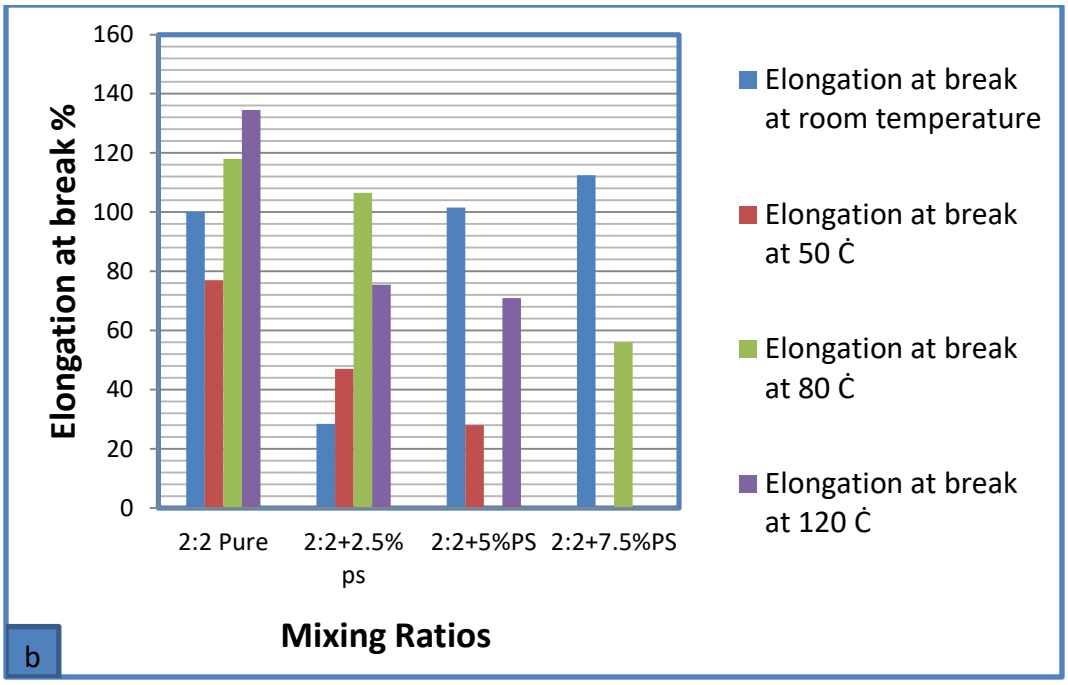
160
140
120
100
80
60
40
20
0
Elongation at break %
2:2 Pure
2:2+2.5% ps
2:2+5%PS
2:2+7.5%PS
Mixing Ratios
Elongation at break at room temperature
Elongation at break at 50 Ċ
Elongation at break at 80 Ċ
Elongation at break at 120 Ċ
b

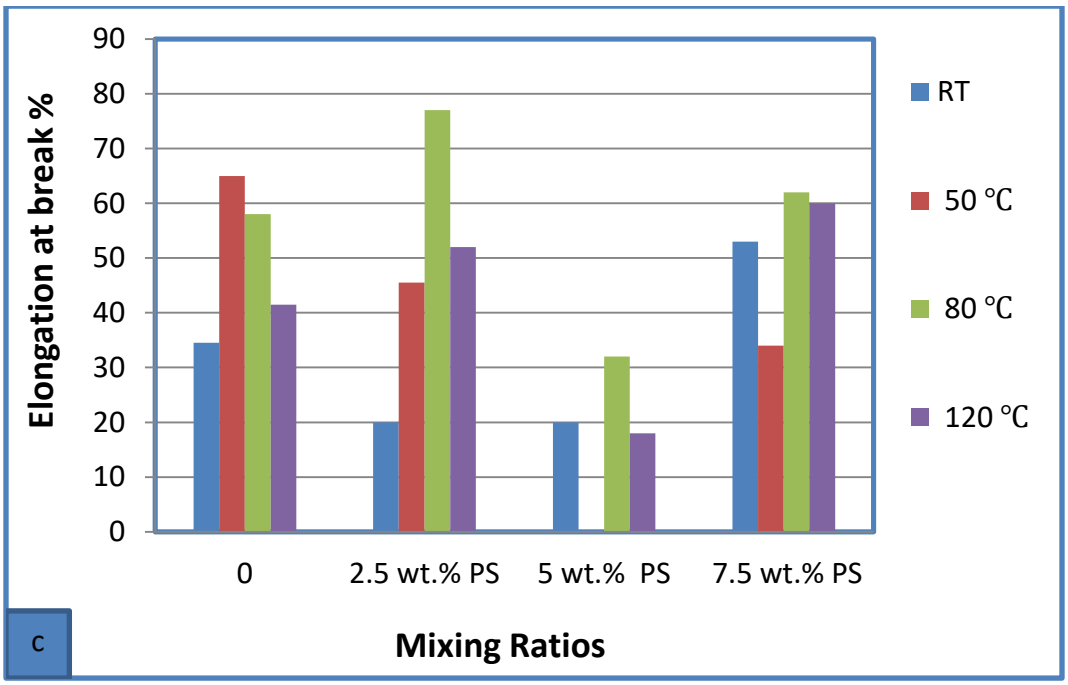
90
80
70
60
50
40
30
20
10
0
Elongation at break %
0
2.5 wt.% PS
5 wt.% PS
7.5 wt.% PS
Mixing Ratios
RT
50 °C
80 °C
120 °C
c

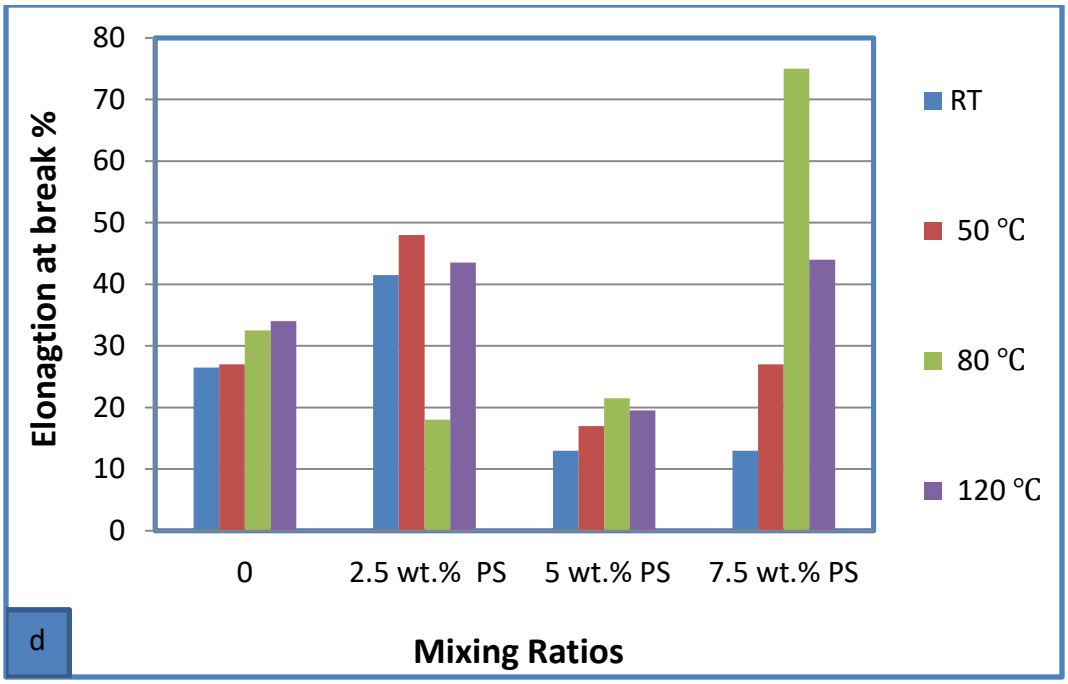

Figure(4.27) : Represent the elongation at break of a: 1:0.5, b:1:1, c:1.5:1 and d:2.5:1.5 unmodified epoxy and blends at different temperature and content of PS.

4.6.2 Hardness Results

Sample hardness is estimated using a shore D durometer, which gauges a material's relative resistance to indentation when a load is applied to the indenter [104]**.** Figure (4.28) summarises the hardness of ratios and shows that it decreased with varying epoxy/hardener ratios while adding polystyrene and keeping the curing temperature constant. 1:0.5 pure and 1:0.5+7.5 weight percent were the highest values. PS: It is important to understand that surface roughness is influenced by the hardness of a given material.

The hardness will decrease as a result of the material plasticizing following its mixing with thermoset polymer epoxy and thermoplastic polymer PS. A reliable indicator of this behaviour will be the roughness levels that dropped after the blending procedure. Epoxy is frequently

described as brittle and deforms under pressure with low elastic strain; but, when mixed with PS, it can change into a more plastic material, as seen in Figure (4-21), which depicts the surface topography. It is important to keep in mind that earlier research looked at thermoplastic materials for epoxy modification. It is noteworthy that earlier research looked into the possibilities of modifying epoxy with thermoplastic polymers in order to toughen it similar to [105]. Epoxy is known to be a brittle material that deforms when stressors are applied with low elastic strain, but when combined with PS, it can change into a material that deforms with more plastic deformation.

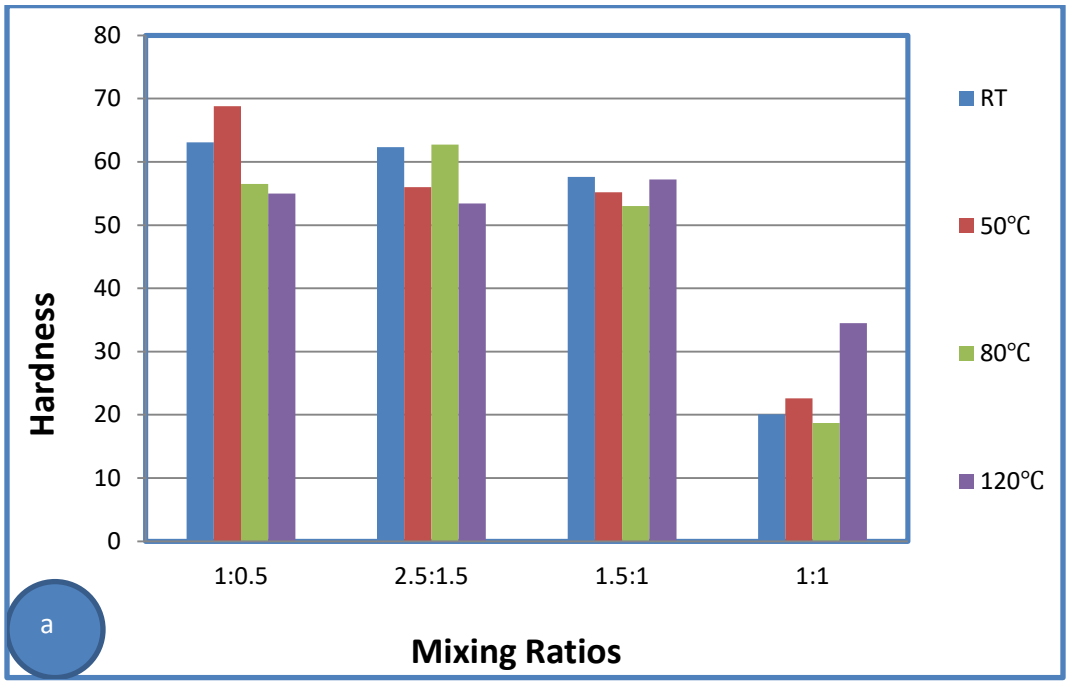

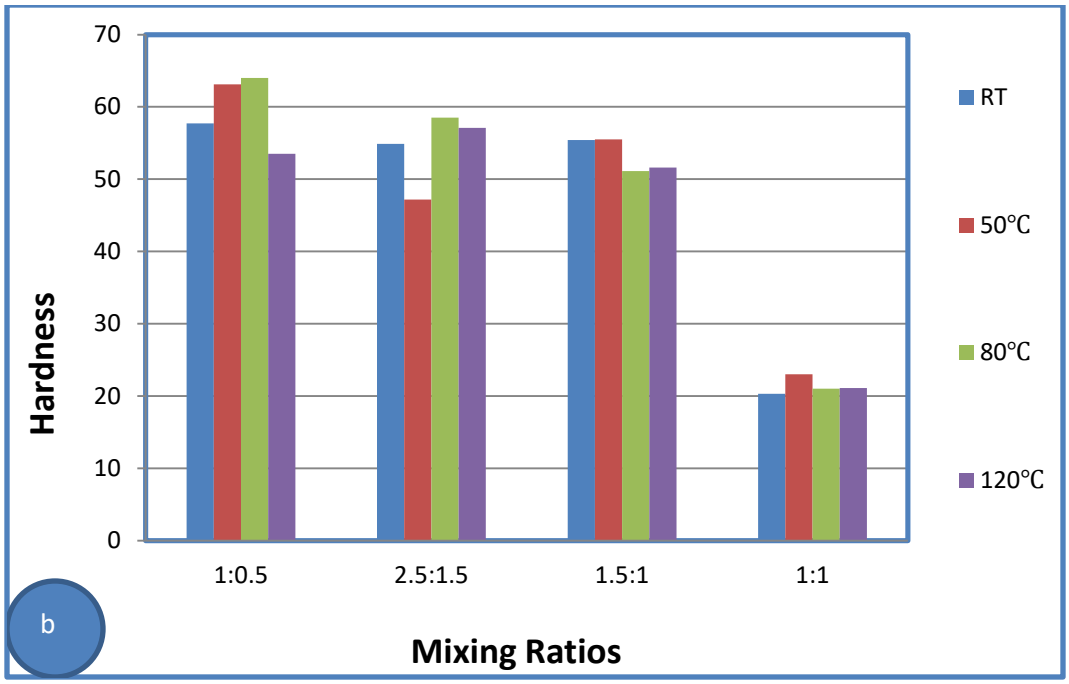
70
60
50
40
30
20
10
0
Hardness
RT
50°C
80°C
120°C
1:0.5
2.5:1.5
1.5:1
1:1
b
Mixing Ratios

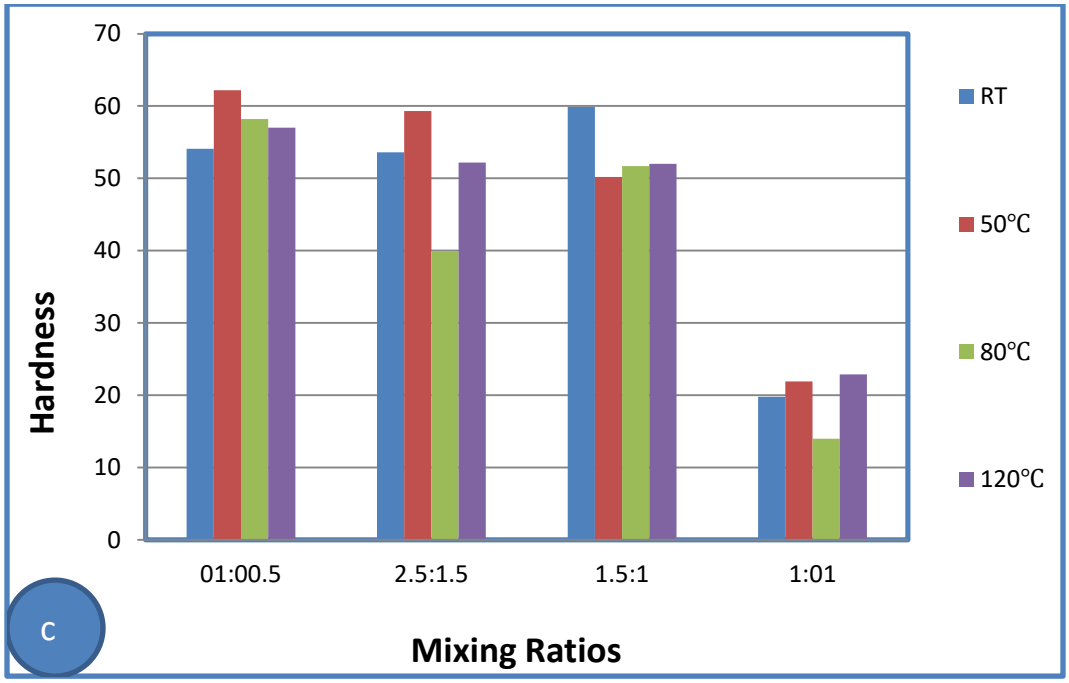
70
60
50
40
30
20
10
0
Hardness
RT
50°C
80°C
120°C
01:00.5
2.5:1.5
1.5:1
1:01
c
Mixing Ratios

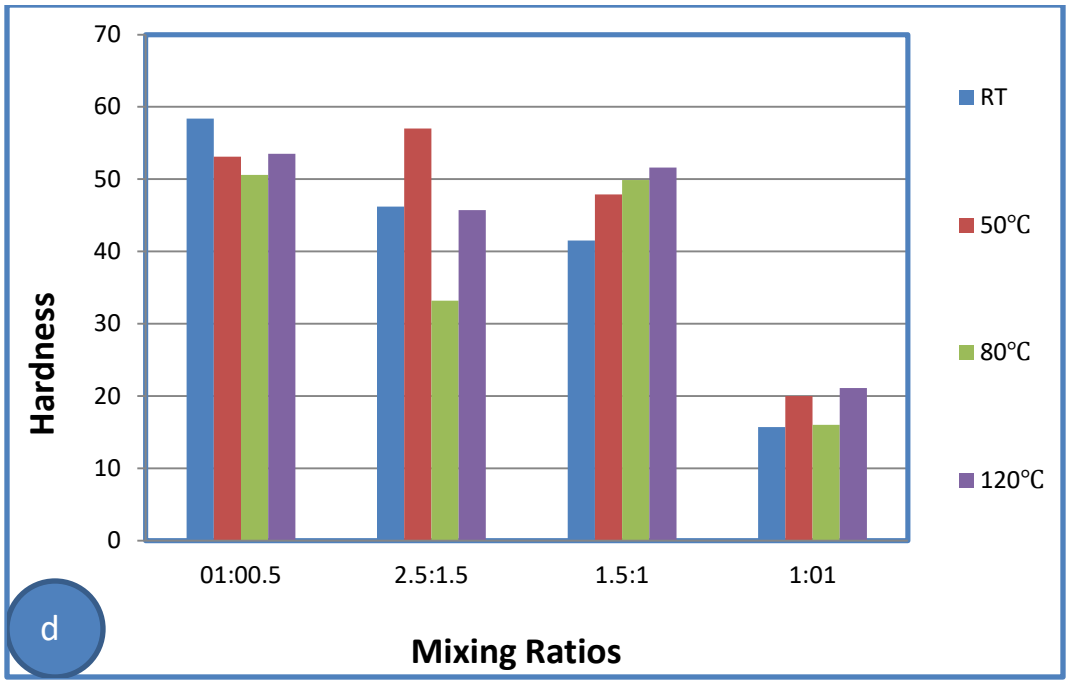

Figure (4.28): Relation between hardness and mixing ratios a: unmodified, b: 2.5 wt.% PS, c: 5 wt.% PS and d: 7.5 wt.% PS of epoxy and its blends at different curing temperature.

4.6.3 Impact Strength Results

In Figure (4.29) the impact strength of the epoxy of samples with the addition of PS exhibits the lowest value at 1:0.5 + 7.5 wt.% PS cured at 120 °C. This results from PS clumping together in one location with gaps that cause stress concentration and may also occur inside of distinct chain, additionally, a hard and compact macromolecular structure is formed, with the dimethoxy group being the only predicted mobility group similar to [107, 108].

These qualities result from the hardener molecule's reactive sites being completely exhausted, which results in a rigid and brittle structure agreement with [107]. The best value is obtained at 1:0.5+5% wt. PS cured at room temperature, as illustrated in Figure (4.29 a).

While the 1.5:1 EP/h ratio is less at 120 °C compared to others (1:0.5 and 2.5:1.5) at 120 °C, which indicates that the formulation is tougher than the epoxy rich formulation and indicates that it is more flexible in this the sample appears like rubber with the ability to absorb more energy or force.

Though more amino hydrogen groups are present in the amino rich formulations (the 2.5:1.5 and 1:0.5 EP/h ratios cured at room temperature show higher impact strength than the 1:1 and 1.5:1 EP/h ratios), the 1:1 EP/h ratio in Figure (4.29 b) shows a higher impact strength for pure ratios while 120 °C than the other ratios. More epoxy rings will be opened during the amino addition reaction, increasing the material's toughness.

A material's ability to withstand impact is one of its key qualities, a difficult polymer is one that needs a lot of energy to break in an impact test. impact test outcomes this test's basic hypothesis is that some of the primary energy that the material's potential energy stores was absorbed by the sample during the rupture.

In comparison to all other resin/hardener ratio formulations, the amine-rich formulation 2.5:1.5 EP/h ratios has the highest impact strength at 80 °C, this suggests that the material can absorb more energy before breaking, where the applied force is dispersed through the molecular structure.

Comparatively speaking, hardness has a smaller value, when the imposed load is too much for the material to bear, its chains begin to break, forming a fracture when combined with a 7.5 wt.% weight percentage of PS, the amino rich 1.5:1 EP/h formulation is showing lower impact strength at 80 °C than the amino rich 2.5:1.5 EP/h formulation. The

behaviour was traced back to the non-reacted locations in the hardener molecule, which break the material similar to [106].

At 120 °C, the curing temperature, other ratios do not demonstrate the same impact strength as the amine-rich 1.5:1 EP/h combined with 7.5 wt.% PS ratio. The findings demonstrated that impact strength at PS increased significantly in comparison to pure epoxy, then increased little and did not increase further, a similar pattern was seen in the results for both fracture toughness and maximal strength it can be because of the disparity in speed between the two tests.

The fracture toughness test was conducted at a somewhat modest speed to allow more PS particles to react and withstand it, the polystyrene polymer was unable to react since the impact test was finished so quickly the heterogeneous distribution of the micro-sized domain may be the cause of this, since it may facilitate the onset and spread of cracks following sudden impact deformation. Charpy impact tests can be used to estimate the blends' macroscopic mechanical behaviour, while fracture toughness investigations can be used to evaluate their micromechanical behaviour.

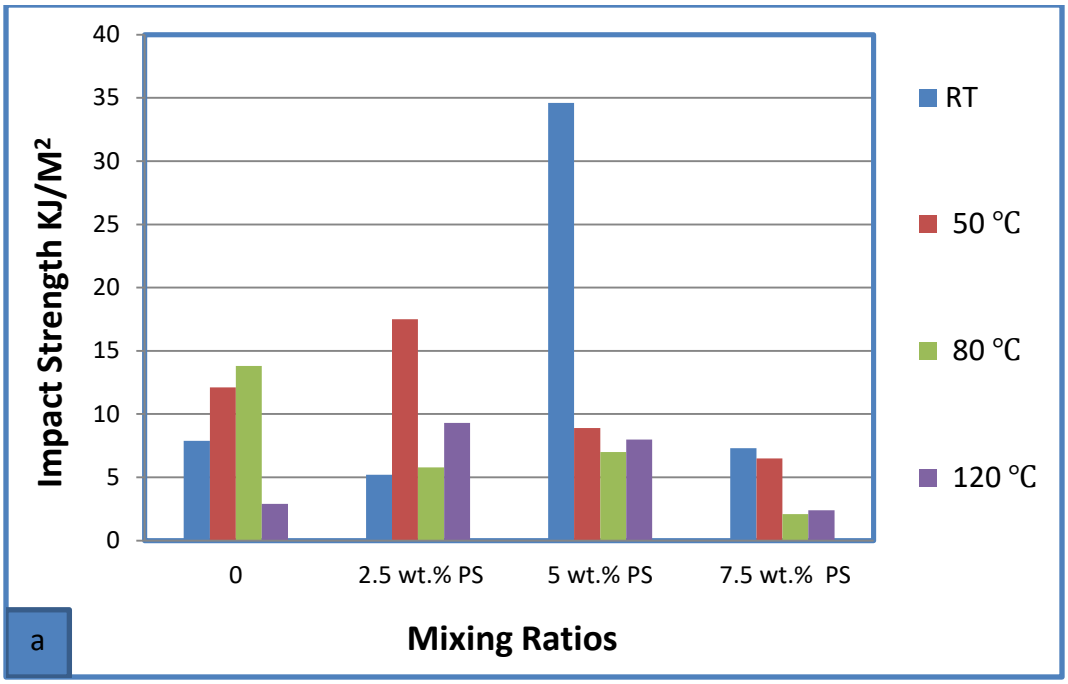
40
35
30
25
20
15
10
5
0
Impact Strength KJ/M²
RT
50 °C
80 °C
120 °C
0
2.5 wt.% PS
5 wt.% PS
7.5 wt.% PS
Mixing Ratios
a

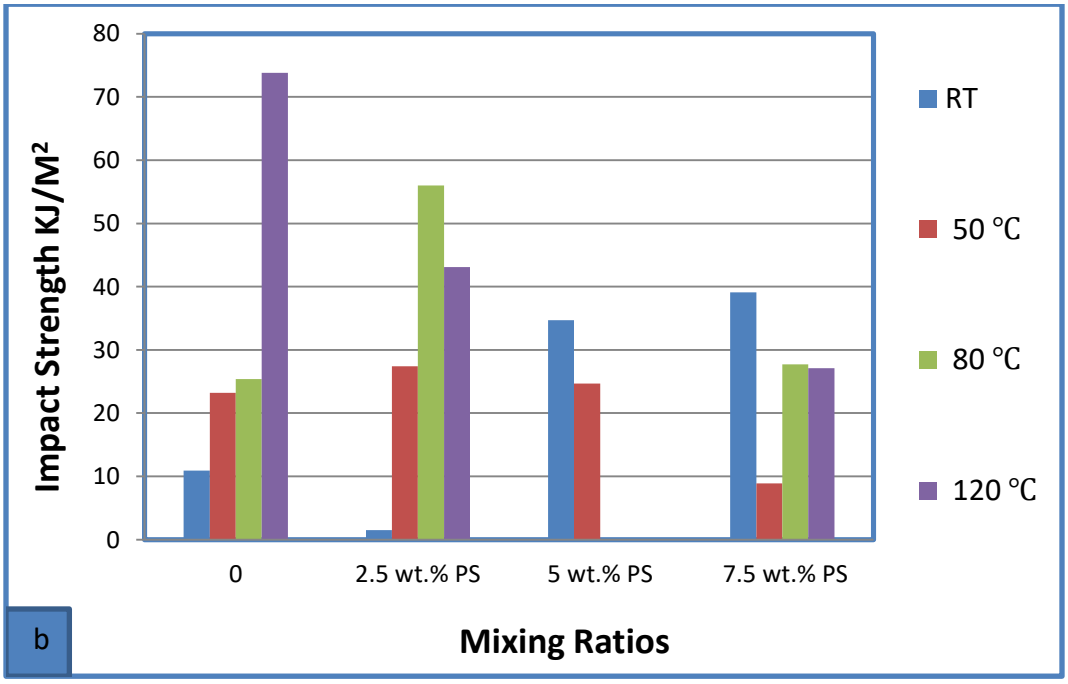
80
70
60
50
40
30
20
10
0
Impact Strength KJ/M²
RT
50 °C
80 °C
120 °C
0
2.5 wt.% PS
5 wt.% PS
7.5 wt.% PS
Mixing Ratios
b

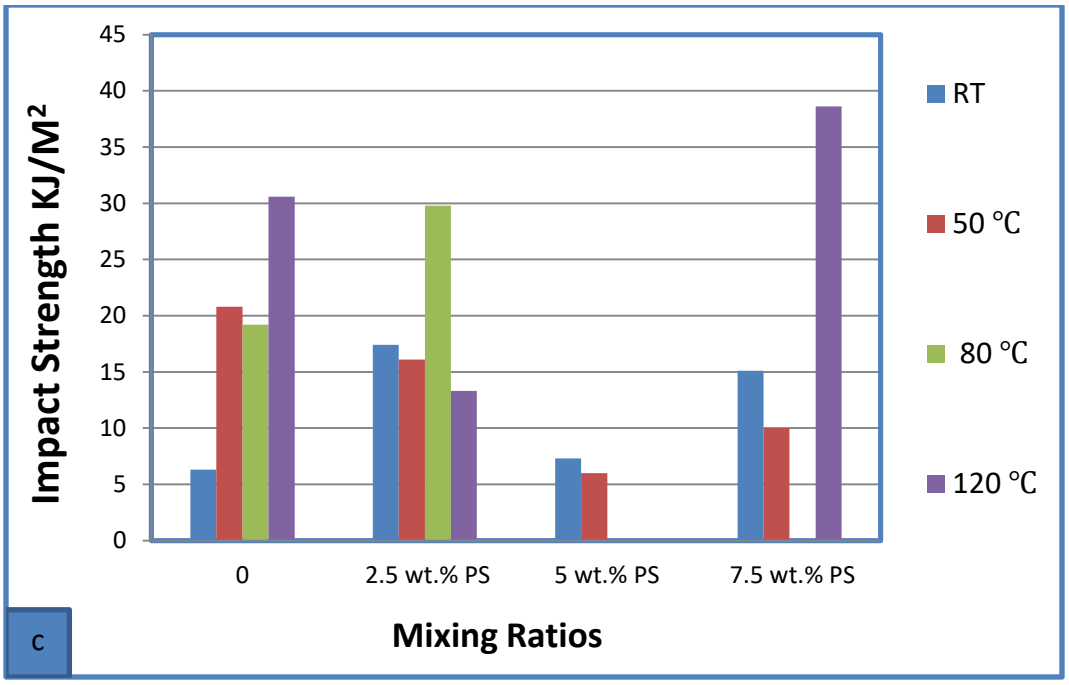

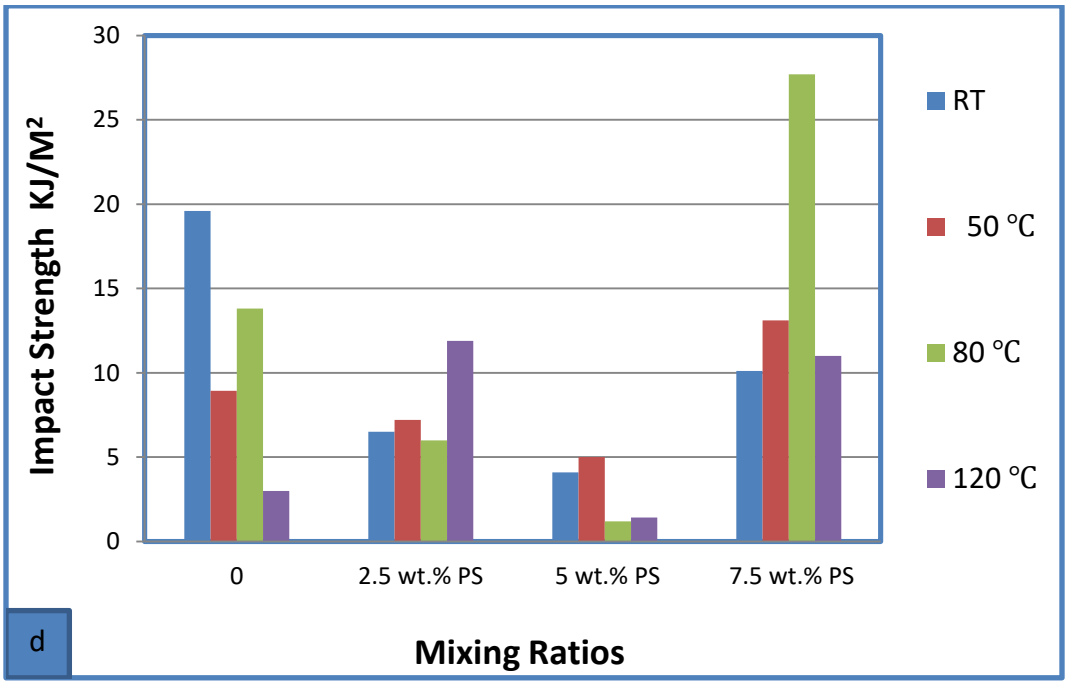

Figure(4.29) : Represent samples of a: 1:0.5, b:1:1, c:1.5:1 and d:2.5:1.5 impact strength of epoxy and its blends at different temperature.

At a curing temperature of 80 °C, Figure (4.29) (c) illustrates how adding PS at a weight of 7.5 wt.% PS to a 1.5:1 formulation increases the impact strength of the epoxy; the highest value was reached at a weight of 2.5:1.5 + 7.5 wt.% PS at 120

°C. Regards, after that, as the PS content increases, the impact strength decreases but does not go below that of pure epoxy; a 1:1 pure value has a better impact strength value than other formation pure values.

This appearance is may be due to the evaporation of solvent which remain a voids that becom stress concetration which may weaken the blends structure or phase separation morphology of the blend, where the PS phase forms scattered domains inside an epoxy matrix the tiny improvement in mechanical characteristics brought about by the addition of PS might be explained by the interfacial adhesion and compatibility between the matrix and the dispersed phase, as well as the softening effect of the flexible PS chains in the hard epoxy matrix similar with [108].

Impact energy is kinetic energy that is absorbed and released through vibration when it collides with a material such as PS that has a second phase of plastic deformation due to the flexibility of its chains as a result, the material is reinforced against impact.

4.6.4 Fracture Toughness Results

Figure (4.30) shows the unmodified epoxy resin and the fracture toughness of polystyrene toughened epoxy with different compositions at different temperatures for curing. The unequal dispersion of PS inside epoxy matrix that was observed at greater polystyrene concentrations prevented any further rise from being noticed after more polystyrene was added. The polystyrene polymer can act as a plasticizer or a flexibilizer when a little amount of polystyrene is introduced to the epoxy matrix. Modified epoxy blends have higher fracture toughness values than raw epoxy blends, and these values

steadily rise with increasing dose levels. These data provide more evidence in favor of the impact strength analyses' conclusions [109]. It is evident that when the maximum load is reached, both pure and modified epoxies exhibit unstable fracture propagation, and the maximum loads for modified epoxies are obviously higher than for their unmodified counterpart similar to [112, 113, 114]. The Figure (4.31) below illustrates the optimal fracture toughness value, which was 1:0.5 + 2.5 wt.% when comparing PS that cured at 120 °C to pure samples and others that cured at different temperatures, it is also evident that under all circumstances and at a 1:1 epoxy to hardener ratio, the value of fracture toughness that give the same response because all of the samples were rubber-like in texture.

This result was also related to the percent's elastic modulus, which had all values equal to the same value and stable. In strongly cross-linked brittle polymers, strong reinforcement particles can achieve a range of effects, regulating the overall increase in fracture toughness through multiple mechanisms, plastic deformation, plastic void expansion, fracture path deflection, and crack pinning are some of these mechanisms.

To identify the extrinsic toughening mechanisms and to describe the interaction between the crack and the reinforcing particles, microscopic investigations of the fracture surfaces were conducted using scanning electron microscopy (SEM).

Because this value is so much less than the toughening's total contribution, the crack deflection mechanism only slightly contributes to the toughening. This could be because the aggregate and PS percentage,

which resemble agglomerated lumps inside the material matrix, are insufficient to deflect the micron-sized fracture point similar to [69]. The influence of the EP/h/PS formulations ratio on the PS fracture mechanism is also investigated in connection to the morphological features of the propagation zones on the impact samples' fracture surface.

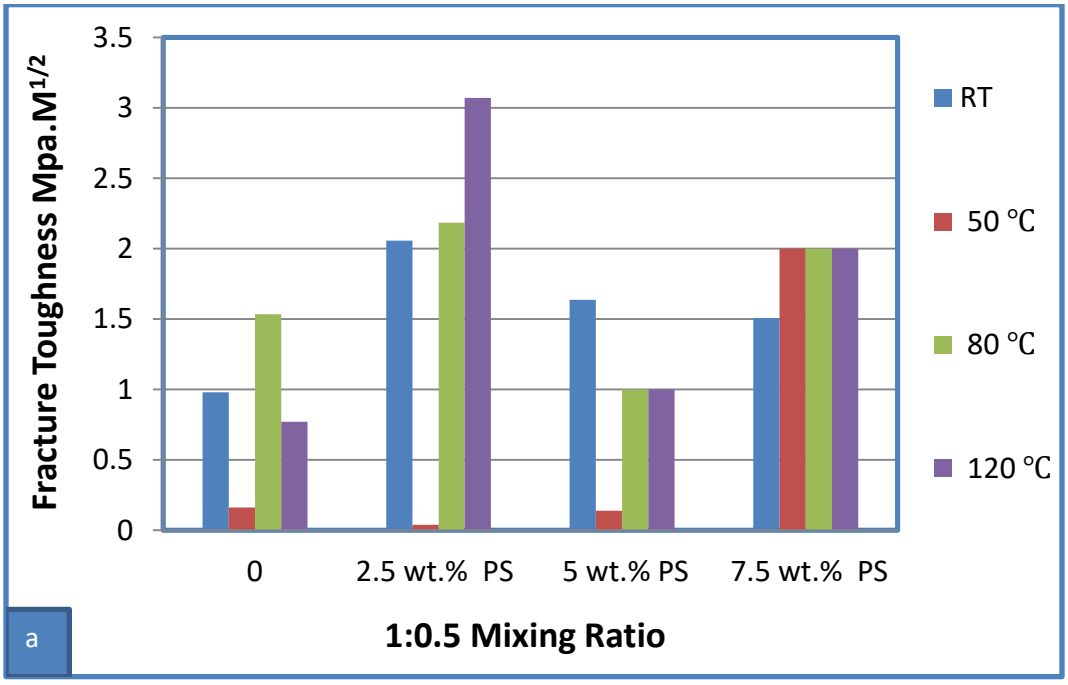

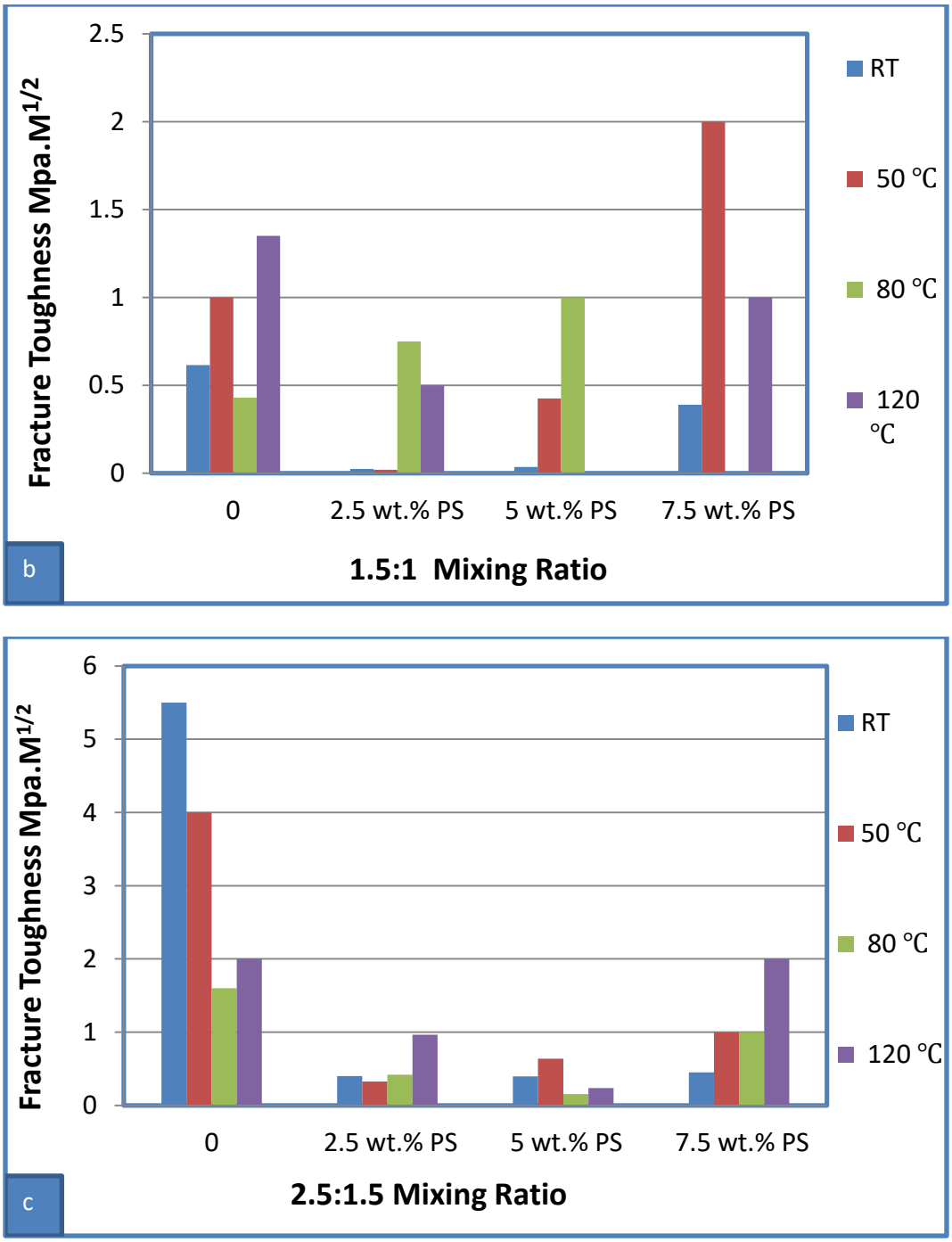

Figure (4.30): Represent the fracture toughness of epoxy with blends at different temperature.

4.7 SEM Results

The cross-sectional SEM pictures of the fractured surface are displayed in Figure (4.31). The images, which illustrate how polystyrene is distributed throughout the epoxy resin polymer matrix, are taken at 20μm magnification for samples that were cured at RT for 24 hours for varying PS concentrations. The SEM pictures of several epoxy/polystyrene blends that cross-sectional views where the raw polystyrene material appears to be scattered throughout the mix matrix Figure (4.30) due to the fact that ordinary epoxy has a smooth fracture surface and a poor barrier to failure similar to [12]. Epoxy networks' amorphous single-phase structure fits with the featureless one-phase morphology observed in SEM micrographs. There have previously been similar SEM photos similar to [113, 114].

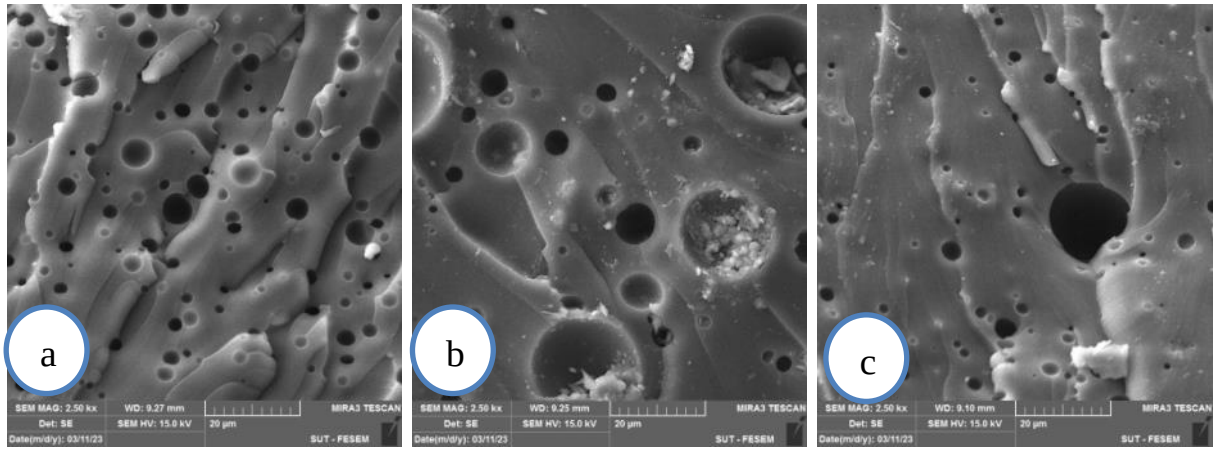

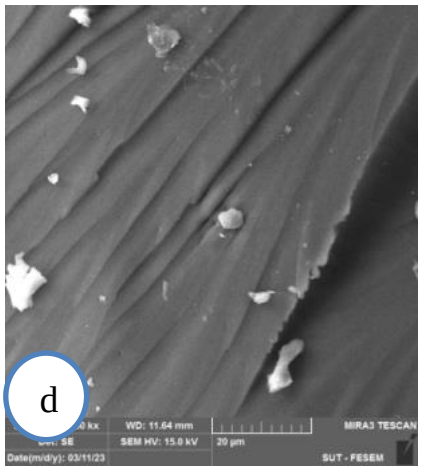

Figure (4.31) : The SEM images at 20µm for samples a: 2:1+7.5 wt. % , b: 2:1+5 wt.%, c: 2:1+2.5 wt. % and d: 2:1pure cured at RT with curing time 24h for different percent of concentration of PS.

Furthermore, a radiating pattern of pure epoxy cleavage plane distribution suggested a brittle fracture with low impact resistance and fracture toughness. The fracture surface of pure epoxy was likewise smoother and flatter. The cross-sectional images clearly show how the addition of polystyrene significantly changed the nature of the fracture.

On the other hand, the fractured surface of the PS-toughened epoxy made it evident that there were two distinct phases present: a scattered Polystyrene phase and a continuous epoxy matrix. The presence of polystyrene will act as the energy dissipation core of the epoxy matrix. In reaction to triaxial stresses close to the crack site, polystyrene would locally yield.

After the occurrence of the polystyrene bridging mechanism in the crack tip zone of the epoxy matrix, cavitation—caused by the solvent that was not evaporating from the mixture or by the polystyrene debonding from the surface led to the growth of the plastic void. In the micrographs, deformation lines were visible stretching across the polystyrene, demonstrating that the ductile fracture had actually happened.

A concentration of small polystyrene particles can allow crack energy to diffuse. Conversely, the fractured surface of the PS-toughened epoxy amply demonstrated the existence of two distinct phases: a dispersed Polystyrene phase and a continuous epoxy matrix, the latter of which will function as the energy dissipation core of the epoxy matrix similar to [115].

In Figure (4.32) for samples cured at 120 ℃ at 4 houres in an oven Phase separation and the emergence of immiscible PS structures in the matrix are indicated by the presence of many spherical holes forms that related to the immiscibility window that phase separation occurs similar to [116]. There is evidence of a micro-phase separation at both low and high PS concentrations, dark patches signify the micro-separated phase which is not miscible with the epoxy matrix, there are a few voids visible in the SEM micrograph. The epoxy matrix's preexisting voids are an inescapable problem, these spaces may serve as stress concentrators, making the hardened epoxy brittle, on the fracture surfaces, heterogeneous morphological surfaces were produced, the micrograph's holes show that the polystyrene distributed throughout the epoxy matrix similar to [117].

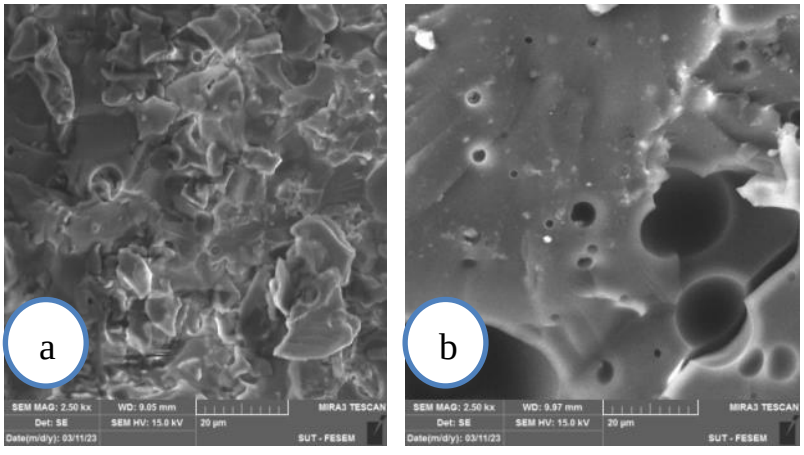

Figure (4.32) : The SEM image at 20µm for samples a: 2:1+7.5 wt. % and b: 2:1+2.5 wt. % cured at 120 ℃ for 4h with different concentration of PS.

Fracture surfaces also exhibit large shear yields and plastic deformations, which point to a characteristic toughness character to decreasing [118], Both the high load EP/PS (5 wt.%) and low load EP/PS (2.5 wt.%) have a rougher fracture surface than pure EP because of the solvents evaporating during the curing process, there are also a few apparent tiny holes similar to [119].

In Fig. (4.33)a large region of the fracture surface micrographed, the harshness of PS/epoxy combinations is demonstrated by it a multilayer fracture with ridges and a wave-like apex is also visible agreement with [120]. Only a small amount of plastic distortion and a few long, twisted threads of material that are periodically apparent similar to [121].

Higher fracture toughness and impact strength can be linked to the SEM micrograph by observing greater roughness and substantial plastic yielding of the polymer matrix at the fracture surfaces, along with twisted leaf-like structures and more cavitations agreement with [122].

It is evident that the second phase gets more aggregated and harder to separate from the epoxy matrix if polystyrene content reaches 7.5% weight. This situation causes the matrix to become more flexible, which lowers its capacity to tolerate tension similar to [123].

A rough surface and numerous PS holes in the epoxy matrix are seen in Figure (4.33), the SEM image at 50μm for different samples cured at RT for 24h with was insufficient interaction between the pure PS and epoxy matrix, which prevented the fracture energy from being effectively dissipated when the external tensile force was applied to the epoxy composites. The tensile test revealed that the PS holes had become the breaking sites and that cracks had started from these holes, resulting in the low tensile strength. The cured epoxy composites filled with PS, however,

show a completely different fracture surface than mixes of pure epoxy and pure PS/epoxy, when dimples emerge, new fracture surfaces are forming which might release more energy and result in an increase in tensile performance. The toughening mechanism of epoxy mixed with thermoplastic components has been explained by a technique known as "crack pinning" according to reports. This method suggests that the stiff PS may have functioned as the impenetrable objects that bowed out the crack and required further force when the loading reaches 7.5 wt.% of PS, a lot of white broken traces are seen on the fracture surface of the epoxy blend these traces are most likely from the agglomerated PS, which accounts for the comparatively lower tensile strength when compared to the cured epoxy composites filled with low loadings of PS similar to [124].

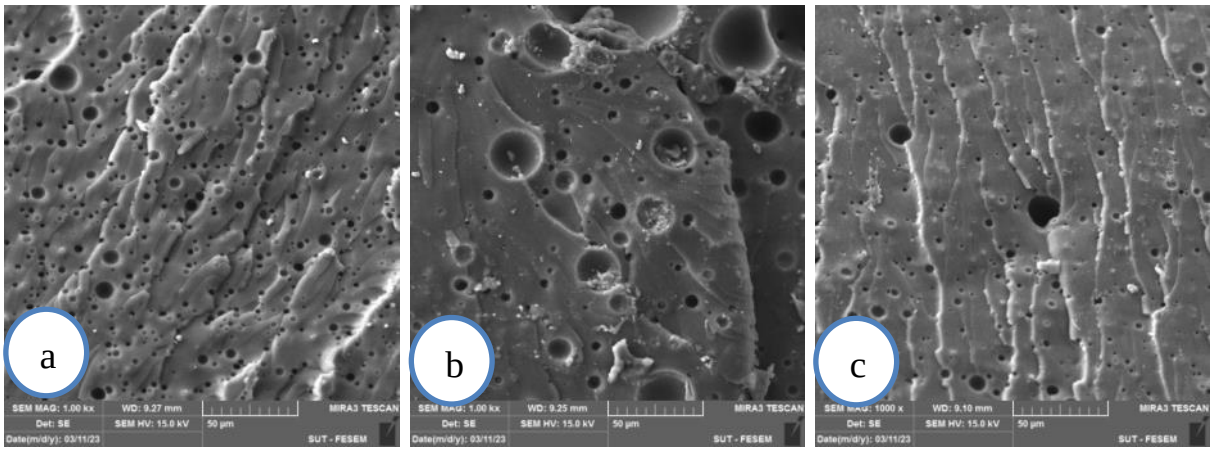

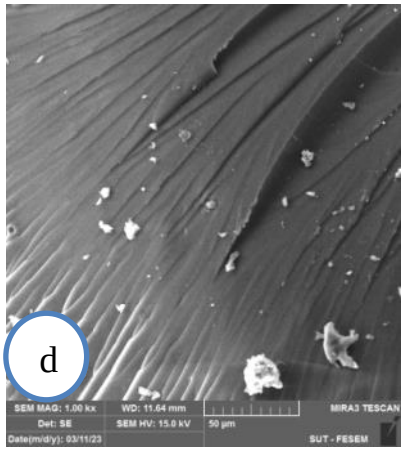

Figure (4.33) : The SEM image at 50µm for different samples a: 2:1+7.5 wt.%, b: 2:1+5 wt.%, c: 2:1+2.5 wt. %and d: 2:1pure cured at RT for 24h with different concentration of PS.

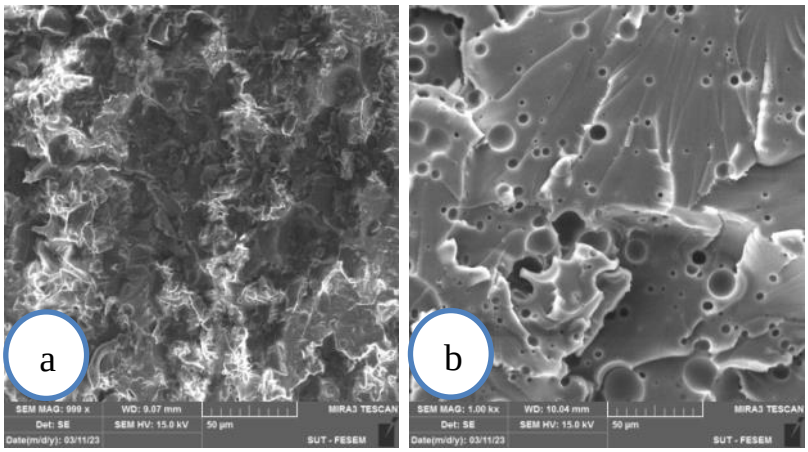

Figure (4.34): The SEM images at 50µm for different samples a: 2:1+7.5 wt.% and 2:1+2.5 wt.% cured at 120 ℃ for 4h with different concentration of PS.

In Figures (4.35), (4.36) , (4.37) and (4.38) showed that the hardened material had voids surrounding many of the regions. This indicates that the epoxy matrix has experienced plastic void expansion, initiated by the debonding of PS. In addition to pure samples, as we will show later, pure samples do not have pinning morphology or voids like other samples do the fracture surface of unmodified epoxy resin and its mixtures is shown

right to left is the direction in which the crack propagates the fracture surface of a brittle thermosetting polymer is frequently glassy and reasonably smooth. Furthermore, the fracture surface of the epoxy modified with polystyrene showed unique features compared to the original epoxy polymer, as seen in all figures. Crack pinning, plastic deformation, crack path deflection, and plastic void expansion are some of these mechanisms, using scanning electron microscopy (SEM), microscopic examinations of the fracture surfaces were made in order to determine the extrinsic toughening mechanisms and to define the interaction between the crack and the reinforcing particles [69]. These variations in morphology are reflected in the fracture toughness data and mechanism, which are discussed subsequently.

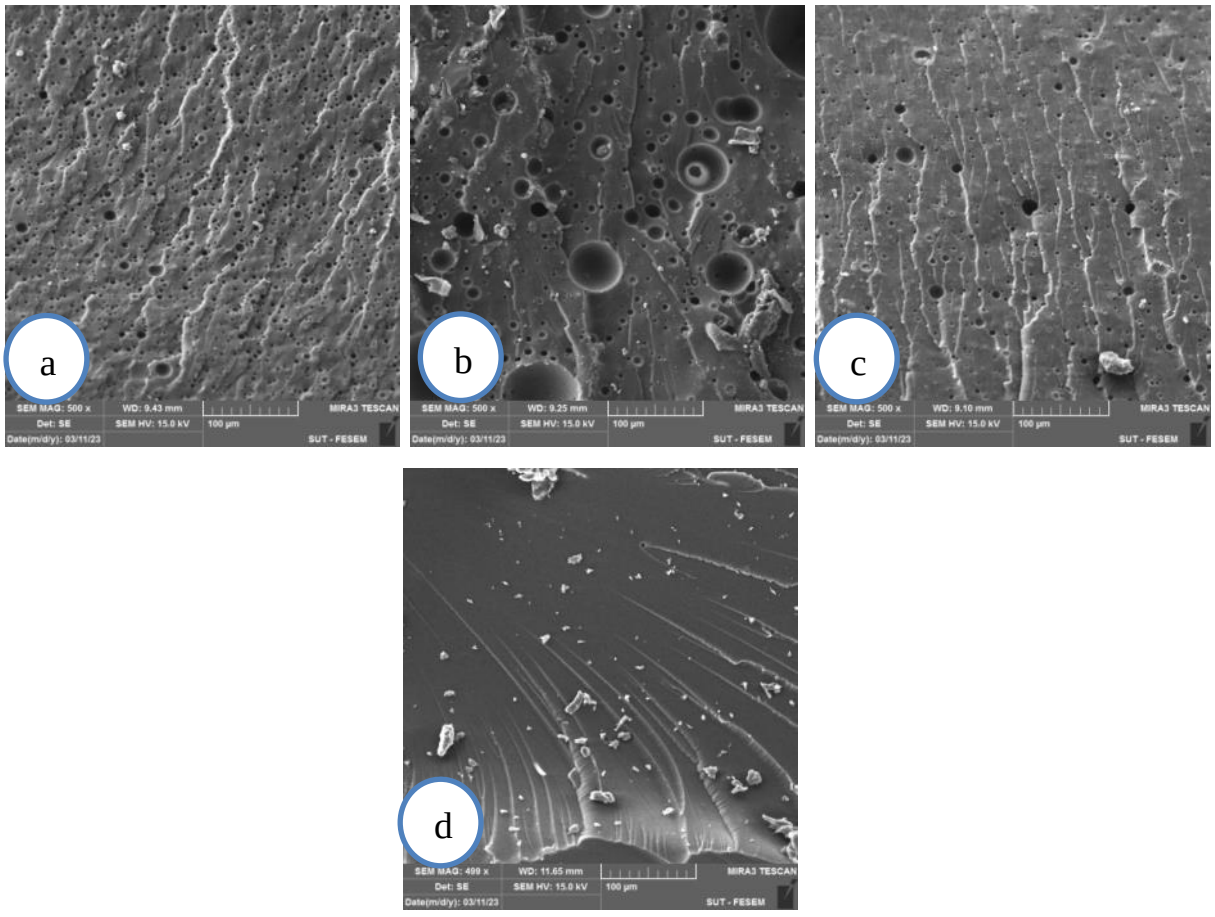

Figure (4.35): The SEM images of different samples a: 2:1+7.5 % wt. PS, b: 2:1+5 % wt. PS c: 2:1+2.5% wt. PS and d: 2:1pure cured at RT of EP/h/PS blends.

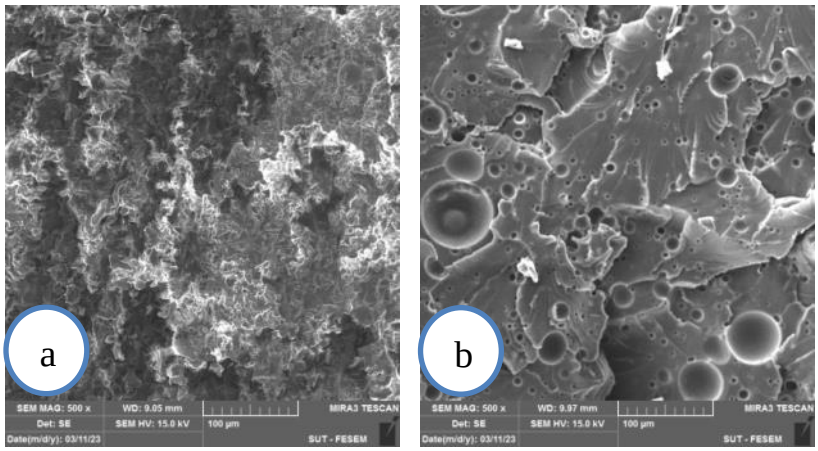

Figure (4.36): The SEM images of different samples a: 2:1+7.5% wt. PS and b: 2:1+2.5 % wt. PS cured at 120°C of EP/h/PS blends.

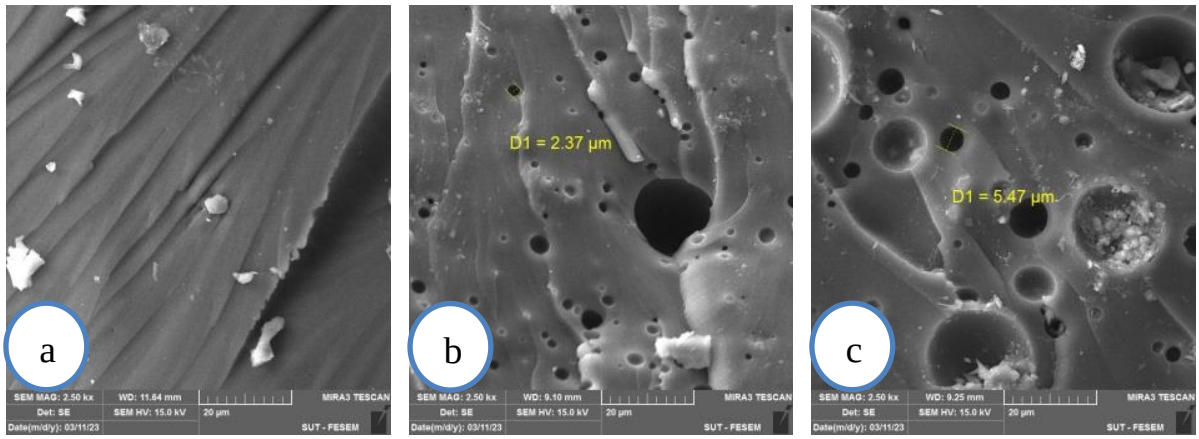

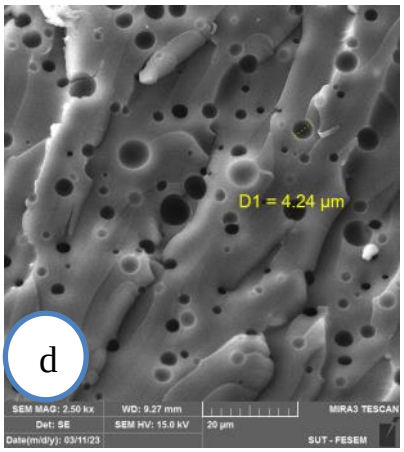

Figure (4.37): The SEM Images of Different Samples a: 2:1 pure, b: 2:1+2.5 % wt. PS, 2:1+5 % wt. PS and 2:1+7.5 % wt. PS cured at RT of EP/h/PS Blends.

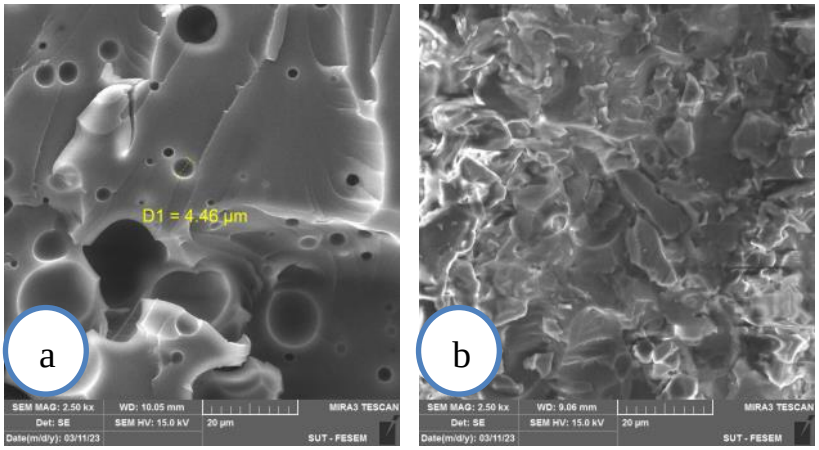

Figure (4.38): The SEM images of different samples a: 2:1+2.5%PS and b: 2:1+7.5%PS cured at 120 ℃ of EP/h/PS blends.

Chapter Five

Conclusions and Recommendations

5.1 The Conclusions

The following conclusions can be made in light of the data collected and the discussion of them in chapter four:

1. The results of DSC epoxy and its blends demonstrated that various parameters affected the kinetics mechanism under various conditions. Additionally, the addition of PS affected Tg, resulting in a decrease in Tg value, indicating the action of the toughening agent on flexibility chains and the plasticizer effect.
2. The thermal stability of epoxy resin and its blends was demonstrated by the TGA data.
3. The FT-IR results for the toughening agent/epoxy blends demonstrated that the polar epoxy polymer and various toughening agents only physically interact with one another rather than undergoing a chemical reaction.
4. In SEM epoxy and its blends images, demonstrates that PS with epoxy matrix that as a result of PS domine phase separation on epoxy matrix with the appearance of pinning morphology in the fracture surface area at RT curing, or as a result of solvent evaporation on the surface of cross section sample including voids and crakes.
5. The tensile strength, elastic modulus, and elongation at break-off were examined. The results demonstrate that, for pure samples under various conditions, the best tensile strength with different curing temperature value was at 1:0.5 pure cured at 80 °C, The best results at formulation 1.5:1 with varying curing temperatures were obtained at 1.5:1 pure at RT, for the blend 2.5:1.5+5 wt.% PS cured

at 120 °C, the formulation 2.5:1.5, with varied curing temperatures, was at 2.5:1.5 pure cured at RT.

6. In a 1:1 formulation, the elastic modulus value was the same for all formulations due to the material's test-related rubber-like appearance. In a 1.5:1 formulation, the best values were found in 1.5:1 pure cured at 50 °C, in a 2.5:1.5 formulation, all formulations show a reduction in their value under all conditions. Elongation at break show that the best values was at 1:0.5+7.5 wt.% PS curing at RT.
7. Formulation 1:1 the best value was 1:1 pure cured 120 °C. At formulation 1.5:1 the best value was 1.5:1+2.5 wt.% PS cured at 80 °C. At formulation 2.5:1.5 the best value was at 2.5:1.5+7.5 wt.% cured at 80 °C.
8. The hardness the best value was at 1:0.5 cured at 50°C.
9. The ability of epoxy compositions to withstand fracture was indicates that at formulation 1:0.5+2.5 wt.% PS cured at 120°C. The formulation 1.5:1 pure, which was cured at RT for 24 hours. The formulation 2.5:1.5, which was cured at RT.
10. The samples' of impact strength was at 1:0.5+5 wt.% PS cured at RT, for 1:1 formulation were cured at 120 °C. For 1.5:1 formulation were at 1.5:1+7.5 wt.% PS was cured at 120°C, and 2.5:1.5+7.5 wt.% cured at 80°C, pure sample cured at 80°C, and pure sample cured at RT.

5.2 Recommendations

1. Using aromatic curing agents such as DDS and DICY etc.,
2. Studying more tests, like the H NMR test and the dynamic mechanical analysis (DMA) test.
3. Using different toughening agents, including polypropylene thermoplastic, Ti powder and micro and nanoparticles, etc.
4. Applying the UV curing method to the curing procedure.
5. Production of bio-based epoxy resin with the inclusion of vegetable oil, like soybean oil, etc.

References

[1] J. Parameswaranpillai, N. Hameed, and E. M. Woo, *Handbook of Epoxy Blends*, 2017, doi :10.1007/978-3-319-40043-3, China.

[2] W. Jau, L. Chen, L. Kang, Y. Chun, C. Zheng, and Y. Wu, "Curing behavior and adhesion properties of epoxy resin blended with phenol-liquefied Cryptomeria japonica," *Eur. J. Wood Wood Prod.*, vol. 0, no. 0, p. 0, 2018, doi: 10.1007/s00107-018-1329-5.

[3] Y. Li, M. Li, and F. Chang, "Kinetics and curing mechanism of epoxy and boron trifluoride monoethyl amine complex system," *J. Polym. Sci. Part A Polym. Chem.*, vol. 37, no. 18, pp. 3614–3624, 1999, doi: 10.1002/(sici)1099-0518(19990915)37:18<3614::aid-pola9>3.3.co;2-q.

[4] M. A. Bashir, "Cure Kinetics of Commercial Epoxy-Amine Products with Iso-Conversional Methods," *Coatings*, vol. 13, no. 3, p. 592, 2023, doi: 10.3390/coatings13030592.

[5] A. Sangregorio, N. Guigo, and E. De Jong, "Kinetics and Chemorheological Analysis of Cross-Linking Reactions in Humins calculate," pp. 1–15, 2019.

[6] R. Hardis, J. L. P. Jessop, F. E. Peters, and M. R. Kessler, "Composite s : Part A Cure kinetics characterization and monitoring of an epoxy resin using DSC , Raman spectroscopy , and DEA," *Compos. Part A*, vol. 49, pp. 100–108, 2013, doi: 10.1016/j.compositesa.2013.01.021.

[7] Z. Zhu, X. Sun, H. Yuan, C. Song, Y. Cao, and X. Li, "Determination of gel time and gel point of epoxy-amine thermosets by in-situ near infrared spectroscopy," *Polym. Test.*, vol. 72, pp. 416–422, 2018, doi: 10.1016/j.polymertesting.2018.11.001.

[8] M. Emad, “Cure Kinetics of Epoxy Resin Studied by Dynamics and Isothermal DSC Data,” vol. 34, pp. 1731–1743, 2016.

[9] I. Kroutilová, L. Matějka, A. Sikora, K. Souček, and L. Stag, “Curing of epoxy systems at sub-glass transition temperature,” *J. Appl. Polym. Sci.*, vol. 99, no. 6, pp. 3669–3676, 2006, doi: 10.1002/app.22548.

[10] V. Y. Ignatenko, S. O. Ilyin, A. V. Kostyuk, G. N. Bondarenko, and S. V. Antonov, “Acceleration of epoxy resin curing by using a combination of aliphatic and aromatic amines,” *Polym. Bull.*, vol. 77, no. 3, pp. 1519–1540, 2020, doi: 10.1007/s00289-019-02815-x.

[11] M. G. Hamed, “Study the tensile strength for epoxy composite reinforced with fibers and particles,” vol. 3, no. 2, 2009.

[12] Z. Wang, F. Liu, W. Liang, and L. Zhou, “Study on Tensile Properties of Nanoreinforced Epoxy Polymer : Macroscopic Experiments and Nanoscale FEM Simulation Prediction,” vol. 2013, 2013.

[13] H. Li, G. Chen, H. Su, D. Li, L. Sun, and J. Yang, “Effect of the stoichiometric ratio on the crosslinked network structure and cryogenic properties of epoxy resins cured at low temperature,” *Eur. Polym. J.*, 2018, doi: 10.1016/j.eurpolymj.2018.10.051.

[14] B. ELLIS, *Chemistry and Technology of Epoxy Resins.*, vol. 59, Springer Science+Business Media Dordrecht 1993, First edition, doi: 10.1007/978-94-011-2932-9.

[15] Clayton May, “Epoxy Resins Chemistry and Technology, Second Edition, 1988, ISBN 0-8247-7690-9.

[16] H. E. Bair, P. K. Gallagher, M. Jaffe, and D. Raucher, “Thermal Characterization of Polymeric Materials,” *Therm. Charact. Polym. Mater.*, 1981, doi: 10.1016/b978-0-12-703780-6.x5001-9.

[17] C. S. Edited by Sabu Thomas and and R. Thomas, *Micro- and Nanostructured Epoxy/Rubber Blends*, vol. 1999, no. December. 2006.

[18] R. Hardis, M. R. Kessler, and M. C. Frank, “Cure kinetics characterization and monitoring of an epoxy resin for thick composite structures by Table of Contents,” 2012.

[19] M. M. Shokrieh, *Residual Stresses in Composite Materials*. 2014. doi: 10.1533/9780857098597.

[20] H. Tsai, Y. Nakamura, and M. Naito, “Materials Advances Strengthening epoxy adhesives at elevated temperatures based on dynamic disulfide bonds †,” no. Scheme 1, pp. 3182–3188, 2020, doi: 10.1039/d0ma00714e.

[21] O. De Andrade Raponi, R. De Andrade Raponi, G. B. Barban, R. M. Di Benedetto, and A. C. Ancelotti, “Development of a simple dielectric analysis module for online cure monitoring of a commercial epoxy resin formulation,” *Mater. Res.*, vol. 20, pp. 291–297, 2017, doi: 10.1590/1980-5373-MR-2017-0067.

[22] S. Xu and X. Song, *Handbook of Epoxy Blends*. 2015. doi: 10.1007/978-3-319-18158-5.

[23] A. Introduction, *Engineering Materials 2 An Introduction to Microstructures, Processing and Design*. 2013. doi: 10.1016/c2009-0-64289-6.

[24] S. Pradhan, P. Pandey, S. Mohanty, and S. K. Nayak, “Insight on the

Chemistry of Epoxy and Its Curing for Coating Applications : A Detailed Investigation and Future Perspectives," vol. 2559, no. May, 2016, doi: 10.1080/03602559.2015.1103269.

[25] Adnan A. Abdulrazak , "A study on the effect of hardener on the mechanical properties of epoxy resin," A Thesis, 2010.

[26] P. I. Karkanas, "Cure modelling and monitoring of epoxy/amine resin systems," *J. Appl. Polym. Sci.*, vol. 77, no. 7, pp. 1419–1431, 1998.

[27] M. Urbaniak and K. Grudziński, "Time-temperature-transformation (TTT) cure diagram for EPY® epoxy system," *Polimery/Polymers*, vol. 52, no. 2, pp. 117–126, 2007, doi: 10.14314/polimery.2007.117.

[28] M. Emad, "Cure Kinetics of Epoxy Resin Studied by Dynamics and Isothermal DSC Data," vol. 34, no. 9, pp. 1731–1743, 2016.

[29] F. Jin, X. Li, and S. Park, "Journal of Industrial and Engineering Chemistry Synthesis and application of epoxy resins : A review," *J. Ind. Eng. Chem.*, vol. 29, pp. 1–11, 2015, doi: 10.1016/j.jiec.2015.03.026.

[30] N. Abdulrazack, "The Effect of Various Hardeners on the Mechanical and Thermal Properties of Epoxy Resin," no. January, pp. 1–5, 2014.

[31] A. Shundo, S. Yamamoto, and K. Tanaka, "Network Formation and Physical Properties of Epoxy Resins for Future Practical Applications," *JACS Au*, vol. 2, no. 7, pp. 1522–1542, 2022, doi: 10.1021/jacsau.2c00120.

[32] G. Gibson, "Handbook of Thermoset Resins," *Brydson's Plastics Materials: Eighth Edition*. pp. 773–797, 2017. doi: 10.1016/B978-0-323-35824-8.00027-X.

[33] J. Brier and lia dwi jayanti, *Polystyrene: Synthesis, Characteristics and Applications*, vol. 21, no. 1. 2020.

[34] C. A. Wilkie, *Polymer Blends Handbook*, Springer New York Heidelberg Dordrecht London, 2014, second edition, doi :10.1007/978-94-007-6064-6.

[35] A. Salisu and Y. S. Maigari, "Polystyrene and its recycling: A review," *Proc. Mater. Sci. Technol.* , no. March, pp. 195–203, 2021.

[36] J. E. Figueruelo, C. M. Gómez, I. S. Monzó, C. Abad, and A. Campos, "Thermodynamic study on phase equilibrium of epoxy resin/thermoplastic blends," *J. Chem. Thermodyn.*, vol. 40, no. 4, pp. 677–687, 2008, doi: 10.1016/j.jct.2007.10.009.

[37] S. Du, Z. Guo, B. Zhang, and Z. Wu, "Cure kinetics of epoxy resin used for," vol. 1347, no. June, pp. 1343–1347, 2004, doi: 10.1002/pi.1533.

[38] N. L. D. Filho, C. X. Cardoso, and H. A. De Aquino, "Relationships between the Curing Conditions and Some Mechanical Properties of Hybrid Thermosetting Materials," vol. 17, no. 5, pp. 935–943, 2006.

[39] K. P. Unnikrishnan and E. T. Thachil, "Toughening of epoxy resins," *Des. Monomers Polym.*, vol. 9, no. 2, pp. 129–152, 2006, doi: 10.1163/156855506776382664.

[40] X. Luo, R. Ou, D. E. Eberly, A. Singhal, W. Viratyaporn, and P. T. Mather, "A Thermoplastic / Thermoset Blend Exhibiting Thermal Mending and Reversible Adhesion," vol. 1, no. 3, 2009, doi: 10.1021/am8001605.

[41] H. Ali Shnawa, "Thermal properties and curing kinetics of epoxy-natural polyphenols based composite," *J. Phys. Conf. Ser.*, vol. 1294, no. 5, pp. 178–

181, 2019, doi: 10.1088/1742-6596/1294/5/052009.

[42] Z. Yang, H. Peng, W. Wang, and T. Liu, “Epoxy Resin/Polymer Blends: Improvement of Thermal and Mechanical Properties,” *J. Appl. Polym. Sci.*, vol. 116, no. 5, pp. 2658–2667, 2010, doi: 10.1002/app.

[43] M. Pramanik, E. W. Fowler, and J. W. Rawlins, “Cure kinetics of several epoxy – amine systems at ambient and high temperatures,” 2014, doi: 10.1007/s11998-013-9565-4.

[44] S. K. Sardiwal, B. V. Sai Anoop, G. Susmita, L. Vooturi, and S. A. Uddin, “Advanced Composite Materials in Typical Aerospace Applications,” *Glob. J. Res. Eng. D Chem. Eng.*, vol. 14, no. 1, pp. 5–10, 2014.

[45] H. Ma, N. Hu, C. Wu, Y. Zhu, Y. Cao, and Q. Q. Chen, “Synthesis and research of epoxy resin toughening agent,” *Springerplus*, 2016, doi: 10.1186/s40064-016-2356-5.

[46] D. A. Lakho, D. Yao, K. Cho, and M. Ishaq, “Study of the Curing Kinetics Towards Development of Fast Curing Epoxy Resins,” vol. 2559, no. June, 2016, doi: 10.1080/03602559.2016.1185623.

[47] B. B. Johnsen, A. J. Kinloch, and A. C. Taylor, “Toughness of Syndiotactic Polystyrene / Epoxy Polymer Blends : Microstructure and Toughening Mechanisms Toughness of Syndiotactic Polystyrene / Epoxy Polymer Blends : Microstructure and Toughening Mechanisms,” no. May 2017, 2006.

[48] E. O. Ozgul and M. H. Ozkul, “Effects of epoxy , hardener , and diluent types on the hardened state properties of epoxy mortars,” *Constr. Build. Mater.*, vol. 187, pp. 360–370, 2018, doi: 10.1016/j.conbuildmat.2018.07.215.

[49] B. Massoumi, M. Abbasian, R. Mohammad-Rezaei, A. Farnudiyan-Habibi, and M. Jaymand, “Polystyrene-modified novolac epoxy resin/clay nanocomposite: Synthesis, and characterization,” *Polym. Adv. Technol.*, vol. 30, no. 6, pp. 1484–1492, 2019, doi: 10.1002/pat.4580.

[50] M. Michel and E. Ferrier, “Effect of curing temperature conditions on glass transition temperature values of epoxy polymer used for wet lay-up applications,” *Constr. Build. Mater.*, vol. 231, p. 117206, 2020, doi: 10.1016/j.conbuildmat.2019.117206.

[51] L. Liu and Y. Chen, “Toughening Study of Epoxy Structural Reinforcement Adhesive in Concrete at Room Temperature Toughening Study of Epoxy Structural Reinforcement Adhesive in Concrete at Room Temperature,” 2019, doi: 10.1088/1757-899X/585/1/012023.

[52] J. L. 1 and S. H. Xingming Bian 1, Rui Tuo 1, Wei Yang 2, Yiran Zhang 1, Qing Xie 1,*, Junwei Zha 3 and 1548; doi:10.3390/polym11101548 Polymers 2019, 11, “Mechanical , Thermal , and Electrical Properties of BN – Epoxy Composites Modified with”.

[53] S. A. Al Bayaty, “Study of Thermal Decomposition Behavior and Kinetics of Epoxy/Polystyrene Composites by using TGA and DSC,” *J. Xi’an Univ. Archit. Technol.*, vol. XII, no. III, 2020, doi: 10.37896/jxat12.03/109.

[54] U. Farooq, J. Teuwen, and C. Dransfeld, “Toughening of Epoxy Systems with Interpenetrating Polymer Network (IPN): A Review,” 2020.

[55] V. E. Resins, “Comparative Study on Toughening Effect of PTS and PTK in Various Epoxy Resins,” pp. 1–13, 2021.

[56] P. D. Sheet, “Sikadur ® -52 LP LOW VISCOSITY INJECTION RESIN,”

no. December, pp. 2–4, 2018.

[57] S. D. Sheet, “Sikadur ® -52 Part B Sikadur ® -52 Part B,” 2018.

[58] C. Polymer and P. Ps, “American Polymers API 390 Polystyrene Contact Songhan Plastic Technology Co ., Ltd .,” p. 51131842.

[59] J. Kjølholt., “Survey of toluene Authors and contributors,” no. June, 2014.

[60] P. M. Piccione *et al.*, “Solvent Selection Methods and Tool,” *Org. Process Res. Dev.*, vol. 23, no. 5, pp. 998–1016, 2019, doi: 10.1021/acs.oprd.9b00065.

[61] S. Liu, M. Li, L. Jia, M. Chen, S. Du, and J. Gong, “Investigation of Drug-Polymer Miscibility, Molecular Interaction, and Their Effects on the Physical Stabilities and Dissolution Behaviors of Norfloxacin Amorphous Solid Dispersions,” *Cryst. Growth Des.*, vol. 20, no. 5, pp. 2952–2964, 2020, doi: 10.1021/acs.cgd.9b01571.

[62] G. Bogoeva-gaceva, “A rapid method for the evaluation of cure kinetics of thermosetting polymers Gordana Bogoeva-Gaceva and Aleksandra Buzarovska,” no. February 2014, 2013, doi: 10.20450/mjcce.2013.303.

[63] Annual Book of ASTM Standard, “Standard Practice for General techniques for Obtaining Infrared Spectra for Qualitative Analysis.” E 1252-98, PP.(1-11), 2002.

[64] Astm, “ASTM D638: Standard Test Method for Tensile Properties of Plastics,” *ASTM Stand.*, no. January, pp. 1–15, 2004.

[65] American Society for Testing and Materials, “ASTM D2240-15 Standard Test Methods for Rubber Property-Durometer Hardness,” *Annu. B. ASTM*

Stand., pp. 1–13, 2015, doi: 10.1520/D2240-15.2.

[66] I. S. 11266, “International Standard International Standard,” *61010-1 © Iec2001*, vol. 2014, p. 13, 2014.

[67] ISO 179-1, “International standard - determination of charpy impact properties,” *Int. Organ. Stand.*, vol. 10406–1:20, pp. 3–6, 2015.

[68] S. T. Methods, “Standard Test Methods for Plane-Strain Fracture Toughness and Strain Energy Release Rate of Plastic Materials 1,” vol. i, pp. 1–10, doi: 10.1520/D5045-14.priate.

[69] M. Zamanian, M. Mortezaei, B. Salehnia, and J. E. Jam, “Fracture toughness of epoxy polymer modified with nanosilica particles: Particle size effect,” *Eng. Fract. Mech.*, vol. 97, no. 1, pp. 193–206, 2013, doi: 10.1016/j.engfracmech.2012.10.027.

[70] T. H. Hsieh, A. J. Kinloch, K. Masania, J. Sohn Lee, A. C. Taylor, and S. Sprenger, “The toughness of epoxy polymers and fibre composites modified with rubber microparticles and silica nanoparticles,” *J. Mater. Sci.*, vol. 45, no. 5, pp. 1193–1210, 2010, doi: 10.1007/s10853-009-4064-9.

[71] Tescan, “Tescan Mira,” 2021.

[72] S. Contents and P. Class, “POLYMER DATA,” 1999.

[73] J. Diani and K. Gall, “Cure Kinetics and Thermal Stability of Micro and Nanostructured Thermosetting Blends of Epoxy Resin and Epoxidized Styrene-Block-Butadiene-Block-Styrene Triblock Copolymer Systems,” *Society*, pp. 1–10, 2006, doi: 10.1002/pen.

[74] M. Martin-Gallego, R. Verdejo, A. Gestos, M. A. Lopez-Manchado, and Q.

Guo, “Morphology and mechanical properties of nanostructured thermoset/block copolymer blends with carbon nanoparticles,” *Compos. Part A Appl. Sci. Manuf.*, vol. 71, pp. 136–143, 2015, doi: 10.1016/j.compositesa.2015.01.010.

[75] L. Ruiz-Pérez, G. J. Royston, J. P. A. Fairclough, and A. J. Ryan, “Toughening by nanostructure,” *Polymer (Guildf).*, vol. 49, no. 21, pp. 4475–4488, 2008, doi: 10.1016/j.polymer.2008.07.048.

[76] J. Wang *et al.*, “Synergistically effects of copolymer and core-shell particles for toughening epoxy,” *Polymer (Guildf).*, vol. 140, pp. 39–46, 2018, doi: 10.1016/j.polymer.2018.02.031.

[77] M. B. Schuster, I. K. de Abreu, D. Becker, and L. A. F. Coelho, “Effects of adding different concentrations of block copolymers in epoxy matrix nanocomposites with carbon allotropic nanoparticles,” *Polym. Compos.*, vol. 42, no. 2, pp. 995–1007, 2021, doi: 10.1002/pc.25881.

[78] L. Tao, Z. Sun, W. Min, and H. Ou, “Improving the toughness of thermosetting epoxy resins via blending triblock copolymers,” pp. 1603–1612, 2020, doi: 10.1039/c9ra09183a.

[79] R. Januszewski, M. Dutkiewicz, M. Nowicki, M. Szołyga, and I. Kownacki, “Synthesis and Properties of Epoxy Resin Modified with Novel Reactive Liquid Rubber-Based Systems,” *Ind. Eng. Chem. Res.*, vol. 60, no. 5, pp. 2178–2186, 2021, doi: 10.1021/acs.iecr.0c05781.

[80] S. H. Mahdi, W. H. Jassim, I. A. Hamad, and K. A. Jasima, “Epoxy/Silicone Rubber Blends for Voltage Insulators and Capacitors Applications,” *Energy Procedia*, vol. 119, pp. 501–506, 2017, doi: 10.1016/j.egypro.2017.07.059.

[81] W. J. Work, K. Horie, M. Hess, and R. F. T. Stepto, “Definitions of terms related to polymer blends, composites, and multiphase polymeric materials (IUPAC Recommendations 2004),” *Pure Appl. Chem.*, vol. 76, no. 11, pp. 1985–2007, 2004, doi: 10.1351/pac200476111985.

[82] C. C. Su, J. H. Lin, and E. M. Woo, “Miscibility windows in ternary polymer blends of a polyester, polymethacrylate and poly(styrene-co-acrylonitrile),” *Polym. Int.*, vol. 52, no. 7, pp. 1209–1216, 2003, doi: 10.1002/pi.1252.

[83] C. Wang, Q. Sun, K. Lei, C. Chen, L. Yao, and Z. Peng, “Effect of Toughening with Different Liquid Rubber on Dielectric Relaxation Properties of Epoxy Resin,” 2020.

[84] D. Hussinaiah, “Synthesis and Characterization of Silicone epoxy resin /poly (methyl methacrylate) Interpenetrating Polymer Networks,” *IOSR J. Eng.*, vol. 4, no. 1, pp. 49–60, 2014, doi: 10.9790/3021-04154960.

[85] S. Roy, R. S. Petrova, and S. Mitra, “Regular article Effect of carbon nanotube (CNT) functionalization in epoxy-CNT composites,” vol. 7, no. 6, pp. 475–485, 2018.

[86] G. Liang and K. Chandrashekhara, “Cure kinetics and rheology characterization of soy-based epoxy resin system,” *J. Appl. Polym. Sci.*, vol. 102, no. 4, pp. 3168–3180, 2006, doi: 10.1002/app.24369.

[87] C. Processes *et al.*, “Study of the Degree of Cure through Thermal Analysis and Raman Spectroscopy in,” 2019.

[88] J. Liang *et al.*, “Experimental Study of Curing Temperature Effect on Mechanical Performance of Carbon Fiber Composites with Application to Filament Winding Pressure Vessel Design,” *Polymers (Basel).*, vol. 15, no. 4,

pp. 1–16, 2023, doi: 10.3390/polym15040982.

[89] W. Peng, X. Chen, and J. Wang, “Study on the curing behavior of polythiol/phenolic/epoxy resin and the mechanical and thermal properties of the composites,” *Mater. Res. Express*, vol. 8, no. 5, p. 55302, 2021, doi: 10.1088/2053-1591/abeb4a.

[90] V. Hermán, H. Takacs, F. Duclairoir, O. Renault, J. H. Tortai, and B. Viala, “Core double-shell cobalt/graphene/polystyrene magnetic nanocomposites synthesized by in situ sonochemical polymerization,” *RSC Adv.*, vol. 5, no. 63, pp. 51371–51381, 2015, doi: 10.1039/c5ra06847a.

[91] A. A. Godbole, “TRACE : Tennessee Research and Creative Exchange Study of UV Curable Rubber-Toughened Epoxy Systems,” 2002.

[92] P. Taylor, “Study of the curing process of an epoxy resin by FTIR spectroscopy Access details : Access Details : [subscription number 789296669],” no. May 2014, 2000, doi: 10.1081/PPT-100101414.

[93] P. Taylor and S. C. Dsc, “Cure Kinetics Study of Two Epoxy Systems with Fourier Tranform Infrared Spectroscopy (FTIR) and Differential Cure Kinetics Study of Two Epoxy Systems with Fourier Tranform Infrared Spectroscopy (FTIR) and Differential Scanning Calorimetry (DSC),” no. July 2013, pp. 37–41, doi: 10.1080/10601325.2012.696995.

[94] P. Maity, S. V Kasisomayajula, and V. Parameswaran, “Improvement in Surface Degradation Properties of Polymer Composites due to Pre-processed Nanometric Alumina Fillers,” no. March, 2008, doi: 10.1109/T-DEI.2008.4446737.

[95] S. Nikafshar *et al.*, “A renewable bio-based epoxy resin with improved

mechanical performance that can compete with DGEBA," *RSC Adv.*, vol. 7, no. 14, pp. 8694–8701, 2017, doi: 10.1039/c6ra27283e.

[96] J. Fang, Y. Xuan, and Q. Li, "Preparation of polystyrene spheres in different particle sizes and assembly of the PS colloidal crystals," *Sci. China Technol. Sci.*, vol. 53, no. 11, pp. 3088–3093, 2010, doi: 10.1007/s11431-010-4110-5.

[97] H. N. Varzeghani, I. A. Amraei, and S. R. Mousavi, "Dynamic Cure Kinetics and Physical-Mechanical Properties of PEG / Nanosilica / Epoxy Composites," vol. 2020, 2020.

[98] Z. Sun, L. Xu, Z. Chen, Y. Wang, and R. Tusiime, "Enhancing the Mechanical and Thermal Properties of Epoxy Resin via Blending with Thermoplastic Polysulfone," 2019, doi: 10.3390/polym11030461.

[99] W. -Y Chiang and C. -Y Huang, "The effect of the soft segment of polyurethane on copolymer-type polyacetal/polyurethane blends," *J. Appl. Polym. Sci.*, vol. 38, no. 5, pp. 951–968, 1989, doi: 10.1002/app.1989.070380516.

[100] L. Wu and S. V Hoa, "Effects of Composition of Hardener on the Curing and Aging for an Epoxy Resin System," 2005, doi: 10.1002/app.22493.

[101] C. Campana *et al.*, "Effect of post curing temperature on mechanical properties of a flax fiber reinforced epoxy composite To cite this version : HAL Id : hal-01772669," 2018.

[102] S. Pandini, F. Baldi, R. De Santis, and F. Bignotti, "Epoxy / Layered-Silicate Nanocomposites : Effect of the Matrix Composition on Large Deformation and Fracture Behavior," pp. 1–2.

[103] C. Barrère-Tricca, J. L. Halary, and F. Dal Maso, “Relationship between epoxy resin properties and weepage of glass-reinforced filament-wound pipes,” *Oil Gas Sci. Technol.*, vol. 57, no. 2, pp. 169–175, 2002, doi: 10.2516/ogst:2002013.

[104] R. H. Bello, L. Antonio, and F. Coelho, “Role of Triblock Copolymers in the Properties of Epoxy Matrices Role of Triblock Copolymers in the Properties of Epoxy Matrices With Carbon Nanoparticles,” no. January, 2019.

[105] A. M. Hameed, E. G. Daway, and M. F. Abd Al Majed, “Morphology and Mechanical Properties of (Epoxy/PVC) Blend,” *Al-Khwarizmi Eng. J.*, vol. 11, no. 3, pp. 47–53, 2015.

[106] K. C. Jajam, M. M. Rahman, M. V. Hosur, and H. V. Tippur, “Fracture behavior of epoxy nanocomposites modified with polyol diluent and amino-functionalized multi-walled carbon nanotubes: A loading rate study,” *Compos. Part A Appl. Sci. Manuf.*, vol. 59, pp. 57–69, 2014, doi: 10.1016/j.compositesa.2013.12.014.

[107] M. N. G. Chanshetti and M. A. S. Pol, “Wear Behavior of TiO 2 and WC Reinforced Epoxy Resin Composites,” pp. 2342–2346, 2016.

[108] Z. Heng, Z. Zeng, Y. Chen, H. Zou, and M. Liang, “Silicone modified epoxy resins with good toughness, damping properties and high thermal residual weight,” *J. Polym. Res.*, vol. 22, no. 11, 2015, doi: 10.1007/s10965-015-0852-x.

[109] S. P. Khatiwada, U. Gohs, R. Lach, G. Heinrich, and R. Adhikari, “A new way of toughening of thermoset by dual-cured thermoplastic/thermosetting blend,” *Materials (Basel).*, vol. 12, no. 3, 2019, doi: 10.3390/ma12030548.

[110] S. Deng, L. Ye, and K. Friedrich, “Fracture behaviours of epoxy nanocomposites with nano-silica at low and elevated temperatures,” *J. Mater. Sci.*, vol. 42, no. 8, pp. 2766–2774, 2007, doi: 10.1007/s10853-006-1420-x.

[111] B. Wetzel, P. Rosso, F. Haupert, and K. Friedrich, “Epoxy nanocomposites – fracture and toughening mechanisms,” vol. 73, pp. 2375–2398, 2006, doi: 10.1016/j.engfracmech.2006.05.018.

[112] Y. Zheng, K. Chonung, G. Wang, P. Wei, and P. Jiang, “Epoxy / Nano-Silica Composites : Curing Kinetics , Glass Transition Temperatures , Dielectric , and Thermal – Mechanical Performances,” 2008, doi: 10.1002/app.

[113] F. N. Alhabill, “Influence of filler / matrix interactions on resin / hardener stoichiometry , molecular dynamics , and particle dispersion of silicon nitride / epoxy nanocomposites,” *J. Mater. Sci.*, vol. 53, no. 6, pp. 4144–4158, 2018, doi: 10.1007/s10853-017-1831-x.

[114] V. Nguyen, A. Vaughan, P. Lewin, and A. Krivda, “The effect of resin stoichiometry and nanoparticle addition on epoxy/silica nanodielectrics,” *IEEE Trans. Dielectr. Electr. Insul.*, vol. 22, no. 2, pp. 895–905, 2015, doi: 10.1109/TDEI.2015.7076790.

[115] R. Aradhana, S. Mohanty, and S. K. Nayak, “High performance epoxy nanocomposite adhesive: Effect of nanofillers on adhesive strength, curing and degradation kinetics,” *Int. J. Adhes. Adhes.*, vol. 84, no. March, pp. 238–249, 2018, doi: 10.1016/j.ijadhadh.2018.03.013.

[116] A. Lavoratti, A. J. Zattera, and S. C. Amico, “Effect of carbonaceous nanofillers and triblock copolymers on the toughness of epoxy resin,” *Polym. Bull.*, vol. 78, no. 10, pp. 5467–5480, 2021, doi: 10.1007/s00289-020-03375-

1.

[117] S. K. Tan, S. Ahmad, C. H. Chia, A. Mamun, and H. P. Heim, “A Comparison Study of Liquid Natural Rubber (LNR) and Liquid Epoxidized Natural Rubber (LENR) as the Toughening Agent for Epoxy,” vol. 3, no. 3, pp. 55–61, 2013, doi: 10.5923/j.materials.20130303.02.

[118] L. Xiao *et al.*, “A renewable tung oil-derived nitrile rubber and its potential use in epoxy-toughening modifiers,” *RSC Adv.*, vol. 9, no. 44, pp. 25880–25889, 2019, doi: 10.1039/c9ra01918a.

[119] R. L. Yongli He, “Effect of nitrogen-doped carbon dots on the anticorrosion properties of waterborne epoxy coatings,” *2D Mater.*, pp. 0–6, 2020.

[120] A. S. Ismail, M. Jawaid, N. H. Hamid, R. Yahaya, and A. Hassan, “Mechanical and morphological properties of bio-phenolic/epoxy polymer blends,” *Molecules*, vol. 26, no. 4, pp. 1–11, 2021, doi: 10.3390/molecules26040773.

[121] Y. Qin, Y. Wang, Y. Wu, Y. Zhang, H. Li, and M. Yuan, “Effect of Hexadecyl Lactate as Plasticizer on the Properties of Poly(l-lactide) Films for Food Packaging Applications,” *J. Polym. Environ.*, vol. 23, no. 3, pp. 374–382, 2015, doi: 10.1007/s10924-014-0702-7.

[122] J. Szymańska, M. Bakar, M. Kostrzewa, and M. Lavorgna, “Preparation and characterization of reactive liquid rubbers toughened epoxy-clay hybrid nanocomposites,” *J. Polym. Eng.*, vol. 36, no. 1, pp. 43–52, 2016, doi: 10.1515/polyeng-2014-0393.

[123] Arundhati, R. Singhal, and A. K. Nagpal, “Thermal and chemical resistance behavior of cured epoxy based on diglycidyl ether of bisphenol-A and thiol

treated liquid polysulfide blends," *Adv. Mater. Lett.*, vol. 1, no. 3, pp. 238–245, 2010, doi: 10.5185/amlett.2010.10172.

[124] H. Gu and C. Ma, "Low Loading of Grafted Thermoplastic Polystyrene Strengthened and Toughened Transparent Epoxy Composites", Issue 17, 2017, May 2017, Journal of Materials Chemistry C 5(17), DOI:10.1039/C7TC00437K.

جمهورية العراق

وزارة التعليم العالي والبحث العلمي

جامعة بابل

كلية هندسة المواد

قسم هندسة البوليمرات والصناعات البتروكيمياوية

تأثير ظروف الانضاج على المحددات الحركية على نظام الايبوكسي وخلائطه

اطروحة مقدمة الى
عمادة كلية هندسة المواد/ جامعة بابل وهي جزء من متطلبات نيل درجة
الدكتوراه فلسفة في هندسة المواد/البوليمر

من قبل

زهراء عمران موسى حسين

بكالوريوس هندسة المواد/ لامعدنية 2011

ماجستير هندسة البوليمرات 2014

بإشراف

أ.د. نجم عبد الامير سعيد

2024 A.D **1445 A.H**

الخلاصة:

في الاونة الاخيرة تزايد الاهتمام نحو راتنج الايبوكسي وخلائطه لذلك من الضروري معرفة حركية التفاعل للايبوكسي والية التقسية للحصول على الخواص المطلوبة لتطبيقات عديدة في مجالات مختلفة.

في هذه الدراسة تم استخدام أربع نسب خلط مختلفة لعينات نقية من الايبوكسي / المصلب مع دراسة حركية التفاعل لراتنجات الايبوكسي النقي , المجموعة الثانية من العينات كانت لحلائط الايبوكسي مع البوليستايرين مع دراسة حركية التفاعل تحت ظروف مختلفة لتقسيو الايبوكسي وخلائطه حيث تتضمن استخدام عدة ظروف وعوامل توثر على الية التقسية بما في ذلك استخدام نسب مختلفة من نسب الايبوكسي للمصلد وكميو اضافة البوليستايرين بالاضافة الى تغير درجة حرارة التقسية وزمن التقسية بالاضافة الى عدة عوامل اخرى.

تم استخدام عدة فحوصات لدراسة تاثير هذه الظروف على حركية التفاعل للايبوكسي وخلائطه من ضمنها TGA، DSC FTIR، ، خصائص الشد ، قوة صلابة الكسر ، قوة التأثير ، الصلابة و SEM .

حيث بينت النتائج التالي:

بناء على النتائج المحصلة ، تم حساب حركية التفاعل لراتنجات الايبوكسي المستخدمة في ظل ظروف معالجة مختلفة ، مثل درجة الحرارة ، والنسب الزمنية للمواد المقواة ، والراتنج إلى العوامل غير المباشرة الأكثر صلابة ، مثل درجة التقسية ووتيرة التفاعل. أظهرت نتائج المسح الضوئي التفاضلي الإيبوكسي وخلطاته أنه ، اعتمادا على الظروف ، قام عدد من العوامل بتغيير آلية الحركية بالإضافة إلى ذلك ، كان لإضافة PS تأثير أقل على Tg مما يشير إلى أن المتانة أظهرت نتائج تحليل FT-IR لعامل التقوية / مزيج الإيبوكسي أن هناك تفاعلا فيزيائيا فقط بين بوليمر الإيبوكسي القطبي والبوليستارين ، وليس أي تفاعل كيميائي مع PS. في صور SEM لمزيج الإيبوكسي ، قام PS بتغيير شكل السطح للمقطع العرضي لعينة الإيبوكسي ، مما يدل على وجود عدة عوامل ادت الى هذه الهيئة للسطح بسبب عدة

عوامـل منهـا تبخـر المـذيب ممـا يـودي الـى تـرك فراغـات ويسـبب تششـققات او انفصـال البوليستايرين عن الايبوكسي ممال يؤدي الى هذه الهيئة.

مما ادى الى تدهور الخواص الميكانية كما تم ملاحظتها سابقا في فصل الرابع للنتائج.